

Engineering baculovirus gene delivery platforms for treating atherosclerotic progression



Sabrina Jasmin Schaly

Biomedical Technology and Cell Therapy Research Laboratory

Department of Biomedical and Bioengineering

Faculty of Medicine and Health Sciences

McGill University, Montreal, Canada

December 2023

A thesis submitted to McGill University in partial fulfillment of the requirement of the degree of Doctor of Philosophy

© Sabrina Jasmin Schaly 2023

Abstract

A single cut sets off a cascading signal in our body to initiate healing. This happens every day without us realizing it. Only when these finely regulated system dysfunctions do we realize, arising in an infection or disease. This is also the case with atherosclerosis, plaque build-up within the arteries causing serious complications. Atherosclerosis is on the rise, affecting a growing number of younger individuals, leading to a diminished quality of life, substantial pain, and numerous serious accompanying comorbidities. Accumulation of fatty deposits, endothelial cell dysfunction, and inflammation causes the artery to close and constrict blood flow causing significant health problems such as limb ischemia and chronic wounds.

Typically, a metal stent forces the artery open, successfully saving millions of lives. However, stents further damage the artery and can lead to in-stent restenosis and thrombosis. But what if we could bypass this dysfunction and injury by providing the proper genes your artery needs to recover? Baculoviruses, extracted from insect cells, have the potential to do just this. These biosafe, non-replicative, non-integrative, low-cost vectors can effectively be engineered to express human genes. The baculovirus gene delivery system was found to be safe with no signs of inflammation, hemolysis, thrombosis, genotoxicity, or cytotoxicity. The baculovirus safety and gene expression can be further improved by encapsulating the baculovirus in an engineered biocompatible and biodegradable polymer. A baculovirus polymer hydrogel system was developed to control and sustain baculovirus delivery. The three genes selected (ADAMTS13, NOS3, and VEGFA) showed favourable properties including angiogenic, prolific for endothelial cells, and regulatory for smooth muscle cells. The genes also prevented reactive oxygen species (ROS) production in both cell types and C-reactive protein (CRP) production in endothelial cells.

By coating these baculoviruses onto a stent, healing can be promoted and the significant morbidity associated with peripheral and coronary artery disease can be prevented.

The novel stents investigated here were proven safe and efficient. The stent system also demonstrated favourable therapeutic properties, including anti-thrombotic, anti-inflammatory, and anti-restenotic. These therapeutic properties suggest a promising alternative stent system for mitigating current complications.

Résumé

Une seule coupure déclenche un signal important dans notre corps pour initier la guérison. Cela arrive tous les jours sans que nous nous en rendions compte. Ce n'est que lorsque ce système très régulé dysfonctionne que nous nous en rendons compte, à cause d'une infection ou d'une maladie. C'est également le cas avec l'athérosclérose, l'accumulation de dépôts gras. Athérosclérose, le dysfonctionnement des cellules endothéliales et l'inflammation provoquent une restriction de l'écoulement sanguin dans l'artère et peut entraîner des problèmes de santé importants tels qu'une ischémie des membres et des plaies chroniques.

En général, un stent métallique est utilisé pour forcer l'ouverture de l'artère et a sauvé des millions de vies. Cependant, cela crée d'autres dommages à l'artère et peut entraîner une resténose et une thrombose intra-stent. Mais et si nous pouvions contourner ce dysfonctionnement et cette blessure en fournissant les protéines appropriées dont votre corps a besoin pour guérir? Les baculovirus, extraits de cellules d'insectes, ont le potentiel de faire exactement cela. Ces vecteurs non-toxiques, non répliatifs, non intégratifs et à faible coût peuvent être conçus pour exprimer des gènes humains de manière efficace. Ces gènes sont utilisés pour synthétiser les gènes nécessaires à la guérison. Le système de distribution de gènes de baculovirus s'est avéré sûr, sans signe d'inflammation, d'hémolyse, de thrombose, de génotoxicité ou de cytotoxicité. La sécurité et l'expression des protéines peuvent être encore améliorées en encapsulant le baculovirus dans un polymère biocompatible et biodégradable modifié. Un système d'hydrogel avec baculovirus a été développé pour contrôler et maintenir la distribution du baculovirus. Les trois gènes sélectionnés (ADAMTS13, NOS3, et VEGFA) ont démontré des propriétés favorables, dont une angiogenèse plus marquée, la prolifération de cellules endothéliales et la régulation des cellules musculaires lisses. Les gènes ont également empêché la production d'espèces réactives de l'oxygène (ROS)

dans les deux types de cellules et la production de protéine C-réactive (CRP) dans les cellules endothéliales. En enrobant des baculovirus exprimant des gènes régulateurs sur un stent, la cicatrisation artérielle peut être favorisée et la morbidité significative associée à la maladie artérielle périphérique peut être évitée.

Les nouveaux stents périphériques étudié ici s'est avéré sûr et efficace. Le système de stent a également démontré des propriétés thérapeutiques favorables, notamment anti-thrombotiques, anti-inflammatoires et anti-resténotiques. Ces propriétés thérapeutiques suggèrent un système de stent alternatif prometteur pour atténuer les complications liées aux stents.

Acknowledgments

Thank you to everyone who supported me throughout my career and studies. I could not have done it without you.

First, I would like to take this opportunity to express my deepest appreciation and gratitude to my supervisor, Dr. Satya Prakash. Thank you for your invaluable support, feedback, and guidance throughout my time at McGill University. Thank you for your unwavering encouragement and for pushing me in every aspect of my work and self-improvement. I also thank my thesis committee members (Dr. Nicole Li-Jessen, Dr. Rosaire Mongrain, and Dr. Robert J. Funnell) for their feedback and support. I would also like to acknowledge the faculty and staff of Biological and Biomedical Engineering for their support and guidance. Moreover, this work would not be possible without the funding support from McGill's BME department, the Canadian Graduate Scholarship Master's (NSERC), the Canadian Graduate Scholarship Doctoral (NSERC), Fonds de Recherche du Québec - Nature et Technologies (FRQNT), and the research grant awarded to Dr. Prakash and Dr. Shum-Tim by the Canadian Institute of Health Research (CIHR).

Thank you to my friends who were a welcome happiness throughout the years. Thank you to my fellow lab members (Paromita, Jacqueline, Rahul, Karan, Merry, Waqar, and Ahmed) for hearing me out, the support, and a good laugh when we all needed it. Thank you to Dr. Michelle Tran for guidance with the thesis writing and submission process.

I would also like to thank the several labs that allowed me to work with them and access their equipment. Specifically, the Neuro Institute and C-BIG Repository; Dr. Kelly Sears and Dr. David Liu at the FEMR; Dr. Maryam Tabrizian and Michael Yitayew in the Biomat'X lab; Dr. Nicholas Audet in the McGill University Imaging and Molecular Biology Platform (IMBP); Petr

Fiurasek and Robin Stein in the Chemical Characterization Facility; and Prof. Richard Leask's lab including Brenden Moeun and Kevin Bates.

Finally, thank you to Maple for making me smile every day and being the best welcome home after long days in the lab. Lastly, to my parents, who gave me every opportunity they never had and worked endlessly to give me the best life possible, a thank you will never be enough. Thank you for listening to my every problem and even troubleshooting experiments with me. I could not have done it without you. A thank you will never be enough. I am forever grateful to my family for their unconditional love and support.

Preface

This thesis was prepared in accordance with McGill University's thesis guidelines. There are twelve chapters in total. The thesis is manuscript-based, including five original articles. I am the first author of the five included papers. Each article contains an abstract, introduction, methods, results, discussion, and conclusion. The thesis also includes a general introduction, literature review, discussion, conclusion, contributions to knowledge, and references.

Table of Contents

<i>Abstract</i>	2
<i>Résumé</i>	4
<i>Acknowledgments</i>	6
<i>Preface</i>	8
<i>List of Figures</i>	11
<i>List of Tables</i>	12
<i>List of abbreviations</i>	13
CHAPTER 1: General introduction	15
Contribution to original knowledge	28
CHAPTER 2: Background and literature review	34
CHAPTER 3: Papers included in this thesis	51
CHAPTER 4: In vitro safety assessment of baculovirus gene delivery	55
Abstract.....	56
Introduction.....	56
Results	57
Discussion	68
Conclusion	70
Materials and Methods	71
Bridging text.....	79
CHAPTER 5: Alginate-chitosan hydrogel formulations sustain baculovirus delivery and VEGFA expression, which promotes angiogenesis for wound dressing applications.	81
Abstract.....	82
Introduction.....	82
Results	84
Discussion	92
Conclusion	94
Materials and Methods	94
Bridging text.....	104
CHAPTER 6: Controlled and customizable baculovirus NOS3 gene delivery using PVA-based hydrogel systems	106
Abstract.....	107
Introduction.....	108

Results and Discussion.....	111
Conclusion.....	126
Materials and Methods.....	126
Bridging text.....	135
<i>CHAPTER 7: Evaluating a tri-gene-eluting dissolvable stent for peripheral artery disease using baculoviruses.....</i>	137
Abstract.....	139
Introduction.....	140
Results.....	144
Discussion.....	161
Conclusion.....	164
Materials and Methods.....	165
Bridging text.....	175
<i>CHAPTER 8: A gene- and drug-eluting (GDES) stent coating to promote re-endothelialization and prevent restenosis due to atherosclerosis.....</i>	177
Abstract.....	179
Introduction.....	180
Results.....	182
Discussion.....	193
Conclusion.....	196
Materials and Methods.....	197
<i>CHAPTER 9: General discussion.....</i>	207
<i>CHAPTER 10: Limitations and future recommendations.....</i>	216
<i>CHAPTER 11: Conclusion.....</i>	218
<i>CHAPTER 12: Summary and claimed original contributions to knowledge.....</i>	219
<i>Appendix.....</i>	224
<i>References.....</i>	226

List of Figures

Figure 1. Thesis outline for the three atherosclerosis treatments investigated	15
Figure 2. Schematic of peripheral artery disease progression	17
Figure 3. Baculovirus gene delivery of ADAMTS13, NOS3, and VEGFA proposed mechanism of action. Boxes in green are the complications common after peripheral artery stenting and boxes in purple are the baculovirus delivered genes	25
Figure 4. Novel stent design strategy and therapeutic mode	27
Figure 5. Lifecycle of baculoviruses and potential use for gene therapy (adapted from Schaly et al., 2021)	42
Figure 6. Mechanism of action and interplay between the three selected genes Error! Bookmark not defined.	
Figure 7. Brightfield images of Sf9 cells infected with baculoviruses	59
Figure 8. Baculovirus gene expression and cytotoxicity in SMC and HUVECs.....	61
Figure 9. Lysosomal activity following baculovirus transduction.....	63
Figure 10. Cytokinesis-block proliferation index (CBPI) in mammalian cells following baculovirus transduction	64
Figure 11. Reactive oxygen species (ROS) and C-reactive protein (CRP) production after baculovirus transduction	66
Figure 12. Blood compatibility of the baculovirus	68
Figure 13. Alginate-chitosan hydrogel morphology.....	85
Figure 14. Baculovirus release and expression from hydrogels.	87
Figure 15. Hydrogel therapeutic properties.	90
Figure 16. Hydrogel cytotoxicity and hemocompatibility studies.....	91
Figure 17. Properties of the PVA-based hydrogels	114
Figure 18. SEM of different PVA-based hydrogel compositions.....	117
Figure 19. Baculovirus elution from PVA-based hydrogels over time	119
Figure 20. Gene expression after baculovirus transduction.....	124
Figure 21. Mammalian cell viability after baculovirus transduction with different MOIs or direct hydrogel incubation	125
Figure 22. HUVEC and SMC viability, proliferation, and CRP production after baculovirus (BV) transduction.....	147
Figure 23. SMC and HUVEC proliferation after BV transduction	149
Figure 24. HUVEC migration and tube formation after baculovirus transduction.....	151
Figure 25. ROS production and vWF cleavage in HUVECs after baculovirus transduction	154
Figure 26. Morphology of the biodegradable stents	156
Figure 27. Mechanical properties of the biodegradable PVA stent	158
Figure 28. Baculovirus release from the PVA-coated stents over time at different conditions..	159
Figure 29. Stent cytotoxicity, hemocompatibility, and cell adhesion.....	161
Figure 31. PVA-coated stent morphology under SEM.....	183
Figure 32. Cell adhesion and blood compatibility for the stent coatings.....	185
Figure 33. Stent coating characterization and degradation.....	187
Figure 34. NOS3 gene expression and therapeutic effect.....	189
Figure 35. NOS3 and Everolimus (EVE) elution from the stent	191
Figure 36. NOS3 and Everolimus (EVE) elution and therapeutic effect together.....	193

List of Tables

Table 1. Comparison of viral vectors for gene therapy	47
Table 2. Hydrogel zeta potential, size, and swelling ratios. The zeta potential of the hydrogels, after being washed and resuspended in Milli-Q water (n = 3/group, 10 runs each). The average size of 10 randomly selected spherical hydrogels. The average swelling ratio of the different hydrogel formulations (10 different hydrogels/group, selected at random).	86
Table 3. PVA-based hydrogel swelling ratio and antimicrobial properties.....	115
Table 4. PVA-based hydrogel loading efficiencies	118

List of abbreviations

Abbreviation	Full name
ADAMTS13	disintegrin and metalloproteinase with a thrombospondin type 1 motif, member 13
ATR-FTIR	attenuated total reflectance Fourier transform infrared spectroscopy
BMS	bare-metal stent
BV	baculovirus
CAD	coronary artery disease
CBPI	cytokinesis-block proliferation index
CLI	critical limb ischemia
CVD	cardiovascular disease
DES	drug-eluting stent
DMSO	dimethyl sulfoxide
FBS	fetal bovine serum
g	gram
GDES	gene- and drug-eluting stent
GES	gene-eluting stent
GFP	green fluorescent protein
GOI	gene of interest
h	hour
HBSS	Hanks balanced salt solution
hpi	hours post infection
HUVEC	human umbilical vein endothelial cells
IC	intermittent claudication
LDH	lactate dehydrogenase
mg	milligram
mL	millilitre
mM	millimolar
MOI	multiplicity of infection
MTT	3-(4,5-dimethylthiazol-2-yl)-2,5-diphenyltetrazolium bromide
nm	nanometer
NMR	nuclear magnetic resonance (spectrometry)
NOS3	nitric oxide synthase 3
NP	nanoparticle
PAD	peripheral artery disease
PBS	phosphate buffer saline
PCR	polymerase chain reaction
PEG	polyethylene glycol
PFU	plaque forming unit

PLGA	poly (DL-lactide-co-glycolide)
PRP	platelet rich plasma
PVA	polyvinyl alcohol
RFP	red fluorescent protein
rpm	rotations per minute
RT	reverse transcription
SD	standard deviation
SEM	scanning electron microscope
Sf	<i>Spodoptera frugiperda</i>
SFM	serum-free media
SMC	smooth muscle cells
SS	stainless steel
STMP	sodium trimetaphosphate
TEM	transmission electron microscope
TU	transduction units
uL	microliter
V	volts
VEGFA	vascular endothelial growth factor A
VLP	virus-like particle

CHAPTER 1: General introduction

This thesis will investigate treatment options for atherosclerotic (arterial plaque build-up)

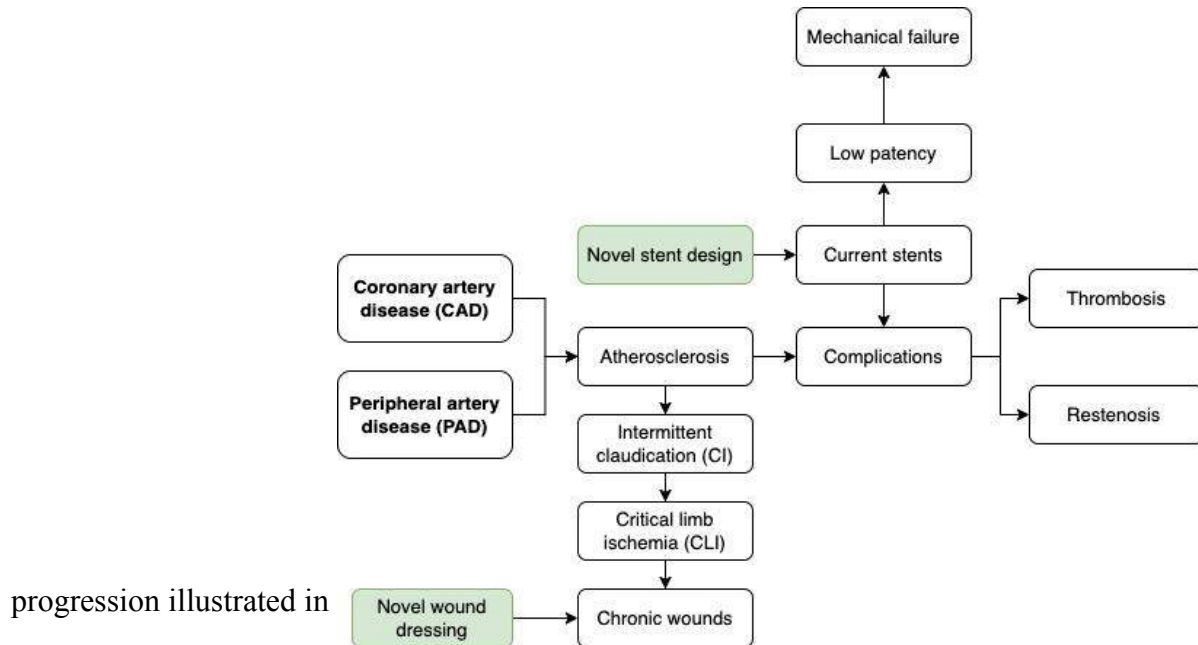


Figure 1. Specifically, peripheral stents, cardiac stents, and wound dressings were designed and optimized using natural polymers and baculovirus gene therapy. The three medical devices were optimized for their safety, efficacy, and therapeutic dose. Suitable properties for a chronic wound dressing were achieved and investigated during this optimization stage, mainly fluid control, cell regeneration, and antimicrobial properties. The novel stent designs tackle one of the main unaddressed complications of current stents, endothelial dysfunction, using baculovirus gene delivery.

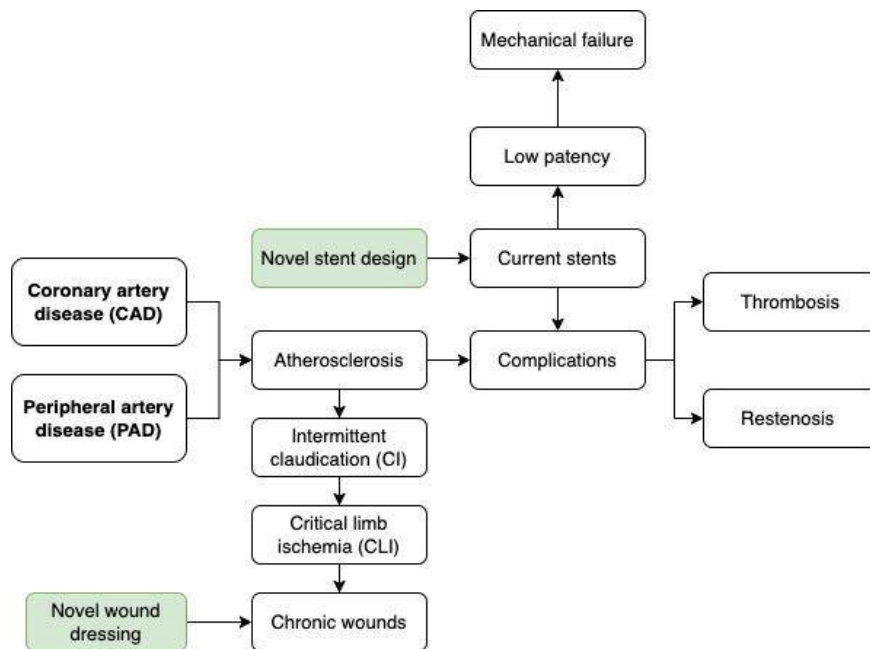


Figure 1. Atherosclerosis; three main treatment options investigated in this thesis

Atherosclerosis

Atherosclerosis is defined as the narrowing of peripheral or coronary arteries leading to an obstruction of blood flow. Atherosclerosis pathology occurs within the arteries' three layers: the tunica interna, tunica media, and tunica externa (also known as the adventitia). The inner layer, tunica interna, mainly comprises endothelial cells that form a confluent layer and are in contact with the flowing blood. The tunica media comprises mostly smooth muscle cells (SMC) and elastic fibers that allow the artery to stretch. The arterial narrowing may be attributed to four key factors within these layers: calcification, inflammation, endothelial dysfunction, and SMC hyperproliferation.

Atherosclerosis is a complex process involving several mechanisms, including endothelial dysfunction, inflammation, neointimal hyperplasia, and thrombosis (depicted in Figure 2). During the initial stages of atherosclerosis, endothelial dysfunction occurs due to several factors, such as

elevated low density lipoprotein (LDL), free radicals, hypertension, stress, obesity, diabetes, infection, and more [1]. The high LDL levels and endothelial dysfunction cause the medial layer to hyperproliferate (termed neointimal hyperplasia). Endothelial dysfunction also impairs vasodilation and vascular resistance. The LDL continues to accumulate in the artery and commences an inflammatory reaction. The activated immune cells translocate into the subendothelial space. Particularly, monocytes are known to translocate and differentiate into inflammatory macrophages [2]. The macrophages take up the LDL and differentiate into foam cells. The foam cells release more growth factors and cytokines, promoting SMC migration and proliferation, contributing to neointimal hyperplasia and restenosis.

During SMC migration, extracellular matrix remodeling can also occur, leading to stiff, stenotic, and calcified blood vessel walls. The macrophages can become overextended and undergo apoptosis, releasing pro-thrombotic factors, damaging microvessels, and contributing to a necrotic core [3]. These factors create a positive feedback loop contributing further to neointimal hyperplasia, inflammation, and plaque development, narrowing the blood vessel. Plaque erosion and rupture can cause thrombi formation, further obstructing blood flow and leading to complications. Consequently, atherosclerosis often comes with significant pain, discomfort, limb ischemia, difficulty breathing, and increases the risk of major cardiovascular events such as

myocardial infarction, stroke, and cerebrovascular disease [4].

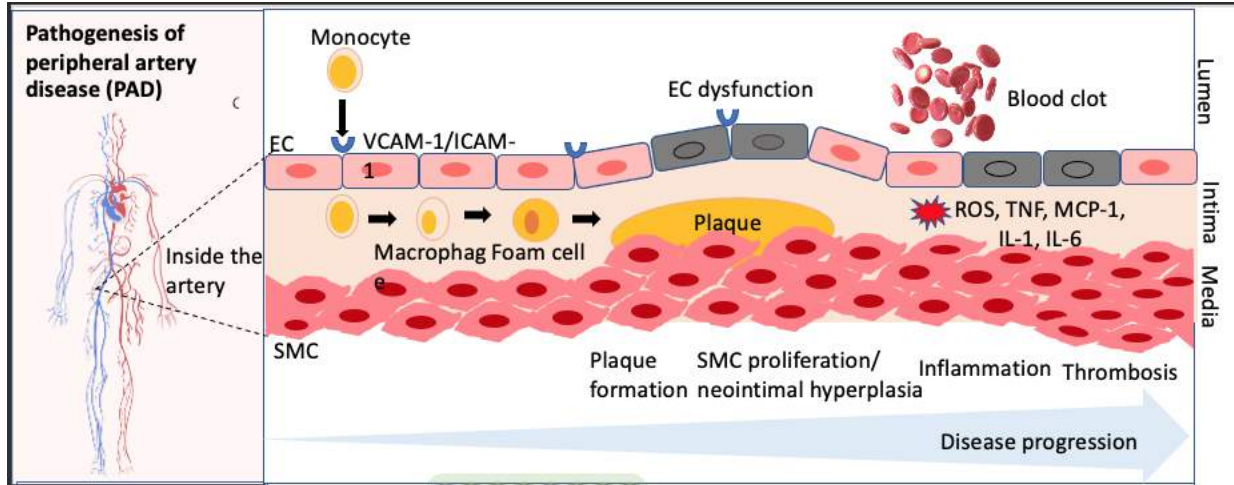


Figure 2. Schematic of peripheral artery disease progression

Peripheral artery disease

Peripheral artery disease (PAD) is most common in the lower extremities, such as the femoral artery (in the thigh), femoropopliteal artery (behind the knee), and the arteries coming from the heart. Historically, PAD burdened people in their 60s and over. Nearly one in five people over 60 have PAD, with an estimated 200 million new cases each yearly [5], [6]. However, more recent data suggest PAD also affects a significant proportion of young adults. Specifically, one to four percent of people aged 25 to 29 have PAD, and this percentage increases steadily with age [7].

People with PAD report a worse quality of life, higher work impairment, and use more healthcare resources compared to people without PAD [8]. Disability associated with PAD has also increased over the past 20 years, indicating a growing issue with an aging population. Moreover, complications and disabilities associated with PAD have a larger burden on women and people in developing countries [7], [9]. Hospitalization is common in people with PAD, with rates averaging 89.5 people per 100,000 [10]. The hospital stay duration ranged from three to nine days,

costing an average of \$15,755 USD per hospitalization. Major adverse limb events occur in almost one out of two (45.8 %) hospitalizations [11],[10]. The death rate is 0.07 and 28.71 per 100,000 people in the age groups 40 – 44 years and 80+ years, respectively [9].

Common symptoms include intermittent claudication, limb ischemia, and pain, all of which contribute to a reduced quality of life. Intermittent claudication (IC) is pain that occurs during movement but not while resting and occurs in nine out of ten symptomatic people [12]. People with symptomatic PAD also have a higher five-year cumulative cardiovascular mortality (13 % compared to 5 %) [12]. Moreover, around one in five (21 %) people with IC are diagnosed with critical limb ischemia. Critical limb ischemia (CLI) is characterized as the severe blockage of blood flow in the lower extremities. CLI leads to chronic wounds that cannot heal due to a lack of blood flow and nutrition. This often leads to amputation, with rates varying from four to twenty-seven percent. However, PAD can often be asymptomatic, leading to a more severe disease progression when diagnosed and complications [13].

Coronary artery disease (CAD)

Coronary artery disease (CAD) is the obstruction of arteries supplying the heart with nutrients and oxygen. The obstructed arteries can often be attributed to atherosclerosis, including calcification, inflammation, endothelial dysfunction, and neointimal hyperplasia [14]. Around one out of 20 people have CAD [15]. CAD is the third leading cause of death yearly, generating a large health and economic burden [16]. CAD accounts for 43 % of all cardiovascular disease deaths [17].

Poor diet, tobacco use, genetics, limited exercise, and an increasingly sedentary lifestyle are key risk factors for developing CAD [18],[19]. High cholesterol, body mass index, blood

pressure, and glucose levels also significantly increase the risk of adverse outcomes. With an increasing trend in these factors, there is also an increase in heart failure and CAD in the younger population. Overall, CAD creates a significant health and economic burden. It is estimated that the US and Europe spend over \$500 and \$150 billion, respectively, on people with CAD [20],[21].

CAD causes shortness of breath, pain in the shoulder or chest, nausea, and dizziness. More severe consequences include heart attack, heart failure, stroke, and death. CAD also increases the risk of severe adverse outcomes following any comorbidity. CAD contributes the most to the loss of Disability Adjusted Life Years (DALYs). The disease burden is highest in low and middle-income countries, accounting for over 7 million deaths annually [22]. Specifically, women tend to receive less aggressive treatment and possess more risk factors contributing to the disease burden [23].

Current atherosclerotic treatments

Atherosclerosis management includes lifestyle changes, medical management, endovascular repair, and surgery [24]. One of the main treatments for CAD and PAD includes implanting a stent to reopen the artery. A stent is used to force open the artery and has successfully saved millions of lives [25]. To insert a stent, a catheter is used to guide it through the arterial network and toward the blocked artery. Once at the occlusion site, the stent is expanded with a balloon or is self-expandable, allowing blood to pass through again.

There are several types of stents, often characterized as bare-metal stents (BMS) or drug-eluting stents (DES). These stents are often composed of 316L stainless steel, nitinol, or cobalt-chromium. Stents vary in geometry, size, expansion method, polymer coating, coating technique, and eluted drug. All these different properties have been tested due to recurrent complications,

mainly thrombosis, restenosis, and stent fracture. Typically, the stent struts are 80 to 200 μM with a degradable or permanent polymer coating under 10 μM thick [26], [27]. In DES, the drug is eluted anywhere from 30 to 180 days.

More recently, fully biodegradable stents have been explored. Biodegradable stents offer several advantages, such as eliminating the foreign body (the stent) and reducing the risk of thrombosis [28]. Complete biodegradation of the stent would also support normal vasomotion and luminal movement. Finally, biodegradable stents allow the possibility of discontinuing dual antiplatelet therapy. Magnesium alloys, zinc calcium alloys, iron alloys, polylactic acid (PLA, PDLA & PLLA), and tyrosine polycarbonate are being investigated [29], [30]. Another approach is using polyvinyl alcohol (PVA), which has the required mechanical strength and elasticity for a stent [31]–[34]. Some research groups created a stent using braided PVA yarn, while others have used 3D printing to create a PVA stent [31]–[33]. Other researchers have shown promising results using dip coating to synthesize PVA biliary duct stents [34]. Although these stents would provide significant advantages, incomplete degradation, lack of mechanical stability, and increased risk of thrombosis have limited their commercial use thus far.

Stenting complications

Stent implantation can cause complications due to incomplete endothelial growth and smooth muscle cell (SMC) hyperproliferation [35]. This is a risk factor for blood clot formation and blood vessel re-narrowing (in-stent restenosis, ISR). Each incidence of ISR requires re-intervention, putting the individual at a greater risk of infection and complications.

Stenting can also induce further damage to the endothelial lining of the artery and can lead to blood vessel re-narrowing and blood clots [35]. Blood vessel narrowing (restenosis) is defined

as a >50 % narrowing of a blood vessel's diameter and occurs in 5-10 % of cases using current drug-eluting stents [36]. ISR invites further calcification making the blood vessel stiff, inefficient and increases the risk of stroke, myocardial infarction, and death. At the very least, this further reduces the individual's quality of life, leading to chest pain, shortness of breath, aches, and general pain. Other common complications include thrombosis, restenosis, calcification, and mechanical failures leading to an increased risk of morbidity, myocardial infarction, stroke, and mortality [37]. One-year patency rates are as low as 76 %, and two-year patency rates are as low as 60 % [38]. With low patency, re-intervention is required increasing the risk of complications and associated morbidity. An alternative and promising approach is the delivery of genes to promote endothelial cell regulation and regrowth.

Another significant consequence of atherosclerosis is the obstruction of blood flow, oxygen, and nutrients. Inadequate tissue perfusion, oxidative stress, endothelial dysfunction, and chronic inflammation can lead to tissue degeneration and often gangrene [39], [40]. These factors also contribute to chronic wounds that are difficult to heal despite interventions.

Gene-eluting stents

Atherosclerosis can cause gene dysregulation, specifically an increase in pro-inflammatory genes and a decrease in healing and anti-inflammatory ones. Thus early-stage interventions promoting proper endothelial function would appear to prevent LDL accumulation, immune cell infiltration, inflammation, and smooth muscle cell hyperproliferation. To achieve this, gene-eluting stents are promising. Several gene-eluting stents have been investigated in pre-clinical settings, including green fluorescent protein, β -galactosidase, Anti-Monocyte Chemoattractant Protein-1, miR-22, nitric oxide, and vascular endothelial growth factor (VEGF) delivery. β -

galactosidase and green fluorescent protein (GFP) expression were used to prove the concept of localized arterial delivery [41],[42]. Anti-Monocyte Chemoattractant Protein-1 stent delivery prevented monocyte infiltration and neointima formation [43]. Comparatively, miR-22 is a microRNA capable of regulating gene expression and degradation [44]. Specifically, miR-22 was used to regulate SMC proliferation and vascular remodeling. The miR-22-loaded stents reduce inflammation, SMC proliferation, and extracellular matrix deposition. Similarly, nitric oxide can inhibit SMC proliferation and dose-dependently reduce blood pressure and arterial stiffening [45]. Specifically, nitric oxide delivery from stents has been shown to prevent neointimal hyperproliferation while maintaining endothelial health and re-endothelialization [46], [47]. Another key gene studied for re-endothelialization is VEGF. One group reported that stent delivery of a VEGF plasmid significantly improved re-endothelialization and reduced ISR [48]. VEGF expression and paclitaxel co-elution have also been studied, resulting in complete re-endothelialization and reduced ISR one month after implantation [49]. These results suggest that two weeks of gene expression is sufficient to recover endothelial function. However, gene-eluting stents are limited by gene fragility, efficiency, loading capacity, and short elution time. Moreover, the organic solvents used during stent coating degrade the gene resulting in restricted loading and efficacy.

Baculoviruses gene delivery for gene-eluting stents

Baculoviruses expression systems, extracted from insect cells, can improve loading efficiency and sustain gene delivery. These biosafe, non-replicative, non-integrative, low-cost vectors can effectively be engineered to express human genes used to synthesize proteins required

for healing [50]. By coating baculoviruses, expressing healing genes, onto a stent, arterial healing can be promoted and prevent significant morbidity and health complications.

Baculoviruses belong to a diverse group of viruses found in insects. Baculoviruses can be genetically modified to enter and mediate gene expression in mammalian cells. However, they do not replicate in vertebrate cells, making them a biologically safe and transient gene delivery vector [50]. This narrow host range prevents complications with pre-existing immunity observed with other viral vectors in humans. Moreover, the 40-50 x 200-400 nm baculovirus capsid can extend to accommodate larger inserts of recombinant DNA (+38 kb), enabling multi-gene expression [51]. They also have low risk regarding biosafety, are classified as safe by regulatory agencies (FDA and Health Canada) and are currently used in human and veterinary therapeutic production. Baculoviruses can easily be amplified for large-scale production using insect cells and serum-free media in suspension, making them cost-effective [52]. The advantages of this system include its safety, large and complex genes can be delivered, and the transient delivery instead of integrative prevents adverse effects sometimes seen with adenoviruses. The baculovirus can also be engineered, encapsulated, and surface modified to optimize gene expression for specific time periods, such as the crucial first two weeks following stent implantation, to promote proper endothelial function. After this two-week period, gene expression should return to base levels to prevent adverse effects, another advantage of baculoviruses.

Previously, Paul et al., (2013b) developed a recombinant baculovirus that expressed VEGF for its angiogenic potential. The baculovirus was then ionically loaded onto a polyamidoamine dendrimer (PAMAM) dendrimer. The Baculovirus-PAMAM complex was then encapsulated in biodegradable poly(D, L-lactic-co-glycolic acid) (PLGA) microspheres. The researchers reported localized gene expression at the stent location, which declined over time. Moreover, there was

evidence of significantly enhanced re-endothelialization, reduction in neointimal formation, and reduced stenosis after 14 days [53].

It is predicted that the delivery of three genes can create a synergistic effect, reducing the dosage required for a therapeutic effect and mitigating off target effects. The three genes selected include ADAMTS13, NOS3, and VEGFA, depicted in

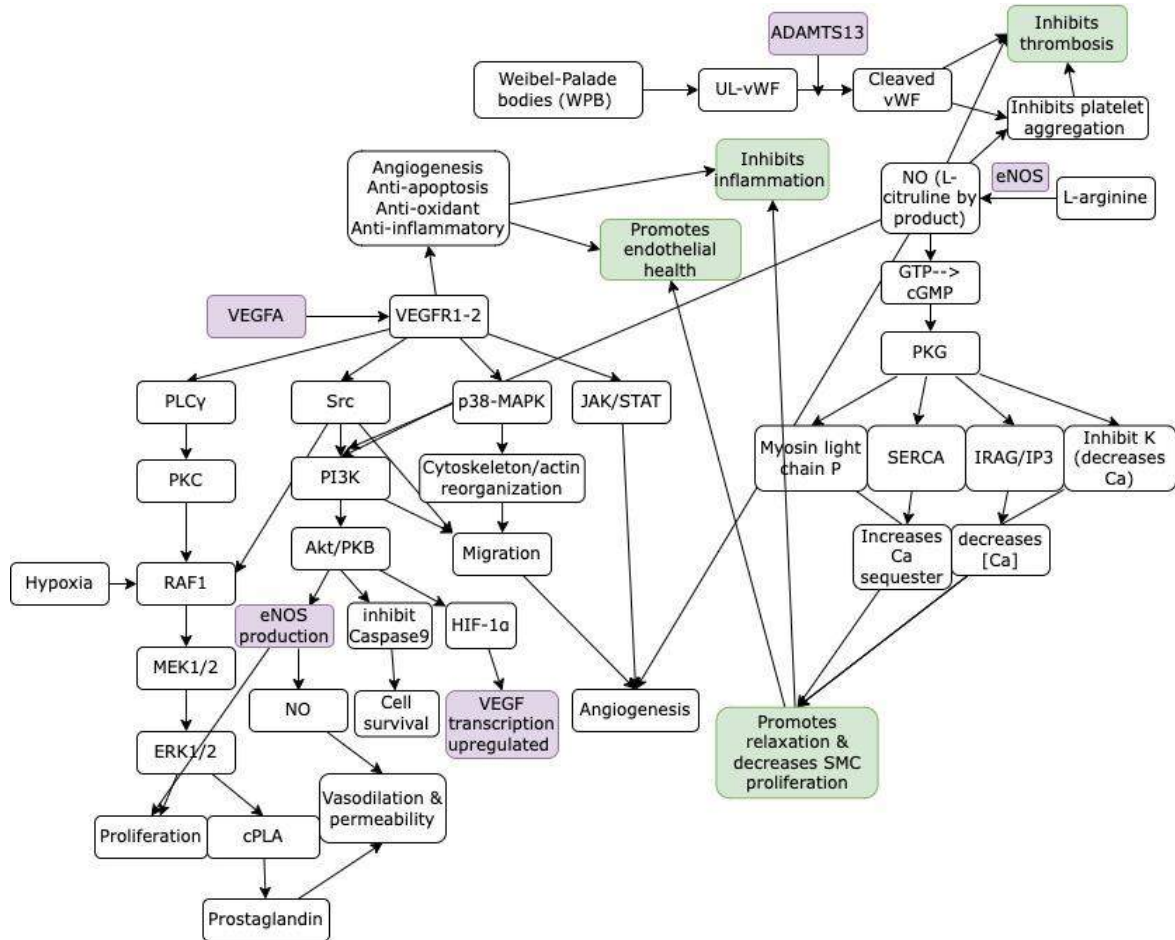


Figure 3. Specifically, NOS3 converts L-arginine to nitric oxide, which signals through a cGMP pathway leading to a decrease in calcium influx [54], [55]. This leads to relaxation (vasodilation), a decrease in the proliferation of SMCs, inhibits inflammation, and promotes endothelial health. Nitric oxide also helps prevent platelet adhesion and thrombosis. Similarly, VEGFA also improves endothelial health, inhibits inflammation, and promotes eNOS production.

However, the VEGFA signalling is through the VEGFR which signals through the p38-MAPK, PLCgamma, and JAK/STAT pathway [56], [57]. ADAMTS13 cleaves vWF to make smaller multimers that are less likely to aggregate and attract platelets to adhere [58]. Both ADAMTS13 and NO₃ inhibit platelet aggregation.

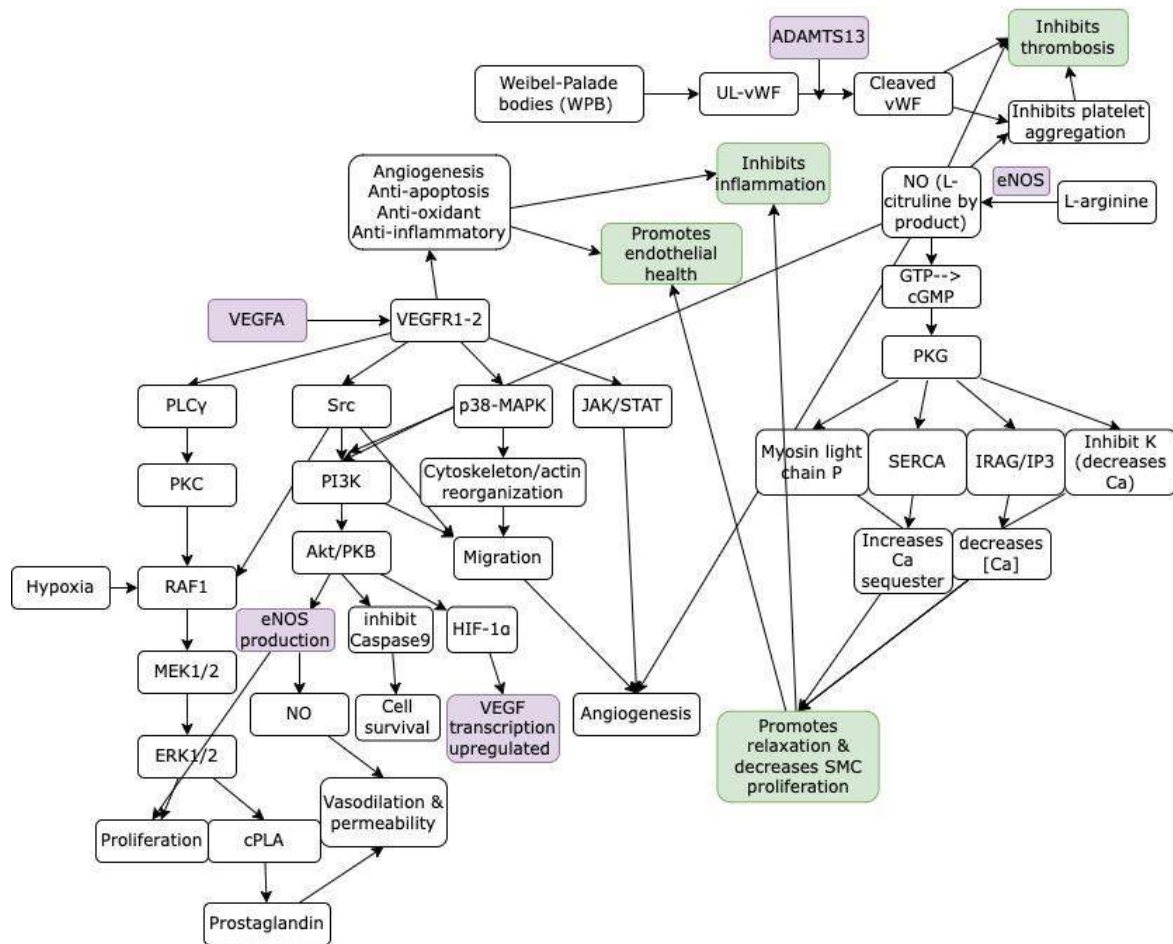


Figure 3. Baculovirus gene delivery of ADAMTS13, NOS3, and VEGFA and their proposed mechanism of action. Boxes in green are the complications common after peripheral artery stenting and boxes in purple are the baculovirus delivered genes.

Collectively, these reports demonstrate the feasibility and efficiency of baculoviruses in using gene-eluting stents. However, further work must be done to optimize the gene delivery,

optimize gene selection, reduce the coating thickness from 200 μM , and create a smooth and uniformly dissolvable stent coating.

Research Hypothesis: Baculovirus gene delivery stent coatings can be used to treat atherosclerosis and prevent currently associated complications. Combining a gene- and drug-eluting stent can promote artery healing, thereby preventing common complications like restenosis and thrombosis.

Research Aims:

- I. To design gene-eluting (ADAMTS13, VEGFA, & NOS3) baculoviruses and evaluate their safety, stability, and efficacy *in vitro* for gene therapy applications.
- II. To create a baculovirus delivery platform to optimize the therapeutic timeframe, efficacy, and safety.
- III. To develop a wound dressing to treat the chronic wounds commonly associated with PAD.
- IV. To optimize the baculovirus doses, gene expression, polymer selection, mechanical properties, and stent coating, and use this information to fabricate optimized stents for PAD and CAD.

Outline of original research

The present research proposal aims to extend our previous baculovirus-delivering stent studies and introduces a new stent combining drug and gene therapy technologies. We propose to coat the Eucatech® chromium cobalt stent with therapeutic baculovirus-entrapping hydrogel to promote endothelial recovery and reduce immune cell infiltration. We hypothesize that the gene-

and drug-eluting stent will offer a new therapeutic approach to the stent technology (Figure 4). The recombinant baculovirus can be used for targeted delivery of three therapeutic transgenes to the damaged vascular wall, concomitant with the slow release of Everolimus drugs from the exposed stent struts to attenuate acute inflammatory conditions.

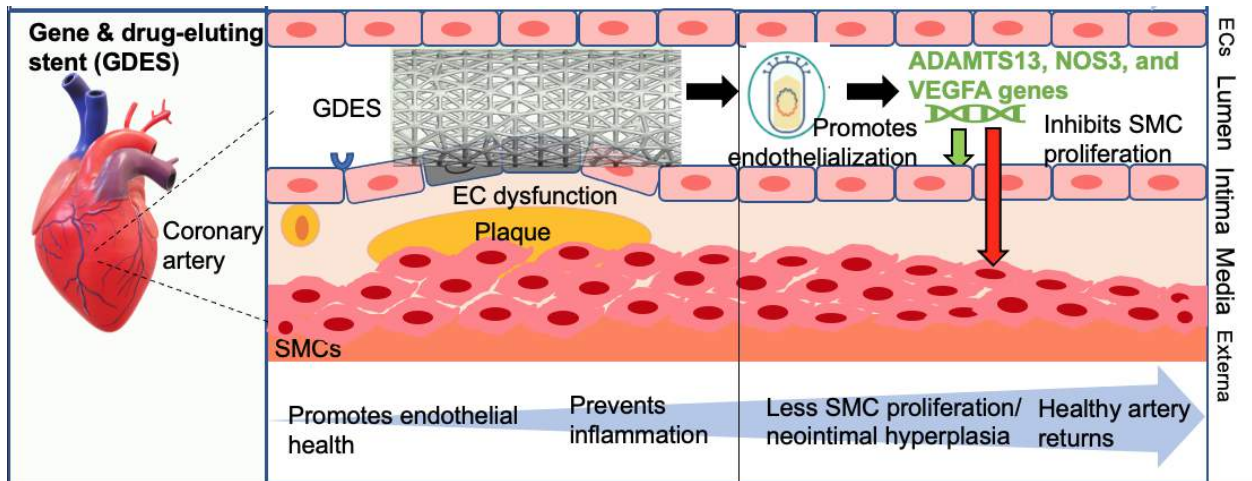


Figure 4. Novel stent design strategy and therapeutic mode

Contribution to original knowledge

Toward my Ph.D. thesis progress, I have contributed to several research articles, book chapters, poster presentations, and conference abstracts. I have also received several grants and awards that supported my research. These accomplishments are listed below.

Original research articles:

1. **Schaly, S.,** Islam, P., Boyajian, J. Thareja, R., L., Abosalha, A., Arora, K., Shum-Tim, D., & Prakash, S. (2023). *In vitro* human safety assessment of RFP and VEGF baculovirus delivery. *Molecular Biotechnology* (to be submitted).
2. **Schaly, S.,** Islam, P., Abosalha, A., Boyajian, J. L., Shum-Tim, D., & Prakash, S. (2022). Alginate-Chitosan Hydrogel Formulations Sustain Baculovirus Delivery and VEGFA Expression Which Promotes Angiogenesis for Wound Dressing Applications. *Pharmaceuticals (Basel, Switzerland)*, 15(11), 1382. <https://doi.org/10.3390/ph15111382>.
3. **Schaly, S.,** Islam, P., Boyajian, J. Thareja, R., L., Abosalha, A., Arora, K., Shum-Tim, D., & Prakash, S. (2023). Controlled and customizable baculovirus NOS3 gene delivery using PVA-based hydrogel systems. *PLoS One*. 2023 Sep 21;18(9):e0290902. doi: 10.1371/journal.pone.0290902. PMID: 37733661; PMCID: PMC10513238.
4. **Schaly, S.,** Islam, P., Boyajian, J. Thareja, R., L., Abosalha, A., Arora, K., Shum-Tim, D., & Prakash, S. (2023). Evaluating a tri-gene-eluting dissolvable stent for peripheral artery disease using baculoviruses. *Science Advances* (To be submitted).
5. **Schaly, S.,** Islam, P., Boyajian, J. Thareja, R., L., Abosalha, A., Arora, K., Shum-Tim, D., & Prakash, S. (2023). A gene- and drug-eluting (GDES) stent coating to promote re-

endothelialization and prevent restenosis due to atherosclerosis. *Science Advances* (To be submitted).

6. **Schaly, S.**, Ghebretatios, M., & Prakash, S. (2021). Baculoviruses in Gene Therapy and Personalized Medicine. *Biologics: targets & therapy*, *15*, 115–132. <https://doi.org/10.2147/BTT.S292692> (Review).
7. **Schaly, S.**, Xiping, W., Probandt, J., & Prakash, S. (2021). COVID-19, probiotics, and the microbiome. Springer Nature. (To be submitted).
8. Ghebretatios, M., **Schaly, S.**, & Prakash, S. (2021). Nanoparticles in the Food Industry and Their Impact on Human Gut Microbiome and Diseases. *International journal of molecular sciences*, *22*(4), 1942. <https://doi.org/10.3390/ijms22041942> (Review).
9. Boyajian, J. L., Ghebretatios, M., **Schaly, S.**, Islam, P., & Prakash, S. (2021). Microbiome and Human Aging: Probiotic and Prebiotic Potentials in Longevity, Skin Health and Cellular Senescence. *Nutrients*, *13*(12), 4550. <https://doi.org/10.3390/nu13124550> (Review).
10. Ahmad W, Boyajian JL, Abosalha A, Nasir A, Ashfaq I, Islam P, **Schaly S**, Thareja R, Hayat A, Rehman Mu, Anwar MA, Prakash S. High-Molecular-Weight Dextran-Type Exopolysaccharide Produced by the Novel *Apilactobacillus waqarii* Improves Metabolic Syndrome: In Vitro and In Vivo Analyses. *International Journal of Molecular Sciences*. 2022; *23*(20):12692. <https://doi.org/10.3390/ijms232012692>
11. Abosalha, A. K., Ahmad, W., Boyajian, J., Islam, P., Ghebretatios, M., **Schaly, S.**, Thareja, R., Arora, K., & Prakash, S. (2023). A comprehensive update of siRNA delivery design strategies for targeted and effective gene silencing in gene therapy and other applications. *Expert opinion on drug discovery*, *18*(2), 149–161. <https://doi.org/10.1080/17460441.2022.2155630> (Review).

12. Abosalha, A. K., Boyajian, J., Ahmad, W., Islam, P., Ghebretatios, M., **Schaly, S.**, Thareja, R., Arora, K., & Prakash, S. (2022). Clinical pharmacology of siRNA therapeutics: current status and future prospects. *Expert review of clinical pharmacology*, 15(11), 1327–1341. <https://doi.org/10.1080/17512433.2022.2136166> (Review).
13. Islam, P., **Schaly, S.**, Abosalha, A. K., Boyajian, J., Thareja, R., Ahmad, W., Shum-Tim, D., & Prakash, S. (2023). Stent Bioengineering: Metamorphosis of Cardiac Stents and Nanotechnology: 14. *Nature Reviews Bioengineering*. (Submitted: NATREVBIOENG-23-0115V1).

Book chapters:

1. **Schaly, S.**, Prakash, S. (2023). Combating the Sustained Inflammation Involved in Aging and Neurodegenerative Diseases with Probiotics. In: Marotta, F. (eds) *Gut Microbiota in Aging and Chronic Diseases. Healthy Ageing and Longevity*, vol 17. Springer, Cham. https://doi.org/10.1007/978-3-031-14023-5_10
2. **Schaly, S.**, Xiping, W., Probandt, J., & Prakash, S. (2022). The Better Forever Diet on mental health. *The Better Forever Diet*: 108-125. Huaxia Publishing House.
3. **Schaly, S.**, Xiping, W., Probandt, J., & Prakash, S. (2022). The Better Forever Diet on the immune system and chronic disease. *The Better Forever Diet*. (2): 70-107. Huaxia Publishing House.
4. Xiping, W., Probandt, J., **Schaly, S.**, & Prakash, S. (2022). The Better Forever Diet on anti-aging and wellness. *The Better Forever Diet*: 126-160. Huaxia Publishing House.

Oral and poster presentations:

1. **Schaly, S., & Prakash, S.** (2021). Baculovirus gene delivery for cardiovascular disease. Biological & Biomedical Engineering Student Society Symposium poster presentation, Montreal, Canada.
2. **Schaly, S., & Prakash, S.** (2021). Baculovirus microparticle gene delivery. Seminars in Biomedical Engineering at McGill University, Montreal, Canada.
3. **Schaly, S., & Lomax, LB.** Sleep architecture can predict ICU patient outcomes following Status Epilepticus. (2020). 499 Final Poster Presentation (Asynchronous due to COVID-19), Kingston, Canada.

Abstracts:

1. **Schaly, S., & Prakash, S.** (2023). A gene- and drug-eluting peripheral stent using a baculovirus-eluting PVA hydrogel coating. American Heart Association Scientific Sessions 2023.
2. **Schaly, S. & Prakash, S.** (2023). Gene-eluting alginate-chitosan hydrogels for peripheral artery disease chronic wound treatment. Fellow Summit. International Association of Advanced Materials. Orlando, Florida.
3. Boyajian, J., Westfall, S., **Schaly, S.,** Arora, K., & Prakash S. (2022). Microbiome potential and limitations in metabolic syndrome: *Lactobacillus fermentum* NCIMB 5221 as metabolic syndrome therapeutics. The Eurobiotech Journal. The European Biotechnology Conference.
4. **Schaly, S.,** Islam, P., Boyajian, J., Ghebretatios, M., & Prakash, S. (2021). Baculovirus gene delivery for coronary artery disease. Journal of the American Heart Association. American Heart Association.

5. Boyajian, J., Westfall, S., **Schaly, S.**, Arora, K., & Prakash, S. (2022). Microbiome potential and limitations in metabolic syndrome: *Lactobacillus fermentum* NCIMB 5221 as metabolic syndrome therapeutics. The European Biotechnology Conference
6. Boyajian, J., Ghebretatios, M., **Schaly, S.**, Islam, P., & Prakash, S. (2021). The novel use of a pro-longevity probiotic formulation for skin aging. The European Biotechnology Conference
7. Liu, R., Winston, G., **Schaly, S.**, Shukla, G., & Lomax, LB. (2021). Prognostic impact of absent sleep architecture on mortality in patients admitted to the intensive care unit in status epilepticus. American Epilepsy Society Annual Meeting.

Awards and research grants:

1. Canadian Graduate Scholarship Doctoral from NSERC (2022-2024): \$105,000
2. Fonds de recherche du Québec – Nature et technologies Doctoral (2021-2025): \$84,000
3. Canadian Graduate Scholarship – Master’s from NSERC (2021-2022): \$17,500
4. Biomedical Engineering Excellence Award at McGill University (2020): \$5,000
5. Canadian Institute of Health Research Stipend (2020-2021): \$21,000

Papers included in this thesis:

Out of these contributions, I have selected five articles to present within this thesis:

1. **Schaly, S.**, Islam, P., Boyajian, J. Thareja, R., L., Abosalha, A., Arora, K., Shum-Tim, D., & Prakash, S. (2023). *In vitro* human safety assessment of RFP and VEGF baculovirus delivery. Molecular Biotechnology (To be submitted).
2. **Schaly, S.**, Islam, P., Abosalha, A., Boyajian, J. L., Shum-Tim, D., & Prakash, S. (2022). Alginate-Chitosan Hydrogel Formulations Sustain Baculovirus Delivery and VEGFA

Expression Which Promotes Angiogenesis for Wound Dressing Applications. *Pharmaceuticals (Basel, Switzerland)*, 15(11), 1382. <https://doi.org/10.3390/ph15111382>.

3. **Schaly, S.,** Islam, P., Boyajian, J. Thareja, R., L., Abosalha, A., Arora, K., Shum-Tim, D., & Prakash, S. (2023). Controlled and customizable baculovirus NOS3 gene delivery using PVA-based hydrogel systems. *PLoS One*. 2023 Sep 21;18(9):e0290902. doi: 10.1371/journal.pone.0290902. PMID: 37733661; PMCID: PMC10513238.
4. **Schaly, S.,** Islam, P., Boyajian, J. Thareja, R., L., Abosalha, A., Arora, K., Shum-Tim, D., & Prakash, S. (2023). Evaluating a tri-gene-eluting biodegradable stent for peripheral artery disease using baculoviruses. *Science Advances* (to be submitted).
5. **Schaly, S.,** Islam, P., Boyajian, J. Thareja, R., L., Abosalha, A., Arora, K., Shum-Tim, D., & Prakash, S. (2023). A gene- and drug-eluting (GDES) stent coating to promote re-endothelialization and prevent restenosis due to atherosclerosis. *Science Advances* (to be submitted).

CHAPTER 2: Background and literature review

Peripheral (PAD) and coronary artery disease (CAD) current treatments

One of the main treatments for coronary and peripheral artery disease includes implanting a stent. A stent is used to force open the artery and has successfully saved millions of lives [25]. To insert a stent, a catheter is used to guide it through the arterial network and toward the blocked artery. Once at the occlusion site, the stent is expanded with a balloon or is self-expandable, allowing blood to pass through again. However, this further damages the endothelial lining of the artery and can lead to blood vessel narrowing and blood clot [35]. Blood vessel narrowing (restenosis) is defined as a >50 % narrowing of a blood vessel's diameter and occurs in 5-10 % of cases with current drug-eluting stents [36].

The first bare-metal stents (BMS)

Stenting and angioplasty are commonly employed for treating cardiovascular diseases. The bare-metal stents (BMS), typically composed of 316L stainless steel or nitinol, can effectively hold open the artery to allow blood passage. However, this BMS design has the highest occurrence of thrombosis and restenosis, 18 % and 2 %, respectively [59]. Further complications arise at the stent site due to incomplete endothelial regrowth and vascular smooth muscle cell (SMC) proliferation. This causes obstruction of the dilated artery, termed in-stent restenosis. To improve this stent design, the next generation of stents must prevent SMC proliferation and promote re-endothelialization. Consequently, drug-eluting stents (DES) have evolved to prevent arterial wall thickening and dampen the immune response to prevent inflammation.

First generation of drug-eluting stents (DESs)

Typically, stent implantation induces a chronic vascular response and inflammation leading to SMC proliferation (neointimal hyperplasia). These challenges sparked the design of several novel DES. DES have a durable polymer coated onto the BMS, permitting slow anti-restenotic drug release. These DES vary in their delivery platform, polymer coating, and drug selection.

The first generation of DES includes paclitaxel and sirolimus-eluting stents. Sirolimus-eluting stents, like Cypher® for coronary arteries, are one example of an approved and commonly used DES. Sirolimus is an antibiotic with immunosuppressive abilities. Specifically, sirolimus binds the cytoplasmic FKBP 12 protein inhibiting smooth muscle division in the G1 and G2 phase [60]. This effectively prevents neointimal hyperplasia. This stainless-steel stent is coated in a durable polymer and releases 80 % of the drug within the first 30 days. Sirolimus-eluting stents demonstrate better kinetics and a wider therapeutic index than BMS and paclitaxel-eluting stents [61]. Paclitaxel-eluting stents have similar characteristics but have a slower drug release rate. Paclitaxel also has a different mechanism of action by binding beta-tubulin within microtubules during mitosis. The microtubule binding also inhibits smooth muscle cell division preventing neointimal formation. A randomized control trial involving 26,616 people determined the efficacy of the first-generation of DES compared to BMS [62]. They reported that the DESs reduced the risk of stent thrombosis, revascularization, death, and myocardial infarction. However, one year after placement, the reduced risk associated with DES was no different than BMS. Moreover, when compared to the first generation of DES, only slight changes in efficacy were found. Specifically, the first-generation sirolimus-eluting stent and the second-generation Everolimus and Zotarolimus-eluting stents showed similar efficacy at preventing revascularization [61]. The

common permanent polymer coatings used in this generation include ethylene-vinyl acetate (PEVA), poly(butyl methacrylate) (PBMA), and styrene isoprene butadiene (SIBBS).

Second generation of drug-eluting stents (DES)

The second generation of DES further improved upon restenosis prevention through drugs from the 'Limus' family, novel permanent polymer coatings, and improved stent design. Common polymer coatings include a combination of PBMA, polyvinylidene fluoride (PVDF-HF), poly(hexyl methacrylate) (PHMA), polyvinylpyrrolidone (PVP), and polyvinyl alcohol (PVA), selected for their strength and drug retention abilities. Classic polymer coatings can be conformal or abluminal with abluminal appearing to have a favourable impact on re-endothelialization. This means they can inhibit SMC proliferation at all areas of contact or only at the surface level. The 'Limus' drugs (Everolimus, Sirolimus, etc.) inhibit mTOR, a major cell growth regulator [60]. Everolimus-eluting stents have a better bioavailability due to their higher affinity for FKBP12. Moreover, the drug also prevents T cell proliferation mitigating a pronounced immune reaction and inflammation [60]. The 2nd generation of DES typically releases 80 % of the drug within the first 30 days following implantation. Everolimus-eluting stents use a durable polymer coated onto a cobalt-chromium or platinum-chromium metal stent. This type of metal has better biocompatibility and is thinner, which has been shown to reduce the risk of thrombosis. The cobalt-chromium metal is also used in Zotarolimus-eluting stents (Endeavor) with 80 % of the drug delivered in the first 10 days. Some Limus-eluting stents include Sirolimus, Zotarolimus, Biolimus A9, and Everolimus. These DES have a similar mechanism of action to Sirolimus by binding FKBP12 protein. Comparatively, Tacrolimus and Pimecrolimus complex with FKBP12 to block the activation of T cell's Nuclear Factor, a major transcription factor that starts an inflammatory

response. This prevents cell cycle activation and proliferation. Tacrolimus-eluting stents have also shown limited stent thrombosis and similar rates of major adverse clinical events [63].

The DES can prevent smooth muscle proliferation and blood vessel re-narrowing through mTOR inhibition. However, this also prevents endothelial cell proliferation and regrowth. This approach reduced the risk of thrombosis and myocardial infarction, but not in-stent restenosis when compared to the first generation of DES [59]. However, the 31,379 people studied showed no difference in mortality between BMS and DES [61]. This indicates that although DES are superior to BMS initially, they have a comparable efficacy after one year. Overall, the 2nd generation of DES mitigates thrombosis, restenosis, and myocardial infarction initially when compared to BMS. However, the rate of complications (blood clots and blood vessel re-narrowing) is still relatively high at 5-10 % and needs to be addressed by future generations of stents [36].

Stents with biodegradable coatings

Permanent polymers, used in the first generation of DES, are associated with delayed healing and triggering inflammation. This increases the risk of late and very late thrombosis [64]. An alternative to current DES is the development of biodegradable stent coatings to prevent polymer-induced inflammation. Biodegradable polymers are mainly composed of lactic or glycolic acid which can be resorbed in the body through hydrolysis. Common polymer examples include polylactic (PLLA, PDLLA), polyglycolic (PGA) and polylactic-co-glycolic (PLGA) copolymers. This led to the production of new stents (such as Osrsiro, Ultimaster, Synergy, BioMatrix Nobori, Combo, and BioMartix Flex®) [26]. These polymer coatings degrade within three to nine months after deployment. This new generation of stents is considered superior to BMS and the 1st generation of DES due to its ability to prevent thrombosis. However, a meta-

analysis of 12 randomized control trials showed no short-term difference in safety or efficacy [65]. This study also reported no difference in myocardial infarction, stent thrombosis, and target vessel revascularization. This indicates biodegradable polymer coatings need further testing and optimization.

Polymer free stents

An alternative option to DES, is omitting the polymer altogether to prevent polymer-induced inflammation. However, this increases the drug elution rate and may decrease the stent efficacy. To counteract this, researchers have created different stent styles. This includes a smooth surface, microporous, nanoporous, and drug-filled stents. In the smooth surface model, the drug release is determined by the drug solubility. For the other non-polymer stent models, the rough surface creates drug-filled holes to improve drug-loading capacity. Some stent design examples include BioFreedom® and Drug-Filled® stents [26]. These polymer coatings provide a transient scaffolding for the blood vessel preventing thrombosis. To determine the safety and efficacy of polymer-free DES several studies have been conducted. A recent meta-analysis of 11 randomized control trials, including 8,616 people, showed no difference in polymer-free DES compared to DES [66]. Specifically, there was no difference in myocardial infarction, target-lesion revascularization, stent thrombosis, cardiac death, late lumen loss, or stenosis diameter. However, the polymer-free DES was associated with a lower incidence of major adverse cardiovascular events. Although this is beneficial, the advances in stent design have yet to generate the golden standard stent.

Biodegradable stents

In support of leaving behind fully formed vasculature and preventing long-term stent-related issues, fully biodegradable or dissolvable stents have been developed. This would have several advantages. 1. A reduction of thrombosis as no foreign material would remain in the vessel [28]. 2. Eliminating a metal stent allows normal vasomotion and luminal movement. 3. The possibility of discontinuing dual antiplatelet therapy. 4. Customizable resorption that emits the drug encapsulated within.

Currently, magnesium alloys, zinc calcium alloys, iron alloys, poly(lactic acid) (PLA, PDLA & PLLA), and tyrosine polycarbonate are being investigated [29], [30]. These polymers typically degrade after three to nine months leaving behind the rebuilt vasculature. Particularly, metallic biodegradable stents have shown promise in providing similar mechanical properties to the original 316L stainless steel stent but are fully biodegradable. In animal models, these stents have shown similar efficacy when compared to current DES and better anti-restenotic properties.

A disadvantage to bioresorbable stents is the poor bioavailability and increased strut thickness to maintain mechanical stability which can damage the blood vessel. Moreover, scaffold collapse has been reported requiring re-intervention [67]. A recent meta-analysis of 16 randomized control trials, including 19,886 people, observed no significant differences between biodegradable and second-generation DES [68]. The difficulty with fully biodegradable stents is ensuring uniform degradation (to prevent pieces from coming off, leading to thrombosis) while maintaining its mechanical stability. Overall, further testing and optimization are needed before these stents become commercially available.

Tethering bioactive molecules to stents

Alternative stenting approaches have also been used to promote re-endothelialization while inhibiting smooth muscle cell proliferation. Some approaches include the addition of antibodies for site-specific delivery, co-eluting stents, and gene-eluting stents. For example, Nakazawa et al., added CD34 antibodies to the surface of sirolimus-eluting stents to attract endothelial cells and promote healing [69]. This preclinical study showed significantly enhanced re-endothelialization using the CD34 antibody, but long-term efficacy has yet to be studied. Advances in co-eluting stents, as well as gene-delivering stents, have also been promising. Titanium nitric oxide has been coated onto stents to deliver nitric oxide particles [70]. Nitric oxide particles dilate the blood vessel and can prevent restenosis and thrombosis. Preclinical studies with titanium nitric oxide coatings demonstrated enhanced safety and comparable efficacy compared to DES. Yang et al. also recently developed a paclitaxel and VEGF gene eluting stent resulting in significantly suppressed restenosis compared to the DES control [49]. Similarly, Paul et al. developed a recombinant baculovirus complexed with Tat/DNA nanoparticles which enhanced re-endothelialization, attenuated stenosis, and prevented neointima formation [71]. Based on these studies, the ideal future stent should possess high flexibility, thin struts, 60-90 day drug elution, stimulate re-endothelialization, prevent thrombosis, and minimize the requirement for double antiplatelet therapy [26].

Gene-eluting stents (GES)

Gene-eluting stents are an alternative treatment approach. However, gene delivery is challenging due to the low gene stability. Plasmid DNA-eluting stents have been shown to express green fluorescent protein (GFP) but had an efficiency rate of one to ten percent [41]. Several gene-eluting stents have been investigated in pre-clinical settings, including GFP, β -galactosidase, Anti-Monocyte Chemoattractant Protein-1, miR-22, nitric oxide, angiopoietin-1, and VEGF delivery.

β -galactosidase and GFP expression were used to prove the concept of localized arterial delivery [41],[42]. Elution of vascular endothelial growth factor (VEGF) and angiopoietin-1 (Ang-1) from stents was reported to prevent restenosis by promoting endothelial health and re-endothelialization [72], [73]. Endothelial nitric oxide synthase (eNOS) has also been studied and effectively suppressed ISR and improved re-endothelialization [74]. However, limitations included low efficiency, incomplete endothelialization, limited thrombosis prevention, and neointimal hyperplasia.

Baculoviruses as gene delivery vectors

Baculoviruses, naturally known to infect *Lepidoptera*, have been exploited for their recombinant protein expression since 1983, enabling the development of a diverse range of therapeutics [75]. Baculoviruses (BVs) naturally mass produce polyhedral capsules, under the control of the polyhedrin promoter, accounting for 25% of the cell protein [76], [77]. Advantageously, the polyhedrin gene can be replaced with the desired gene of interest enabling over-expression of the gene of interest. This large and natural amplification feature makes baculoviruses an attractive option for gene delivery in stent applications expressing significantly more genes than plasmid delivery alone. Baculovirus gene delivery systems enable site-specific delivery, mitigating adverse effects, and improving the therapeutics [53]. This easily modifiable gene therapy system may be the cost-effective and efficient backbone needed to advance transient gene therapy. BVs typically have a transgene expression window of seven to fourteen days which can be optimized or extended based on the disease [78]. The ease of genetically manipulating baculoviruses for gene therapy applications is shown below in Figure 5.

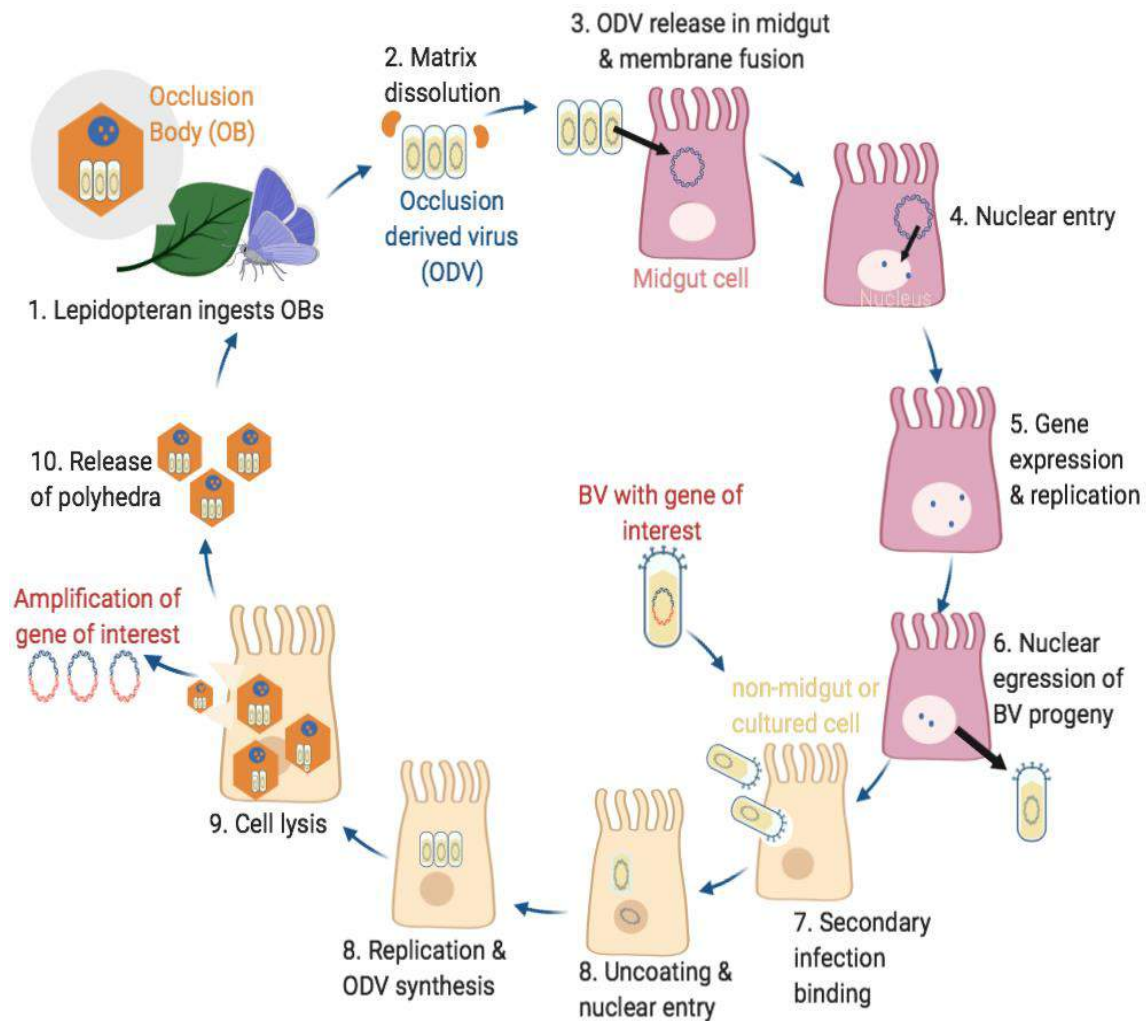


Figure 5. Lifecycle of baculoviruses and potential use for gene therapy (adapted from Schaly et al., 2021)

Baculoviruses naturally mass produce polyhedral capsules, under the control of the polyhedrin promoter, accounting for 25 % of the cell protein [76], [77]. Advantageously, the polyhedrin gene can be replaced with the desired gene of interest enabling over-expression of the gene of interest. This large and natural amplification feature makes baculoviruses an attractive option for gene delivery in stent application expressing significantly more gene than plasmid delivery alone. The insect cell lines can also be genetically engineered to produce properly glycosylated proteins using baculoviruses [79], [80]. Human glycosylation patterns are essential

for therapeutic uses as it enables proper effector functions such as antibody-dependent cellular cytotoxicity (ADCC). Moreover, N-glycans' presence significantly enhances the antibody binding efficiency to Fc receptors [79]. Baculoviruses can also be grown in serum free media, in bioreactors, without carbon dioxide, at room temperature, making them a scalable and cost-effective method for protein production [81]. Moreover, they have already been used in several human therapeutics including cancer treatment, vaccines, and regenerative medicine indicating their large potential [82]–[84]. This easily modifiable gene delivery system may be the cost-effective, safe, and therapeutic solution to promoting endothelialization and preventing SMC proliferation following atherosclerotic stenting.

Baculovirus vectors have already been implemented in several successful studies, including cancer treatment, vaccines, and regenerative medicine [82]–[84]. The large cloning capacity of baculoviruses enables transgene of expression of large multi-complex proteins both *in vivo* and *ex vivo*. This is particularly useful for use in anticancer therapy, stem cell regeneration and in vaccine development. Specifically, a toxin vector for diphtheria toxin A has been developed to eliminate malignant glioma cells within the brain [85]. Other BVs expressing normal epithelial cell specific-1 and herpes simplex virus-1 thymidine kinase have shown similar promising results in eliminating glioblastoma and gastric cancer cells [86],[87]. Moreover, angiogenesis-dependent tumours have been treated with a hybrid sleep beauty-Baculovirus vector to prolong antiangiogenic fusion protein expression (endostatin and angiostatin) [88]. Lin et al engineered bone marrow-derived mesenchymal cells (BMSCs) to express bone morphogenetic protein 2 and VEGF enabling enhanced femoral bone repair and bone quality [89]. Similarly, for myocardial infarction therapy, baculoviruses can be engineered to expressed Angiopoietin-1 to increase capillary density and reduce infarct sizes in rats [71].

BVs also have a large potential in virus-like particle (VLP) and vaccine production. One of the first vaccines using baculoviruses, called FluBlok®, used the hemagglutinin antigen as a subunit vaccine to elicit a protective immune response [90]. This technique has been extended into other vaccines such as human papillomavirus, prostate cancer, and familial lipoprotein lipase deficiency [82],[91],[92]. The three vaccines expressed HPV-L1 protein, granulocyte-macrophage colony-stimulating factor, and an AAV vector with lipoprotein lipase transgene, respectively. Moreover, administering baculoviruses could eliminate malaria parasites in mice livers and elicit a protective humoral and cellular immune response [93]. Alternatively, the scalability of BV expression systems is beneficial for the mass production of molecules like VLPs. Baculoviruses are predicted to generate 415 million 10 µg/dose vials of anti-flu vaccines in one week compared to the six-month standard using chicken embryos [94]. The high protein production and efficacy support using baculoviruses as a promising vaccine vector and scalable approach to personalized medicine. Baculoviruses have also been used to develop more recent COVID-19 vaccines. Specifically, baculoviruses were used to produce viral S protein and receptor binding domain protein in three subunit vaccine candidates and for VLP production in the fourth vaccine [95].

The display of surface proteins can also direct cell-specific uptake of baculoviruses. Fc receptors, folate, and epidermal growth factor (EGF) have been used to dictate the baculovirus selectivity [96]. Rätty et al. exploited the avidin-biotin interaction to increase transduction efficiency while expressing biotinylated EGF causing the system to target EGF-displaying cells [97]. Polyethylene glycol (PEG)-folate has also been displayed on the baculovirus surface to target the Fc receptors displayed specifically on malignant cells enabling targeted gene delivery [98]. In comparison, BVs displaying human epidermal growth factor-2 (HER2) single-chain variable domain fragments (scFV) while expressing Apoptin bind specifically HER2 positive SK-BR-3

breast cancer cells reducing cancer cell viability [99]. Similarly, a BV expressing BIMs, a potent apoptosis inducer, results in the selective death of Hepatitis C virus-positive cells only [100]. Selectively treating an individual's malfunctioning or impaired cells can mitigate traditional medical treatments' side effects and systemic effects, significantly improving the quality of treatment, care, and life.

Baculoviruses have a large therapeutic potential as vaccine vectors, anticancer therapy, and recombinant protein production. Limitations such as the immune response, complement activation and baculovirus fragility may be quickly overcome through further genetic engineering. Despite these limitations, the biosafety, relative ease of production, low cytotoxicity, and non-replicative nature in mammalian cells, associated with baculoviruses, continue to make it an advantageous method for gene therapy and personalized medicine. Moreover, baculoviruses have an immense potential to be optimized for each disease and individual through further gene and dose modifications. The simple extraction and manipulation of insect cells provide a cost-effective method for gene therapy and personalized medicine.

Baculovirus limitations and advantages

A few limitations are associated with baculovirus in gene therapy, hindering its wide-scale use and production. Specifically, BV expression systems can induce an immune response producing inflammatory cytokines and chemokines and activating the complement pathway. This can lead to an unnecessary immune response and viral genome degradation. Upon serum contact, baculoviruses activate RIG-I/IPS-1 or cyclic GMP-AMP synthase/stimulator of interferon genes (cGAS/STING) pathway, which can suppress transgene expression [101]. Moreover, baculoviruses exhibit transient gene expression, typically lasting seven to fourteen days in most

cell lines, including CHO, HeLa, and BHK [78]. However, several gene insertions or modifications have been able to extend gene expression and prevent immune complement recognition [88], [102], [103]. Transgene expression can also be prolonged by shielding the baculovirus from the immune system using a polymer coating. This prevents immune activation and prolongs gene expression and its associated therapeutic effect. Alternatively, the transient gene expression mitigates safety concerns providing potential in vaccine vector or adjuvant field. Another limitation of baculovirus vector systems is the virus's fragility. Previous researchers have reported a half-life of only 173 hours at 27 °C and around eight hours at 37 °C [104]. Moreover, defective interfering (DI) particles accumulate during serial cell culture passages. DI particle accumulation can be reduced by using a low MOI or removing the non-homologous origin from the SeMNPV baculovirus genome, preventing DI formation for 20 cell passages [105].

Baculoviruses provide a relatively safe, scalable, and cost-effective vector for gene therapy [81]. Baculoviruses' biosafety, large cloning capacity, low toxicity, and non-replicative nature make it an attractive vector for stent coatings. One of the main advantages is the non-toxic nature of baculoviruses within mammalian cells and the inability to hinder their growth [81], [106], [107]. Baculoviruses provide transient gene expression that is higher than plasmid delivery and safer than alternative viral delivery systems (Table 1). Specifically, baculoviruses provide a safer alternative to lentiviral, retroviral, and adenoviral vectors, all of which are human pathogens and are capable of producing replication-competent viruses (RCV) [108]. Moreover, baculoviruses' inability to integrate into the host DNA or chromosomes further supports its biosafety and use in gene delivery. Baculoviruses also provide significantly higher expression compared to plasmid or other viral gene delivery due to the lack of pre-existing immunity and protected delivery (with the viral capsid). Unlike adenoviruses, baculoviruses do not elicit a potentially fatal humoral and cellular immune

response [109]. Despite the high specificity of baculovirus, they can be engineered to transduce both dividing and non-dividing cell lines or only specific cell types [110]. This specificity is beneficial in diseases where only specific cells are to be targeted, such as the cells directly in contact with the stent. Another advantage over other viral vectors is baculoviruses' large cloning capacity, enabling insertions up to 38 kb compared to other viral vectors, which only have a capacity of under 7.5 kb [51]. Moreover, large-scale insect culture processes are already well-established, can be stored for 1+ years at 4 °C, and can easily be scaled up for mass production [52]. This makes it a feasible approach with a long shelf life. Baculoviruses are a biosafe and low-cost vector capable of site-specific and enhanced gene delivery compared to alternative methods [50]. Moreover, their high but transient gene delivery is ideal for stent applications, whereby gene delivery is only required for the initial three weeks until healing is completed.

Table 1. Comparison of viral vectors for gene therapy (adapted from Schaly et al. 2021)

Feature	Baculovirus	Adeno-associated virus	Lentivirus	Retrovirus
Size	80-180 kb	8.5 kb	8 kb	7-11 kb
DNA or RNA	dsDNA	ssDNA	ssRNA	ssRNA
Cloning capacity	38 kb	5 kb	9 kb	8 kb
Max viral titer	2x10 ⁸	1x10 ¹¹	1x10 ⁹	1x10 ⁹
Tropism	Dividing and non-dividing cells	Dividing and non-dividing cells	Dividing and non-dividing cells	Dividing cells
Safety	Non-toxic	Inflammatory response & toxicity	Insertional mutagenesis	Insertional mutagenesis
Ease of scale-up	High	Low	Low	Low
Immunogenicity	Low	Low	Low	Low
Integration	Non-integrating	Non-integrating	Integrating	Integrating
Expression	Transient	Stable: site-specific integration	Transient or stable	Stable

Baculoviruses in localized stent delivery

Given the literature above, baculoviruses may be the solution to promoting re-endothelialization and inhibiting smooth muscle cell proliferation within stented arteries using three different genes (ADAMTS13, NOS3, and VEGFA). VEGFA and NOS3 both help regulate the cells lining the artery and promote their healing which can reduce inflammation and blood vessel re-narrowing [111], [112]. VEGF release from bioactive stents has been shown to significantly increase reendothelialization and prevent in-stent restenosis *in vivo* [113]. Comparatively, NOS3 and ADAMTS13 genes were selected for their ability to regulate blood coagulation, prevent platelet adhesion which could lead to thrombosis, and promote endothelial health and migration for re-endothelialization [112], [114], [115]. NOS3 plays a key role in vascular homeostasis, vascular dilation, and protects the intima from platelet aggregation and leukocyte adhesion [116]. It also prevents SMC proliferation and endothelial dysfunction. This is crucial in the initial two weeks after stent implantation to regulate vascular function and promote an anti-inflammatory environment. Similarly, ADAMTS13 cleaves vWF which prevents platelet aggregation and blood clotting (supported by Everolimus), which is required for the first month after stent implantation. High vWF and low ADAMTS13 levels are associated with major cardiovascular events, thrombosis, and PAD progression [114], [115]. The three genes selected (ADAMTS13, NOS3, and VEGFA) may exert an additive effect on each other, resulting in superior arterial healing (**Error! Reference source not found.**). This additive effect will be investigated. Moreover, proper healing and endothelial function would prevent downstream complications, including thrombosis, ISR, and low patency.

The baculovirus can also be encapsulated to prolong transgene expression past the typical seven-day window. Polymeric encapsulation can also increase stability, solubility, prolong gene expression, and promote site specificity, which allows for a lower dosage and less toxicity [117],

[118]. Finally, the optimized baculovirus encapsulated in a hydrogel can be coated onto a stent to provide a localized therapeutic effect. Different layers, polymers, and methods will be employed and optimized for safety and efficacy.

Baculovirus encapsulation

Cell and bacterial encapsulation have been extensively investigated, showing promising results in localized treatment with sustained efficacy [124]. Bioencapsulation, also termed artificial cells, are one method to preserve the baculovirus therapeutic window and protect the genes from the immune system. Baculovirus encapsulation prevents immune inactivation, effectively shielding the virus from the immune system. Artificial cells are capable of delivering enzymes, drugs, genes, microbes, hormones, vaccines, and hemoglobin [119]. They have applications in medical devices, drug delivery, blood substitutes, gene therapy, regenerative medicine, agriculture, nanomedicine, and more. The artificial cell composition can include natural, biodegradable, or permanent polymers commonly including lipids, PEG, PLGA, and PLA. Specifically, natural polymers such as alginate and chitosan are common for their biocompatibility and biodegradability, safety, and feasibility [16–19]. Similarly, PVA and polylactic substitutes are commonly selected for their inherent biosafety and hemocompatibility [167][168]. Another benefit of PVA is the tunability of its mechanical properties. Specifically, the tensile strength, toughness, elongation, and elastic modulus can vary significantly depending on the ions used during the aggregation [169].

Significance in designing and fabricating GESSs

This dissolvable baculovirus delivery system will demonstrate the potential use of baculoviruses in gene therapy and stenting. The cost-efficient system can mitigate common complications, be more accessible to all people, and save many more lives. Given the information provided above, the gold standard would be the development of a stent enabling site-specific delivery, highly efficient gene delivery, high retention, functionality, and viability at the target site. Given the literature, baculoviruses may be the golden ticket to this medical advancement. Coating stents with baculoviruses that express healing genes can promote arterial healing and potentially prevent the significant morbidity associated with atherosclerosis. This also allows its use on other stent types and arteries. The coating can be integrated into upcoming fully biodegradable stents to mitigate further complications and improve the quality of life of those impacted by PAD and CAD.

CHAPTER 3: Papers included in this thesis

This is a manuscript-based thesis. The thesis is comprised of five original research articles.

Original research articles included in this thesis:

1. **Schaly, S.,** Islam, P., Boyajian, J. Thareja, R., L., Abosalha, A., Arora, K., Shum-Tim, D., & Prakash, S. (2023). *In vitro* human safety assessment of RFP and VEGF baculovirus delivery. *Molecular Biotechnology* (To be submitted).

For this paper, I investigate the safety of direct baculovirus gene delivery for human therapeutics. Baculoviruses have been extensively studied for vaccine and recombinant protein production but not for direct human administration. Thus, I investigated the cytotoxicity, hemocompatibility, genotoxicity, and lysosomal activity in human SMCs and HUVECs following baculovirus transduction. Overall, I determined that baculovirus gene delivery to SMCs and HUVECs is efficient and safe.

2. **Schaly, S.,** Islam, P., Abosalha, A., Boyajian, J. L., Shum-Tim, D., & Prakash, S. (2022). Alginate-Chitosan Hydrogel Formulations Sustain Baculovirus Delivery and VEGFA Expression Which Promotes Angiogenesis for Wound Dressing Applications. *Pharmaceuticals (Basel, Switzerland)*, 15(11), 1382. <https://doi.org/10.3390/ph15111382>.

In this paper, I demonstrated the feasibility and efficacy of sustained and controlled baculovirus delivery using alginate-chitosan hydrogels. This is one of the few papers published on controlling virus gene delivery over ten days. Moreover, the hydrogel formulation had significant beneficial properties in chronic wounds, common in PAD. Specifically, I found that the hydrogel formulation improved cell migration, proliferation, and angiogenesis. Moreover, the hydrogels

have an encapsulation efficiency of 99.9 %, no cytotoxicity, antimicrobial properties, good blood compatibility, promote hemostasis, and maintain a moist wound healing environment.

- Schaly, S.,** Islam, P., Boyajian, J. Thareja, R., L., Abosalha, A., Arora, K., Shum-Tim, D., & Prakash, S. (2023). Controlled and customizable baculovirus NOS3 gene delivery using PVA-based hydrogel systems. *PLoS One*. 2023 Sep 21;18(9):e0290902. doi: 10.1371/journal.pone.0290902. PMID: 37733661; PMCID: PMC10513238.

In this paper, I customized and optimized baculovirus gene delivery using polyvinyl alcohol (PVA). I varied the amount of baculovirus and duration of elution using different polymer hydrogels and loading methods. Overall, baculovirus could be eluted for five to 25 days, enabling sustained delivery. Passive absorption of the baculovirus into PVA hydrogels exhibited the highest baculovirus loading (96.4 ± 0.6 %). Moreover, the sustained NOS3 delivery from the baculovirus would benefit both chronic wounds from PAD and as a stent coating. NOS3 promotes nitric oxide and nitrate production and can effectively be delivered using baculoviruses. Nitric oxide regulates cell proliferation, promotes blood vessel vasodilation, and inhibits bacterial growth. This is a novel gene delivery method that has not been reported previously.

- Schaly, S.,** Islam, P., Boyajian, J. Thareja, R., L., Abosalha, A., Arora, K., Shum-Tim, D., & Prakash, S. (2023). Evaluating a tri-gene-eluting dissolvable stent for peripheral artery disease using baculoviruses. *Science Advances* (to be submitted).

In this paper, I investigated a novel dissolvable tri-gene eluting stent for peripheral artery disease. I found that the co-elution of two genes (ADAMTS13 and NOS3) significantly improved wound healing and angiogenesis of HUVECs to allow for proper re-

endothelialization. The two genes also selectively inhibited SMC proliferation and cleaved proteins involved in blood clotting preventing neointimal hyperplasia and thrombosis, respectively. Moreover, the novel stent was optimized, anti-thrombotic, and enabled sustained baculovirus delivery over ten days allowing for the proper therapeutic window. This stent had similar mechanical properties to metal stents, excellent hemocompatibility, noncytotoxic, and sustained baculovirus delivery. This is one of the first papers to investigate a multi-gene eluting stent and this formulation of dissolvable stents for PAD.

5. **Schaly, S.,** Islam, P., Boyajian, J. Thareja, R., L., Abosalha, A., Arora, K., Shum-Tim, D., & Prakash, S. (2023). A gene- and drug-eluting (GDES) stent coating to promote re-endothelialization and prevent restenosis due to atherosclerosis. *Science Advances* (to be submitted).

Coronary artery disease (CAD) occurs in one out of every 20 people over the age of 20. One common cause of CAD is atherosclerosis (plaque build-up). Currently, a bare-metal or drug-eluting stent is used to force open the artery, but current stents have complications including blood clotting and arterial re-narrowing. To mitigate these complications, a novel gene- and drug-eluting (GDES) stent was developed. The novel gene- and drug-eluting stent (GDES) coating shows favourable properties *in vitro*. The dual factor elution assists with re-endothelialization, inhibiting inflammation, and preventing smooth muscle cell proliferation leading to restenosis. The stent coating is also flexible, without cracks or breakage during expansion or degradation, reducing the risk of thrombosis. The PVA stent coating is hemocompatible and fully dissolvable, reducing the risk of polymer-induced inflammation long-term. Overall, the stent system may improve clinical outcomes by mitigating current

complications such as thrombosis, restenosis, polymer-induced inflammation, and endothelial dysfunction.

CHAPTER 4: *In vitro* safety assessment of baculovirus gene delivery

Sabrina Schaly¹, Paromita Islam¹, Jacqueline L. Boyajian¹, Rahul Thareja¹, Ahmed Abosalha^{1,2}, Karan Arora¹, Dr. Dominique Shum-Tim⁴, and Dr. Satya Prakash^{1,*}

¹ Biomedical Technology and Cell Therapy Research Laboratory, Department of Biomedical Engineering, Faculty of Medicine and Health Sciences, McGill University, 3775 University Street, Montreal, Quebec, H3A 2B4, Canada

² Pharmaceutical Technology Department, Faculty of Pharmacy, Tanta University, Tanta 31111, Egypt

³ Division of Cardiac Surgery, Royal Victoria Hospital, McGill University Health Centre, McGill University, Faculty of Medicine and Health Sciences, Montreal, Quebec H3G 2M1, Canada *

* Corresponding author: satya.prakash@mcgill.ca

Contributions of the author: I am the first author and contributed to all experiments and manuscript preparation.

Molecular Biotechnology

(To be submitted)

Abstract

Baculovirus gene delivery has shown promise as an insecticide, vaccine vector, and recombinant protein production for human therapies. However, baculovirus vectors for direct human gene therapy has yet to be fully evaluated. Hence further safety studies in human cells are warranted. Here, we investigate the safety of red fluorescent protein (RFP) and vascular endothelial growth factor (VEGF) baculovirus delivery *in vitro* in endothelial and smooth muscle cells. Our safety assessment investigates genotoxicity, hemocompatibility, cell viability, cell proliferation, and inflammatory response (C-reactive protein and reactive oxygen species production) of baculovirus gene delivery. We test multiplicities of infection (MOI) ranging from ten to 1000, revealing an excellent safety profile with no signs of inflammation, hemolysis, cytotoxicity, thrombosis, and cell proliferation dependent on the gene delivered and cell type.

Keywords: baculovirus, gene delivery, safety assessment, cytotoxicity, genotoxicity, lysosomes, hemocompatibility, VEGF

Introduction

Baculoviruses are efficient mammalian gene delivery vectors after adding a mammalian promoter directly upstream of the gene of interest [81]. Research has indicated an excellent biosafety profile with low immunogenicity. They also have a cloning capacity 30 times larger than other viral vectors enabling complex protein expression [51]. Finally, they are affordable with little cost for scale-up and can be grown at room temperature without a carbon dioxide requirement.

There are several approved baculovirus products already on the market. Upon this discovery, several products have been investigated. Baculoviruses have been used in vaccine production, regenerative medicine, and cancer therapy [125]. There are currently four FDA-accepted human

products (Cervarix®, Provenge®, Glybera®, and Flublok®). There are also five FDA-accepted veterinary products (Porcilis® Pesti, BAYOVAC CSF E2®, Circumvent® PCV, Ingelvac CircoFLEX®, and Porcilis® PCV). Current pre-clinical studies are investigating virus-like particle production in baculoviruses for the Norwalk, Porcine, Bluetongue, Poliovirus, and other vaccine candidates [126].

Common genes delivered by baculoviruses include fluorescent proteins and growth factors [127], [128]. VEGF is a common growth factor present in the body. VEGF is responsible for several steps in angiogenesis, including blood vessel formation, cell migration, and cell proliferation [129], [130]. It also plays a role in several diseases that have yet to be fully elucidated. RFP is another common gene used for easy monitoring and visualization [127], [128].

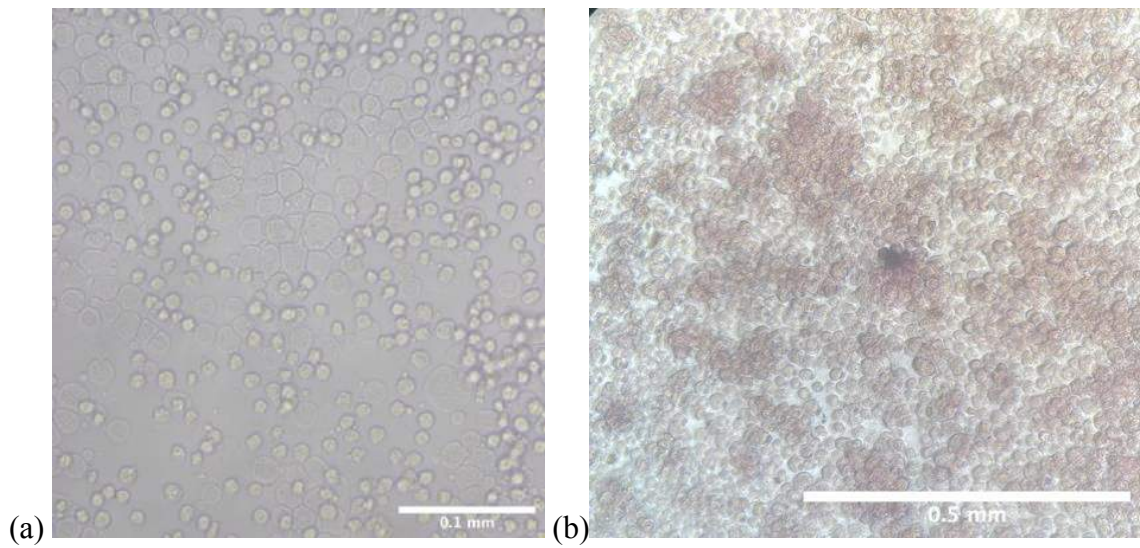
However, the virus's fragility limits baculovirus gene therapy and has not been studied extensively for direct human gene therapy. The majority of papers report mammalian transduction at room temperature and not at typical human physiological conditions (37 °C), which would be required for direct human gene therapy [131], [132]. Consequently, safety studies have been limited, with the few available reporting no adverse effects. Here we investigate the efficiency and safety of baculovirus gene therapy in humans *in vitro* at physiological conditions.

We investigate the genotoxicity, hemocompatibility, cytotoxicity, and inflammatory response (C-reactive protein and reactive oxygen species production) in smooth muscle and endothelial cells. We also investigate lysosomal activity after baculovirus transduction, as this is the main method of cellular viral degradation [133]. This information will provide further insight into the *in vitro* safety of the baculovirus. This information will support future *in vivo* research and the use of baculoviruses as a human gene delivery technique.

Results

Baculovirus gene expression and biosafety

We created a baculovirus that expresses GFP in insect cells and RFP in mammalian cells, termed GFP-baculovirus, to allow for visualization and monitoring of the gene delivery process (Figure 6). At the same time, we created a baculovirus that delivered VEGF, termed VEGF-baculovirus. As the amount of baculovirus added increased, the percentage of fluorescent cells also increased. There is a significant increase in the percent of fluorescent cells with an MOI of 1000 compared to lower MOIs. The percentage of fluorescent cells was also maintained over 72 hours in both cell types.



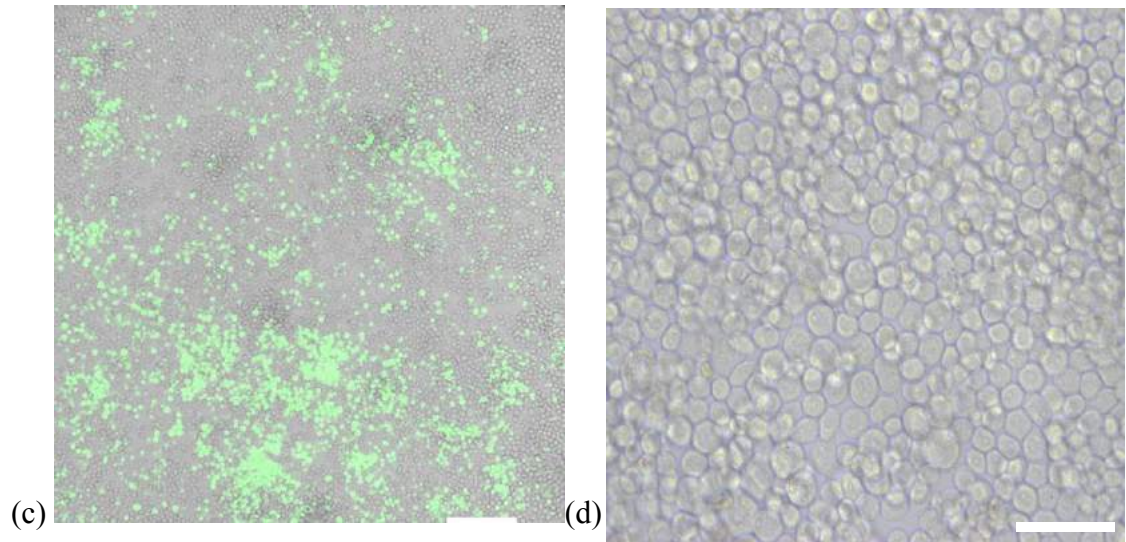
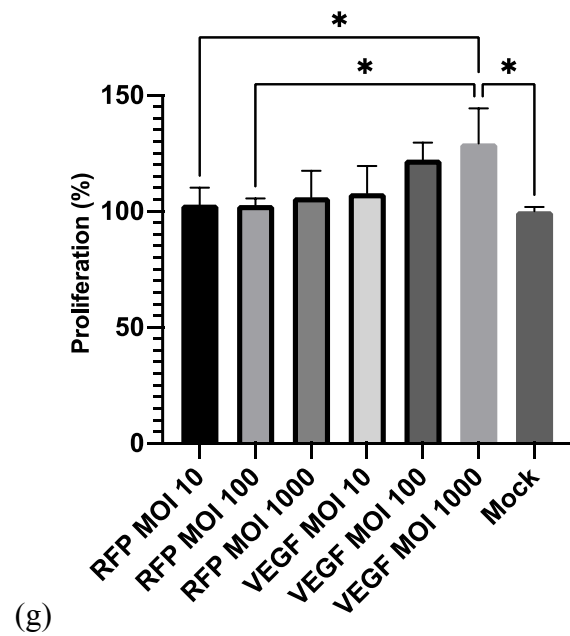
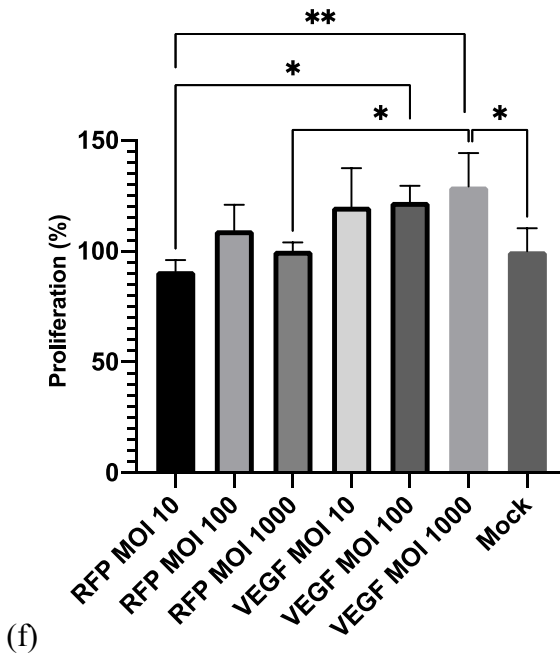
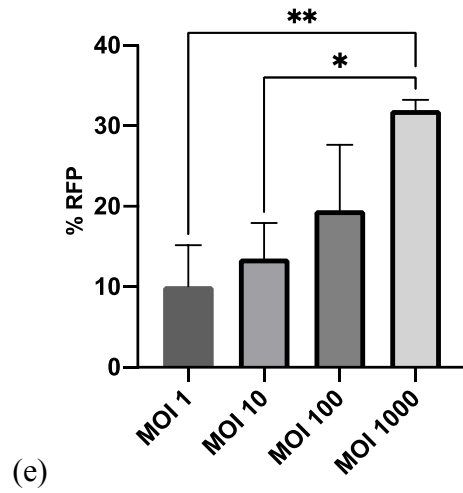
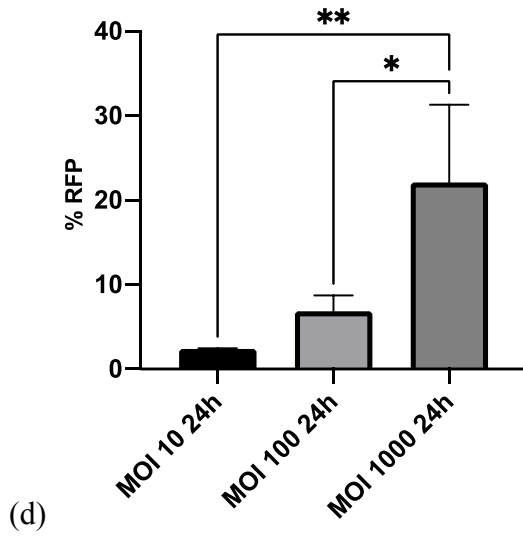
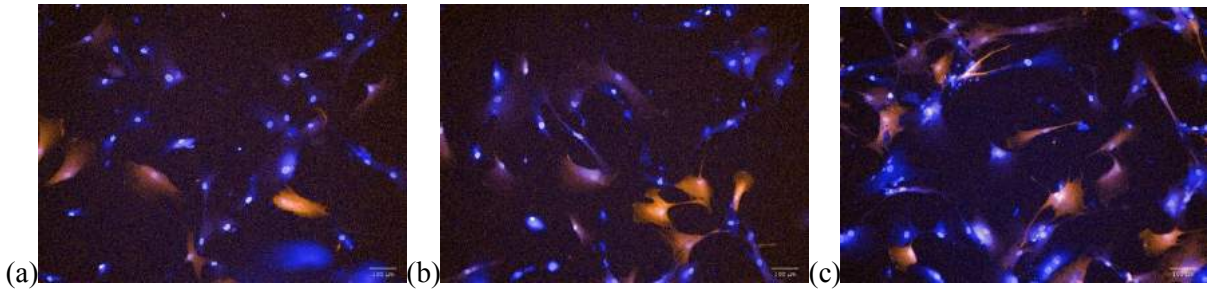


Figure 6. Brightfield images of Sf9 cells infected with baculoviruses

(a) Phase contrast image of Sf9 cells four days after initial transfection. (b) Sf9 cell infected with baculovirus expressing VEGFA titrated using a FastPlax Titration Kit. (c) Brightfield overlaid with a green fluorescent image of Sf9 cells infected with baculovirus expressing EGFP after four days. Scale bar= 0.5 mm. (d) Uninfected Sf9 cells after four days of incubation. Scale bar= 0.1 mm.

Since efficient gene expression was observed with MOIs above ten, we studied the impact on cell proliferation and viability (Figure 7). The GFP-baculovirus did not alter HUVEC or SMC proliferation at any MOI compared to mock transduced cells. There were no changes in cell proliferation after 24 and 48 hours. Comparatively, the VEGF-baculovirus significantly increased cell proliferation at an MOI of 1000, consistent with the gene function. Lower MOIs of the VEGF-baculovirus also increased proliferation but not significantly in both cell types. No reduction in viability was observed after transduction with the GFP-baculovirus or VEGF-baculovirus at lower MOIs. However, at an MOI of 1000, a significant reduction in SMC viability but not HUVEC viability was reported after either gene was delivered.



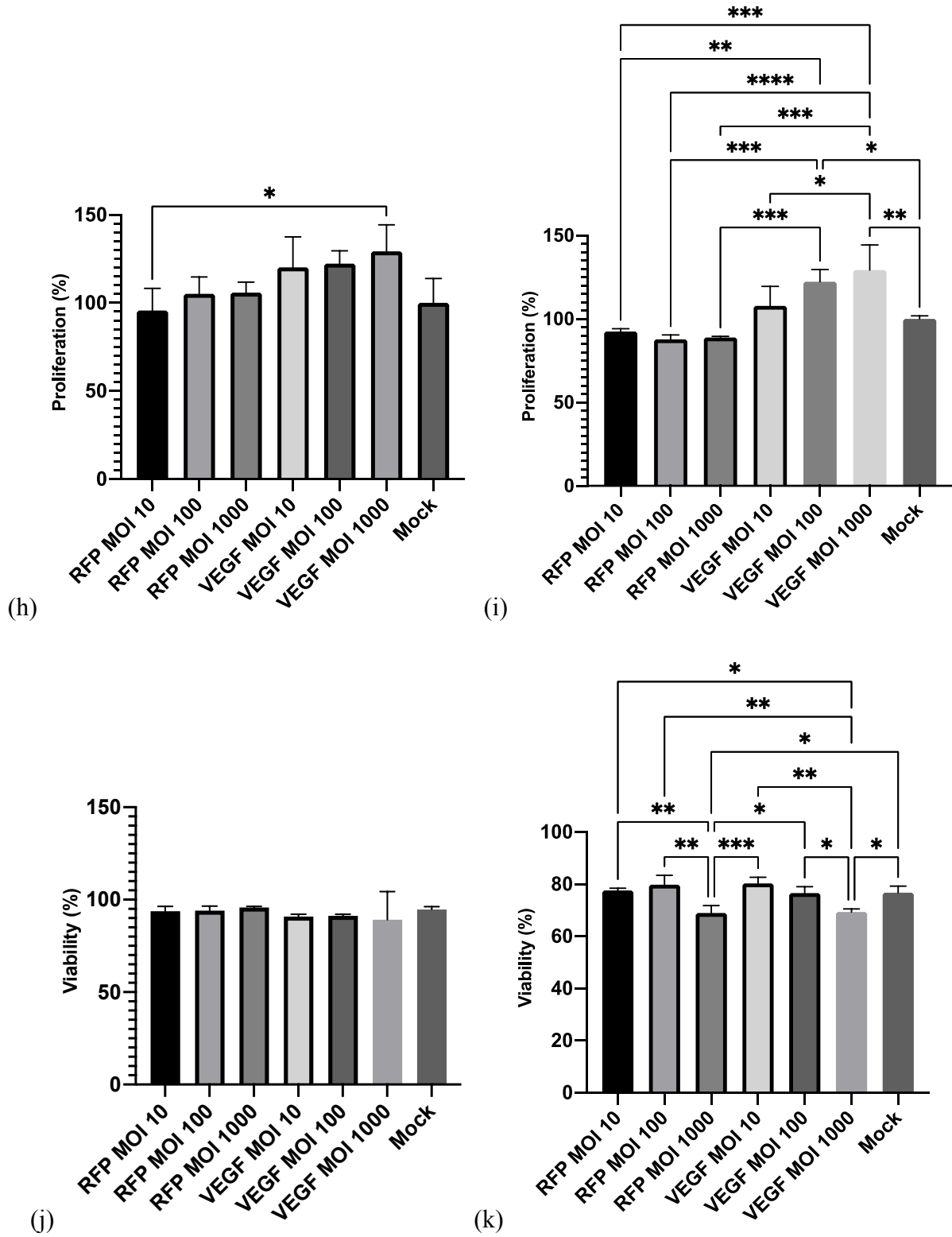


Figure 7. Baculovirus gene expression and cytotoxicity in SMC and HUVECs

(a-c) Fluorescence images of DAPI-stained SMCs transduced with different MOIs of baculovirus expressing RFP; (a) MOI 10, (b) MOI 100, and (c) MOI 1000. Percent of fluorescent cells after baculovirus transduction; (d) fluorescent HUVECs and (e) fluorescent SMCs. HUVEC proliferation after (f) 24 hours and (g) 48 hours. SMC proliferation after (h) 24 hours and (i) 48 hours. Cell viability after BV transduction; (j) HUVEC viability and (k) SMC viability.

Lysosomal activity after baculovirus gene delivery

Lysosomes play a key role in viral clearance and degradation [134]. To determine if baculovirus gene delivery impacts lysosomal activity, lysosomes were stained with LysoTracker Red after baculovirus transduction. The lysosomal activity was monitored using a previously established method [135]. The lysosomal activity significantly (p -value < 0.05) decreased 24 hours after baculovirus transduction with higher doses (MOI 100 and 1000) compared to an MOI of 10 (Figure 8). However, no difference in lysosomal activity was found between the baculovirus treatments and mock cells. After 48 hours, lysosomal activity returned to the base level for all groups.

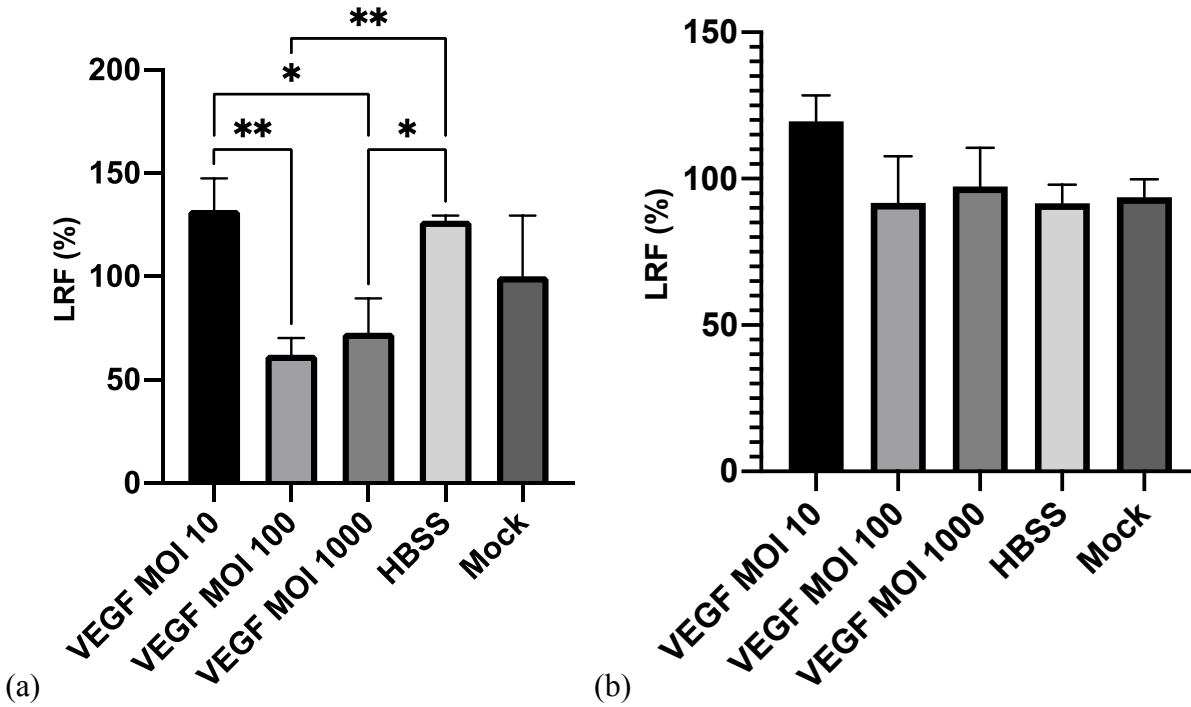


Figure 8. Lysosomal activity following baculovirus transduction

(a) Lysosomal relative fluorescence (LRF) 24 hours after baculovirus transduction. (b) LRF 48 hours after baculovirus transduction.

Baculovirus genotoxicity assessment

Gene delivery may interfere with cellular chromosomal stability leading to the creation of micronuclei. However, no significant difference in the number of micronuclei was present between different baculoviruses. All treatment groups and mock transduced cells contained significantly fewer micronuclei than the DMSO-positive control group. Overall, there was no evidence of genotoxicity in HUVECs or SMCs, as indicated by the cytokinesis-block proliferation index (CBPI), which accounts for micronuclei presence (Figure 9).

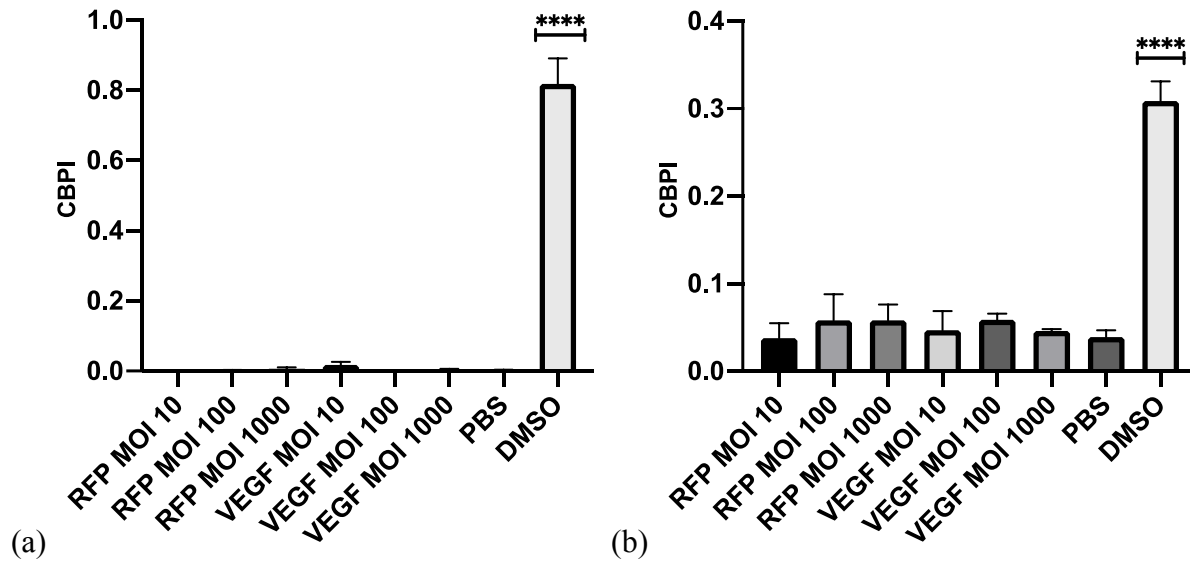


Figure 9. Cytokinesis-block proliferation index (CBPI) in mammalian cells following baculovirus transduction

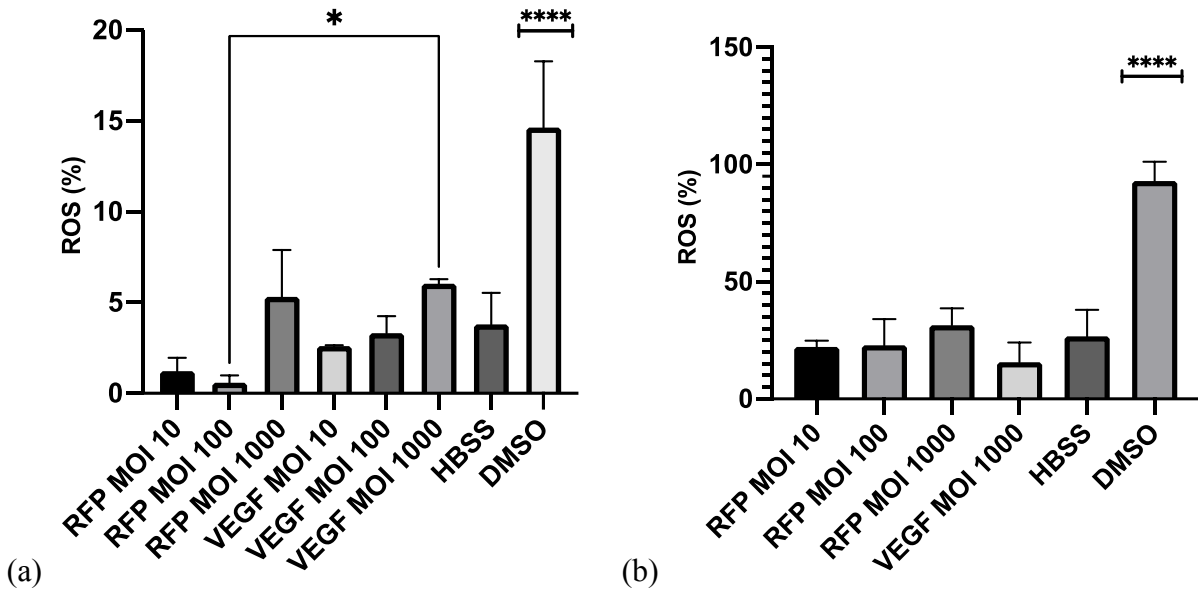
(a) CBPI in HUVECs after BV transduction. (b) CBPI in SMCs after BV transduction.

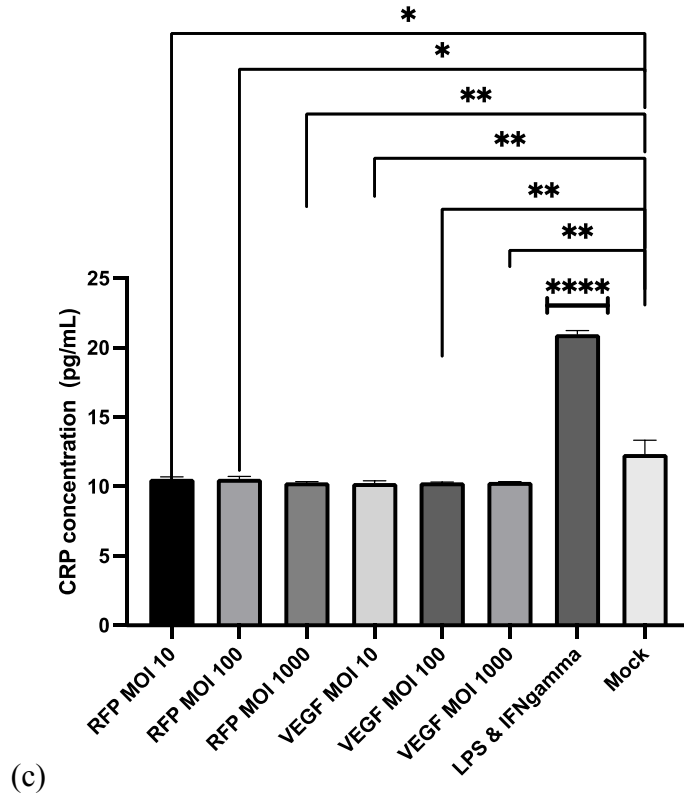
Non-inflammatory response to baculovirus gene delivery

The generation of reactive oxygen species was evaluated after baculovirus transduction to investigate its potential to create an inflammatory environment. Reactive oxygen species (ROS) production was evaluated for both baculoviruses with differing amounts (MOIs) seen in Figure 10a-b. In SMCs, all treatment groups created significantly fewer ROS than the DMSO control. There was no significant production of ROS with any MOI. HUVEC produced similar results, with all treatment groups producing significantly less ROS than the DMSO control and similar ROS to the mock transduced cells.

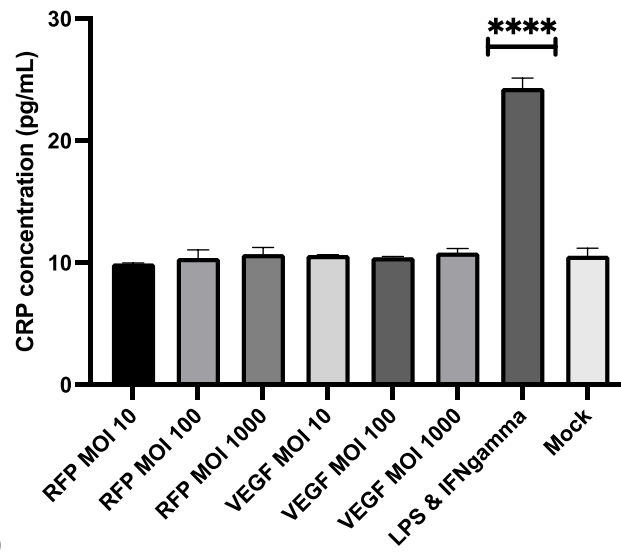
C-reactive protein (CRP) production and associated inflammation due to baculovirus gene delivery was also investigated. The CRP levels were evaluated after exposure to different MOIs of the baculovirus. No significant increase in CRP levels was detected, even at MOIs as high as

1000 (Figure 10c-d). Moreover, CRP levels were reduced in HUVECs after baculovirus transduction compared to mock transduced HUVECs.





(c)



(d)

Figure 10. Reactive oxygen species (ROS) and C-reactive protein (CRP) production after baculovirus transduction

(a) Percentage of HUVECs expressing ROS. (b) Percentage of SMCs expressing ROS. (c) CRP production in HUVECs. (d) CRP production in SMCs.

Blood compatibility of the baculovirus

Blood compatibility of the baculoviruses was evaluated using a standard hemolysis assay. Different concentrations of the baculovirus and the suspension media were tested with no significant hemolytic effect (Figure 11). The baculovirus showed no significant hemolysis, below 2 %, even at high amounts (10^8 TU/mL or 1 mL). Moreover, no significant change in blood clotting was observed after baculovirus addition compared to insect cell media and the PBS control.

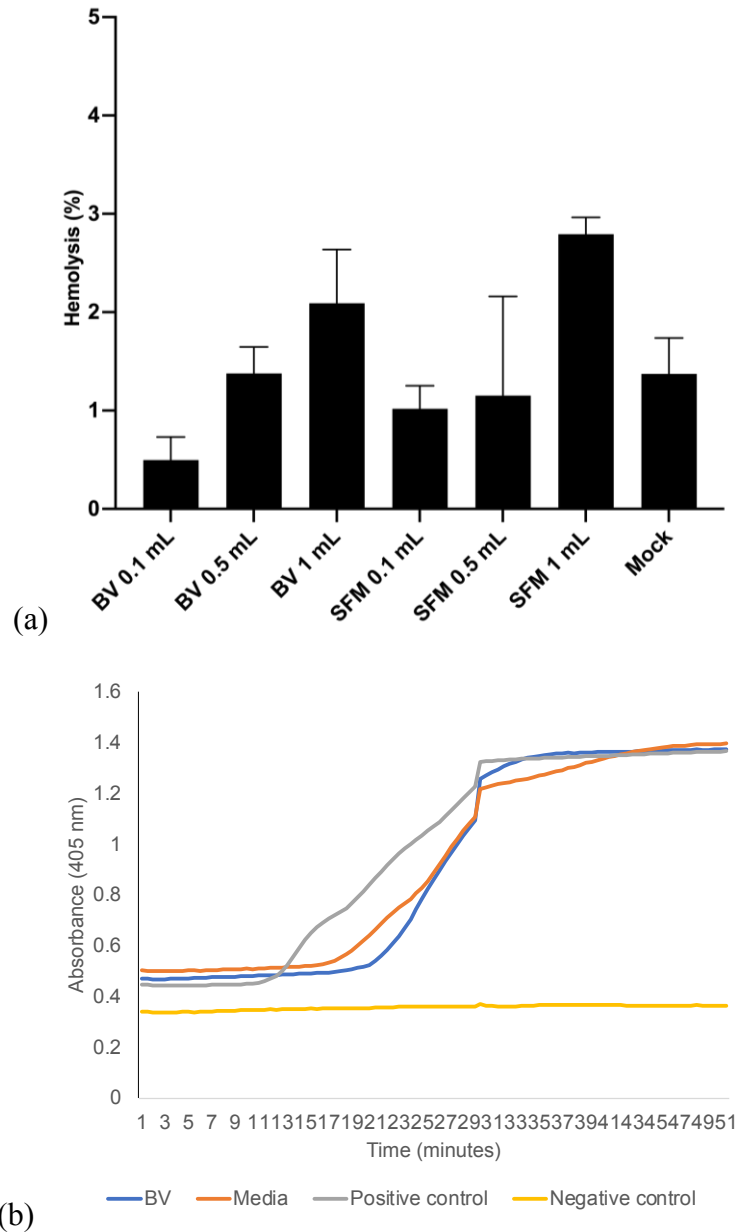


Figure 11. Blood compatibility of the baculovirus

(a) Hemolysis (%) after exposure to baculoviruses or serum-free media (SFM). (b) Blood clotting after baculovirus addition.

Discussion

Here we demonstrate the *in vitro* safety of baculovirus gene delivery. Overall, baculoviruses are an effective gene delivery system. The number of cells expressing the delivered

gene reached over 30 % despite the high physiological temperatures employed. As the amount of baculovirus was added, the relative amount of that gene expressed increased significantly.

Beneficially, most dosages of baculovirus did not reduce cell viability. When MOIs above 1000 were used, HUVEC and SMC viability significantly decreased. However, it would be difficult physiologically to obtain an MOI above 1000, given the sheer number of cells within the human body and the maximum dosage feasible. As expected, the baculovirus expressing VEGF increased cell proliferation, whereas the baculovirus expressing RFP did not alter cell proliferation. This is expected because VEGF is a common growth factor that stimulates cell proliferation, migration, and angiogenesis [136], [137].

Baculovirus gene delivery showed no evidence of genotoxic effects. Specifically, 24 and 48 hours after transduction, no increase in cytokinesis-block proliferation index (CBPI) was observed compared to the mock transduced cells. All treatment groups and the mock transduced had a CBPI significantly lower than the cells treated with a 20 % (v/v) solution of DMSO to induce genotoxicity [138]. The same results were shown in both SMCs and HUVECs.

The immune response to baculovirus gene delivery was also investigated by measuring C-reactive protein (CRP) and reactive oxygen species (ROS) production. ROS plays a crucial role in inflammation and viral clearance [139]. Baculovirus-induced ROS production was comparable to mock transduced cells after 48 hours. The mock transduced cells and baculoviruses, expressing different genes, produced significantly less ROS than the DMSO positive control. Similarly, CRP production did not increase after RFP-baculovirus or VEGF-baculovirus transduction. Even at an MOI of 1000, there was no significant difference in CRP production between treatments or the mock transduced cells.

Baculoviruses have been shown to enter cells via a clathrin-mediated endocytosis [133]. Following entry, some virus is often cleared through lysosomes. Typically, lysosomes assist with virus degradation and have been shown to play a similar role with baculoviruses [133]. Interestingly, lysosomal activity was reduced after the initial baculovirus transduction compared to lower MOIs. However, after 48 hours, lysosomal activity returned to base levels compared to the mock transduced cells. Together, these findings indicate that baculovirus may hijack lysosomes within the first 24 hours, but after 48 hours, they resume their usual activity.

Future work should investigate the method of viral clearance and the role lysosomes play in this. Moreover, given the *in vitro* safety shown here, future *in vivo* safety assessments should be conducted. *In vivo* studies can further confirm the immune response within a three-dimensional environment.

We report some limitations to baculovirus delivery such as reduced transduction efficiency at physiological conditions. The reduction in baculovirus gene delivery efficiency at 37 °C indicates a reduction in virus viability and stability at higher temperatures. This is supported by previous studies [140]. Thus, higher amounts of baculovirus are needed to meet the same transduction efficiency. However, overall baculoviruses do have a promising outlook for gene therapy applications with no evidence of genotoxicity or inflammatory responses. We also report good hemocompatibility and no direct impact on cell proliferation or viability at lower doses.

Conclusion

Baculovirus gene delivery to mammalian cells is efficient and safe. Specifically, even high doses of the baculovirus, well above the therapeutic window, were non-cytotoxic, hemocompatible, non-genotoxic, and non-inflammatory in both smooth muscle and endothelial

cells. These results support its use in further vaccine development, cancer treatment, and gene therapy applications for humans [125].

Materials and Methods

Cell culture

Human umbilical vein endothelial cells (HUVECs) and smooth muscle cells (SMCs) were maintained in T-25 flasks in a 37 °C, 5 % CO₂ incubator. Medium 199 was used with 0.02 mg/mL endothelial growth supplement, and 10 % (v/v) fetal bovine serum was used to culture the SMCs and complete endothelial growth medium (Sigma Aldrich, Burlington, MA, USA) was used to culture the HUVECs. Cells were used within five passages upon receiving.

Insect cell culture

Sf9 insect cells (Sigma Aldrich, Burlington, MA, USA) were maintained at 27 °C in BacVector medium (Sigma Aldrich) in T-75 flasks or 250 mL shake flasks (Erlenmeyer, CA). The Sf9 cells were subcultured 2-3 times weekly and shaken at 130 rpm.

Gene cloning

Human VEGFA in a pcDNA3.1+eGFP vector and GFP-RFP in a pBakPak9 plasmid were purchased from GenScript (Piscataway, NJ, USA). The VEGFA gene was excised from the original plasmid using EcoRI and NotI restriction enzymes (Thermo Fisher, Waltham, MA, USA). The recipient plasmid, pOET6, was cut using the same enzymes. The gene fragments and cut plasmid were run on a 1 % (m/v) agarose gel for one hour at 90 Volts. The DNA bands were visualized, excised, and purified using NEB's Gel Extraction Kit. The VEGFA gene was ligated, using Instant Sticky End Ligase (NEB, Whitby, ON, CA), into the pOET6 plasmid (MJS Biolynx Inc., Brockville, ON, Canada). The new plasmid was then chemically transformed into DH5alpha E. coli and selected for using ampicillin resistance. Next, 200 µL of the bacteria were plated on an

LB agar plate containing ampicillin and grown overnight. The next day, the resistant colonies containing each gene of interest were selected and grown overnight in 5 mL of Luria Broth media to amplify the plasmid. The plasmid was then extracted and purified using NEB's plasmid purification kit. The concentration and purity of the plasmid was checked using a NanoDrop (Thermo Fisher) and used for all future virus production steps. The pBakPak9 plasmid was used as is and designed to express GFP in insect cells (polyhedron promoter) and RFP in mammalian cells (cytomegalovirus promoter).

Baculovirus production

Baculovirus production was performed following the supplier's protocol previously described [141]. Briefly, 5×10^5 Sf9 cells, in an exponential growth phase, were seeded into a 12-well plate one hour before virus transfection. Next, 200 ng of the plasmid with each gene was added to 100 ng of flashBAC DNA (MJS Biolynx Inc., Brockville, ON, Canada), 0.48 μ L of TransIT Insect Reagent, and 100 μ L PBS and incubated at room temperature for 15 minutes. The transfection mixture was then added to the Sf9 cells and incubated overnight at 27 °C. The next day, 0.5 mL of BacVector media (Sigma Aldrich) was added. Five days after transfection, the culture medium was harvested, centrifuged at 1000 x g for 10 min, and stored at 4 °C. This generated the P₀ virus stock and was added to 100 mL of Sf9 cells at a concentration of 2×10^6 cells/mL. The infected Sf21 cells were agitated at 130 rpm for four days before harvesting the culture medium as described above. This generated P₁ baculovirus stock expressing VEGFA or GFP-RFP.

Baculovirus titration

The baculovirus P₁ stock was titrated using two methods. The fluorescent titration was calculated using the EGFP expressed by the baculovirus. The Fast Plax Titration kit (Sigma Aldrich) was used to calculate the titration of the three other baculoviruses.

For the fluorescent titering assay, 5×10^5 Sf9 cells/well were seeded into a 12-well plate and incubated for one hour. During the incubation, the virus was diluted using insect cell medium (1:10, 1:25, 1:50, 1:75, 1:100). The cell media was then aspirated off the Sf9 cells and 100 μ L of the virus dilution was added to each well. The plate was incubated for one hour and then an additional 0.5 mL of insect cell media was added to each well and incubated at 27 °C. The next day, the number of fluorescent cells was counted in each well with less than 40 % of fluorescent cells. The following equation was used to calculate the titration:

$$\text{Transduction Units (TU)/mL} = (\text{number of cells transduced} \times \text{percent of fluorescent cells} \times \text{dilution factor}) / (\text{transduction volume in mL})$$

Baculovirus transduction

The titrated baculovirus stock was diluted as necessary and used to transduce mammalian cells (SMCs & HUVECs) in 96 well plates. After three hours of incubation, the virus inoculum was removed and replaced with fresh cell media. The cells were incubated for 24 to 48 hours to allow for viral gene expression. Fluorescent images of the cells were taken at different time points and stained with DAPI at 48 hpi. Images were acquired using the Columbus Image Data Storage and Analysis System (PerkinElmer, USA) and the Operetta® CLS automated microscope.

Baculovirus gene expression

HUVECs were seeded into a 96-well plate and incubated overnight. The HUVECs were then transduced with different baculovirus MOIs for three hours, after which the virus inoculum was removed and replaced with fresh cell media. Twenty-four hours post-infection, the media was

frozen at -80 °C for the CRP ELISA and the total RNA from each well was extracted using Bio-Basic's Total RNA Extraction Kit. The extracted RNA was then mixed with Luna Universal One Step RT-qPCR kit (NEB, Whitby, ON, CA) and VEGFA primers (Bio-Rad, Hercules, CA, USA). The mixture was then placed into the Eco Illumina PCR® system. Amplification was carried out for 40 cycles with 35 seconds (denaturation), 55 °C for 35 seconds (annealing), and 72 °C for 25 seconds (extension).

MTT proliferation assay

To determine the impact of the baculovirus transduction and gene expression on cell proliferation, an MTT toxicity kit (Sigma Aldrich, St. Louis, MI, USA) was used. As above, different MOIs of BV were added to HUVEC and SMCs and incubated for three hours. After three hours, the baculovirus transduction media was removed and replaced with fresh cell media. Twenty-four to forty-eight hours after transduction, 0.01 mL of AB Solution (MTT) was added to each well 24 hpi. The cells were incubated for two hours at 37 °C to allow MTT cleavage. After one hour, 0.1 mL of isopropanol with 0.04 N HCl was added to each well. The isopropanol solution was mixed thoroughly via pipetting. The plate was then read using an EnSpire Multimode plate reader (Perkin Elmer, USA) with a wavelength of 570 nm.

Live dead assay

A Live Dead Assay was employed to determine the baculovirus cytotoxicity. First, 1×10^4 cells/well were seeded into a 96-well plate and incubated overnight. The next day, different BV MOIs were added to each well in triplicate and incubated for three hours. Media alone or DMSO was used as a control. After three hours, the transduction media was removed, and fresh media was added. The cells were left for 24 to 48 hours to allow for baculovirus gene expression. At the designated time point, 5 μ L of 1 mM Calcein AM and 5 μ L of 2.5 mg/mL propidium iodide (both

from Thermo Fisher) were added to 10 mL of cell media. Next, 100 μ L of this solution was added to the cells and incubated at 37 °C for 30 minutes. After 30 minutes, the plate was imaged using the Operetta Image system (five images per well) and analyzed using Columbus.

Micronucleus assay

An *in vitro* micronucleus assay, in compliance with the Organization of Economic Cooperation and Development Guidelines for Testing of Chemicals no. 487, was used to determine if the virus induces genotoxic effects [142]. First, 2×10^5 cells/well were seeded into a 96-well plate. Next, different MOIs of the baculovirus were used to transduce the cells as described above. PBS and DMSO were used as the negative and positive controls, respectively. A 20 % (v/v) solution of DMSO was applied as this has been shown to induce the most genotoxicity [138]. Twenty-four hpi, the cells were fixed with paraformaldehyde and stained with DAPI (Sigma Aldrich). The cytokinesis-block proliferation index (CBPI) was calculated using the following equation [142], [143]:

$$\text{CBPI} = \frac{[(n^{\circ} \text{ mononucleate cells}) + (n^{\circ} \text{ binucleate cells} \times 2) + (n^{\circ} \text{ multinucleate cells} \times 3)]}{\text{total } n^{\circ} \text{ cells}}$$

Lysosomal activity assay

The lysosomal activity was monitored using a method adapted from McNeil et al. with slight modifications [135]. First, HUVECs were transduced with baculovirus for three hours. After transduction, fresh media was added to the cells and incubated for 24 or 48 hours. LysoTracker Red (Thermo Fisher) was added to the cells at the designated time points. Columbus was then used to calculate the LysoTracker red fluorescence (LRF). The percent of LRF was calculated using the following equation.

$$\% \text{ LRF} = \frac{(\text{Emission of BV transduced cells}) - (\text{Emission of cell-free BV blank})}{\text{Emission of cell-free BV blank}}$$

(Emission of cell-free media blank) – (Emission of cell media)

Reactive oxygen species (ROS) assay

To determine if the baculovirus induces ROS, mammalian cells were seeded into 96-well plates and incubated overnight as above. Next, different MOIs of the baculovirus were added to the cells and incubated for three hours. After three hours, the virus inoculum was removed and replaced with fresh media. The following day, a ROS kit (Abcam ab186027, Waltham, Boston, MA, USA) was used to evaluate ROS production following the supplier's instructions. The plate was imaged using the Operetta microscope system. The mean well intensity and number of cells expressing ROS were calculated using Columbus.

C-reactive protein (CRP) ELISA

CRP is a marker for inflammation and infection [144]. A CRP ELISA was employed to determine if the baculovirus or subsequential gene production induces CRP (Ab260058, Abcam). The frozen samples from the baculovirus gene expression were treated and added to the ELISA per the supplier's protocol.

Hemocompatibility studies

The potential hemolysis of the baculovirus and the baculovirus-delivered genes was evaluated using an established method. All tested samples were immersed into 5 mL PBS in a 15 mL centrifuge tube. Next, 4 mL of citrated blood was mixed with 5 mL PBS and 0.1 mL of the diluted blood was added to each sample. The samples were incubated at 37 °C for one hour and then centrifuged at 1000 rpm for 10 minutes. The supernatant containing the lysed hemoglobin was placed into a 96-well plate and the absorbance was read at 545 nm. A standard hemolysis curve was generated by mixing different dilutions of PBS with distilled water. The absorbance was

measured, and the percent hemolysis was plotted against absorbance to create the standard curve. This standard curve was used to determine the percent hemolysis for all samples.

The impact of baculovirus on blood clotting time was also investigated using a protocol adapted from Alexandre et al. [145]. Briefly, whole blood from the donors was centrifuged at 10,000 rpm for 10 minutes to separate the platelet-rich plasma (PRP). During the centrifugation, 100 μ L dilutions of the baculovirus and suspension media were prepared in a 96-well plate (none, 1:2, 1:4, and 1:8 dilutions). Next, 50 μ L of the PRP was added to each well in triplicate. Finally, 100 μ L of 0.025 M calcium chloride was added to each well to initiate clotting. Wells with PBS were used as the controls, with no calcium chloride added to the negative control group. The plate was read every 30 seconds for 45 minutes at 405 nm using the same plate reader as previously mentioned.

Statistical analysis

All results are reported as a mean \pm standard deviation (SD) of triplicates. GraphPad Prism (version 9.0.0 for Windows, GraphPad Software, San Diego, California USA, www.graphpad.com) was used for all one-way ANOVA data analysis with a post-hoc Tukey's test.

Supplementary Materials: All data is presented within the manuscript.

Author Contributions: Conceptualization, S.S. and S.P.; methodology, S.S.; validation, S.S. and S.P.; formal analysis, S.S.; investigation, S.S.; resources, S.P.; data curation, S.S.; writing—original draft preparation, S.S.; writing—review and editing, S.P., A.A, J.L.B., & P.I.; visualization, S.S., S.P., A.A, J.L.B., & P.I.; supervision, S.P.; project administration, S.P.; funding acquisition, S.P. All authors have read and agreed to the published version of the manuscript.

Funding: This work was supported by a research grant from the Canadian Institute of Health Research (CIHR) to Dominique Shum-Tim and Satya Prakash. S.S. is fully funded by the Canadian Graduate Scholarship-Doctoral from the Natural Sciences and Engineering Research Council (NSERC). P.I. is funded by the Islamic Development Bank Scholarship (2020-245622). A.A. is fully funded by a scholarship from the Ministry of Higher Education of the Arab Republic of Egypt. R.T. and K.A. are funded by the Canadian Graduate Scholarship-Master's from NSERC.

Acknowledgments: We thank the Facility for Electron Microscopy Research of McGill University (SEM equipment), McGill Chemistry Characterization Facility (H-NMR), Mariam Tabrizian's Biomat'X lab, and McGill University Imaging and Molecular Biology Platform (IMBP) equipment or services (image acquisition).

Conflicts of Interest: The authors declare no conflicts of interest.

Copyright: This is an open-access article under the CC BY-NC-ND license (<http://creativecommons.org/licenses/by-nc-nd/4.0/>).

Bridging text

Confirming the baculovirus gene delivery system's *in vitro* safety and efficiency is the first step to generating a gene-eluting stent. Direct human baculovirus gene therapy studies have been limited. Experiments ranging from hemocompatibility, cytotoxicity, and inflammation were conducted to confirm that our specific baculovirus system is safe.

First, proper gene expression from the baculovirus was confirmed. The green (GFP) and red fluorescent protein (RFP) expressed by the control baculovirus were used for monitoring gene expression. The other baculovirus gene expression was evaluated using RT-qPCR to measure mRNA levels of the specific GOI. As the amount of baculovirus was added, the levels of the gene of interest also rose.

Given that gene expression is confirmed I wanted to investigate the overall *in vitro* safety. I specifically looked at hemocompatibility, which is important given that the baculovirus will be in direct contact with the blood as either a wound dressing or stent system. Beneficially, I found that the baculovirus did not change the blood clotting time or cause hemolysis of blood cells. I also investigated the cytotoxicity of the baculovirus using an MTT proliferation and Live Dead Assay. Overall, I found that even high doses of the baculovirus did not significantly impact SMC or HUVEC viability. However, the proliferation depended on the gene being expressed by the baculovirus as desired. Cytotoxicity experiments are important to determine the therapeutic index and safety range. Especially for medical devices, a large safety margin is essential. Next, I looked at the inflammatory environment. Atherosclerotic disease progression occurs with an increase in inflammation, so it is important that the baculovirus gene delivery does not further contribute to this. Specifically, C-reactive protein (CRP) and reactive oxygen species (ROS) are one of the first signs of inflammation in PAD and CAD. I found that baculovirus transduction and gene expression

did not significantly increase ROS or CRP. I also investigated if baculovirus gene delivery altered lysosomal activity to see if the virus could hijack typical cellular responses. This could cause downstream and unintended consequences. However, I found no significant change in lysosomal activity after 48 hours.

All the above-mentioned tests were conducted on every baculovirus. However, the paper only includes the baculoviruses expressing VEGF and RFP was shown. Overall, from these tests, I concluded that baculovirus gene delivery is safe and efficient. With direct baculovirus gene delivery, a single dose can only be given, and the gene expression lasts only a few days. The next step would be to create a baculovirus delivery system capable of controlled and sustained baculovirus delivery. The delivery length can then be optimized to express the duration of the therapeutic window for the specific application. For example, the following two weeks after stent implantation are the most important for restoring proper endothelial function and thus baculovirus gene delivery and gene expression should last this long.

There are several methods for controlling and sustaining baculovirus delivery. Methods include nanoparticle encapsulation, hydrogel loading, targeted delivery, and more. I investigated all options but found that hydrogel loading demonstrated the best safety and efficiency. The following two papers will investigate different hydrogel formulations for baculovirus gene delivery.

CHAPTER 5: Alginate-chitosan hydrogel formulations sustain baculovirus delivery and VEGFA expression, which promotes angiogenesis for wound dressing applications.

Schaly, S., Islam, P., Abosalha, A., Boyajian, J. L., Shum-Tim, D., & Prakash, S. (2022). Alginate-Chitosan Hydrogel Formulations Sustain Baculovirus Delivery and VEGFA Expression Which Promotes Angiogenesis for Wound Dressing Applications. *Pharmaceuticals (Basel, Switzerland)*, 15(11), 1382. <https://doi.org/10.3390/ph15111382>.

Contributions of the author: I am the first author and contributed to all experiments and manuscript preparation.

Pharmaceuticals IF 5.215

(Published)

Abstract

Hydrogel wound dressings are effective in providing a wound-healing environment but are limited by their ability to promote later stages of revascularization. Here, a biosafe recombinant baculovirus expressing VEGFA tagged with EGFP is encapsulated in chitosan-coated alginate hydrogels using ionic cross-linking. The VEGFA, delivered by the baculovirus, significantly improves cell migration and angiogenesis to assist with wound healing and revascularization. Moreover, the hydrogels have an encapsulation efficiency of 99.9 %, no cytotoxicity, antimicrobial properties, good blood compatibility, promote hemostasis, and enable sustained delivery of baculoviruses over eight days. These hydrogels sustain baculovirus delivery and may have clinical implications in wound dressings or future gene therapy applications.

Keywords: baculovirus; encapsulation; wound healing; angiogenesis; gene delivery; VEGFA; revascularization; wound dressing; targeted delivery; alginate; chitosan

Introduction

Baculoviruses (BVs) are insect viruses that can be genetically engineered to express recombinant growth factors within a host. This property makes them effective for short-term gene therapy, including wound dressings [1–3]. Baculoviruses are also safer than alternative viral delivery systems. Specifically, many alternative viral delivery systems (lentiviral, retroviral, and adenoviral vector) are human pathogens capable of producing replication-competent viruses [108]. Moreover, the baculoviruses' inability to integrate into the host DNA or chromosomes further supports its biosafety and use in gene delivery [50]. Baculoviruses also provide significantly higher gene expression than plasmid or other viral gene delivery due to the lack of pre-existing immunity.

This is unlike adenoviruses which elicit a humoral and cellular immune response preventing re-administration [146].

Moreover, due to their high specificity, they can be genetically engineered to target only specific cell types [110]. In addition, baculoviruses can be easily scaled up, mitigating the cost typically associated with gene delivery [77]. Baculoviruses provide a biosafe, low-cost, low cytotoxicity, non-replicative vector with a large cloning capacity [1–3]. Thus far, baculoviruses have shown promising results in treating several diseases (such as atherosclerosis, prostate cancer, and gastric cancer) in humans and animals [82], [87], [113]. Still, their full potential has yet to be exploited. However, some limitations must be overcome first, including serum inactivation, virus fragility, and consequential transient delivery [101], [104].

Encapsulation of baculoviruses provides a promising avenue to overcome these limitations and sustain baculovirus delivery. Specifically, natural polymers such as alginate and chitosan are biocompatible and biodegradable, have extensive human safety studies, and are cost-effective options for encapsulation [16–19]. Alginate also has antimicrobial properties, can be cross-linked with calcium chloride and exhibits reversible binding to VEGF, leading to a sustained release [120]. Similarly, chitosan has anti-inflammatory, antimicrobial, and antioxidant properties [121]. Chitosan can also be complex with negatively charged particles such as baculoviruses to sustain delivery and improve transduction efficiency [122]. The polymeric capsules can also increase stability, solubility, prolong gene expression, and promote site specificity which allows for a lower dosage and less cytotoxicity [123].

Moreover, baculovirus encapsulation prevents immune inactivation, effectively shielding the virus from the immune system. Cell and bacterial encapsulation have been extensively investigated, showing promising results in localized treatment with sustained efficacy [124].

However, the efficiency and effectiveness of baculovirus encapsulation have yet to be shown and applied.

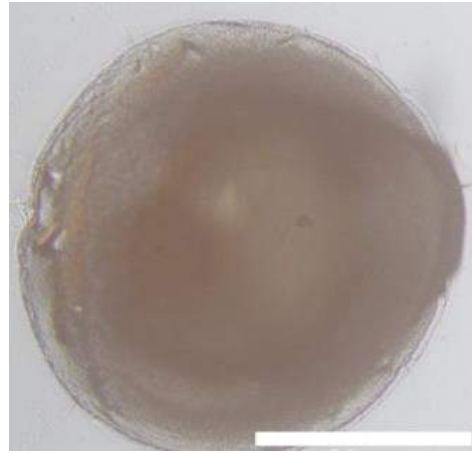
Wound healing is a complex process involving four main stages, including coagulation, inflammatory, proliferative, and remodeling phase [147]. The coagulation and inflammatory phase include platelet aggregation to help with blood clotting and removing bacteria. These platelets release growth factors to attract immune cells. The proliferative phase then commences, which includes angiogenesis, epithelialization, collagen deposition, and more. The final stage includes remodeling and when scar formation can occur. One method to enhance healing is to provide a wound dressing that provides an antimicrobial and moist environment [148]. The moist environment can promote cell migration, angiogenesis, and epithelialization leading to significantly improved healing at the injury site [25–27]. Specifically, hydrogels synthesized from different polymers have been shown to be effective, and some even elute growth factors, antibiotics, or pain medication to promote healing and prevent scar formation [149], [150]. For instance, vascular endothelial cell growth factor A (VEGFA) is known to be one of the most potent pro-angiogenic factors and plays a key role in wound healing [30–32]. Specifically, VEGFA promotes endothelial cell migration, proliferation, and capillary tube formation. Furthermore, intradermal VEGF injections have accelerated diabetic wound-healing [151], [152]. Here, we investigate hydrogel delivery of baculoviruses expressing VEGFA to promote cell migration and angiogenesis as a potential candidate for wound dressing applications.

Results

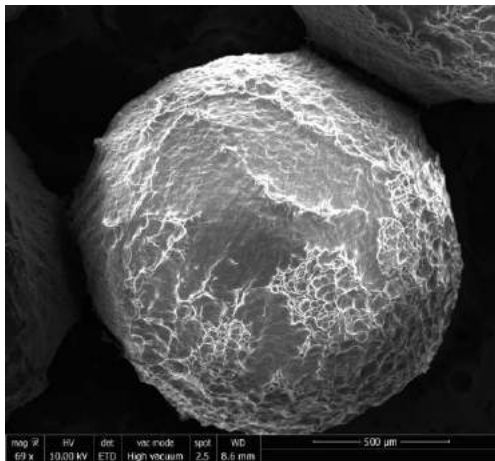
Hydrogel Formulation Morphology



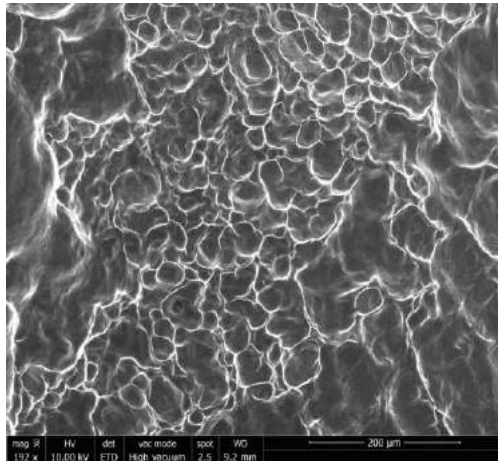
(a)



(b)



(c)



(d)

Figure 12. Alginate-chitosan hydrogel morphology.

(a-b) Brightfield images of the hydrogels swollen in PBS at 4 \times , the scale bar represents 1 mm. **(a)** Alginate hydrogel; **(b)** alginate hydrogel coated with chitosan; **(c,d)** SEM images of the dried hydrogels at different magnifications.

The spherical hydrogels formed instantly upon dropping the alginate virus solution into the calcium chloride cross-linking solution. The resultant alginate–BV hydrogels were coated with chitosan (termed alginate–chitosan hydrogels). The chitosan coating on the alginate capsules changed the surface morphology, as seen in Figure 12a,b. The hydrogels were observed under a

brightfield microscope revealing hydrogels around 2 mm in diameter with a smooth surface appearance. The surface was more closely evaluated using FEI Quanta 450 SEM revealing a more rigid surface (Figure 12c,d). The hydrogel characteristics are outlined below in Table 2.

Table 2. Hydrogel zeta potential, size, and swelling ratios. The zeta potential of the hydrogels, after being washed and resuspended in Milli-Q water (n = 3/group, 10 runs each). The average size of 10 randomly selected spherical hydrogels. The average swelling ratio of the different hydrogel formulations (10 different hydrogels/group, selected at random).

Property	Alginate	Alginate–BV	Alginate–Chitosan	Alginate–Chitosan–BV
Zeta potential (mV ± SD)	-2.67 ± 0.87	-2.85 ± 1.66	6.62 ± 0.35	-0.13 ± 0.42
Size (mm ± SD)	2.17 ± 0.06	2.12 ± 0.07	2.21 ± 0.10	2.37 ± 0.10
Swelling ratio (average ± SD)	1.51 ± 0.05	1.48 ± 0.05	1.54 ± 0.07	1.65 ± 0.07

The hydrogel stability was observed over several months, with most of the hydrogels remaining intact after three months at room temperature and 4 °C. However, the baculovirus diffused over time, so the hydrogels must be freshly prepared. The hydrogels swelled ~1.5-fold after initial drying in a 37 °C incubator and then slightly over time in PBS, saline, and at a pH of 4. Hydrogel swelling was observed over one month with no significant size difference over time. Moreover, the hydrogels dissolved more quickly in an acidic environment (pH of 4).

Baculovirus (BV) Activity and Elution from the Hydrogels

The supernatant from the freshly formed hydrogels was used to determine the encapsulation efficiency. The encapsulation efficiency of the hydrogels was 99.9 %. Moreover, the baculovirus was released in a sustained manner over eight days. The virus activity was assessed in human umbilical vein endothelial cells (HUVECs), as seen in Figure 13.

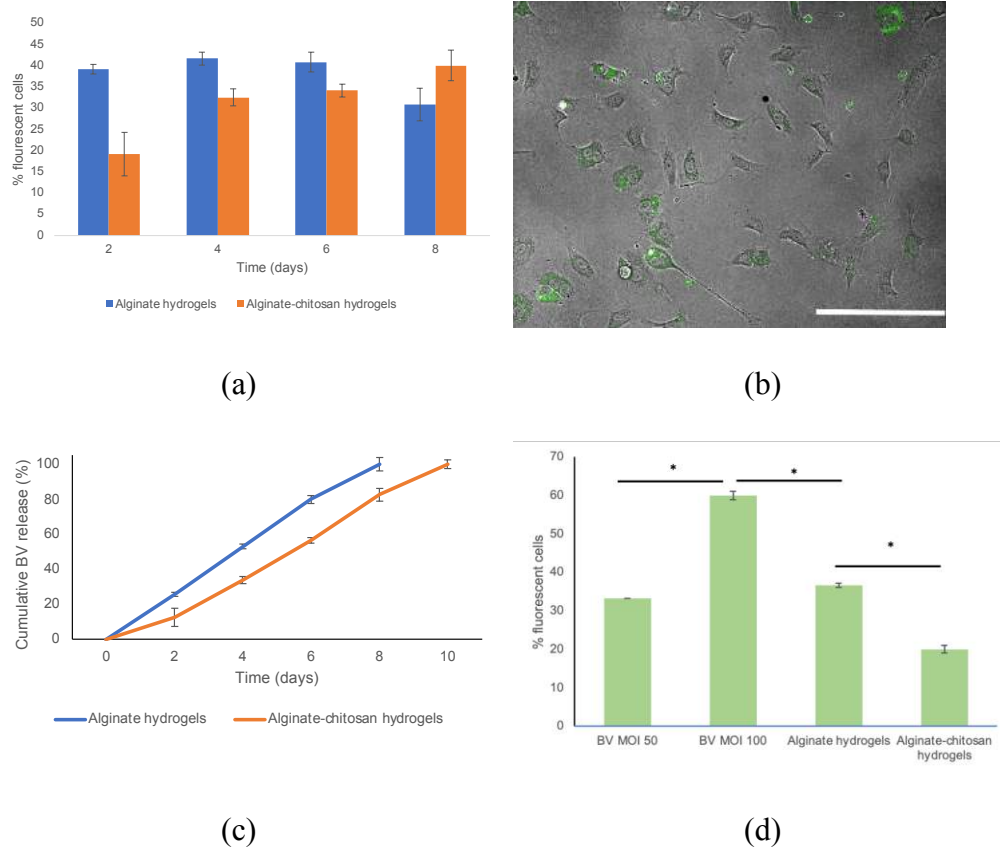


Figure 13. Baculovirus release and expression from hydrogels.

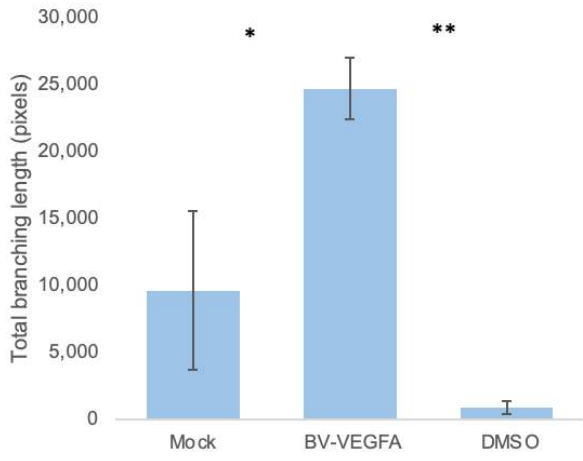
(a) Percentage of fluorescent HUVECs after transduction with baculovirus eluted from hydrogels. **(b)** Brightfield image overlaid with a fluorescent image of HUVECs transduced with baculovirus eluted from alginate-chitosan hydrogels on day 3 at 20× magnification, scale bar = 200 μm. **(c)** Cumulative BV release (%) from alginate and alginate-chitosan hydrogels. **(d)** Percentage of fluorescent HUVECs after transduction with BVs or hydrogel suspension media, 24 hpi. $n = 3$ per group for each experiment. * Indicates a significance of $p < 0.05$

Both hydrogels provided sustained baculovirus elution. The alginate hydrogels had a larger initial burst release of baculovirus than those coated with chitosan. Up to 41 % of cells expressed the VEGFA-EGFP when transduced with the alginate-baculovirus hydrogels on day 4. Comparatively, up to 40 % of cells expressed the gene of interest when transduced with the baculovirus eluted from the alginate-chitosan hydrogels on day 8. The virus elution also remained

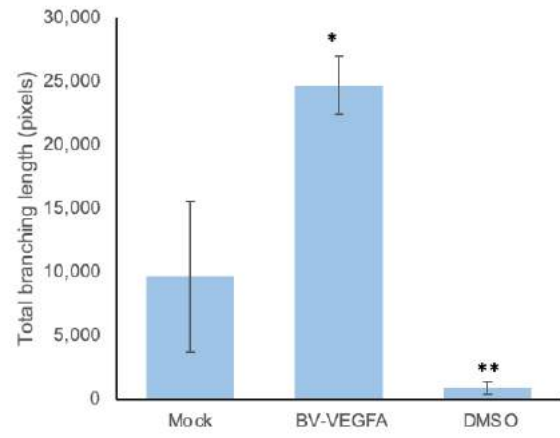
stable over eight days for the alginate hydrogels and over 10 days for the alginate–chitosan hydrogels. The baculovirus elution slowly diminishes over time. Hydrogel delivery improves the therapeutic efficacy by releasing the baculovirus over several days instead and all at once if left unencapsulated. The baculovirus VEGFA delivery increased VEGFA expression up to 25.76-fold with an MOI of 50 compared to the mock-infected cells (PBS).

Hydrogel formulations delivering baculovirus demonstrate therapeutic potential over seven days

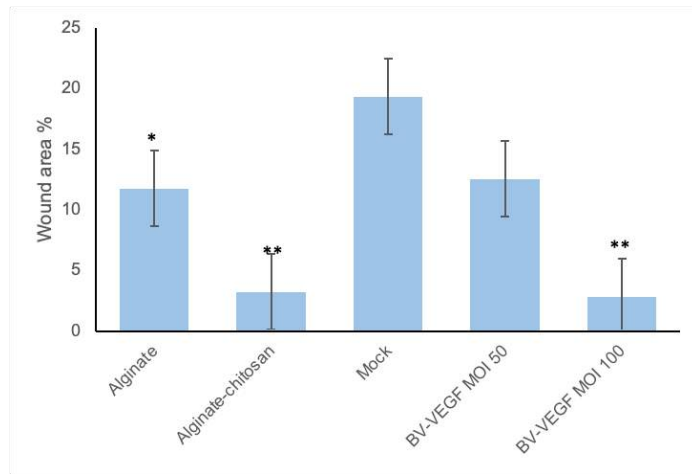
The baculovirus eluted from the hydrogels maintained activity. The baculovirus-hydrogel system demonstrated beneficial properties, including no cytotoxicity, good blood compatibility, antimicrobial properties, and significantly improved wound healing and angiogenesis compared to the mock cells (Figure 14). VEGFA activity was maintained from the baculovirus, as demonstrated by the improved cell migration over time. Both hydrogels significantly improved cell migration in HUVECs over the course of seven days (Figure 14). Moreover, the alginate hydrogels demonstrated significantly less cell migration when compared to chitosan-coated hydrogels. However, the alginate hydrogels were still significantly better at promoting wound healing compared to the mock-infected cells (Figure 14c). Angiogenesis also significantly improved with the baculovirus treatment, as shown by the longer branching and increased number of nodes after tube formation (Figure 14a,b). The hydrogels also prevented *E. coli* and *C. albicans* growth directly below and inhibited *C. albicans* growth surrounding the alginate–chitosan hydrogels (Figure 14i).



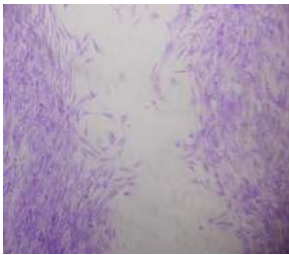
(a)



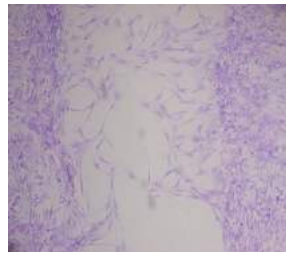
(b)



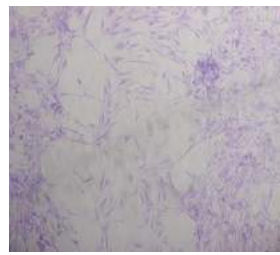
(c)



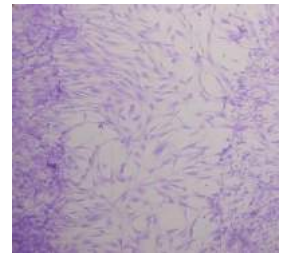
(d)



(e)



(f)



(g)

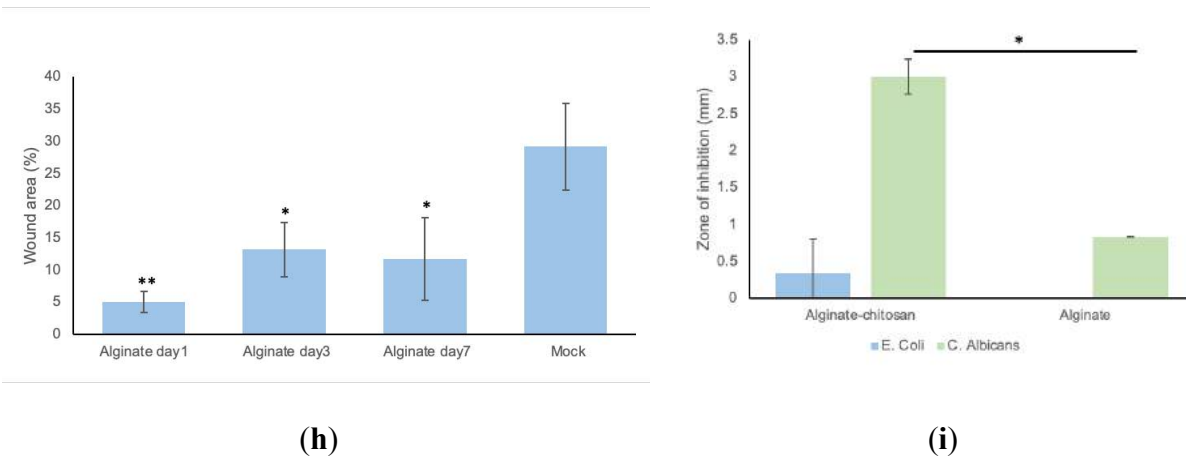


Figure 14. Hydrogel therapeutic properties.

(a) Total branching length of tube formation after treatment with BV expressing VEGFA compared to the mock transduced cells. (b) A number of junctions formed during angiogenesis assay compared to the mock transduced cells. (c) Wound area remaining after hydrogel or baculovirus treatment for 12 h compared to the mock transduced cells. (d–g) Brightfield images of wound area 12 h after wounding and staining with crystal violet at 10 \times ; (c) mock transduced and (d) transduced with BV released from alginate hydrogels on day 8; (e) transduced with BV released from chitosan–alginate hydrogels on day 8; (h) control baculovirus transduction with a MOI of 100; (g) wound area (%) after hydrogel treatment over time compared to the mock cells. (i) Growth inhibition zone of bacteria from alginate and alginate–chitosan hydrogels using the antimicrobial disc diffusion method. $n = 3$ per group. * Indicates a significance of $p < 0.05$ and ** indicates a significance of $p < 0.005$ (see the Appendix for additional data).

The baculovirus delivery system also demonstrated a high safety profile. Specifically, there was no significant decrease in proliferation or viability in the hydrogel-treated cells compared to the mock-infected cells. The baculovirus significantly improved cell proliferation compared to the mock transduced cells (Figure 15a). The viability also remained high for all treatment groups, above 94.3 %, with no significant difference except for the alginate hydrogels (Figure 15b). Moreover, the baculovirus and hydrogel delivery system demonstrated blood biocompatibility

with no significant hemolysis (Figure 15c). The baculovirus, gene expression, and hydrogel formulations all showed negligible hemolysis, below 5 %. The hydrogels also promoted whole blood clotting over time compared to the polystyrene “mock” control (Figure 15d). Overall, the baculovirus-eluting hydrogels demonstrated no cytotoxicity or antimicrobial properties, and improved cell migration and angiogenesis.

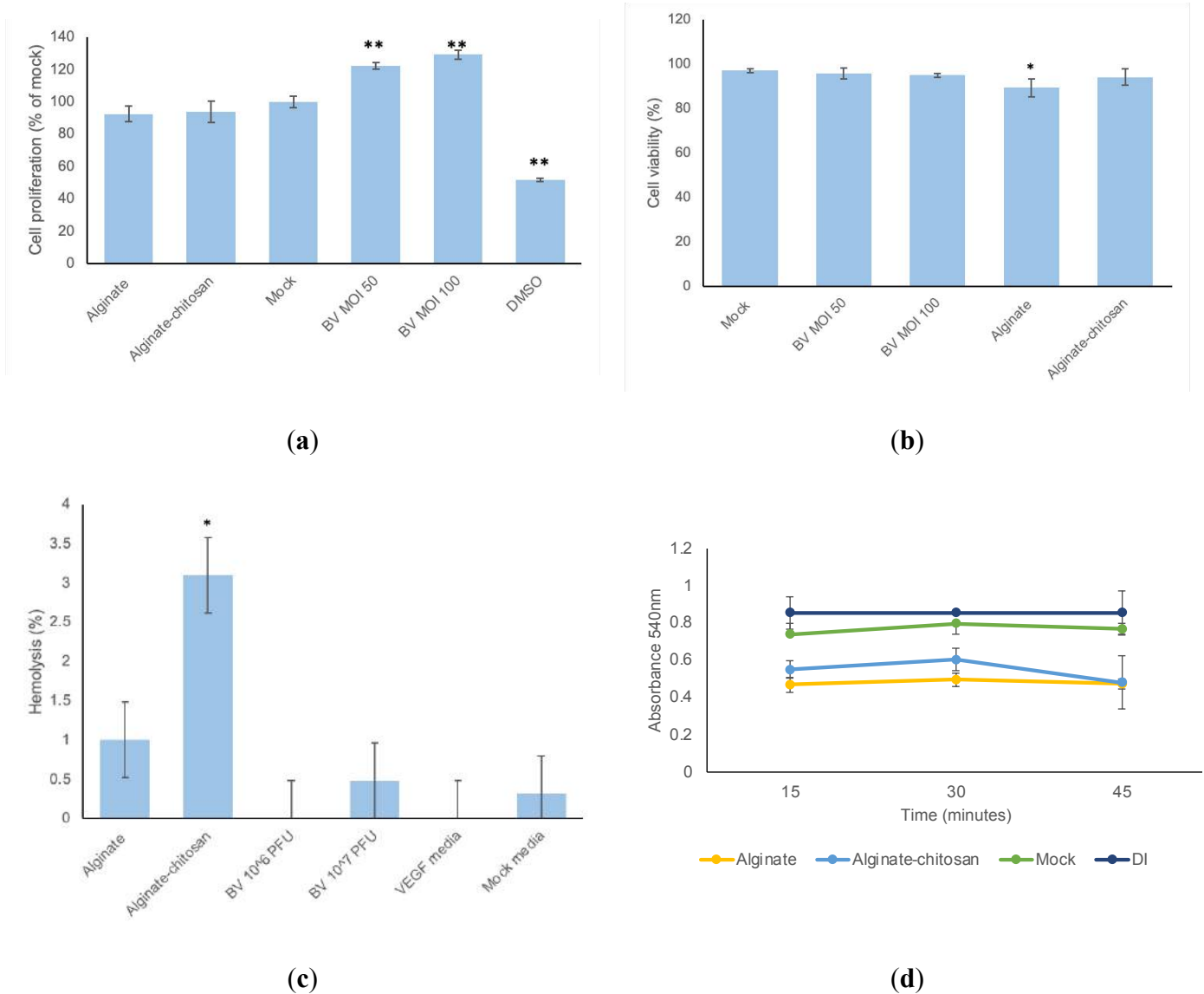


Figure 15. Hydrogel cytotoxicity and hemocompatibility studies.

(a) MTT proliferation assay with HUVECs after treatment with different hydrogels or the BV compared to the mock transduced cells. (b) HUVEC viability (%) after BV transduction or hydrogel incubation for

24 h compared to the mock cells. (c) Compared to the mock cell media, hemolysis (%) of the hydrogels, baculovirus (BV), and VEGFA expressed from the BV. (d) Whole blood clotting on the surface of the hydrogels compared to polystyrene (mock) and deionized water (control). $n = 3$ per group and repeated twice. * indicates $p < 0.05$ and ** indicates $p < 0.005$.

Discussion

The hydrogel delivery formulation presented here is cost-effective, requiring few resources and natural polymers (alginate and chitosan) that are widely abundant and inexpensive. Alginate and chitosan are also known for their excellent biocompatibility, bioadhesion, and biodegradability [153]. Moreover, the hydrogels do not require harsh solvents, promoting their safety and preventing baculovirus inactivation during synthesis. The hydrogels are also easily pre-sterilized to avoid bacterial contamination in the wound.

The ionically cross-linked hydrogels were smooth and demonstrated good stability at various temperatures and osmotic gradients. Their stability at different temperatures is also beneficial to improve the feasibility and allows for sufficient storage time before expiration. Moreover, their stability in saline, PBS, and at a pH of 4 demonstrates their ability to perform in various physiological conditions. A pH of 4 would be comparable to the acidic environment observed as wounds begin to heal [154]. Moreover, a 1 (v/v) % concentration of acetic acid has been shown to be effective against a wide range of bacteria and fungi, effectively preventing infection and multi-resistant bacteria [155]. Beneficially, the chitosan coating is dissolved in acetic acid, which creates an acidic environment to promote wound healing [154]. Moreover, hydrogel swelling is important for bacterial entrapment and microbial growth inhibition [156].

The high baculovirus encapsulation (99.9 %) promotes the system's deliverability and minimizes costs with the little virus going to waste. The baculovirus elution was sustained over

eight days, overcoming the transient baculovirus delivery previously reported [101], [104]. Moreover, sustained baculovirus elution has a vast potential in chronic wound environments, whereby healing is a slow process. The virus activity also remained active and was capable of transducing 40 % of cells with an MOI of 50. Overall, this delivery system can prolong baculovirus delivery with a therapeutic effect.

The baculovirus eluted from the hydrogels also possessed beneficial properties for wound-healing applications, including no cytotoxicity, good blood compatibility, and significantly improved wound healing and angiogenesis compared to the mock cells. Specifically, there was no significant difference in proliferation or viability in the hydrogel-treated cells compared to the mock-infected cells. Moreover, the baculovirus and hydrogel delivery system demonstrated blood biocompatibility with no significant hemolysis. The hydrogels also promoted blood coagulation over time (15–45 min), effectively preventing excessive bleeding and creating a barrier for the wound. The VEGFA expression from the baculovirus hydrogels also significantly improved HUVEC migration over eight days leading to improved considerably wound healing.

Moreover, the baculovirus delivery significantly improved tube formation in the angiogenesis assay, which can assist with wound revascularization. The chitosan coating demonstrated the best wound-healing ability, which may be attributed to improved baculovirus transduction due to the positively charged chitosan and slightly acidic pH created by the polymer coating [157]. Overall, the chitosan coating prolonged baculovirus delivery and improved wound healing, cell proliferation, and antimicrobial resistance.

Some limitations include investigating the immune and cytokine response and other growth factors. The possibility of fibromatosis due to growth factor elution should also be investigated. However, preliminary studies reveal that VEGF promotes fibrogenesis but is also needed for

fibrosis resolution [158]. Future studies should also investigate the in vivo impact on healing with reference to the immune response and the several organ systems at play. Overall, these baculovirus-eluting hydrogels enable sustained baculovirus delivery which releases VEGFA to promote cell migration, proliferation, and tube formation along with beneficial safety properties in vitro. The baculovirus-eluting hydrogels may have future applications in wound healing through the promotion of angiogenesis.

Conclusion

Baculovirus' VEGFA gene delivery to endothelial cells is efficient and safe. Alginate and chitosan–alginate hydrogels, with an encapsulation efficiency of 99.9%, can prolong virus delivery and increase the therapeutic window. Moreover, the encapsulated baculovirus maintained its activity and was released in a sustained manner over eight days. The virus transduction efficiency can reach over 40% with the hydrogel delivery system. The baculovirus elution stimulates tube formation, cell proliferation, and cell migration, all contributing to angiogenesis. This may be beneficial for chronic wound-healing applications. Moreover, this is proof of concept that encapsulation can prolong baculovirus elution, making it a candidate for several gene therapy applications.

Materials and Methods

Insect cell culture

Sf21insect cells (Invitrogen Life Technologies, Carlsbad, CA, USA) were maintained at 27 °C in SF900 II serum-free medium in T-75 flasks or 250 mL shake flasks (Erlenmeyer, CA, USA). The Sf21 cells in the shake flasks were maintained in a shaking incubator at 130 rpm. The cells were subcultured two to three times weekly to maintain the exponential growth phase.

Gene cloning

The human VEGFA in a pcDNA3.1 + eGFP vector was purchased from GenScript USA. The EGFP-tagged VEGFA gene was excised from the original plasmid using EcoRI and XbaI Fast Digest restriction enzymes (Thermo Fisher, Waltham, MA, USA). The resultant genes of interest were run on a 1 % (*m/v*) agarose gel containing SYBR Green (Thermo Fisher) at 100 Volts. After one hour, the DNA bands were visualized using a blue light transilluminator (miniPCR bio, Boston, MA, USA). Each gene fragment was excised and purified using NEB's Gel Extraction Kit. The genes of interest were each ligated, using Instant Sticky End Ligase (NEB), into the pOET6 plasmid with compatible sticky ends. The VEGFA-eGFP-pOET6 plasmid was then chemically transformed into DH5 α *E. coli* (Thermo Fisher) and selected for using the ampicillin resistance present within the pOET6 plasmid (MJS BioLynx Inc., Brockville, ON, Canada). Different LB agar plates were streaked with different dilutions of the transformed bacteria and grown overnight. The next day, the resistant colonies containing the gene of interest were selected and grown overnight to amplify the plasmid. The plasmid was then extracted and purified using NEB's plasmid purification kit. The resultant purified pOET6 plasmid, each with a gene of interest, was used for all future virus production steps or frozen at -20 °C for future use.

Baculovirus production

The supplier's protocol was followed for baculovirus production [28]. In an exponential growth phase, 5×10^5 Sf21 cells were seeded into a 12-well plate one hour before virus transfection. Next, 200 ng of VEGFA-EGFP-pOET6 plasmid was added to 100 ng of flashBAC DNA (Oxford Expression Technologies, Oxford, UK), 0.48 μ L of TransIT Insect Reagent (MJS BioLynx, Brockville, ON, Canada), and 100 μ L PBS and incubated at room temperature for 15 min. The transfection mixture was then added to the Sf21 cells and incubated overnight at 27 °C. The next day, 0.5 mL of SFM-II was added. Five days after transfection, the

culture medium was harvested and centrifuged at $1000\times g$ for 10 min. The supernatant was collected and stored at 4 °C (P_0 virus stock). To amplify the baculovirus, 100 mL of Sf21 cells were diluted to 2×10^6 cells/mL in SF900II medium, and 0.4 mL of P_0 virus stock was added. The infected Sf21 cells were agitated at 130 rpm for four days before harvesting the culture medium as described above. This generated P_1 baculovirus stock expressing VEGFA.

Baculovirus titration

The baculovirus was titrated using viral plaque assays or endpoint dilutions to determine the initial stock concentration and encapsulation efficiency, respectively. For the plaque assay, 0.5×10^6 cells were seeded into each well of a 12-well plate and incubated for one hour. A sample of the P_1 virus stock was used to make serial dilution (down to 10^{-7}). After the one-hour incubation, the media was removed from each well and 100 μ L of each dilution (10^{-4} to 10^{-7} dilutions) was added to a well in triplicate. The infected Sf9 cells were incubated at room temperature for 1 h, after which the 100 μ L of inoculum was removed. For the plaque assay, a 1 % (*m/v*) agarose-SFM-II overlay was added to the side of each well. The overlay solidified at room temperature, after 0.5 mL of SFM-II was added. The plate was then incubated at 27 °C for 4 days. After 4 days, 0.5 mL of neutral red (0.25 mg/mL) was added to each well and incubated for 3 hours. After 3 hours, the neutral red stain was removed, and the plates were inverted to allow the plaques to clear. Wells with 10 to 30 plaque-forming units (PFUs) were counted, and the plaque count was averaged to determine the viral titer using the following equation.

$$\text{Titer of virus (pfu/mL)} = (\text{average plaque count}) \times (\text{dilution factor}^*) \times (10^{**}).$$

* Dilution factor = the inverse of the dilution used on the counted plate.

** Multiply by 10 because 0.1 mL was applied to each dish.

For the endpoint dilution, 10,000 Sf21 cells were seeded per well in a 96-well plate and incubated for 1 hour. During this time, serial dilutions of the virus were made using SFM-II (down to 10^{-10}). After the one hour incubation, each virus dilution was added to 10 separate wells. The plate was then incubated for five days and observed for cytopathic effect (CPE) in each well. The titer was calculated using the following equation.

$$\text{Titer (pfu/mL)} = 10(1 + Z (X - 0.5))$$

where Z is Log 10 of the starting dilution (1 for a ten-fold dilution) and X is the sum of the fractions of CPE-positive wells.

Endothelial cell culture

Human umbilical vein endothelial cells (HUVECs) were purchased from Sigma Aldrich. The HUVECs were maintained in T-25 flasks in a 37 °C, 5 % CO₂ incubator. A complete endothelial growth medium (Sigma Aldrich, St. Louis, MI, USA) was used to culture the HUVECs. Cells were used within 4–5 passages upon receiving.

Spherical hydrogel preparation

Ionic cross-linking was employed for virus encapsulation under aseptic conditions. First, a 4 % (*m/v*) sodium alginate, 2 % (*m/v*) chitosan with 0.5 % (*v/v*) acetic acid, and 100 mM calcium chloride solution was prepared (Sigma Aldrich and Bio-Basic, Markham, ON, Canada). The sodium alginate and chitosan were sterilized in the autoclave for 20 min. The calcium chloride was sterilized using a 0.20 µm filter. Next, 1.5 mL of sodium alginate solution was mixed with either sterile water for the mock hydrogels or baculovirus stock in a 50:50 ratio. The remaining 2 % (*m/v*) alginate solution was then loaded into a 5 mL syringe and added dropwise, using a 30-gauge needle, into a beaker containing 20 mL of calcium chloride, stirring on the lowest possible setting. The hydrogels formed instantly and were allowed to solidify in the beaker for 10 min. After this,

the calcium chloride solution was aspirated off, and 1 mL of the 2 % (*m/v*) chitosan solution was added for 5 minutes. The supernatant was saved to determine the encapsulation efficiency. The hydrogels were washed with PBS three times and finally resuspended in PBS to evaluate the virus elution over time.

Hydrogel morphology and swelling

To observe the morphology, freshly formed hydrogels were imaged under an inverted microscope using brightfield at 4 × magnification. The size of 10 random hydrogels was measured using ImageJ. Some of the spherical hydrogels were dried overnight, imaged, and measured to determine the swelling ratio using the following equation:

$$\text{Swelling ratio} = \text{Weight}_{\text{swollen}} / \text{Weight}_{\text{dry}}$$

Scanning electron microscopy (SEM)

The uncoated and coated hydrogels were removed from suspension and dried overnight in a 37 °C incubator. They were then visualized using a FEI 450 Quanta SEM under high vacuum at 10 kV.

Zeta potential

The hydrogels were resuspended in MilliQ water. Next, a zeta potential analyzer with electrophoretic laser Doppler anemometry (Brookhaven Instruments Corporation, Holtsville, New York, NY, USA) was used to determine the surface charge of the hydrogels. Zeta Potential Analyzer version 3.57 software was used to determine the zeta potential. Each measurement was obtained after taking the average of the ten runs.

Encapsulation efficiency of the hydrogel delivery formulation

The supernatant from the virus encapsulation process was preserved and titrated to determine the encapsulation efficiency.

Encapsulation efficiency % = encapsulated virus concentration/ initial virus concentration \times 100 %

Hydrogel stability

The stability of the hydrogels was evaluated using an osmotic pressure and a rotational stress test. The osmotic pressure test was performed by transferring 50 microcapsules into deionized water in a flask. The rotational stress test consisted of transferring 50 microcapsules into a hypotonic solution (deionized water) and shaking it at 150 rpm at 37 °C for several days. The hydrogels were also resuspended in PBS pH 7.4, saline solution, or PBS pH 4 (addition of HCl) and shaken to test their stability in a variety of environments.

Antimicrobial studies

The antimicrobial properties of the alginate and alginate–chitosan hydrogels were tested using an adapted disc diffusion method [159]. Briefly, *E. coli* was grown in Luria-Bertani (LB) medium, and *C. albicans* were grown in YPD media. Dilutions of the bacteria were spread on LB agar or YPD agar plates to determine the number of colony-forming units (CFU). The bacteria were diluted to 10^8 CFU/mL and 100 μ L was spread onto fresh LB/YPD agar plates. The different hydrogels were plated onto the plates containing *E. coli* or *C. albicans* and incubated at 37 °C for up to 24 hours. A drop (10 μ L) of penicillin was used as a negative control. After 24 h, the area of growth inhibition was observed and measured.

Baculovirus release and activity

Release studies were performed by incubating freshly formed hydrogels, containing baculovirus in 2 mL of PBS. The supernatant (baculovirus in PBS) was removed and replaced with fresh PBS every 24 h until all virus was released. The hydrogel suspension media was then used to transduce mammalian cells (HUVECs) in 96-well plates to determine the virus activity.

Baculovirus transduction

The hydrogel suspension media or the virus stock itself was added to either HUVECs, in black 96-well plates (Corning 3603) and incubated at 37 °C. After three hours of incubation, the virus or hydrogel suspension media was removed and replaced with fresh cell media. The cells were incubated for 24–48 h to allow for viral gene expression. These cells were then imaged using the green and blue fluorescent filter in the ImageXpress Micro[®] Confocal High-Content Imaging System (Molecular Devices, San Jose, CA, USA). At 24 hours, the cells were imaged using brightfield and fluorescent microscopy (green filter). At 48 h, the percent of fluorescent cells was compared to the number of cells using DAPI staining for the nuclei (blue filter) and a green filter for the EGFP-tagged VEGFA expression.

Baculovirus gene expression

VEGFA PCR primers were purchased from Bio-Rad. HUVECs (2×10^4 cells/well) were seeded into a 48-well plate and incubated overnight. The HUVECs were then transduced with different MOIs of baculovirus for three hours after which the virus inoculum was removed and replaced with fresh cell media. At 24 hours post-infection (hpi), the media was saved for the angiogenesis assay, and the total RNA from each well was extracted using Bio-Basic's Total RNA Extraction Kit. The extracted RNA was then mixed with the Luna Universal One-Step RT-qPCR kit (NEB) and primers. The mixture was then placed into the Eco Illumina PCR[®] system. Amplification was carried out for 40 cycles with 35 s (denaturation), 55 °C for 35 s (annealing), and 72 °C for 25 s (extension).

MTT proliferation assay

An MTT cell growth assay kit was purchased from Sigma Aldrich. As above, different MOIs of BV and the hydrogel supernatant were added to HUVECs (10,000 cells/well in a 96-well plate) and incubated for three hours. PBS and DMSO were used as a positive and negative control,

respectively. After three hours of incubation, the baculovirus supernatant was removed and replaced with fresh media. Next, 24 hpi, 0.01 mL of AB Solution (MTT) was added to each well. The cells were incubated for 4 hours at 37 °C to allow MTT cleavage. After one hour, 0.1 mL of isopropanol with 0.04 N HCl was added to each well. The isopropanol solution was mixed thoroughly via pipetting. The plate was then read using an EnSpire Multimode plate reader (Perkin Elmer, Waltham, MA, USA) with a wavelength of 570 nm.

Live Dead assay

A Live Dead Assay was employed to estimate the hydrogels' cytotoxicity. First, 2×10^4 HUVECs/well were seeded into a 48-well plate and incubated overnight. The next day, the hydrogels were added to each well in triplicate and incubated. Media alone or DMSO was used as a control. After 24 hours, 5 μ L of 1 mM Calcein AM and 5 μ L of 2.5 mg/mL propidium iodide (both from Thermo Fisher) were added to 10 mL of cell media. This solution was then added to the cells in the 48-well plate and incubated at 37 °C for 30 min. After 30 min, the cells were imaged (three random images per well) using the green and red filters on the Leica DMIL microscope with a Canon T3i camera. ImageJ 'analyze particles' was used to count the number of live (green) and dead (red) cells.

Hemocompatibility studies

Blood samples from two individuals were obtained from Innovative Research and tested independently in triplicate. One sample was from a Male 49, Hispanic and one from a female 29, white. The potential hemolysis of the virus itself, gene expression, and the hydrogels were evaluated. Briefly, all tested samples were immersed into 5 mL of PBS in a 15 mL centrifuge tube. Next, 4 mL of citrated blood was mixed with 5 mL PBS and 0.1 mL of the diluted blood was added to each sample. The samples were incubated at 37 °C for one hour and then centrifuged at 1000

rpm for 10 min. The supernatant containing the lysed hemoglobin was placed into a 96-well plate, and the absorbance was read at 545 nm. The negative and positive control was PBS and deionized water, respectively. The following equation was used to determine the % hemolysis.

$$\text{Hemolysis (\%)} = ((\text{OD}_{\text{sample}} - \text{OD}_{\text{negative control}}) / (\text{OD}_{\text{positive}} - \text{OD}_{\text{negative}})) \times 100 \%$$

Blood clotting on the hydrogels was also evaluated using a method described by Sabino et al. (2020) [160]. Briefly, the hydrogels were placed into a 24-well plate. Next, 7 μL of whole blood was pipetted onto the surface of the hydrogels. At 15, 30 and 45 min, deionized water was added to each sample and incubated for 5 minutes. The resulting supernatant was removed, and the absorbance was read on a 96-well plate at 540 nm. As a control, 7 μL of whole blood in distilled water was used as a control where no blood clotted onto a biomaterial surface. A ‘mock’ polystyrene surface was also used to compare the blood coagulation properties of the hydrogels.

Wound healing assay

Growth factors, such as VEGFA, induce endothelial cell migration, as demonstrated by a wound-healing or scratch assay [161]. HUVECs were seeded in 96-well plates and grown to confluency. Twenty-four hours before scratching the cells, the cells were transduced with baculovirus. Specifically, the wells were incubated with baculovirus for two hours (PBS was used as a mock), and then the virus solution was replaced with fresh cell media. The next day, a straight wound was generated down the middle of each well using a 200 μL pipette tip. After 12 hours, the cells were visualized and imaged using a Leica DMIL microscope with a Canon T3i camera. After 24 hours, the cells were fixed with 4 % (w/v) paraformaldehyde and stained with crystal violet (Thermo Fisher). The wound-healing ability was evaluated using an open-access ImageJ plugin [162].

Endothelial tube formation assay

To confirm the angiogenic potential of VEGFA released from the baculovirus a standard angiogenesis assay was performed as described elsewhere with slight modifications [163]. First, the supernatant from baculovirus transduced cells (containing the eluted VEGFA) was added as the angiogenic stimulator. Endothelial cell media with VEGF was used as a positive control, and DMSO (a known inhibitor of angiogenesis) was used as the negative control [164]. The cells were then incubated until tube formation was observed. After 2 hours, the wells were imaged using a phase contrast microscope. The images were analyzed using an ImageJ plugin [165].

Statistical analysis

All experiments were performed at least twice on different days and with three replicates each time. The values are expressed as the mean \pm standard deviation for each experiment. SPSS (SPSS Inc., Chicago, IL, USA, IBM version 28) was used to perform all statistical analyses and ImageJ was used for all image analyses. A p-value of less than 0.05 was considered statistically significant.

Copyright: This is an open-access article under the CC BY-NC-ND license (<http://creativecommons.org/licenses/by-nc-nd/4.0/>).

Bridging text

In this paper, I have created a baculovirus-eluting hydrogel that is stable, antibacterial, hemocompatible, and sustains baculovirus VEGFA gene delivery. The hydrogel system can sustain baculovirus elution over eight to ten days, depending on the formulation. The hydrogel system was stable over a month, even at accelerated conditions. Moreover, the chitosan-coated hydrogel demonstrated antibacterial properties and was capable of swelling to prevent wound infection and remove wound debris. The baculovirus hydrogel systems did not induce hemolysis and promoted blood coagulation. Improved blood coagulation is an important aspect of a wound dressing to help prevent excessive bleeding. Moreover, the sustained baculovirus elution leads to sustained VEGFA elution (expressed by the BV). VEGFA assists with cell migration, proliferation, and angiogenesis, which is important for promoting initial wound healing. This system can support chronic wound recovery by regenerating an endothelial layer, promoting revascularization, and preventing infection.

The enhanced cell proliferation, migration, and angiogenesis are also beneficial for the initial days after stent implantation, whereby the damaged endothelial arterial lining can benefit from the effects of localized VEGFA delivery. Moreover, enhanced angiogenesis would promote increased blood flow and vascularization, restoring nutrient and blood delivery. However, the hydrogel is not stable enough to be a stent coating and the promotion of blood coagulation is not beneficial for stenting applications. Consequently, I wanted to investigate alternative polymers. I chose to stick with natural and biodegradable sources so they could more easily integrate with new biodegradable stent systems. I investigated several polymers, including alginate, chitosan, polyvinyl alcohol (PVA), poly lactic-co-glycolic acid (PLGA), polylactic acid (PLA), dextran, polyethylene glycol (PEG), and gelatin. The following paper will focus on creating a customizable

and controlled hydrogel system for stent coating using the polymers mentioned before and different synthesis or loading methods.

CHAPTER 6: Controlled and customizable baculovirus NOS3 gene delivery using PVA-based hydrogel systems

**Sabrina Schaly¹, Paromita Islam¹, Jacqueline L. Boyajian¹, Rahul Thareja¹, Ahmed Abosalha^{1,2},
Karan Arora¹, Dominique Shum-Tim³, and Satya Prakash^{1,*}**

¹ Biomedical Technology and Cell Therapy Research Laboratory, Department of Biomedical Engineering, Faculty of Medicine and Health Sciences, McGill University, Montreal, Quebec, Canada

² Pharmaceutical Technology Department, Faculty of Pharmacy, Tanta University, Tanta 31111, Egypt

³ Division of Cardiac Surgery, Royal Victoria Hospital, McGill University Health Centre, McGill University, Faculty of Medicine and Health Sciences, Montreal, Quebec, Canada

* Corresponding author: satya.prakash@mcgill.ca (SP)

Contributions of the author: I am the first author and contributed to the design, experiments, and manuscript preparation.

PLOS One

(Published)

Abstract

Nitric oxide synthase 3 (NOS3) eluting polyvinyl alcohol-based hydrogels have a large potential in medical applications and device coatings. NOS3 promotes nitric oxide and nitrate production and can effectively be delivered using insect cell viruses, termed baculoviruses. Nitric oxide is known for regulating cell proliferation, promoting blood vessel vasodilation, and inhibiting bacterial growth. The polyvinyl alcohol (PVA)-based hydrogels investigated here sustained baculovirus elution from five to 25 days, depending on the hydrogel composition. The quantity of viable baculovirus loaded significantly declined with each freeze-thaw from one to four ($15.3 \pm 2.9\%$ vs. $0.9 \pm 0.5\%$, respectively). The addition of gelatin to the hydrogels protected baculovirus viability during the freeze-thaw cycles, resulting in a loading capacity of $94.6 \pm 1.2\%$ with sustained elution over 23 days. Adding chitosan, PEG-8000, and gelatin to the hydrogels altered the properties of the hydrogel, including swelling, blood coagulation, and antimicrobial effects, beneficial for different therapeutic applications. Passive absorption of the baculovirus into PVA hydrogels exhibited the highest baculovirus loading ($96.4 \pm 0.6\%$) with elution over 25 days. The baculovirus-eluting hydrogels were hemocompatible and non-cytotoxic, with no cell proliferation or viability reduction after incubation. This PVA delivery system provides a method for high loading and sustained release of baculoviruses, sustaining nitric oxide gene delivery. This proof of concept has clinical applications as a medical device or stent coating by delivering therapeutic genes, improving blood compatibility, preventing thrombosis, and preventing infection.

Keywords: baculovirus, gene delivery, PVA hydrogel, nitric oxide, controlled release, freeze-thaw, medical device coating

Introduction

Polyvinyl alcohol (PVA) is one of the most versatile synthetic polymers used in medical applications. PVA has several applications, including tissue engineering, dental implants, drug delivery systems, wound dressings, contact lenses, cosmetics, and more [166]. PVA's popularity may be attributed to its inherent biosafety and hemocompatibility [167]. Even when administered orally, PVA demonstrates low toxicity (a lethal dose of 15-20 g/kg), is poorly absorbed in the gastrointestinal system, and is not mutagenic [168]. Another benefit of PVA is the tunability of its mechanical properties. Specifically, the tensile strength, toughness, elongation, and elastic modulus can vary significantly depending on the ions used during the aggregation [169]. The properties of the PVA can be further customized by adding other polymers or particles. Previously, chitosan, cellulose, Gellan Gum, protein, starch, nanotubes, and nanoparticles, and more have been used to alter PVA's properties [170]. Moreover, the solution temperature and synthesis method (ex., cross-linker) alter the polymer's strength and elasticity. These modifiable properties are beneficial when customizing hydrogels for different medical applications.

The addition of different polymers to PVA also provides new biological properties. For example, gelatin is a natural polymer that promotes cell attachment in tissue engineering applications and cell spheroids [171]. Gelatin is also non-toxic, non-immunogenic, low-cost, and widely available [172]. Gelatin has been investigated and used in drug delivery carriers, bioinks, tissue engineering, and wound dressings. Alternatively, chitosan has anti-inflammatory, antimicrobial, and antioxidant properties [173]. Also, chitosan can bind negatively charged particles, including baculoviruses to improve transduction efficiency. Adding chitosan has been shown to increase the tensile strength and elastic modulus while decreasing the elongation of PVA-

chitosan films [170]. Finally, polyethylene glycol (PEG) was selected for its biocompatibility and controlled drug release properties [174].

Hydrogels are helpful delivery platforms for drugs, proteins, genes, or growth factors to treat several diseases. PVA-based hydrogels have been studied for treating colon cancer, sustained ibuprofen delivery, and medical device coatings [175]–[177]. Specifically, nitric oxide-releasing coatings are beneficial for their enhanced biocompatibility, inhibition of thrombosis, and antibacterial properties. Moreover, nitric oxide inhibits platelet adhesion and reduces smooth muscle cell proliferation, which are beneficial hemocompatibility properties [177]. Nitric oxide also has antimicrobial effects and prevents biofilm creation [178], [179]. These properties make PVA hydrogels promising for medical device coatings, specifically stent coatings.

Stenting is a common treatment for coronary artery disease. However, damage to the arterial cells, mainly endothelial and smooth muscle cells (SMCs), leads to complications such as in-stent restenosis (ISR) and thrombosis. Different stent coatings have been developed, including drug-eluting stents to prevent inflammation and ISR. Alternatively, nitric oxide delivery regulates blood coagulation, prevents platelet adhesion, prevents thrombosis, prevents SMC proliferation, and promotes endothelial health and migration for re-endothelialization [180]. NOS3 also plays a key role in vascular homeostasis and protects the intima from platelet aggregation and leukocyte adhesion [116]. NOS3 expression is crucial in the initial two weeks after stent implantation to regulate vascular function and promote an anti-inflammatory environment [180]. Controlled NOS3 delivery could thus prevent platelet aggregation and SMC hyperproliferation, mitigating complications such as thrombosis and in-stent restenosis, respectively.

There are challenges associated with eluting genes from hydrogels. Some limitations include burst release, growth factor degradation, and low loading efficiency. One limitation

associated with PVA hydrogels, is their hydrophilicity, making hydrophobic drug loading challenging and leading to an initial burst release [181]. However, this limitation can be overcome by optimizing the synthesis method, adding additional polymers, or an additional coating [181], [182]. One method to extend and control gene elution is through a viral delivery system. Specifically, baculoviruses are insect cell viruses that allow transient gene delivery in humans [183]. Baculoviruses are also non-toxic, have low immunogenicity, and provide transient yet high gene expression [81], [106], [107][77],[113], [125]. Compared to other viral vectors such as adenoviruses, retroviruses, and lentiviruses, baculoviruses have lower immunogenicity, lower cost, higher biosafety, larger cloning capacity (300+ kb), and are easier to scale up [125]. Baculoviruses also demonstrate higher gene expression than direct gene delivery due to the protective virus capsid [113]. However, baculovirus stability has been reported to decline quickly at temperatures matching or exceeding room temperature [140]. To mitigate this, the PVA hydrogel delivery system was developed to prevent baculovirus decline and provide controlled release. In addition, baculovirus encapsulation within hydrogels can prevent immune inactivation, effectively shielding the virus from the immune system and promoting its stability. The polymer gene delivery platform also promotes site-specificity by releasing virus directly at the contact site [123]. The site specificity allows for a lower dosage and improves the therapeutic range.

Here, we develop and investigate a PVA-based baculovirus eluting delivery system. We will investigate how PVA-based hydrogels can overcome limitations associated with baculovirus gene delivery. Different hydrogel synthesis methods are explored to determine their impact on virus stability and loading efficiency. Moreover, polymers are added to the PVA hydrogels to modify PVA's properties. Specifically, we investigate how the elution duration, hydrogel properties, and gene dosage can be controlled and customized. Controlled baculovirus elution

studies have been limited [136]. To our knowledge, this is the first study optimizing PVA-based hydrogels containing baculovirus gene delivery vectors. This is used as a proof of concept that PVA-baculovirus hydrogels can be tunable to treat a wide variety of diseases and are a promising option for medical device coating.

Results and Discussion

Morphology, swelling, antibacterial, and hemocompatibility of PVA-based hydrogels

First, freeze-thawed PVA hydrogels were investigated for sustained baculovirus delivery. Up to four freeze-thaw cycles were used. For one, two, three, and four freeze-thaw cycles, the hydrogels are named PVA1, PVA2, PVA3, PVA4, respectively. The number of freeze-thaw cycles was optimized to maximize baculovirus entrapment. The functionality of baculoviruses diminished with every freeze-thaw cycle. However, to maintain mechanical strength, two freeze-thaw cycles were used. Consequently, unless otherwise stated, two freeze-thaw cycles were employed for all subsequent hydrogels. Next, different polymers were added to the PVA solution before casting, which altered the baculovirus entrapment and release. Chitosan, PEG-8000, or gelatin were added to the PVA solution, termed PVA-chitosan, PVA-PEG, and PVA-gelatin, respectively. After this, the baculovirus was added and the solution mixed. After two freeze-thaw cycles, the hydrogels were removed and incubated in HBSS to test the virus elution over time.

The properties of the PVA-based hydrogels were evaluated via ATR-FTIR, swelling ratios, antimicrobial properties, and surface morphology using scanning electron microscopy (SEM). The addition of each polymer was confirmed with ATR-FTIR, with new peaks indicating the presence of gelatin, chitosan, or PEG-8000. The PVA base had the characteristic FTIR peaks for the hydroxyl group ($3200\text{-}3600\text{ cm}^{-1}$), C-H stretching ($2850\text{-}3000\text{ cm}^{-1}$), the carbonyl group (1745 cm^{-1}), and CH_2 wagging (1400 cm^{-1}). Gelatin also had a characteristic peak due to N-H stretching

(3200-3600 cm^{-1}). The amide bond within the gelatin also added an additional peak at 1540-1650 cm^{-1} . PEG-8000 added peaks for the hydroxyl groups and C-H stretching. The ether bond within PEG also added a peak around 1100-1200 cm^{-1} . Moreover, the hydrogels maintained a similar morphology despite the addition of other polymers.

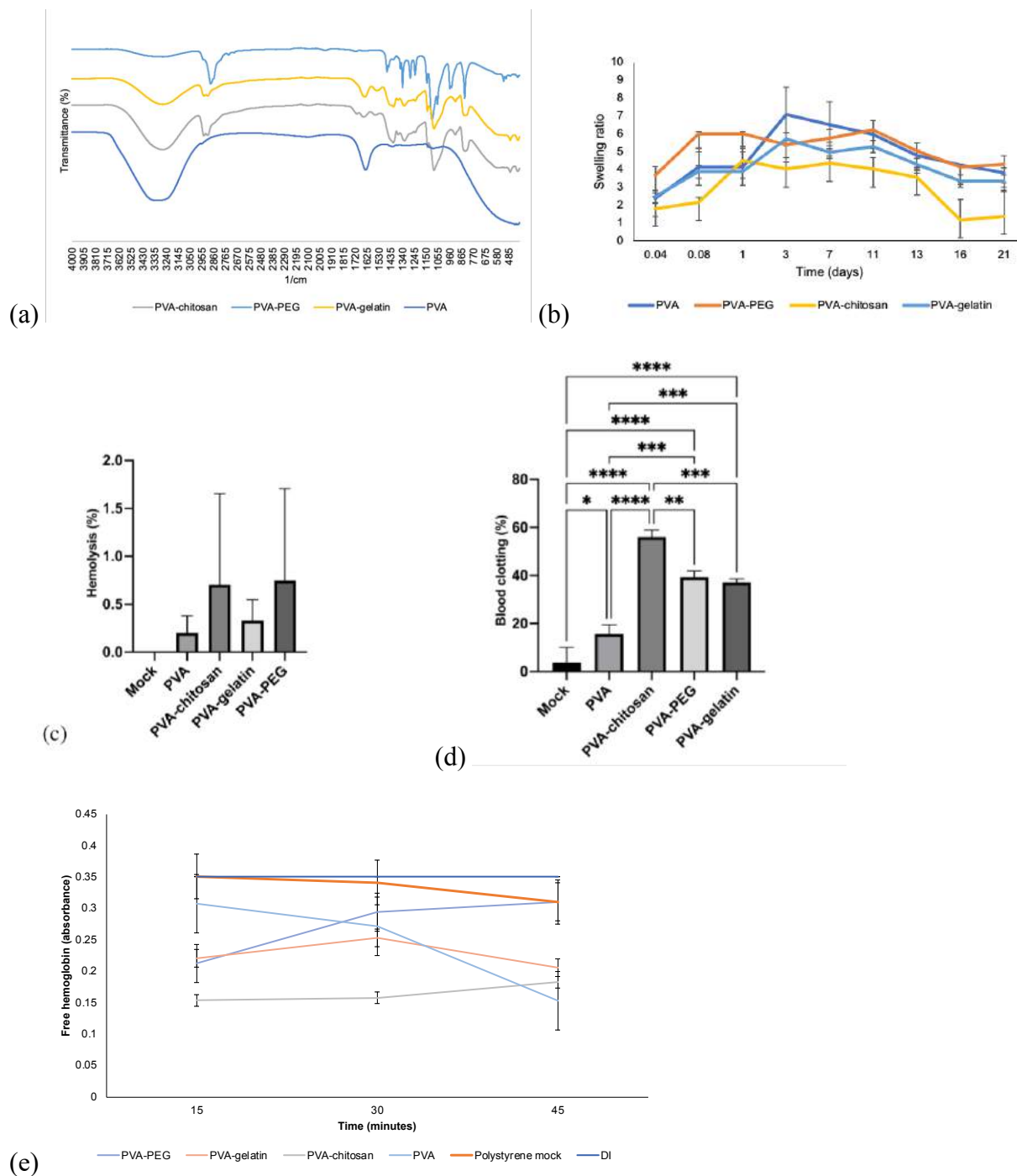


Figure 16. Properties of the PVA-based hydrogels

(a) ATR-FTIR of PVA-based hydrogels. (b) PVA-based hydrogel swelling over time. (c) Hemolysis of red blood cells after incubation with PVA-based hydrogels. (d) Blood coagulation on the surface of the PVA-based hydrogels after 45 minutes of incubation. (e) Blood coagulation on the surface of the PVA-based hydrogels after incubating over time.

The hydrogels initially swelled up to three times their weight after incubating in HBSS for one hour. After two hours, most hydrogels had reached their peak swelling capacity. The PVA-based hydrogels had different swelling ratios depending on the polymer addition. The maximum swelling ratio varied from 4.0 to 7.1 (Table 3). The swelling increased over time, peaking at day three. After day three, the swelling ratio slowly decreased until the original weight was achieved from day one indicating suitable stability over 21 days. Passive baculovirus diffusion onto the PVA hydrogel was the most efficient and thus the stability was evaluated over two months. Overall, no significant change in weighted stability was observed over the 56 days tested at accelerated conditions (37 °C and 150 rpm). The antimicrobial properties of the hydrogels were also investigated (Table 3). All hydrogels blocked bacterial growth directly beneath (2.0 ± 0.1 mm), but only PVA-chitosan resulted in a one-millimeter growth inhibition zone of *E. coli* (3.0 ± 0.1 mm) but not *C. Albicans*. This was compared to a growth inhibition zone of 3.0 ± 0.5 mm using 500 units of penicillin-streptomycin control solution.

Table 3. PVA-based hydrogel swelling ratio and antimicrobial properties

Hydrogel type	Maximum swelling ratio (average \pm SD)	Antimicrobial inhibition (mm \pm SD)
PVA	7.1 ± 1.5	2.0 ± 0.1
PVA-PEG	6.0 ± 0.2	2.0 ± 0.1
PVA-chitosan	5.7 ± 3.4	3.0 ± 0.1
PVA-gelatin	4.0 ± 0.6	2.0 ± 0.1

The PVA-based hydrogels also demonstrated hemocompatibility. The blood compatibility was evaluated using a standard hemolysis and blood coagulation assay. After the one-hour incubation, some degree of hemolysis was observed after incubating the blood samples with the hydrogels (Figure 16c). However, all the hydrogels were considered non-hemolytic with hemolysis below 2.0 %. The PVA-chitosan and PVA-PEG hydrogels produced the largest variation in

hemolysis. Comparatively, the PVA and PVA-gelatin hydrogels demonstrated the least hemolytic potential (below 0.5 %).

Blood was also added directly to the surface of the hydrogels and incubated for different amounts of time. Each hydrogel composition impacted blood clotting differently (Figure 16d-e). Compared to the polystyrene mock control, significantly more blood was clotted to the PVA hydrogel ($p < 0.05$). Blood coagulation was also significantly higher ($p < 0.00005$) for the PVA-gelatin, PVA-PEG, and PVA-chitosan hydrogels compared to the mock control. Overall, the PVA hydrogel showed the least blood coagulation (15.5 ± 3.8 %) and PVA-chitosan showed the most (56.0 ± 2.85 %), as indicated by the limited free hemoglobin after washing the hydrogels with deionized water. The PVA hydrogels maintained a similar smooth appearance under SEM despite adding other polymers (Figure 17). These properties could be used to customize the hydrogels for specific applications. For example, the PVA-chitosan hydrogel prevented *E. Coli* growth (antibacterial) and promoted blood coagulation. The PVA-chitosan hydrogel was also capable of swelling four-fold to maintain a moist environment, indicating its suitability for wound dressing applications [184], [185]. Comparatively, the PVA hydrogel creates a smooth surface with minimal blood coagulation, indicating a potential use for vascular grafts or other applications requiring an anti-thrombotic polymer [186]. Finally, the PVA and PVA-gelatin hydrogels demonstrated the best baculovirus retention and sustained delivery making them useful for long term applications such as medical device or stent coatings [47].

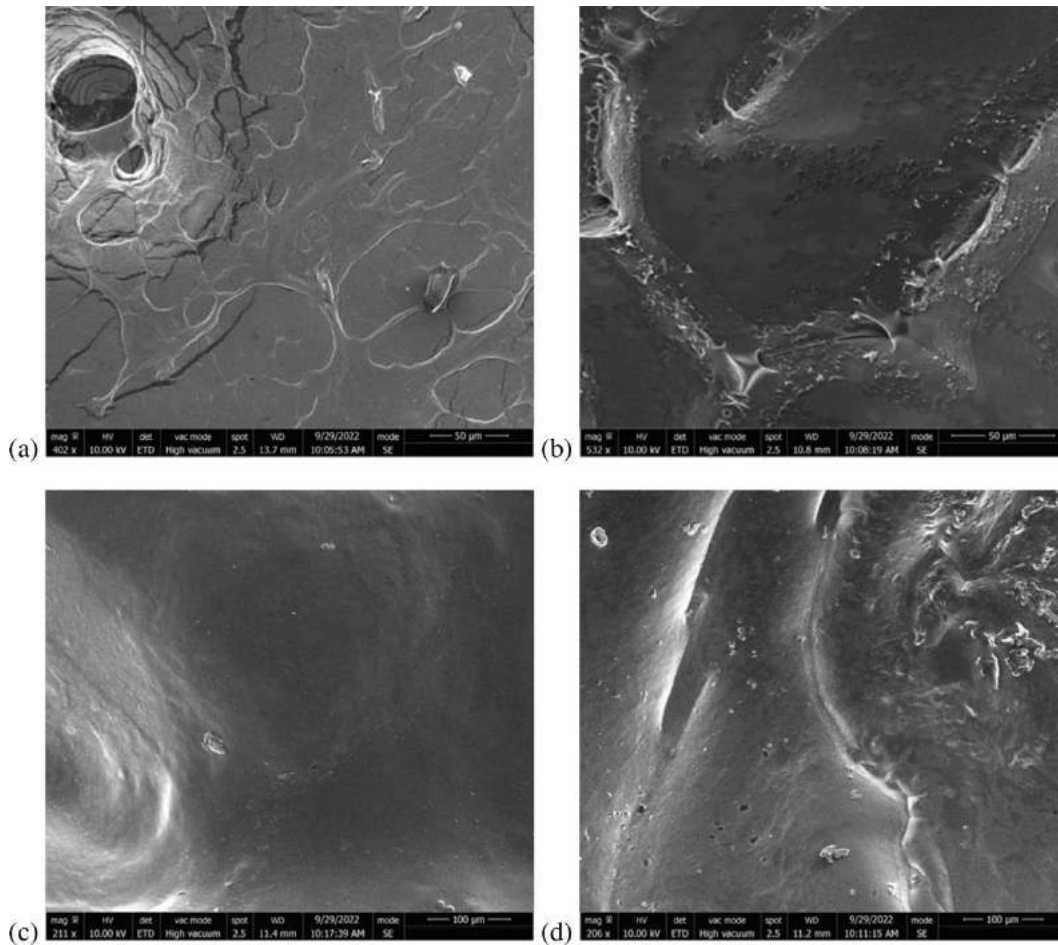


Figure 17. SEM of different PVA-based hydrogel compositions

(a) PVA, (b) PVA-PEG, (c) PVA-chitosan, and (d) PVA-gelatin.

Baculovirus production and elution from PVA-based hydrogels

We created two different baculoviruses. One baculovirus expressed EGFP in insect cells and RFP in mammalian cells. The second baculovirus expressed nitric oxide synthase three (NOS3) in mammalian cells. The baculovirus was amplified in 100 mL of Sf9 cells in BacVector media. The virus supernatant was collected and titrated using a fluorescent titrating assay or FastPlax titration kit with dilutions for an accurate estimate. The Sf9 cells were imaged 48 hours

after infection, at the first sign of EGFP expression. The final titration was calculated to be 1.4×10^8 TU/mL for the EGFP-baculovirus and 1.0×10^8 PFU/mL for the NOS3-baculovirus.

Table 4. PVA-based hydrogel loading efficiencies

Hydrogel type	Loading efficiency (% \pm SD)
PVA1	15.3 ± 2.9
PVA2	11.8 ± 1.0
PVA3	3.7 ± 2.1
PVA4	0.9 ± 0.5
PVA passive absorption	96.4 ± 0.6
PVA-PEG	0.4 ± 0.7
PVA-chitosan	2.3 ± 1.7
PVA-gelatin	94.6 ± 1.2

Before the freeze-thaw cycles, the baculovirus stock was added directly to the PVA-based hydrogels. After the designated freeze-thaw cycles, the hydrogels were removed from the casting well plate and incubated in HBSS. At the designated time points, the HBSS was removed and added to Sf9 cells to determine the baculovirus elution over time. The baculovirus viability significantly decreased with each freeze-thaw cycle (Figure 18). The hydrogel loading efficiency varied for each freeze-thaw cycle, ranging from 15.3 ± 2.9 % to 0.9 ± 0.5 % (Table 4).

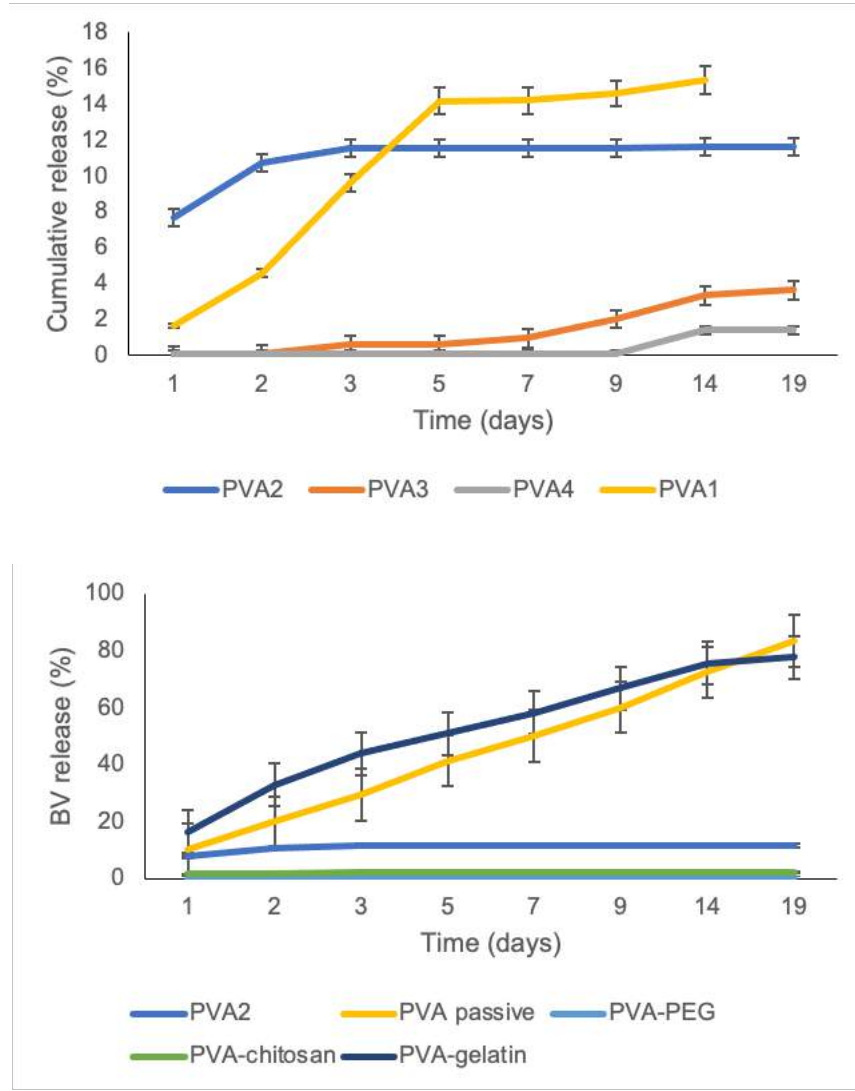


Figure 18. Baculovirus elution from PVA-based hydrogels over time

(a) BV elution from PVA hydrogels based on the number of freeze-thaw cycles. (b) BV elution from different PVA-based hydrogel compositions.

The addition of different polymers improved baculovirus entrapment and elution from the hydrogels. Specifically, adding PEG to the PVA hydrogel prolonged the baculovirus elution compared to the PVA2 hydrogel. The majority of the virus was eluted between days three to five for the PVA-PEG hydrogel. Similarly, adding chitosan to the PVA seemed to reduce the amount

of baculovirus entrapped and released over time and may be attributed to chitosan's binding to negatively charged virus particles. Comparatively, adding gelatin significantly improved baculovirus retention and controlled release over time compared to all other freeze-thawed PVA-based hydrogels.

Once all the baculovirus was eluted, the total amount was used to determine the hydrogel loading efficiency. The loading efficiency varied from $0.4 \pm 0.7 \%$ to $94.6 \pm 1.2 \%$ depending on the hydrogel composition, listed in Table 2. For most of hydrogels, the baculovirus was eluted in the first three days, such as for PVA2 and PVA-chitosan. The PVA-gelatin hydrogel and the PVA hydrogel loaded passively with baculovirus after the freeze-thaw cycles demonstrated the most baculovirus elution (Figure 18). Specifically, the passive absorption of baculovirus into PVA hydrogels resulted in a loading efficiency of $96.4 \pm 0.6 \%$. Similarly, the PVA-gelatin hydrogels had a loading efficiency of $94.6 \pm 1.2 \%$. The elution from these hydrogels also lasted over 23 days.

Adding different polymers (chitosan, gelatin, and PEG) to PVA hydrogels controlled baculovirus elution and loading. Baculovirus elution was sustained with all hydrogels. The elution time varied from 5 to 25 days. All hydrogels exhibited a slow first-order release of the baculovirus that eventually plateaued. With each freeze-thaw cycle, the amount of viable baculovirus within each hydrogel diminished significantly, consistent with previous results [187]. The amount of baculovirus encapsulated varied between freeze-thaw cycles as seen in Table 4. The addition of gelatin preserved the baculovirus viability during the freeze-thaw cycles compared to the other hydrogels. This supports previous studies where a gelatin coating maintains transfection efficiency and DNA stability [188], [189]. The baculovirus viability in PVA-gelatin hydrogels was comparable to the hydrogels loaded passively with baculovirus, not exposed to any freeze-thaw

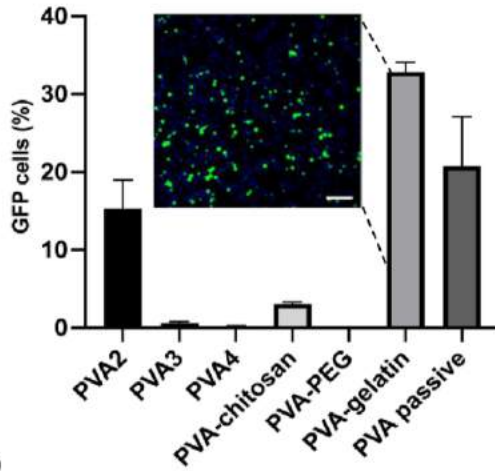
cycles. Passive loading of baculoviruses into PVA hydrogels exhibited the highest loading efficiency with sustained release. When 2×10^7 TU of baculovirus were added, the loading efficiency was 96.4 ± 0.6 %. When 4×10^7 was loaded onto the PVA hydrogel, the loading efficiency dropped to 88.3 ± 0.6 %. However, given the higher initial concentration, more baculovirus was loaded onto second hydrogel overall. The different baculovirus doses and release times observed here can be customized to fit the medical application. For example, wound healing may require a sustained gene delivery over a couple of days, whereas PVA-coated stents require sustained delivery over approximately two weeks.

The optimal storage conditions for the baculovirus-eluting hydrogels include storing the virus in the dark at 4 °C for a couple months or at -80 °C for long term storage to preserve the virus titer and viability [190]. Similarly, the hydrogels can be stored at -20 °C or dried at 4 °C with no loss in weight after a month. Storing the baculovirus loaded hydrogel is less ideal as the baculovirus elutes over time.

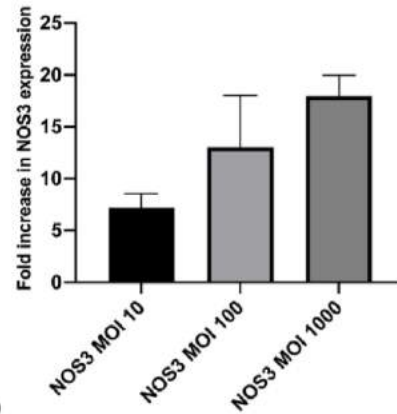
NOS3 delivery from eluted baculoviruses

The different PVA-based hydrogels were incubated in HBSS, and the supernatant was removed and replaced with fresh HBSS at the designated time points. The collected supernatant was added to Sf9 insect cells and used to transduce HUVECs to determine baculovirus release and activity over time. The baculovirus demonstrated efficient gene expression in both SMCs and HUVECs. As the amount of virus added (MOI) increased, the number of fluorescent cells or NOS3 expression also increased. The EGFP expression is shown below (Figure 19a). Similarly, the NOS3-baculovirus increased NOS3 expression increased dose-dependently. The highest dose, an MOI of 1000, increased NOS3 levels 17-fold compared to the mock transduced cells (Figure 19b). NOS3 promotes formation of nitric oxide and nitrate [191]. The media from the transduced cells

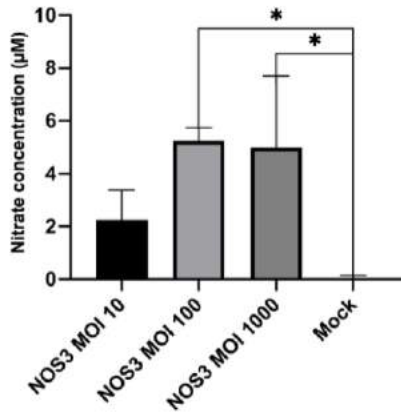
was also used to measure nitrate formation (Figure 19c). Nitrate concentration was increased up to 8-fold compared to mock transduced cells. Nitric oxide and nitrate are effective antimicrobial agents against gram positive and gram negative bacteria preventing biofilm formation [192], [193]. The antimicrobial assay showed similar results, with high doses of NOS3 (MOI 100 to 1000) significantly reducing bacterial cell growth (Figure 19d). The baculovirus expressing NOS3 had a comparable response to 10 μ M of nitrate. NOS3 and nitric oxide are also known for their role in cardiovascular health specifically regulating blood pressure through vasodilation, preventing endothelial dysfunction, and reducing arterial stiffness [45]. Even at a MOIs of 1000, no difference in cell proliferation was observed with the EGFP-baculovirus. Comparatively, high amounts of the NOS3-baculovirus significantly reduced SMC proliferation. An MOI of 100 and 1000 of NOS3 also increased HUVEC proliferation without impacting viability (Figure 19e-f).



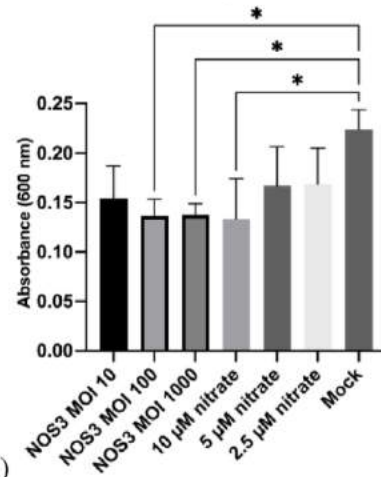
(a)



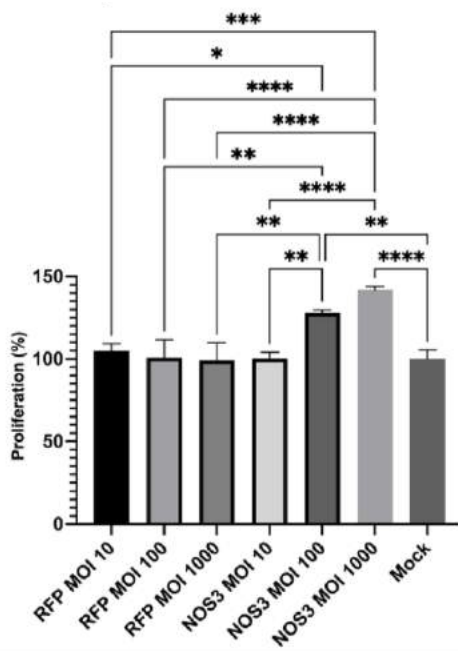
(b)



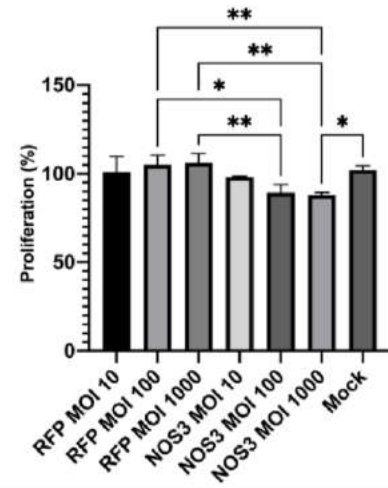
(c)



(d)



(e)



(f)

Figure 19. Gene expression after baculovirus transduction

(a) EGFP-baculovirus expression in Sf9 cells eluted from hydrogels after one day. The EGFP expression from a PVA-gelatin hydrogel is presented as a fluorescent image of DAPI-stained Sf9 cells (the scale bar represents 0.5 mm). (b) NOS3 expression based on baculovirus MOI. (c) Nitrate concentration after BV transduction. (d) Bacterial growth inhibition in the presence of NOS3 and nitrate. (e) HUVEC proliferation after BV transduction. (f) SMC proliferation after BV transduction.

Cytotoxicity of the PVA-based hydrogels eluting NOS3 expressing baculovirus

The baculovirus was non-cytotoxic in SMCs and HUVECs, even in high amounts (Figure 20). Different amounts (MOIs) of the baculovirus were tested, ranging from one to 1000. Even at a MOIs of 1000, no difference in viability was observed with the baculovirus. The PVA-based hydrogels were also incubated directly with SMCs or HUVECs. Similarly, the PVA-based hydrogels were non-cytotoxic to SMCs and HUVECs. The hydrogels did not significantly reduce cell proliferation or viability compared to the mock cells (Figure 20). The PVA-PEG hydrogel reduced the cell viability the most after 48 hours. Comparatively, the PVA and PVA-gelatin hydrogels maintained the highest cell viability and proliferation.

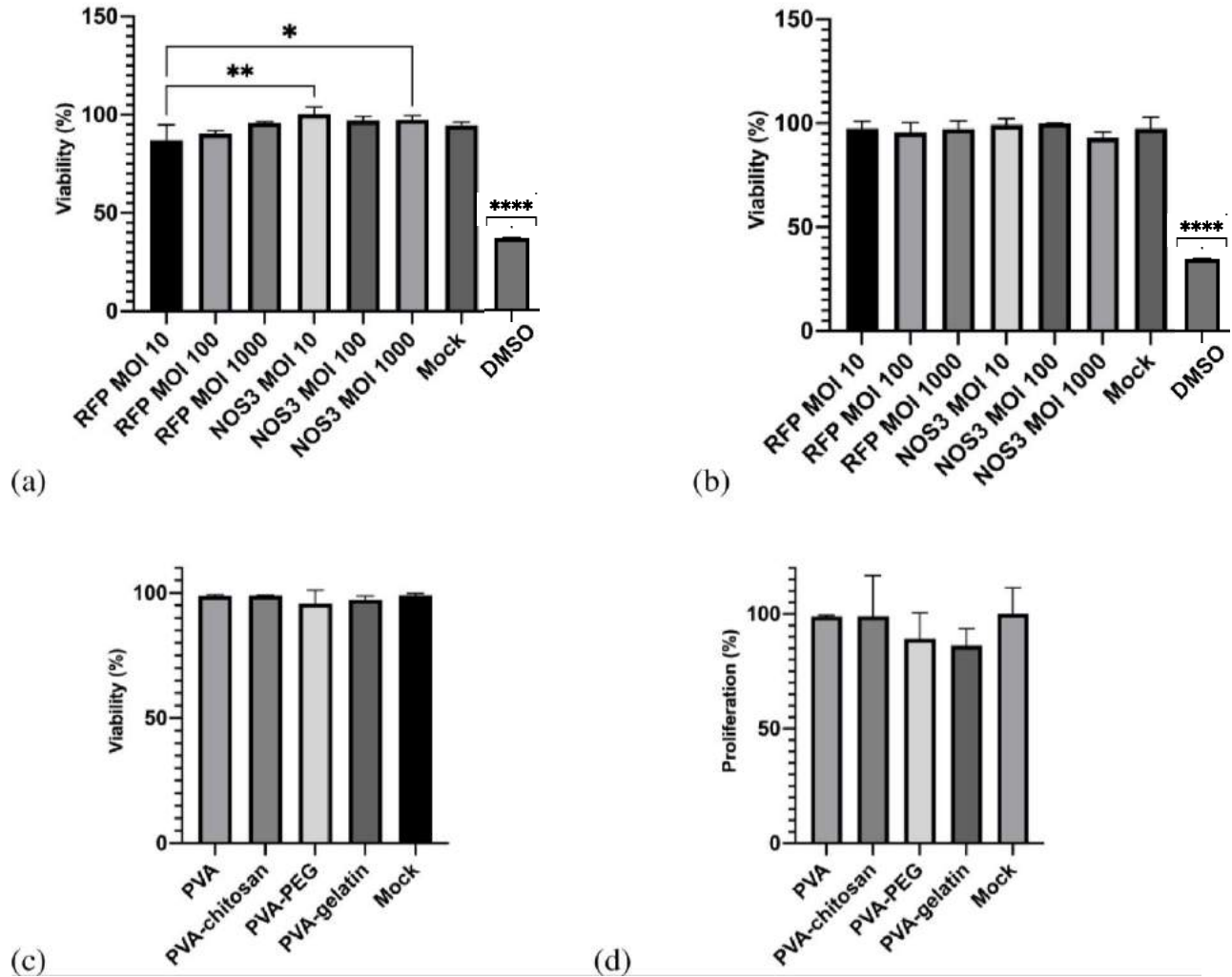


Figure 20. Mammalian cell viability after baculovirus transduction with different MOIs or direct hydrogel incubation

(a) HUVEC viability 48 hours after BV transduction. (b) SMC viability 48 hours after BV transduction. (c) HUVEC viability after incubating with different hydrogels for 48 hours. (d) HUVEC proliferation after hydrogel incubation for 48 hours.

The PVA baculovirus delivery system exhibits excellent safety properties. Specifically, no significant difference in cell proliferation or viability was observed after baculovirus transduction in both SMCs and HUVECs. Even at MOIs above 1000, no cell proliferation or viability change was noted with the EGFP-baculovirus. A significant decrease in SMC proliferation was observed

with higher NOS3 levels as expected [177]. Similarly, no significant difference in viability or proliferation was observed after incubation with the different hydrogels. This indicates that the baculovirus-eluting PVA delivery system does not pose cytotoxic effects on the cells. This study supports previous research reporting that baculoviruses and PVA hydrogels are non-toxic in mammalian cells [167], [194]. Future work can focus on specific clinical applications to optimize the baculovirus delivery system. Moreover, the customized system could be tested *in vivo* to confirm its therapeutic application.

Depending on the required therapeutic time frame and cell type, the baculovirus elution amount and time can be customized for each disease. The PVA-based hydrogels presented here would be suitable for medical device coatings. Specifically, PVA-gelatin stent coatings eluting NOS3 would be beneficial due to the antithrombotic properties, safety, and sustained gene delivery. This controlled baculovirus delivery system can be tailored to the countless diseases requiring gene or growth factor delivery. Similarly, adding another polymer, such as chitosan, gelatin, or PEG, can alter the PVA properties. To our knowledge, this is the first study optimizing PVA-based hydrogels containing baculovirus gene delivery vectors.

Conclusion

PVA-based hydrogel delivery of baculoviruses to mammalian cells is efficient, safe, and customizable. The hydrogel delivery system exhibited good blood compatibility and was non-cytotoxic to SMCs and HUVECs. The baculovirus loading efficiency reached 96.4 ± 0.6 % and was sustained for up to 25 days. The delivery system can be further customized by adding other polymers, loading methods, or additional freeze-thaw cycles. These alterations can change the hydrogel's mechanical properties and gene elution, specific for each therapeutic application.

Materials and Methods

Hydrogel synthesis

A 20 % (m/v) solution of PVA (MW 60,000 from Sigma Aldrich) was made by dissolving PVA in distilled water at 100 °C and 500 rpm. Meanwhile, a 5 % (m/v) gelatin solution was made in PBS. A and 1 mg/mL chitosan solution was made in PBS with 0.5 % (v/v) glacial acetic acid. The three solutions were autoclaved at 120 °C for 15 minutes and then cooled to room temperature. An equal amount of PVA was poured into each well of a 48-well plate. Next, 100 µL of the 1 % (m/v) gelatin, 1 mg/mL chitosan, or 0.1 % (v/v) PEG 8000 (Thermo Fisher) was added to the designated wells to create a PVA-gelatin, PVA-chitosan, or PVA-PEG hydrogels, respectively. The PVA-based hydrogels were stirred with a pipette tip and then baculovirus stock solution was added to each solution and stirred a final time. Water was added to hydrogels to serve as a mock. The hydrogels were frozen overnight and thawed for two hours to constitute one freeze-thaw cycle. The freeze-thaw cycle was repeated one to four times depending on the hydrogel.

Attenuated Total Reflectance- Fourier Transform Infrared (ATR-FTIR) spectroscopy

The spectra of the different hydrogels were obtained using an FTIR Spectrum II (Perkin Elmer) with ATR. The data were normalized to the background spectrum without a hydrogel. Next, the hydrogels were clamped down and a spectral range of 400-4000 cm^{-1} was recorded with four scans and a resolution of 1 cm^{-1} .

Hydrogel swelling and degradation

The hydrogels were dried overnight at 37 °C. The next day the hydrogels were weighed, and 1 mL of Hanks Balanced Salt Solution (HBSS) was added to each hydrogel. At the designated time points, the hydrogel was removed from the HBSS and weighed. The swelling ratio was calculated using the following equation:

$$\text{Swelling ratio} = \text{Weight}_{\text{swollen}} / \text{Weight}_{\text{dry}}$$

Disc diffusion antimicrobial studies

The antimicrobial properties of the PVA-based hydrogels were tested using an adapted disc diffusion method [159]. *E. coli* and *C. Albicans* were grown in Luria-Bertani (LB) and YPD media, respectively. The number of colony-forming units (CFU) was calculated by plating dilutions of the bacteria and incubating overnight. Based on the calculated CFU, 100 μ L of 10^8 CFU/mL was spread onto fresh LB or YPD agar plates. The PVA-based hydrogels were plated on top of the bacteria and incubated 37 °C for 24 hours. A drop (5 μ L) of penicillin was used as a negative control. After 24 hours, the area of growth inhibition was observed and measured.

Scanning electron microscopy (SEM)

The PVA-hydrogels were dried overnight at 37 °C before being imaged. A FEI 450 Quanta SEM was used at the Facility for Electron Microscopy Research at McGill University. A high vacuum and a voltage of 10 kV were applied.

Mammalian cell culture

Human umbilical vein endothelial cells (HUVECs) and smooth muscle cells (SMCs) were maintained in T-25 flasks in a 37 °C, 5 % CO₂ incubator. The HUVECs were purchased from Sigma and the SMCs from Coriell Institute for Medical Research (Camden, NJ, USA). Medium 199 was used with 0.02 mg/mL endothelial growth supplement, 10 % fetal bovine serum was used to culture the SMCs, and complete endothelial growth medium (Sigma Aldrich) was used to culture the HUVECs. Cells were used within five passages upon receiving.

Insect cell culture

Sf9 insect cells (Sigma Aldrich, Burlington, MA, USA) were maintained at 27 °C in BacVector medium (Sigma Aldrich) in T-75 flasks or 250 mL shake flasks (Erlenmeyer, CA). The Sf9 cells were subcultured 2-3 times weekly and shaken at 130 rpm.

Gene selection

The NOS3 gene was purchased from GenScript (Piscataway, NJ, USA). and cloned into a pOET6 plasmid (MJS Biolynx Inc., Brockville, ON, Canada) containing the cytomegalovirus (CMV) promoter. GenScript also provided a pBackPak9 plasmid expressing EGFP and RFP under a polyhedron and CMV promoter, respectively. The concentration and purity of the plasmid were confirmed using a NanoDrop (Thermo Fisher, Waltham, MA, USA) and were used for all future virus production steps.

Baculovirus production

The supplier's protocol was followed as previously described for baculovirus production [141]. In an exponential growth phase, 5×10^5 Sf9 cells were seeded into a 12-well plate one hour before virus transfection. Next, 200 ng of the pBakPak9 plasmid was added to 100 ng of flashBAC DNA (MJS Biolynx Inc., Brockville, ON, Canada), 0.48 μ L of TransIT Insect Reagent, and 100 μ L PBS and incubated at room temperature for 15 minutes. The transfection mixture was then added to the Sf9 cells and incubated overnight at 27 °C. The next day, 0.5 mL of BacVector media was added. Five days after transfection, the culture medium was harvested, centrifuged at 1000 x g for 10 minutes, and stored at 4 °C. This generated the P₀ virus stock and was added to 100 mL of Sf9 cells at a concentration of 2×10^6 cells/mL. The infected Sf9 cells were agitated at 130 rpm for four days before harvesting the culture medium as described above. This generated P₁ baculovirus stock expressing a red fluorescent protein (RFP) or NOS3.

Baculovirus titration

The EGFP-baculovirus was titrated using a fluorescent titering assay. First, 5×10^5 Sf9 cells/well were seeded into a 12-well plate and incubated for one hour. During the incubation, the virus was diluted using insect cell medium (1:10, 1:25, 1:50, 1:75, 1:100). The cell media was then

aspirated off the Sf9 cells and 100 μ L of the virus dilution was added to each well. The plate was incubated for one hour and then an additional 0.5 mL of insect cell media was added to each well and incubated at 27 °C. The next day, the number of fluorescent cells was counted in each well with less than 40 % of fluorescent cells. The following equation was used to calculate the titration: $\text{Transduction Units (TU)/mL} = (\text{number of cells transduced} \times \text{percent fluorescent} \times \text{dilution factor}) / (\text{transduction volume in mL})$

The NOS3-baculovirus was titrated using the FastPlax Titer kit from Sigma Aldrich as specified by the supplier.

Baculovirus elution from the hydrogels

The hydrogels were incubated in 1 mL of Hanks Balanced Salt Solution (HBSS). All the HBSS was removed and replaced with fresh HBSS at the designated times. The amount of baculovirus in the HBSS was quantified using the Fluorescent titering assay described above. The HBSS containing the baculovirus was also used to transduce mammalian cells.

Baculovirus transduction

The hydrogel suspension media (virus in HBSS) was removed and baculovirus stock was used to transduce mammalian cells (SMCs and HUVECs), in 96-well plates. After three hours of incubation, the virus inoculum was removed and replaced with fresh cell media. The cells were incubated for 48 hours to allow for viral gene expression. Fluorescent images of the cells were taken at different time points and stained with DAPI at 48 hpi. Images were acquired using the Columbus Image Data Storage and Analysis System (PerkinElmer, USA) and the Operetta® CLS automated microscope. Image acquisition (Fluorescence) and analysis (Columbus and Harmony) was performed with the McGill University Imaging and Molecular Biology Platform (IMBP) equipment and services.

Reverse transcription-quantitative polymerase chain reaction (RT-qPCR)

To perform RT-qPCR, cells were transduced as described above. Twenty-four hours after transduction, the cell RNA was extracted using an RNA extraction kit (Bio Basic) and stored at -80 °C until use. Luna Universal One-Step RT-qPCR kit (New England Biolabs, Ipswich, MA, USA) was used to reverse transcribe the stored RNA. Primers for NOS3 and β -actin reference genes were purchased from Bio-Rad (Hercules, CA, USA) and mixed with the RNA and primers at the supplier-defined concentrations. The reaction was run on an Illumina Eco Real-Time PCR machine (San Diego, CA, USA) as directed by the supplier (NEB).

MTT proliferation assay

An MTT proliferation assay (Sigma Aldrich, St. Louis, MI, USA) was used. As above, different BV MOIs were added to HUVEC and SMCs and incubated for three hours. After three hours of incubation, the baculovirus supernatant was removed and replaced with fresh cell media. For the PVA-based hydrogels, cells were seeded into 24 well plates, placed into the well, and incubated for 48 hours.

For the MTT assay, 0.01 mL of AB Solution (MTT) was added to each well 48 hpi. The cells were incubated for two hours at 37 °C to allow MTT cleavage. After two hours, 0.1 mL of isopropanol with 0.04 N HCl was added to each well. The isopropanol solution was mixed thoroughly via pipetting. The plate was then read using an EnSpire Multimode plate reader (Perkin Elmer, USA) with a wavelength of 570 nm.

Live Dead assay

A Live Dead Assay was employed to estimate the hydrogels' cytotoxicity using Calcein AM and propidium iodide (Thermo Fisher, Waltham, MA, USA). A 96-well plate was seeded with

cells, as described above, and transduced with different MOIs of the baculovirus. DMSO and regular cell media were used as the controls.

For the hydrogels, 2×10^4 HUVECs/well were seeded into a 48-well plate and incubated overnight. The next day, the PVA hydrogels were added to each well and incubated.

After 48 hours, 5 μ L of 1 mM Calcein AM and 5 μ L of 2.5 mg/mL propidium iodide were added to 10 mL of cell media. This solution was then added to the cells in the 48-well or 96-well plates and incubated at 37 °C for 30 minutes. After 30 minutes, the cells were imaged using the Operetta High-Content Analysis system and the percentage of live cells was calculated using Columbus (Perkin Elmer).

Griess assay

A Griess assay kit was used to measure nitrate production following the supplier's instruction (Thermo Fisher, Waltham, MA, USA). A standard curve was used to calculate nitrate concentration in HUVECs after BV transduction expressing NOS3.

Antibacterial assay for NOS3 and nitrate

The antibacterial properties of NOS3 and nitrate were investigated using broth dilutions to determine the minimal inhibitory concentration. *E. coli* from the hydrogel antimicrobial studies was used. First, the bacteria were diluted to 10^6 CFU/mL and 100 μ L was added to each well of a 96-well plate. Next, 100 μ L of the cell media supernatant containing NOS3 or sodium nitrate (10, 5, and 2.5 μ M) was added to the wells. Cell media without NOS3 and HBSS was added as the control. The plate was read on the HTS7000 microplate reader every two hours for 8 hours to create a bacterial growth curve.

Hemocompatibility studies

Two blood samples were purchased from Innovative Research (Male 49, Hispanic and female 29, white; Novi, MI, USA). A standard hemolysis assay was performed by immersing all samples into 5 mL of PBS in a 15 mL centrifuge tube. Next, 4 mL of citrated blood was added to 5 mL PBS. To each sample, 0.1 mL of diluted blood was added. The samples were incubated at 37 °C for one hour and then centrifuged at 1,000 rpm for 10 min. All supernatants were placed into a 96-well plate and read at 545 nm. The negative and positive control was PBS and deionized water, respectively. The following equation was used to determine the percent hemolysis.

$$\text{Hemolysis (\%)} = ((\text{OD}_{\text{sample}} - \text{OD}_{\text{negative control}}) / (\text{OD}_{\text{positive}} - \text{OD}_{\text{negative}})) \times 100\%$$

Blood coagulation on hydrogels was evaluated using an adapted method by Sabino et al. (2020) [160]. Briefly, the hydrogels were placed into a 24-well plate and 7 μL of whole blood was pipetted onto the surface. After the designated time point, deionized water was added to each well for 5 minutes. The hydrogel supernatant was added to a 96-well plate and read at 540 nm. For controls, 7 μL of whole blood was added to distilled water and a ‘mock’ polystyrene surface was also used to compare the blood coagulation properties of the hydrogels.

Statistical analysis

Unless otherwise stated, all results are reported as a mean \pm standard deviation (SD) in triplicates. GraphPad Prism (version 9.0.0 for Windows, GraphPad Software, San Diego, California USA, www.graphpad.com) was used for all one-way ANOVA data analysis and graph creation. Ethics approval was not required for the study.

Author Contributions: All authors have read and agreed to the published version of the manuscript.

Funding: This work was supported by a grant from the Canadian Institute of Health Research (CIHR, grant 252743) to Dominique Shum-Tim and Satya Prakash. S.S. is fully funded by the

Canadian Graduate Scholarship-Doctoral from the Natural Sciences and Engineering Research Council (NSERC, 569661-2022). P.I. is funded by the Islamic Development Bank Scholarship (2020-245622). A.A. is fully funded by a scholarship from the Ministry of Higher Education of the Arab Republic of Egypt. R.T. and K.A. are funded by the Canadian Graduate Scholarship-Master's from NSERC. The funders had no role in study design, data collection and analysis, decision to publish, or preparation of the manuscript.

Acknowledgments: We thank the Facility for Electron Microscopy Research of McGill University (SEM equipment), McGill Chemistry Characterization Facility (ATR-FTIR), and the McGill University Imaging and Molecular Biology Platform (IMBP, Operetta High Content microscope) for equipment usage and services.

Conflicts of Interest: The authors declare no conflicts of interest.

Copyright: This is an open-access article under the CC BY-NC-ND license (<http://creativecommons.org/licenses/by-nc-nd/4.0/>).

Bridging text

I have used different polymers and hydrogel synthesis methods in this paper to customize and control baculovirus delivery. The customizable baculovirus delivery is beneficial to sustain delivery for each disease-specific therapeutic window. Depending on the hydrogel formulation, I could vary baculovirus elution from five to 23 days. Gelatin was effective at preserving baculovirus viability even through multiple freeze-thaw cycles. BV elution from PVA-gelatin demonstrated the longest elution time. Similarly, passive loading of the PVA hydrogel with baculovirus enabled sustained baculovirus delivery over 25 days. With sustained baculovirus elution, NOS3 delivery was also sustained over this time. Moreover, the hydrogel system demonstrated excellent safety with no reported cytotoxicity.

The NOS3-eluting PVA hydrogel coating has a promising potential as a stent coating. NOS3 inhibits SMC proliferation which would help prevent neointimal hyperplasia. Additionally, NOS3 helps with vasodilation of the artery, which would benefit atherosclerosis treatment in PAD and CAD. Finally, NOS3 has a regulatory role and can help regulate endothelial function and fight off bacteria. This would help with re-endothelialization and preventing infection. To apply this hydrogel system as a stent coating, further studies are needed to verify its properties and therapeutic effect. The following paper will examine the mechanical properties, stent coating process, safety, and baculovirus elution.

The paper will also investigate three genes to determine which one(s) should be incorporated into the stent coating. The three genes are VEGFA, NOS3, and ADAMTS13. The second thesis paper reported that VEGFA helps promote re-endothelialization through the cell proliferation, migration, and angiogenesis presented in the second thesis paper. The third thesis paper reports the properties of NOS3, including potential benefits for vasodilation, re-

endothelialization, and inhibiting neointimal hyperplasia. The fourth paper investigates the therapeutic effects of ADAMTS13. Specifically, its potential as an anti-thrombotic agent.

CHAPTER 7: Evaluating a tri-gene-eluting dissolvable stent for peripheral artery disease using baculoviruses

Sabrina Schaly¹, Paromita Islam¹, Kevin Bates², Jacqueline L. Boyajian¹, Rahul Thareja¹, Ahmed Abosalha^{1,3}, Dr. Dominique Shum-Tim⁴, and Dr. Satya Prakash^{1,*}

¹ Biomedical Technology and Cell Therapy Research Laboratory, Department of Biomedical Engineering, Faculty of Medicine and Health Sciences, McGill University, 3775 University Street, Montreal, Quebec, H3A 2B4, Canada

² Department of Chemical Engineering, McGill University, 3610 University Street, Montreal, Quebec, H3A 0C5, Canada

³ Pharmaceutical Technology Department, Faculty of Pharmacy, Tanta University, Tanta 31111, Egypt

⁴ Division of Cardiac Surgery, Royal Victoria Hospital, McGill University Health Centre, McGill University, Faculty of Medicine and Health Sciences, Montreal, Quebec, H3G 2M1, Canada

* Corresponding author: satya.prakash@mcgill.ca

Contributions of the author: I am the first author and contributed to all experiments and manuscript preparation.

Science Advances

(To be submitted)

Abstract

Peripheral artery disease (PAD) is common, affecting nearly one in five people over 60, leading to the obstruction of peripheral arteries. More recent data suggests that PAD is also infiltrating younger generations, with one to four percent of people aged 25 to 29 diagnosed with PAD. PAD is mainly caused by atherosclerosis and consequential thrombosis. Atherosclerosis is characterized by plaque build-up within the artery leading to restenosis, calcification, and thrombi formation. Often, a bare-metal or drug-eluting stent will be used to force the artery open. These stents are highly effective but do come with complications such as restenosis, thrombosis, and endothelial dysfunction. To combat these complications a novel PVA-based stent eluting three genes (ADAMTS13, NOS3, and VEGFA) was developed. The three genes have a significant and additive effect resulting in inhibition of smooth muscle cell proliferation, promotion of endothelial cell proliferation, cleaving vWF to prevent initial blood clotting, preventing the inflammation, and reducing reactive oxygen species production. The three genes are delivered using insect cell viruses (baculoviruses) which enables efficient and sustained delivery over two weeks with an excellent safety profile. Moreover, the stent system is stable, flexible, and has a high tensile strength. The stent is also non-cytotoxic and anti-thrombotic by preventing platelet adhesion and blood coagulation on the surface. Overall, the novel stent exhibits beneficial mechanical and cellular properties with the potential to mitigate current peripheral stenting complications using gene therapy.

Keywords: Atherosclerosis, peripheral artery disease, dissolvable stent, gene-eluting stent, nitric oxide, VEGF, ADAMTS13

Introduction

Peripheral artery disease (PAD) is defined as the narrowing of peripheral arteries leading to the obstruction of blood flow. PAD is most common in the lower extremities, including the femoral, femoropopliteal arteries, and the arteries coming from the heart. Nearly one in five people over 60 have PAD, with an estimated 200 million new cases each year worldwide [5], [6]. People with PAD report a worse quality of life, higher work impairment, and use more healthcare resources compared to people without PAD [8]. Moreover, complications and disabilities associated with PAD have a larger burden on women and people in developing countries [7], [9]. Disability associated with PAD has also increased over the past 20 years, indicating a growing issue with an aging population. Historically, PAD burdened people in their eighties. However, more recent data suggest PAD affects a significant proportion of young adults as well. Specifically, one to four percent of people aged 25 to 29 have PAD and this percent increases steadily with age [7].

PAD is mainly caused by atherosclerosis and consequential thrombosis. Atherosclerosis may include stenosis (69 %), intimal thickening, fibroatheroma, fibrocalcific lesions, or luminal thrombi (49.1 %) [195]. PAD pathology occurs within the three layers of peripheral arteries; the tunica interna, tunica media, and tunica externa (also known as the adventitia). The inner layer, tunica interna, is mostly composed of endothelial cells that form a confluent layer and are in contact with the flowing blood. The tunica media comprises mostly smooth muscle cells (SMC) and elastic fibers that allow the artery to stretch. Arterial narrowing may be attributed to four key factors within these layers, including calcification, inflammation, endothelial dysfunction, and SMC hyperproliferation.

Atherosclerosis is a complex process involving several mechanisms including endothelial dysfunction, inflammation, neointimal hyperplasia, and thrombosis. During PAD, endothelial dysfunction occurs due several factors such as elevated low-density lipoprotein (LDL), free radicals, hypertension, stress, obesity, diabetes, infection, and more [1]. The high LDL levels and endothelial dysfunction cause the medial cell layer to hyper proliferate (termed neointimal hyperplasia). Endothelial dysfunction also impairs vasodilation and vascular resistance. The LDL continues to accumulate in the artery and commences an inflammatory reaction. The activated immune cells translocate into the subendothelial space. Particularly, monocytes are known to translocate and differentiate into inflammatory macrophages [2]. The macrophages take up the LDL and differentiate into foam cells. The foam cells release more growth factors and cytokines promoting SMC migration and proliferation contributing to the neointimal hyperplasia. Several studies have reported that high levels of C-reactive protein (CRP) and reactive-oxygen species (ROS) contribute to the inflammatory response and disease progression [144], [196]. During the SMC migration and proliferation, extracellular matrix remodelling can also occur leading to stiff, stenotic, and calcified blood vessel walls. The macrophages eventually become overextended and undergo apoptosis releasing pro-thrombotic factors, damaging microvessels, and contributing to a necrotic core [3]. Plaque erosion and rupture can cause thrombi formation further obstructing blood flow and leading to clinical complications. These factors create a positive feedback loop contributing further to neointimal hyperplasia, inflammation, and plaque development, all of which narrow the blood vessel. Consequently, PAD often comes with significant pain, discomfort, limb ischemia, stroke, and increases the risk of major cardiovascular events such as myocardial infarction and coronary artery disease [4].

One of the main treatments for PAD is implanting a stent to force open the artery. Stents have saved millions of lives [25]. However, stenting further damages the endothelial lining of the artery and can lead to blood vessel re-narrowing and blood clotting [35]. Blood vessel narrowing (restenosis) is defined as a >50 % narrowing of a blood vessel's diameter and occurs in 5-10 % of cases using current drug-eluting stents [36]. Peripheral artery stents have the highest rates of complications among the different types of stents.

Despite the advances seen in many coronary artery stents, peripheral stent options are still limited, with bare-metal and paclitaxel-eluting stents being the most common. Moreover, common complications include thrombosis, restenosis, calcification, and mechanical failures leading to an increased risk of morbidity, myocardial infarction, stroke, and mortality [37]. One-year patency rates are as low as 76 %, and two-year patency rates are as low as 60 % [38]. With low patency, re-intervention is required increasing the risk of complications and associated morbidity. In-stent restenosis (ISR) invites further calcification making the blood vessel stiff, inefficient, and increases the risk of stroke, myocardial infarction, and death. At the very least, this further reduces the individual's quality of life, leading to chest pain, shortness of breath, aches, and general pain. Finally, mechanical stent failures are common given the large diameter and flexibility needed from peripheral stents. Stent fracture rates vary from 15.3 - 53.3 % depending on the stent used and anatomical location [197], [198].

More recently, fully biodegradable or dissolvable stents have been explored. These stents offer several advantages, such as eliminating the foreign body (the stent), which could reduce the risk of thrombosis [28]. Complete biodegradation of the stent would also support normal vasomotion and luminal movement. Finally, biodegradable stents would allow the possibility of discontinuing dual antiplatelet therapy. Currently, magnesium alloys, zinc calcium alloys, iron

alloys, polylactic acid (PLA, PDLA & PLLA), and tyrosine polycarbonate are being investigated [29], [30]. Another approach is the use of polyvinyl alcohol (PVA), which has the required mechanical strength and elasticity for a stent [31]–[34]. Some research groups created a stent using braided PVA yarns, while others have utilized 3D printing to create a PVA stent [31]–[33]. Other researchers have shown promising results using dip coating to synthesize PVA biliary duct stents [34].

Given the literature, promoting proper endothelial function would appear to prevent LDL accumulation, immune cell infiltration, inflammation, and smooth muscle cell hyperproliferation. Early-stage interventions to promote endothelial health could thus prevent current downstream complications, including thrombosis, in-stent restenosis, calcification, and low patency. To promote endothelial health, we have selected three genes involved in endothelial cell regulation (ADAMTS13, NOS3, and VEGFA). Vascular endothelial growth factor A (VEGFA) stimulates endothelial cell migration and proliferation from other locations to promote site-specific reendothelialization [113], [136]. VEGF released from bioactive stents has been shown to significantly increase reendothelialization and prevent in-stent restenosis *in vivo* [113]. Similarly, nitric oxide synthase 3 (NOS3) plays a key role in vascular homeostasis, vascular dilation, and protects the intima from platelet aggregation and leukocyte adhesion [116]. NOS3 also prevents SMC proliferation and endothelial dysfunction. This is crucial in the initial two weeks after stent implantation to regulate vascular function and promote an anti-inflammatory environment. Finally, ADAMTS13 cleaves vWF, which prevents platelet aggregation and blood clotting. High vWF and low ADMTS13 levels are associated with major cardiovascular events and thrombosis [114], [199]. Together, these three genes were selected for their ability to promote endothelial function

and prevent blood coagulation which would promote re-endothelialization and mitigate thrombosis, respectively [111], [112], [200].

To improve gene stability and elution, baculovirus expression vectors were selected. Baculoviruses are a biosafe and low-cost vector capable of site-specific and enhanced gene delivery compared to alternative methods [50]. Moreover, their high but transient gene delivery is ideal for stent applications, whereby gene delivery is only required for the initial two weeks until healing is completed. Encapsulating the baculovirus in a stent coating can also prolong transgene expression past the typical four-day window [78]. Viral hydrogel encapsulation can also increase stability, solubility, prolong gene expression, and promote site specificity which allows for a lower dosage and less toxicity [117]. Finally, the optimized baculovirus hydrogel can be coated onto a stent to provide a localized therapeutic effect.

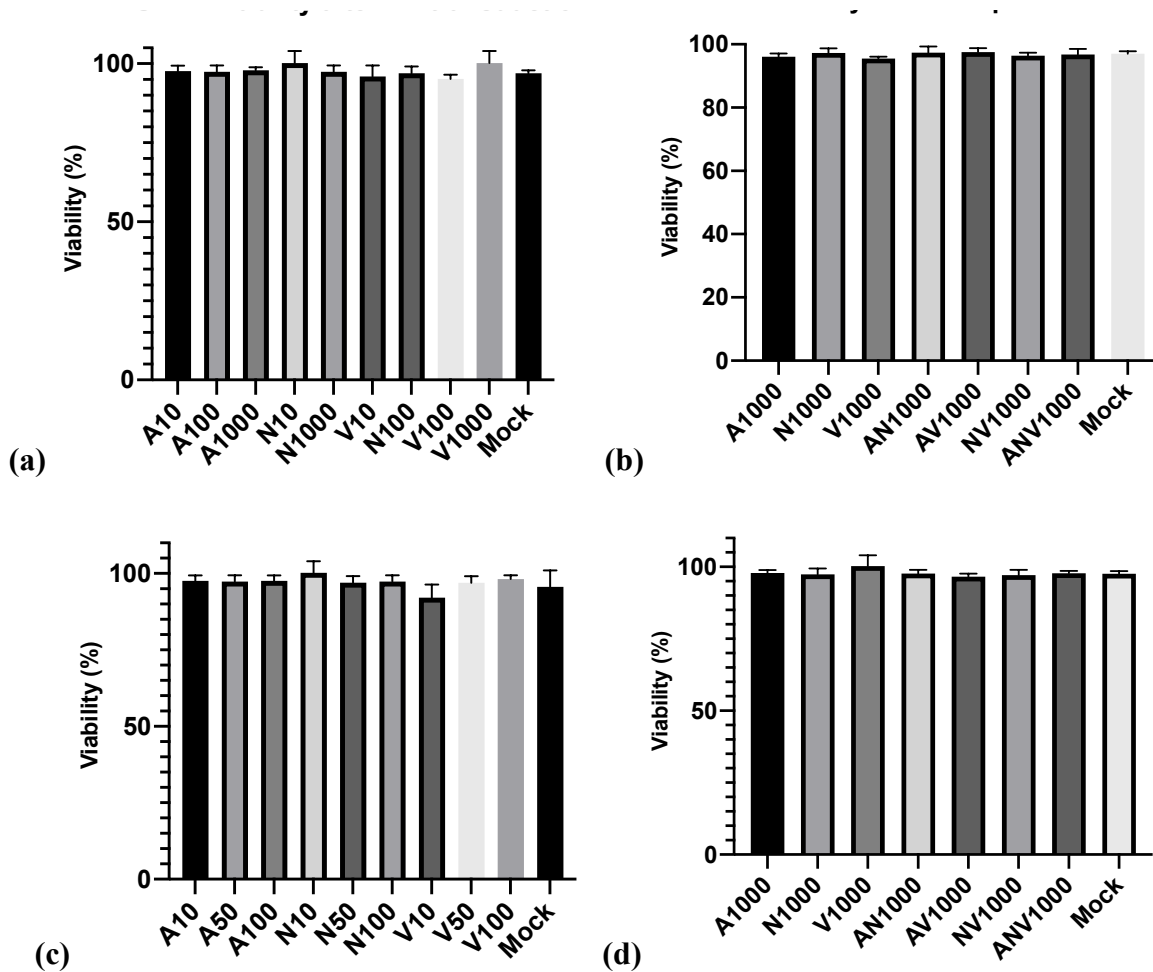
Results

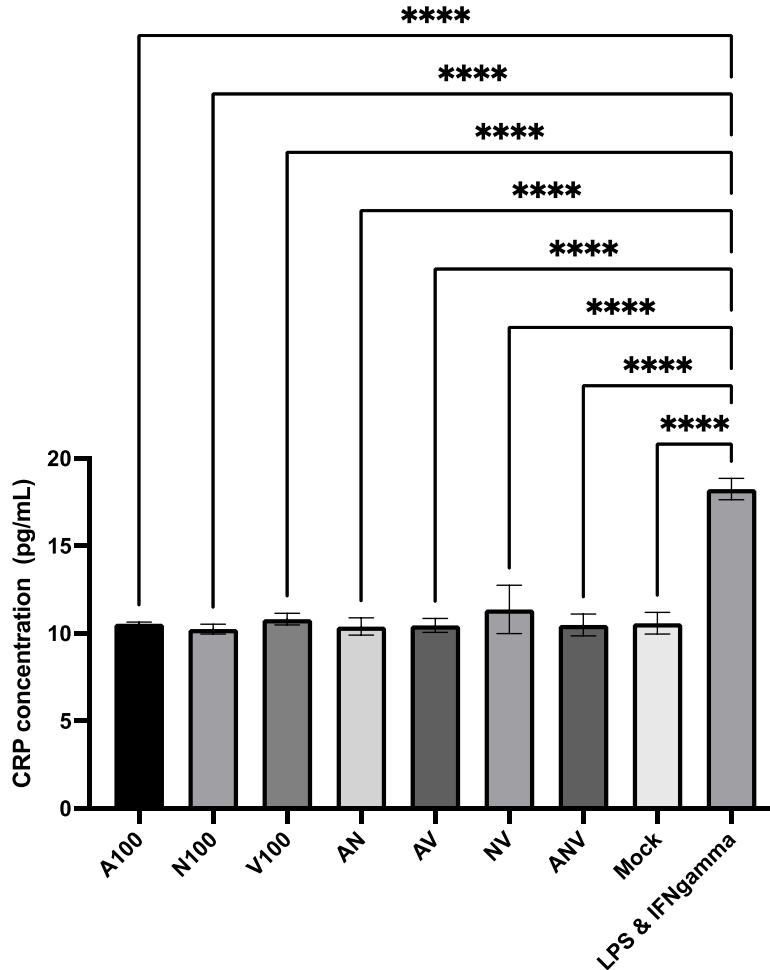
Baculovirus (BV) production and expression

Four different baculoviruses were produced. The final titration for baculoviruses expressing ADAMTS13, NOS3, VEGFA, and RFP were 1.25×10^8 , 1.7×10^8 , 3.5×10^8 , and 1.0×10^8 TU/mL, respectively. The baculovirus expressing a green fluorescent protein (GFP) in insect cells and red fluorescent protein (RFP) in mammalian cells was used to monitor the baculovirus production and elution from the stent. The three baculoviruses expressing the genes of interest (ADAMTS13, NOS3, and VEGFA) were tested for their *in vitro* safety. Different amounts of the virus, multiplicity of infection (MOI), were investigated, ranging from one to 1000 (Figure 21a-d). An MOI of 1000, well above the therapeutic range, was investigated to observe possible adverse effects. The baculoviruses expressing different genes are denoted as follows ADAMTS13 (A),

NOS3 (N), VEGFA (V), ADAMTS13-NOS3 (AN), NOS3-VEGFA (NV), ADAMTS13-VEGFA (AV), and ADAMTS13-NOS3-VEGFA (ANV) with the following number representing the MOI. No significant decrease in viability was observed in smooth muscle cells (SMCs) or human umbilical vein endothelial cells (HUVECs) transduced with baculovirus. The baculoviruses expressing different genes were also tested together to determine if any combination impacted the cellular response and overall safety. Again, no significant decrease in viability was observed when multiple different baculoviruses were added together (ANV).

***In vitro* safety of baculovirus gene delivery**





(f)

Figure 21. HUVEC and SMC viability, proliferation, and CRP production after baculovirus (BV) transduction

(a) HUVEC viability after single BV transduction. (b) HUVEC viability after transduction with multiple BVs. (c) SMC proliferation after BV transduction. (d) SMC proliferation after transduction with multiple BVs. (e) CRP production in HUVECs, all groups were significantly (****) different from the cells treated with LPS and IFN γ . (f) CRP production in SMCs after baculovirus transduction. Abbreviations are for ADAMTS13 (A), NOS3 (N), VEGFA (V), ADAMTS13-NOS3 (AN), NOS3-VEGFA (NV), ADAMTS13-VEGFA (AV), and ADAMTS13-NOS3-VEGFA (ANV) with the following number representing the MOI used.

After transduction, the baculovirus gene delivery and expression was also tested for C-reactive protein (CRP) production (Figure 21e-f). We observed no significant increase in CRP production compared to mock transduced SMCs but significantly less CRP than cells treated with inflammatory compounds such as lipopolysaccharides (LPS) and interferon-gamma (IFN γ). Moreover, baculovirus gene expression, except for a high dose of ANV1000, reduced CRP levels in HUVECs compared to mock transduced cells. Again, all CRP levels after baculovirus transduction were significantly lower than HUVECs treated with LPS and IFN γ .

Baculovirus gene delivery: therapeutic effect

Following initial stent implantation, promoting endothelial regulation, growth, and migration is required for re-endothelialization and to reduce downstream complications. To determine if the genes can help promote this therapeutic effect, we investigated cell proliferation, migration, and angiogenesis after baculovirus transduction.

HUVEC and SMC proliferation varied depending on the gene expressed, MOI, and cell type (Figure 22). Lower MOIs (10 and 50) did not change SMC proliferation compared to mock transduced cells. Only high MOIs of the baculovirus significantly changed SMC proliferation compared to the mock. Specifically, ADAMTS13 expression (MOI 100) significantly reduced SMC proliferation ($p < 0.005$). Comparatively, NOS3 expression (MOI 100) also reduced SMC proliferation but not significantly. Comparatively, VEGFA at an MOI of 100 significantly promoted SMC proliferation ($p < 0.05$) compared to the mock cells. When multiple genes were expressed together, no significant changes in SMC proliferation were observed.

HUVEC proliferation did not significantly change the initial 48 hours post-infection (hpi) at lower MOIs for ADAMTS13 and VEGFA. VEGF increases HUVEC proliferation in a dose-dependent manner but not significantly at lower doses. An MOI of 100 of ADAMTS13 and

VEGFA significantly increased HUVEC proliferation. All MOIs of NOS3 significantly increased HUVEC proliferation in a significant and dose-dependent manner. NOS3 expression (MOI 100) increased HUVEC proliferation most significantly (***) compared to the mock transduced cells. Similarly, when different genes were expressed together (ANV), HUVEC proliferation increased significantly for all treatment groups.

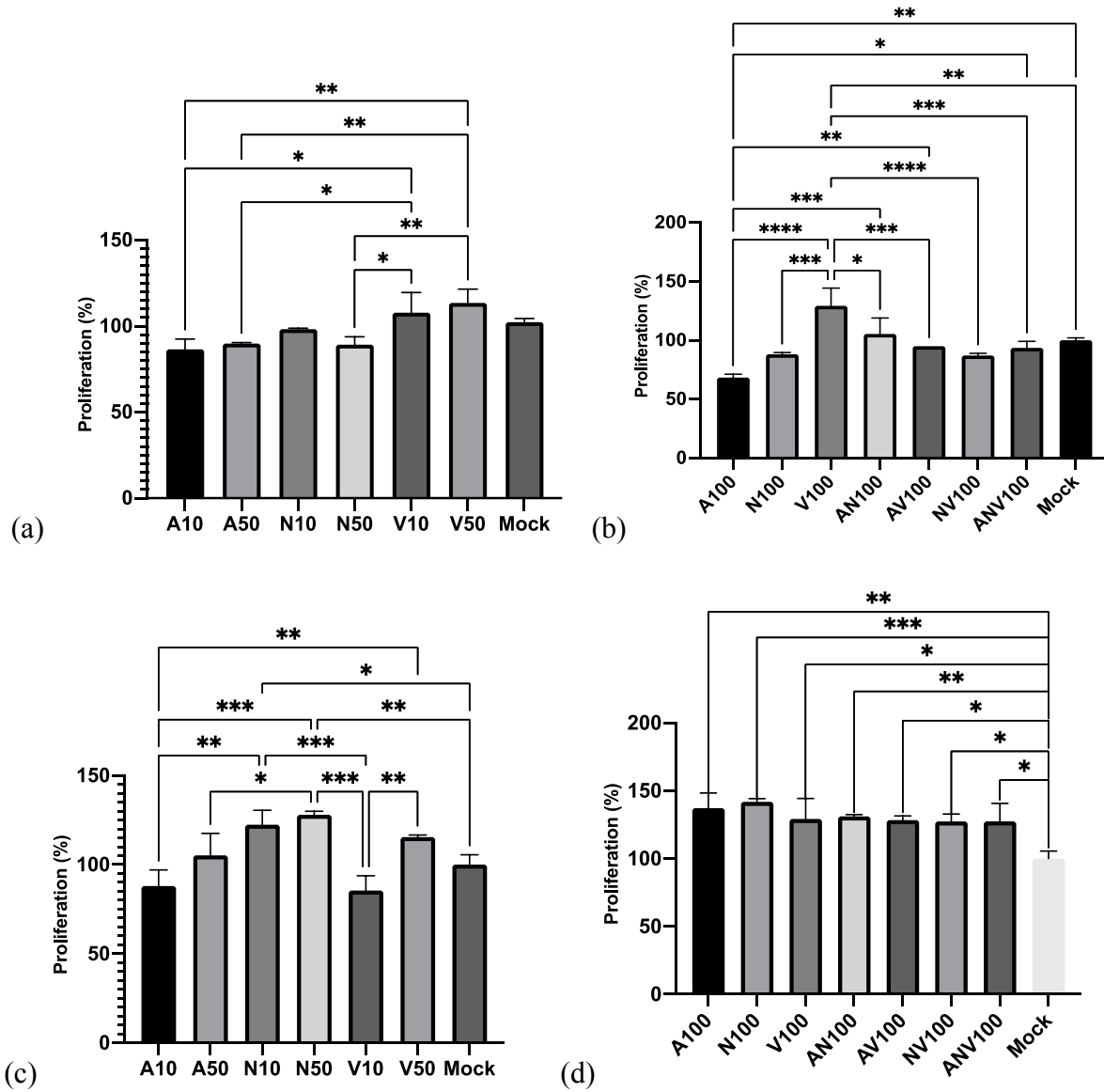


Figure 22. SMC and HUVEC proliferation after BV transduction

(a) SMC proliferation 48 hours after single BV transduction. (b) SMC proliferation 48 hours after transduction with multiple BVs. (c) HUVEC proliferation after BV transduction. (d) HUVEC proliferation after transduction with multiple BVs.

A scratch and angiogenesis assay were also performed to evaluate re-endothelialization potential *in vitro* (Figure 23). To determine the lowest dose possible that still create a therapeutic effect, a range of MOIs were tested. The scratch assay revealed significant HUVEC migration with NOS3 and VEGFA delivery, but not ADAMTS13. Combinations of different genes all exhibited significantly improved cell migration. Specifically, ADAMTS13-NOS3 ($p < 0.0005$) and NOS3-VEGFA ($p < 0.005$) demonstrated the most significant cell migration following wounding when the genes were expressed together. For dual and triple gene expression studies, we tested MOIs half that of individual genes to see if there was an additive effect. AN and AV combinations had a similar response to NOS3 alone despite only using half the MOI of each baculovirus. Overall, AN, N, and NV gene expression resulted in the most prominent cell migration, with almost complete wound healing after 12 hours. The angiogenesis assay showed similar results (Figure 23f-g). Low doses of ADAMTS13 (MOI 10) had an inhibitory effect on angiogenesis. Comparatively, low doses of NOS3 and VEGFA (MOI 10 and 50) did not influence angiogenesis branching length compared to the mock group. Only an MOI of 100 of VEGA and NOS3-VEGFA (NV) significantly stimulated blood vessel formation as indicated by the longer branching length.

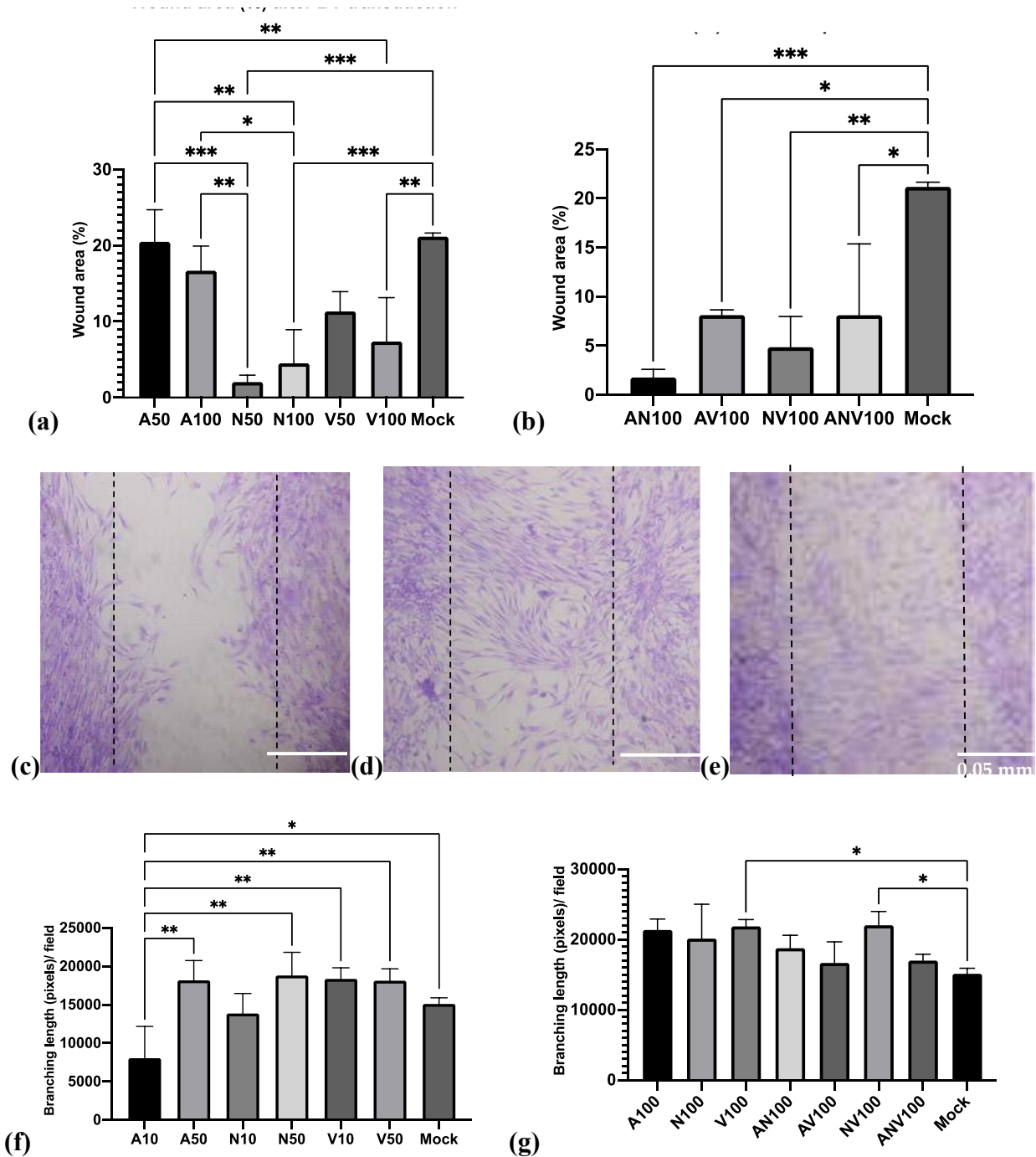
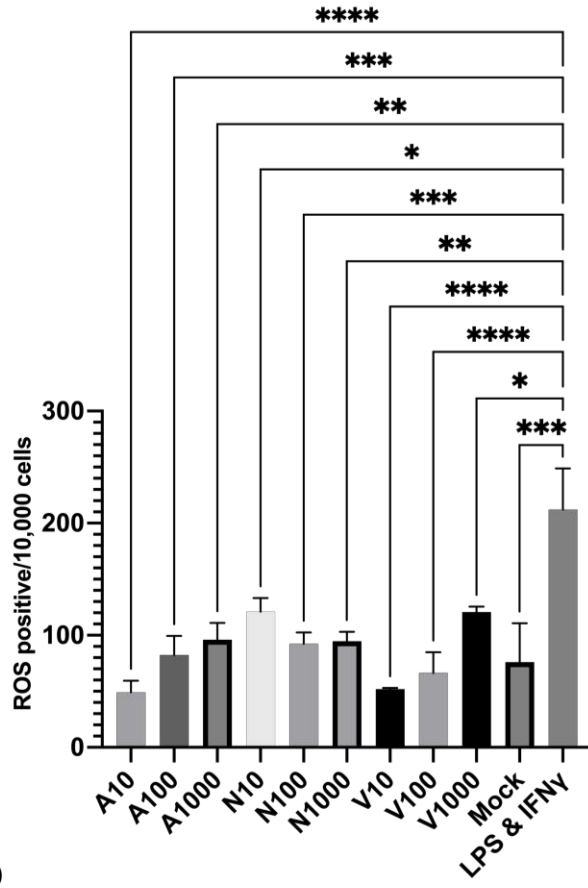


Figure 23. HUVEC migration and tube formation after baculovirus transduction

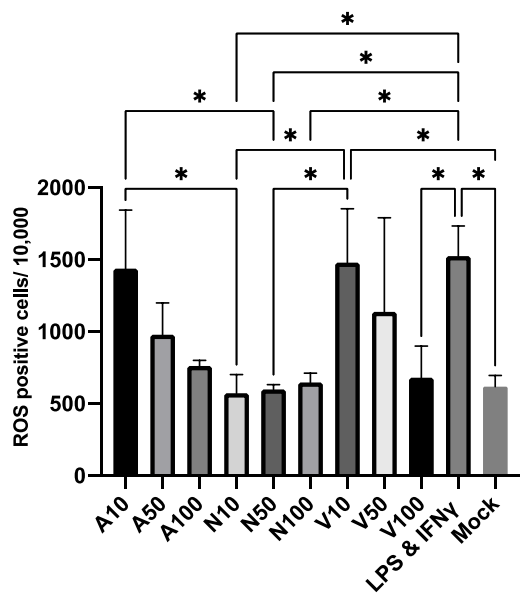
(a) Cell migration after baculovirus transduction and wounding. (b) Cell migration after multiple baculovirus transduction expressing different genes simultaneously. (c-e) Brightfield image of wounded area 12 hours after wounding and staining with crystal violet; (c) mock transduced cells,

(d) VEGFA transduced cells, and (e) ANV transduced cells. (f) Angiogenesis assay branching length after baculovirus gene elution addition. (g) Angiogenesis assay branching length after multiple baculovirus gene elution addition. Abbreviations are for ADAMTS13 (A), NOS3 (N), VEGFA (V), ADAMTS13-NOS3 (AN), NOS3-VEGFA (NV), ADAMTS13-VEGFA (AV), and ADAMTS13-NOS3-VEGFA (ANV). (Please see the Appendix for additional data).

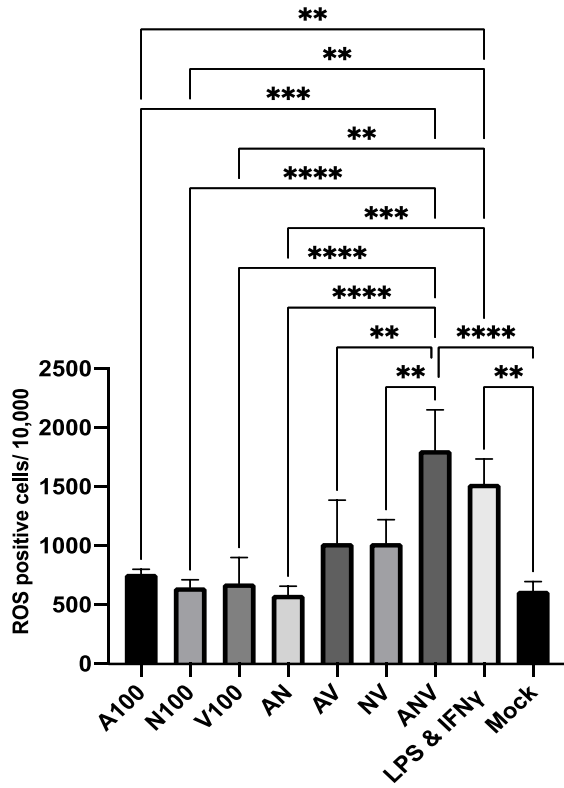
To determine if baculovirus gene delivery induced reactive oxygen species (ROS) production, a ROS assay was employed. The baculovirus itself and the delivered genes did not appear to induce ROS production (Figure 24a). However, the baculovirus gene delivery should also promote an anti-inflammatory and healing environment. To create an inflammatory environment, as seen in PAD, cells were pre-treated with lipopolysaccharide (LPS) and interferon-gamma (IFN γ) 24 hours before baculovirus transduction. As expected, LPS and IFN γ generated significant reactive oxygen species (ROS) in all cells. Next, the cells were transduced with baculoviruses expressing the different genes to observe their anti-inflammatory properties (Figure 24b-c). ADAMTS13 expression created a dose-dependent reduction in ROS levels, although not significant. NOS3 expression significantly reduced ROS production at all MOIs (10, 50, and 100). VEGFA (V) expression generated a dose-dependent decrease in ROS production with a significant decrease at the highest dose (MOI 100). ADAMTS13-NOS3 (AN) reduced ROS production most significantly when the genes were expressed together. All the genes expressed simultaneously (ANV) did not reduce ROS production compared to the LPS and IFN γ treated group.



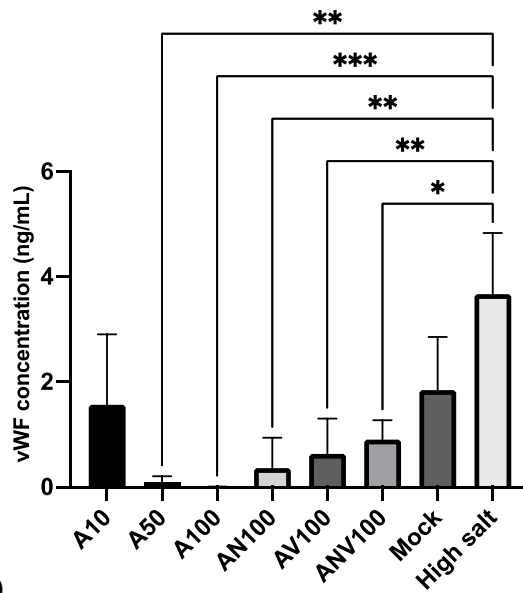
(a)



(b)



(c)



(d)

Figure 24. ROS production and vWF cleavage in HUVECs after baculovirus transduction

(a) ROS production in HUVECs after baculovirus transduction. (b) ROS production in HUVECs after LPS stimulation and then baculovirus transduction. (c) ROS production in HUVECs after

LPS stimulation and then baculovirus (A, N, V, AN, AV, NV, and ANV) transduction. (d) ADAMTS13 cleavage of vWF after baculovirus transduction and gene expression.

Finally, to evaluate vWF cleavage by ADAMTS13, vWF production was stimulated using a high salt concentration (285 mosmol/kg) as shown previously [33]. With high vWF levels, we investigate if the delivery of ADAMTS13 by baculoviruses reduced vWF levels (Figure 24d). We see a dose-dependent and significant decrease in vWF levels with ADAMTS13 (MOIs 10 to 1000). An MOI of 100 is sufficient to return vWF levels to the base level. Combination gene expression of ADAMTS13 with either VEGFA or NOS3 also significantly reduced vWF levels with an MOI of 50 each.

Stent coating and characterization

Now that the optimal baculovirus dosage has been determined, the stent delivery system was optimized. A 10 % (m/v) and 20 % (m/v) PVA solution was freeze-thawed several times, but this failed to maintain its shape. Instead, the PVA was cross-linked with 15 % (m/v) STMP and 30 % (m/v) NaOH [201]. A custom 3D cast was created and cross-linked PVA solution was poured into it. The resulting stent was removed from the cast the following day and revealed striations every 200 μm , due to the 3D printer resolution, under the SEM (Figure 25a). Alternatively, a 2 mm diameter stainless steel tube was dipped into the solution to create a layer-by-layer stent. After drying, the PVA stent was taken off the tube and imaged under SEM revealing a smooth surface (Figure 25b-d). The top view from the stent revealed a thickness of $210.4 \pm 10.2 \mu\text{m}$. The fully dissolvable PVA stent had a dried inner diameter of 3 mm and swelled in HBSS to an inner diameter of 5 mm.

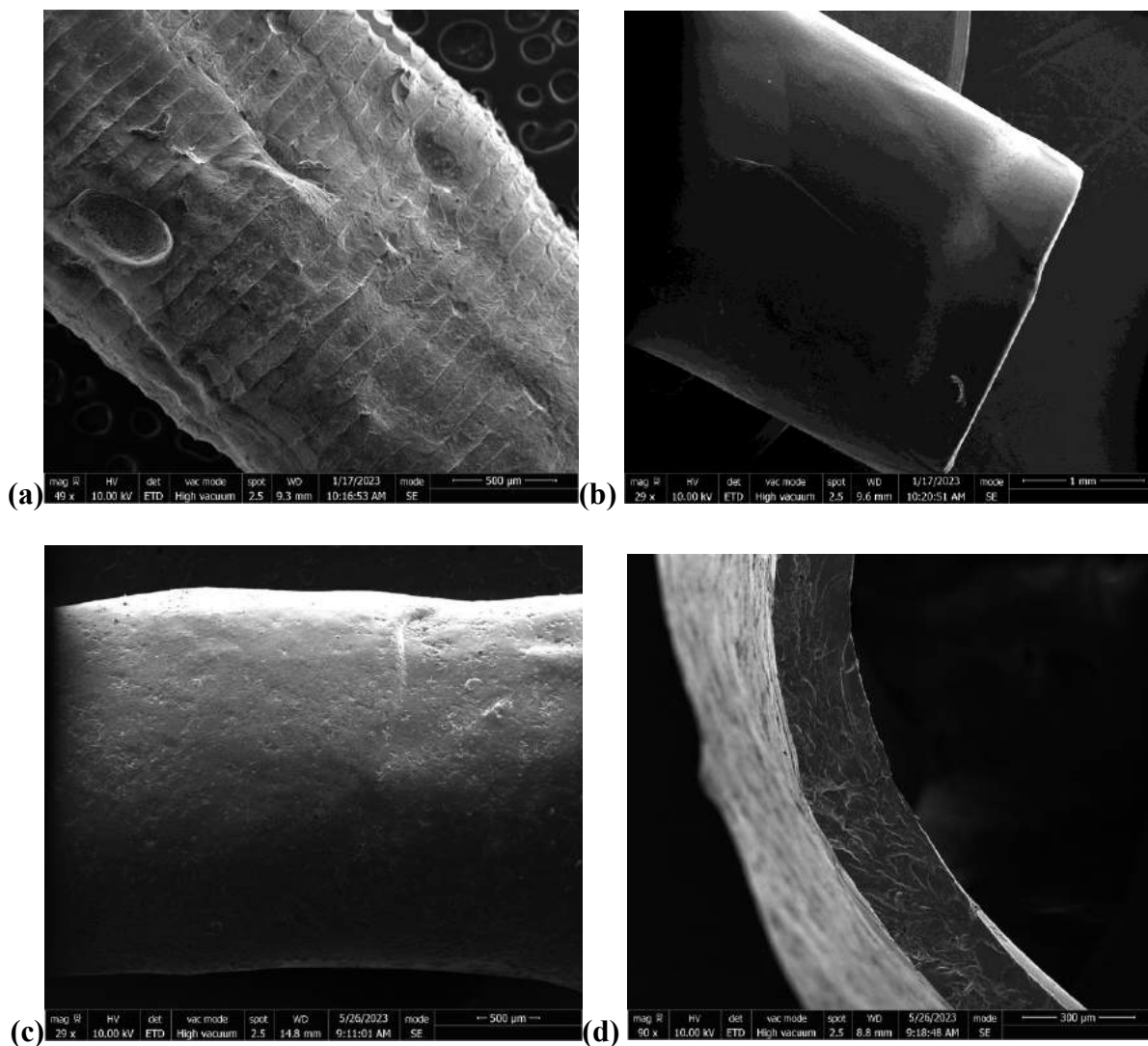
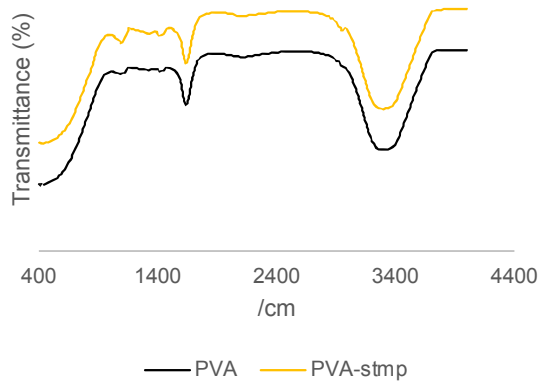


Figure 25. Morphology of the dissolvable stents

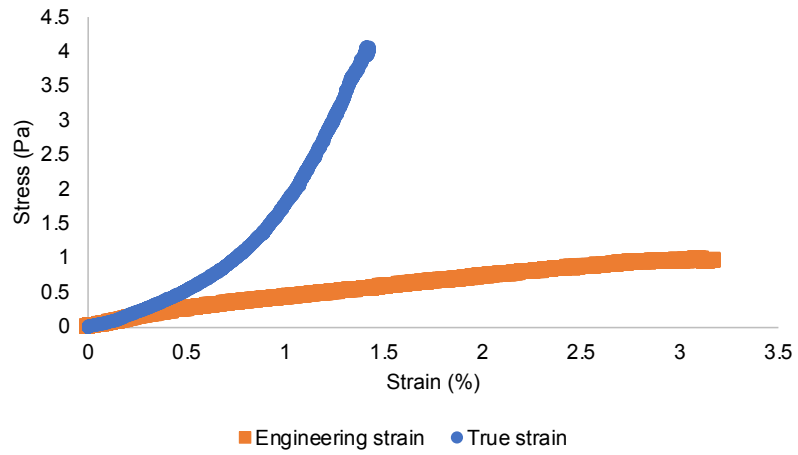
(a) A dissolvable PVA stent created using a 3D-printed cast. (b-c) A biodegradable PVA stent created using dip coating. (d) top SEM view of biodegradable stent.

The chemical and mechanical properties of the stent and coating was also investigated using swelling tests, FTIR, and tensile testing (Figure 26). The key peaks for PVA were presenting including, 3300 cm^{-1} (OH group), 1100 cm^{-1} (C-O stretching), and 720 cm^{-1} and 1400 cm^{-1} (CH_2 in PVA). FTIR analysis also revealed peaks around 1060 and 1230 cm^{-1} due to the addition of the STMP crosslinker and PO_3^- bond creation. The PVA stent had good mechanical strength with a modulus of elasticity of $1.47 \pm 0.3\text{ MPa}$. The modulus was calculated as the slope of the stress-

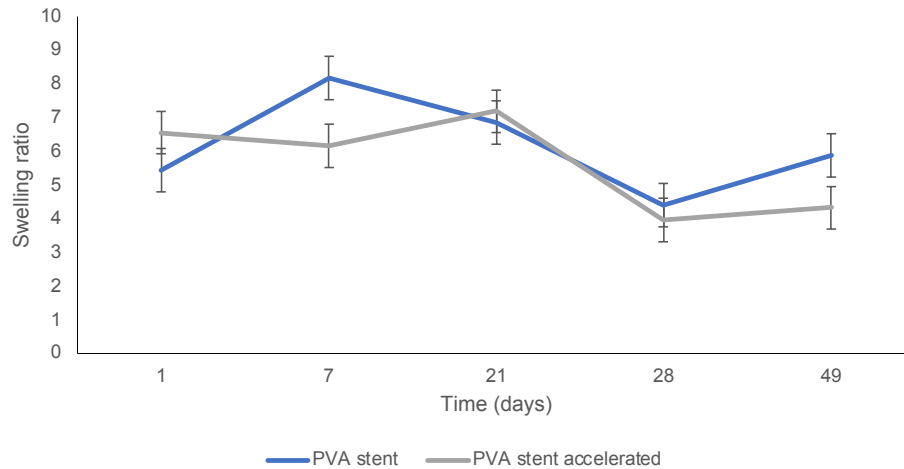
strain curve at 60 % strain. Meanwhile, the mechanical strength was also maintained with two of the three samples slipping before breaking and the final sample breaking at 600 % stretch. Moreover, the swelling ratio and degradation of the stent was investigated, revealing stable degradation over two months.



(a)



(b)



(c)

Figure 26. Mechanical properties of the dissolvable PVA stent

(a) ATR-FTIR analysis of the PVA stent. (b) Uniaxial tensile testing of the stent. (c) Stent swelling ratio over time.

Next, passive diffusion was used to load the stent with baculovirus (BV). Different amounts of the baculovirus were added to determine the change in loading potential (Figure 27). When 2.0×10^7 TU/mL and 4.0×10^7 was diffused onto the PVA stent, the loading efficiencies were $30.9 \pm 1.9\%$ and $38.6 \pm 3.8\%$, respectively. The higher BV dose was used for all subsequent experiments. The baculovirus elution was sustained for up to 10 days. Baculovirus elution from the stent was also stable and remained viable even in 50 % serum.

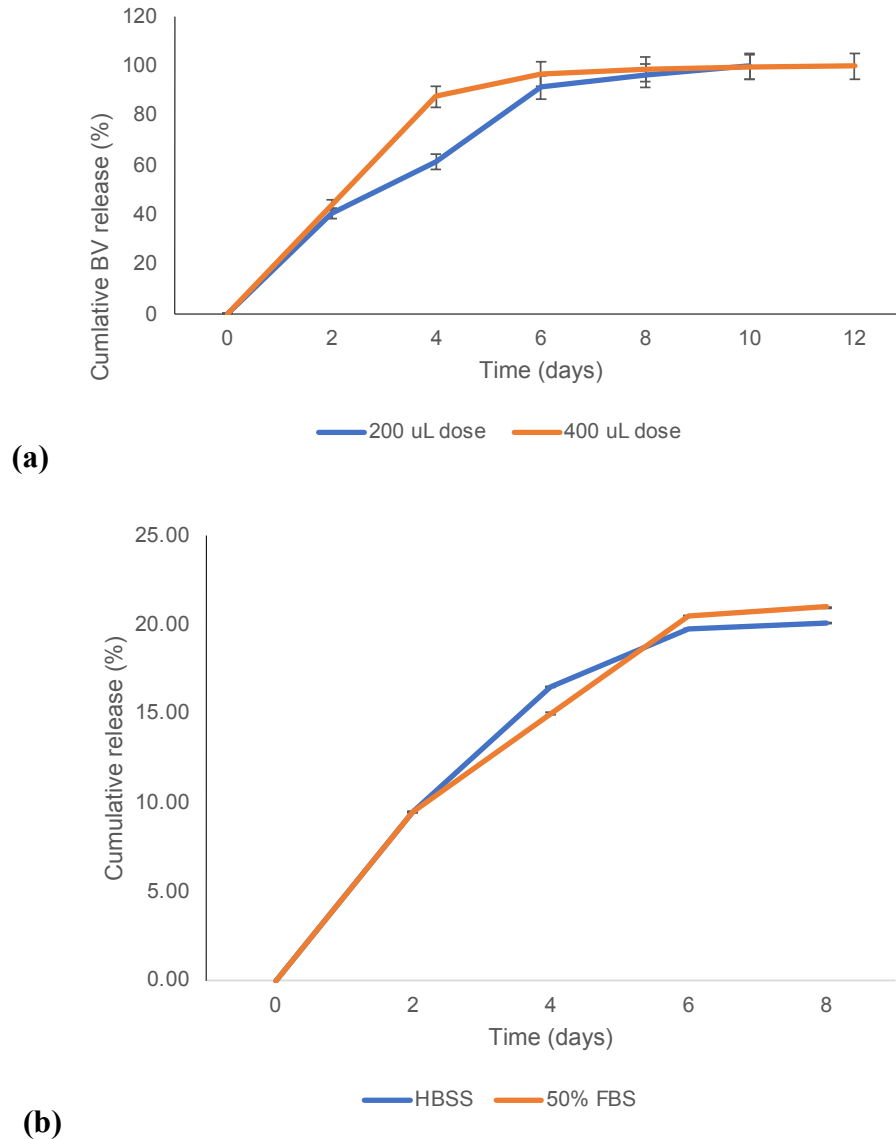
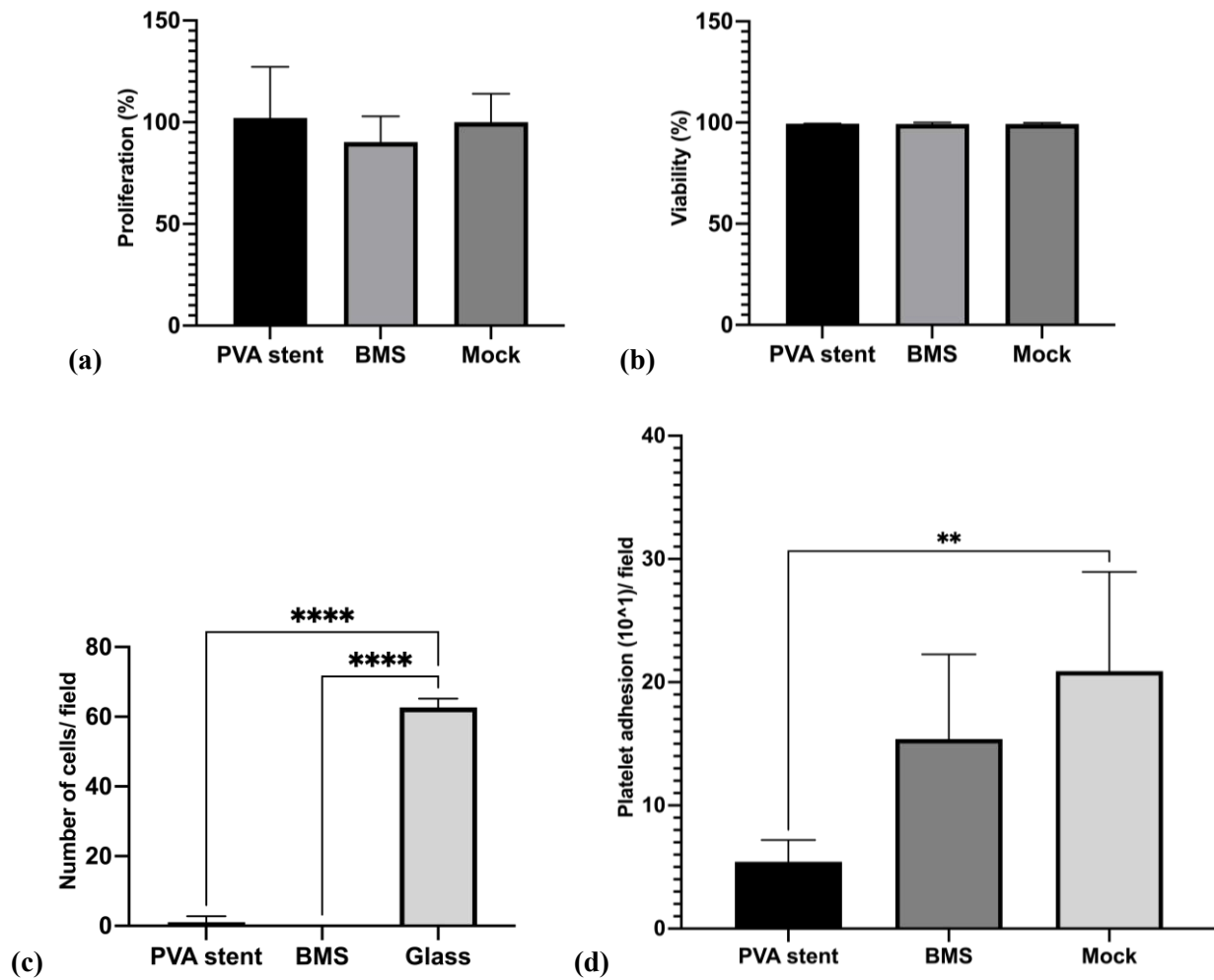


Figure 27. Baculovirus release from the PVA-coated stents over time at different conditions
 (a) BV release from PVA-coated stents based on initial loading. (b) Cumulative BV transduction unit release in Hank's Balanced Salt solution (HBBS) and 50 % (v/v) serum.

The toxicity and hemocompatibility of the stent were also investigated given its direct contact to arterial blood (Figure 28). To ensure the stent coating was non-cytotoxic, a Live Dead and MTT proliferation assay was performed after 48 hours of stent incubation (Figure 28a-b). There was no significant change in cell viability or proliferation after incubation with a bare-metal or PVA stent compared to the mock control. HUVECs were also seeded directly onto the stent to

see if it supported direct cell growth but saw identical cell attachment compared to the BMS (Figure 28c). Similarly, platelet-rich plasma was harvested and seeded onto different stents to determine if they promote platelet adhesion (Figure 28d). Platelets adhered significantly less to the PVA stent than the polystyrene control. Also, the stent did not induce hemolysis (Figure 28e). Moreover, the PVA stent significantly reduced blood coagulation compared to the BMS and polystyrene surface (Figure 28f).



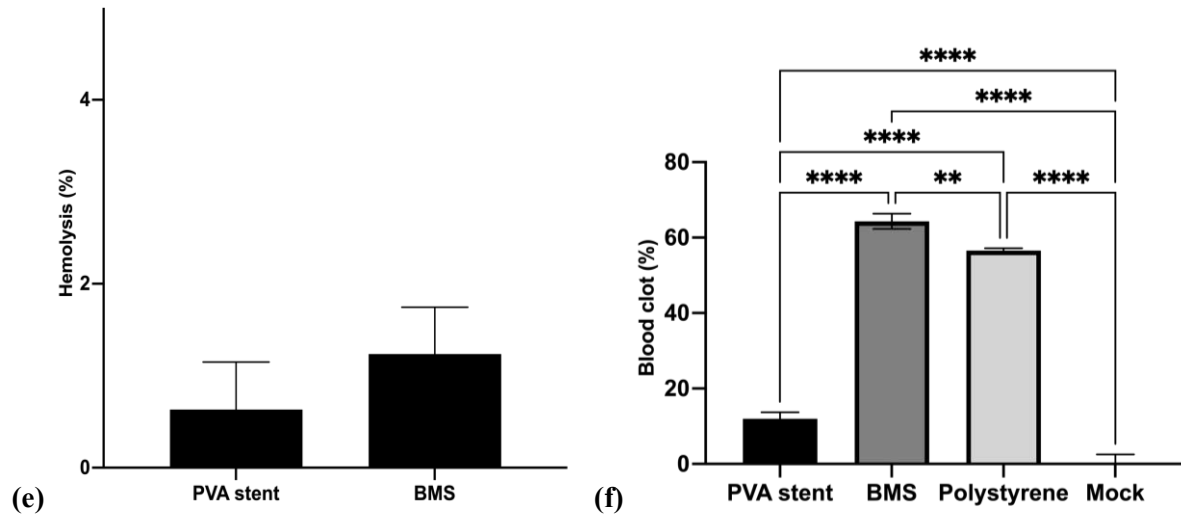


Figure 28. Stent cytotoxicity, hemocompatibility, and cell adhesion

(a) Cell proliferation after stent incubation. (b) Cell viability after stent incubation. (c) HUVEC adhesion to the stents. (d) Platelet adhesion to the stents. (e) Hemolytic potential of the stent system. (f) Blood coagulation on the stent.

Discussion

The gold standard peripheral stent would be capable of site-specific delivery, highly efficient gene delivery, high retention, functionality, and anti-thrombotic properties. Baculoviruses provide an efficient and site-specific delivery method of three genes (ADAMTS13, NOS3, and VEGFA) that can work additively to promote reendothelialization, prevent thrombosis, and prevent smooth muscle cell proliferation mitigating in-stent restenosis. Short-term baculovirus gene delivery can return arterial homeostasis to the diseased artery. Baculovirus gene delivery was reported to be non-inflammatory (CRP and ROS levels) and hemocompatible.

Baculovirus gene delivery is efficient, safe, and feasible. The lack of carbon dioxide or serum requirements and large scalability in shake flasks make this approach feasible [202]. Moreover, baculovirus gene delivery resulted in a significant increase in each gene of interest (GOI). Even high doses of the baculovirus were safe, with no evidence of cytotoxicity in SMCs or

HUVECs. Moreover, the baculovirus and genes did not induce C-reactive protein (CRP) or ROS production, which would indicate an initial inflammatory response. This is particularly important as the gene delivery should not contribute to the disease pathogenesis. CRP is elevated (up to 1000-fold) at sites of infection and inflammation, particularly in cardiovascular events [144]. High CRP levels have been associated with restenosis, major adverse cardiovascular events, and tripled the risk of developing peripheral vascular disease [203], [204]. CRP is a reliable marker for predicting adverse cardiovascular events and atherosclerosis [203], [205].

The genes delivered by the baculovirus also had significant beneficial therapeutic effects. Specifically, VEGFA promoted HUVEC proliferation ($p < 0.05$), migration ($p < 0.005$), and angiogenesis ($p < 0.05$) as reported elsewhere [137]. This would be significant for the initial stages after stent implantation to promote endothelial cell migration for complete arterial re-endothelialization, preventing downstream restenosis [48], [49]. VEGF and nitric oxide (NO) appear to interact heavily with reports of VEGF delivery also increasing NO levels [48]. NOS3 delivery alone also promoted HUVEC migration ($p < 0.0005$). Comparatively, NOS3 (MOI of 100) promoted HUVEC proliferation ($p < 0.0005$) without promoting SMC proliferation which is an important factor in promoting endothelialization while preventing neointimal hyperplasia [180], [206]. NOS3 also inhibited ROS production after LPS-induction ($p < 0.005$) which would help create an anti-inflammatory environment at the site of stent implantation. Reactive oxygen species (ROS) have a complex role in atherosclerosis and PAD. ROS can further contribute to the disease pathogenesis through several pathways [196]. However, more regulatory ROS molecules like nitric oxide can promote VEGF-induced endothelial function and migration which is important for PAD treatment following stenting [207]. Finally, ADAMTS13 delivery was functional and cleaved vWF in a dose-dependent manner [199]. ADAMTS13, naturally secreted from healthy endothelial

cells, was selected for its potential anti-thrombotic properties [208]. ADAMTS13 is a metalloproteinase that cleaves large multimers called von Willebrand factor (vWF) into smaller pieces and prevents early stages of platelet aggregation [199], [200]. This would have a beneficial antithrombotic property for the stent. The anti-thrombotic activity of ADAMTS13 can work additively with the PVA coating.

Overall, either NOS3-VEGFA or ADAMTS13-NOS3 delivery showed the most promising therapeutic effects *in vitro*. Specifically, ADAMTS13-NOS3 delivery promoted HUVEC migration ($p < 0.0005$), promoted HUVEC proliferation ($p < 0.005$), regulated SMC proliferation, reduced ROS production ($p < 0.0005$), and cleaved vWF ($p < 0.0005$) compared to mock cells. NOS3-VEGFA delivery significantly stimulated HUVEC proliferation ($p < 0.05$), migration ($p < 0.005$), and angiogenesis ($p < 0.05$) which may help promote re-endothelialization following stent implantation. The novel stent design elutes the baculovirus for ten days resulting in gene expression for over fourteen days. Beneficially, previous studies report that gene elution for as little as ten to fourteen days is sufficient to achieve significant therapeutic benefits [48], [209]. Moreover, baculovirus viability and elution were not hindered in the presence of serum, which typically forms 55 % of blood.

The stent itself also possesses antithrombotic, mechanically sound, and flexible features. Moreover, the stents have an excellent shelf-life. The dried stent and baculovirus stock should be stored separately for over one year [190]. Prior to implantation, the stent can be incubated overnight in the baculovirus stock to passively load the baculovirus as reported in this paper.

The stent coating also showed favourable mechanical properties. The stent swelled 1.67-fold in diameter in saline and serum. Previous studies have reported that PVA stents have a higher or comparable radial force ($6.6 \pm 0.6 \text{ mN mm}^{-2}$) to BMS ($4.4 \pm 0.3 \text{ mN mm}^{-2}$) [210]. However,

the stent maintained flexibility which is important for peripheral arteries which are subjected to continuous movement and bending. Specifically, the PVA stent has a lower modulus of elasticity (1.47 ± 0.3 MPa) compared to 193 GPa for stainless steel and 45 GPa for magnesium based stents [211]. The stent also showed stable degradation with minimal loss over the accelerated two-month testing.

The cytotoxicity and hemocompatibility of the stent system was also evaluated. Beneficially, no cytotoxicity or difference in cell proliferation was observed with direct cell incubation. Moreover, minimal platelet adhesion and whole blood coagulation were observed, which is important to maintain an anti-thrombotic surface. The stent also demonstrated no signs of hemolysis. Finally, cellular adhesion rates were similar to commercial bare-metal stents (BMS). Similar to previous studies, the stent exhibited a smooth surface which is important from an anti-thrombotic perspective and to prevent immune cell accumulation, which could lead to thrombosis [34].

Future studies should be conducted *in vivo* to confirm the therapeutic efficacy and safety. The stent can also be modeled and scaled up or down to fit in different arteries. As the artery becomes larger a bigger stent is also required enabling more baculovirus to be loaded to reach the therapeutic threshold. This also allows its use on other stent types and anatomical locations. The coating can even be integrated into metal stents or other polymer-based stents to mitigate complications and improve the quality of life of those impacted by PAD.

Conclusion

Overall, the baculovirus-eluting PVA stent fabricated here may mitigate current peripheral stent complications including in-stent restenosis, endothelial dysfunction, and thrombosis. The genes delivered by the baculovirus promote endothelial recovery, endothelial migration, and

prevent inflammation. The gene delivery matches the therapeutic timeline while maintaining a very high safety profile (no signs of cytotoxicity, inflammation, or hemotoxicity). The genes and PVA provide an anti-thrombotic coating by preventing platelet adhesion and blood coagulation. The PVA stent also acts as a physical barrier to prevent SMC hyperproliferation. Meanwhile, the stent itself demonstrated sufficient mechanical strength yet flexibility to improve stent patency. These improvements may reduce complications and improve clinical outcomes mitigating the health and economic burden of PAD.

Materials and Methods

Insect cell culture

Sf9 cells (Novagen, Sigma Aldrich, Burlington, Massachusetts, United States) were maintained in T75 flasks or 250 mL shaker flasks at 27 °C. To maintain the exponential growth phase, the cells were subcultured two to three times per week, using BacVector media (Sigma Aldrich). The shaker flasks were rotated at 130 rpm.

Gene cloning

Three human genes (ADAMTS-13, NOS3, and VEGFA) were purchased from GenScript (Piscataway, NJ, USA). EcoRI and NotI were used to cut out the gene of interest (GOI) and ligate it into a pOET6 plasmid (MJS Biolynx Inc., Brockville, ON, Canada). Each gene was inserted following the CMV promoter using Instant Sticky End Ligase (NEB, Ipswich, Massachusetts, USA). The complete plasmid was then transformed into chemically competent DH5 alpha *E. Coli* (Thermo Fisher). The colonies containing the gene of interest and ampicillin resistance were selected and amplified. The plasmid was then purified from the *E. coli* using NEB's plasmid purification kit. The final plasmid structures were confirmed using a restriction enzyme gel check and NanoDrop (Thermo Fisher, Waltham, Massachusetts, USA) and used for all future steps.

Baculovirus transfection

One hour before the transfection, 0.5×10^6 Sf9 cells/well were seeded into a 12-well plate. Next, 40 μ L of PBS, 200 ng of the plasmid, 200 ng of the flashBAC, and 0.48 μ L of TransIT reagent were mixed and incubated for 15 minutes at room temperature. Next, 0.5 mL of the insect media was aspirated, leaving 0.5 mL remaining. The baculovirus transfection mix was then added dropwise to the wells. PBS was used as a mock control. The plate was incubated overnight and the next day, 0.5 mL of insect media was added to each well. The plate was then incubated for another four days before the media containing the Po baculovirus stock was harvested. A baculovirus expressing GFP in Sf9 cells was generated as a control for easy monitoring and titration.

Baculovirus amplification

The P₀ baculovirus stock was used to amplify each baculovirus with the specified gene of interest. First, 100 mL of Sf9 cells were diluted to a concentration of 2×10^6 Sf9 cells/mL in a shake flask. Next, 0.5 mL of the original P₀ baculovirus stock was added to the cells and the flask was incubated for four days. After four days, the cells were centrifuged at $300 \times g$ for 10 minutes and the viral suspension media (P₁) was collected and stored in the dark at 4 °C.

Baculovirus titration

The baculovirus P₁ stock was titrated using two methods. The fluorescent titration was calculated using the GFP expressed by the baculovirus. The Fast Plax Titration kit (Sigma Aldrich) was used to calculate the titration of the three other baculoviruses as described by the supplier. For the fluorescent titering assay, 1.0×10^4 Sf9 cells/well were seeded into a 96-well plate and incubated for one hour. During the incubation, the virus was diluted using insect cell medium (1:10, 1:50, 1:100, 1:1000, and 1:10000). The cell media was then aspirated off the Sf9 cells and 50 μ L of the virus dilution was added to each well. The plate was incubated for one hour and then

an addition 0.5 mL of insect cell media was added to each well and incubated at 27 °C. Twenty-four hours after, the number of fluorescent cells was counted in each well with less than 40 % of fluorescent cells. The following equation was used to calculate the titration:

Transduction Units (TU)/mL= (number of cells transduced x percent of fluorescent cells x dilution factor)/ (transduction volume in mL)

Mammalian cell culture (human smooth muscle and umbilical vein endothelial cells)

Human umbilical vein endothelial cells (HUVECs) and smooth muscle cells (SMCs) were cultured at 37 °C in a 5 % CO₂ incubator. were cultured in complete endothelial growth media (Sigma Aldrich, St. Louis, MI, USA). The SMCs (Coriell Institute for Medical Research, Camden, NJ, USA) were cultured in M199 media supplemented with 10 % FBS and 0.02 mg/mL endothelial cell growth supplement (Sigma Aldrich). The cell media was changed every second day and the cells were subcultured just prior to confluency. All cells were used before passage five.

Baculovirus transduction

First, 1.0×10^4 mammalian cells/well were seeded into a 96 black well plate with a clear bottom (Corning3603, Thermo Fisher, Waltham, MA, USA) and incubated overnight at 37 °C with 5 % CO₂. The next day, the cell media was removed, and the designated amount of baculovirus was added to each well. The baculovirus was incubated with the cells for three hours before being aspirated and replaced with fresh cell media. The plate was then incubated as before for 24 to 48 hours before being used in the experiments listed below.

Percent of cells expressing red fluorescent proteins (RFP) and relative fluorescent units

After the baculovirus transduction, the 96-well plate was read on an EnSpire multiplate reader (Perkin Elmer, Waltham, Massachusetts, USA) at 588 nm. Next, the cells were imaged using an Operetta High Content Analysis System (Perkin Elmer) using bright field or fluorescent

red and blue filters. The number of cells was counted for each image and compared to the number of cells expressing the red fluorescent protein (RFP) using Columbus (Perkin Elmer). Nine images were taken of each well and all treatments were done in triplicate.

Reverse transcription-quantitative polymerase chain reaction (RT-qPCR)

For RT-qPCR, cells were transduced as described above with each of the viruses individually and in combination. Twenty-four hours after transduction, the cell RNA was extracted using an RNA extraction kit (Bio Basic, Markham, ON, Canada) and used immediately or stored at -80 °C until use. Primers for ADAMTS13, NOS3, VEGFA, and Beta-actin reference gene were purchased from Bio-Rad (Hercules, CA, USA). The RNA, primers, and polymerase solution were mixed as described by the Luna Universal One-Step RT-qPCR kit (New England Biolabs, Ipswich, MA, USA). The reaction was run on an Illumina Eco Real-Time PCR machine ® (San Diego, CA, USA) as directed by the supplier. Amplification was carried out for 45 cycles with 35 s (denaturation), 55 °C for 35 s (annealing), and 72 °C for 25 s (extension).

MTT proliferation assay

For the MTT proliferation assay, the baculovirus transduction protocol was followed as described above. The next day (24 hpi), 50 µL of 5 mg/mL MTT was added to each well and incubated for three hours. Next, 35 µL of 37 % HCl was added to 10 mL of isopropanol. This solution was mixed and 100 µL was added to each well and mixed via pipetting. The absorbance of the plate was measured at 570 nm using an EnSpire multimode plate reader.

To evaluate the impact of the stent on cell proliferation, the PVA stent was added to a 24-well plate containing mammalian cells. After incubation, the stent was removed and 200 µL of 5 mg/mL MTT was added to each well. The cells were then incubated for three hours, and a 0.04 N hydrochloride solution diluted in isopropanol was added and mixed thoroughly. The cell

supernatant containing the dissolved MTT was placed into a 96-well plate and read at 570 nm using the same EnSpire plate reader as above.

Live Dead assay

For the live dead assay the mammalian cells were transduced as described above. After 24 or 48 hours, a 2X live dead stain was diluted in 10 mL of cell media using 50 μ L of 1 mM Calcein AM and 50 μ L of 2.5 mg/mL Propidium Iodide. Next, 100 μ L of the live dead stain was added to each well. The plate was incubated for 30 minutes and then imaged using the same Operetta microscope system. The live dead cell count was performed using Columbus.

A similar approach was adopted with direct stent incubation, in a 12-well plate, to determine the impact on cell viability.

Scratch or wound healing assay

An in vitro scratch assay was performed as previously described with slight modifications [212]. Again, HUVECs were seeded into 96-well plates and grown until confluency. Once they were confluent, the cells were transduced with different MOIs of the baculovirus for three hours. The virus inoculum was aspirated, and fresh media was added. Twenty-four hours after baculovirus transduction, the wells were scraped with a p200 pipette tip. After twelve hours, the wells were imaged when some wounds had healed. The images were analyzed using an ImageJ plugin [162].

Endothelial tube formation assay (angiogenesis assay)

To determine the angiogenic properties of the baculovirus-eluted genes, an endothelial tube formation assay was performed as previously described [163]. Cultrex (50 μ L) reduced growth factor basement membrane (Bio-Techne, Minneapolis, MN, USA) was added to the bottom of each well of a 96-well plate. The plate was then incubated for 30 minutes before 2×10^4

HUVECs/well were seeded on top. Finally, 50 μ L of cell media supernatant from previously transduced cells was added. The cells were incubated at 37 °C in a 5 % CO₂ incubator for four hours or until well-defined vasculature could be seen. Cell media or DMSO were used as positive and negative controls, respectively.

Reactive oxygen species (ROS) assay

To induce an inflammatory environment, cells were pre-treated with 50 μ L of 100 ng/mL lipopolysaccharide (LPS) and interferon-gamma (IFN γ). Following treatment, cells were transduced with different MOIs of the baculovirus to determine if the gene expression reduces ROS production. The transduction protocol was followed as above. Forty-eight hours after treatment, a ROS kit (Abcam 186029, Waltham, Boston, USA) was used to measure ROS production as described by the supplier.

Stent fabrication

The self-expandable PVA stents were generated as previously described with slight modifications [201]. Briefly, 20 mL of 10 % (m/v) PVA was made in sterile water at 90 °C and 700 rpm. Next, 200 μ L of 15 % (m/v) sodium trimetaphosphate (STMP) was added, stirring the solution for five minutes. Finally, 80 μ L of 30 % (m/v) sodium hydroxide was added to the PVA solution and stirred for another five minutes. A stainless-steel tube with a diameter of three millimeters was dipped into the PVA solution and dried for 15 minutes. This process was repeated seven times. After the seventh dip, the stent was placed in a -20 °C freezer overnight. The next day, the stent was removed from the tube and dried at 37 °C overnight. Finally, the stent washed with 85 % (v/v) ethanol followed by sterile PBS for sterilization prior to further studies. The same process was employed for the Eucatech® PVA-coated stent without stent removal.

Stent coating morphology with scanning electron microscopy (SEM)

The self-expandable PVA stents were dried overnight at 37 °C before being imaged. A high vacuum and a 10 kV voltage were used with the FEI 450 Quanta SEM at the Facility for Electron Microscopy Research (FEMR).

Baculovirus release from the stent

The coated stent was dried overnight at 37 °C before incubating the stent in a baculovirus stock solution to allow passive absorption. As previously reported, passive absorption was selected to maintain virus activity compared to direct incorporation. The stent was incubated at 27 °C overnight before removing the stent and placing it into a clean new well. Next, 1 mL of HBSS was added to cover the stent. The HBSS was removed at designated times to determine the amount of baculovirus released over time.

Hemolysis assay

Blood samples from two individuals (Male 49, Hispanic and female 29, white; Innovative Research Inc, Novi, Michigan) were tested independently in triplicate. The hemolysis of the stents was evaluated using whole blood. Briefly, the stents were immersed into 1 mL of PBS in a 15 mL centrifuge tube. Next, 4 mL of citrated blood was mixed with 5 mL PBS and 0.1 mL of the diluted blood was added to each sample. The samples were incubated at 37 °C for one hour and then centrifuged at 1000 rpm for 10 minutes. The supernatant containing the lysed hemoglobin was placed into a 96-well plate, and the absorbance was read at 545 nm. A standard curve for the hemolysis was also generated using dilutions of PBS and deionized water and compared. The negative and positive control was PBS and deionized water, respectively. The following equation was used to determine the percent hemolysis.

$$\text{Hemolysis (\%)} = ((\text{OD}_{\text{sample}} - \text{OD}_{\text{negative control}}) / (\text{OD}_{\text{positive}} - \text{OD}_{\text{negative}})) \times 100\%$$

Blood coagulation assay

Blood coagulation on the stents was also evaluated using a method described by Sabino et al. [160]. Briefly, the stents were placed into a 24-well plate. Next, 7 μL of whole blood was pipetted onto the surface of each stent. At 15, 30 and 45 min, deionized water was added to each sample and incubated for 5 minutes. The resulting supernatant was removed, and the absorbance was read on a 96-well plate at 540 nm. As a control, 7 μL of whole blood in distilled water was used as a control where no blood clotted onto a biomaterial surface. A ‘mock’ polystyrene surface was also used to compare the blood coagulation properties of the hydrogels.

Platelet adhesion assay

A platelet adhesion assay using a lactate-dehydrogenase (LDH) kit (abcam, Waltham, Boston, USA) was performed as previously described [213]. First, platelet rich plasma (PRP) was obtained by centrifuging the blood at 1000 x g for 20 minutes. The platelet concentration was 952 ± 98 platelets/ μL and were allowed to rest for 30 minutes. Meanwhile, the stents were added to a 24-well plate and washed with PBS. The stents were then covered with 200 μL of the PRP and incubated for one hour at 37 °C. After the incubation, the stents were carefully removed and washed with PBS. The stents were then incubated with 50 μL of 2 % (m/v) Triton X-100 diluted in PBS for 30 minutes at 37 °C to lyse the adherent platelets. Next, 50 μL of the lysed platelet solution was used for the LDH assay. The supplier’s protocol was followed and a standard curve for platelet and NADH activity was created to verify assay accuracy. The lysed platelet standard curve was used to determine the adherent platelet concentration.

Tensile testing

To perform the tensile testing, a flat PVA sheet was generated using the same stent synthesis method mentioned above. Once the PVA sheet was fully dried a 3D printed ‘cookie cutter’ was used to cut out a dumbbell shape as described in ISO37:2017. The thickness of the

films was measured in triplicate using a Mitutoyo Litematic VL-50A. Next, the thin films were tested on a Shimadzu Uniaxial tensile and compression tester with a strain rate of 1 %. Sandpaper was added to the clamps to help secure the PVA and prevent slipping.

Statistical analysis

All results are reported as a mean \pm standard deviation (SD) of triplicates, p-values less than 0.05 were considered significant. GraphPad Prism (version 9.0.0 for Windows, GraphPad Software, San Diego, California USA, www.graphpad.com) was used for all one-way ANOVA data analysis with a post-hoc Tukey's test.

Funding: This work was supported by a research grant from the Canadian Institute of Health Research to Dominique Shum-Tim and Satya Prakash (CIHR grant 252743). S.S. is fully funded by the Canadian Graduate Scholarship-Doctoral Award from the Natural Sciences and Engineering Research Council (NSERC, 569661-2022). P.I. is funded by the Islamic Development Bank Scholarship (2020-245622). K.B. is funded by The Fonds de recherche du Québec – Nature et technologies (FRQNT) Doctoral Scholarship. A.A. is fully funded by a scholarship from the Ministry of Higher Education of the Arab Republic of Egypt. R.T. is funded by the Canadian Graduate Scholarship-Master's from NSERC.

Data Availability Statement: All data is contained within the article.

Acknowledgments: We thank the Facility for Electron Microscopy Research of McGill University (SEM equipment), McGill Chemistry Characterization Facility (ATR-FTIR), and the McGill University Imaging and Molecular Biology Platform (Fluorescent Operetta Microscope) for their equipment and services.

Copyright: This is an open-access article under the CC BY-NC-ND license (<http://creativecommons.org/licenses/by-nc-nd/4.0/>).

Bridging text

In the previous paper, I investigated three different genes individually and additively. All genes did not significantly reduce cell viability, even at high doses (MOI 1000). Similarly, all genes did not induce CRP or ROS production, markers of inflammation, even at high MOIs. Cell proliferation depended on the cell type and gene expressed by the baculovirus.

Each gene demonstrated its own therapeutic benefit. VEGFA significantly promoted cell proliferation, migration (wound healing study), and angiogenesis. However, VEGFA was not cell-type specific and exerted these effects on SMCs and HUVECs. This would recruit both HUVECs and SMCs to the site and could contribute to neointimal hyperplasia. Comparatively, NOS3 inhibited SMC proliferation preventing the early stages of neointimal hyperplasia. NOS3 did not significantly impact HUVEC proliferation. NOS3 also significantly improved HUVEC migration which assists with re-endothelialization. Moreover, lower doses of NOS3 (MOI 10 and 100) were able to significantly reduce ROS after LPS-induced inflammation (to mimic the inflammatory environment seen in PAD). ADAMTS13 reduced SMC proliferation at high doses but not HUVEC proliferation. ADAMTS13 also cleaved von Willebrand Factor (vWF), which is a clotting factor involved in the initial stages. Transduction with baculoviruses expressing ADAMTS13 significantly reduced vWF levels after being treated with high salt to induce vWF secretion.

The genes were also tested together to determine if there was any relationship. The therapeutic effect of ADAMTS13, NOS3, and VEGFA varied slightly when expressed with each other. ADAMTS13 and NOS3 significantly improved HUVEC proliferation but not SMC proliferation. AN expression significantly improved HUVEC migration. AN expression also significantly reduced ROS production after LPS-induced inflammation. Overall, I found that

ADAMTS13 and NOS3 (termed AN) together had the best properties and were loaded onto the stent.

The stent coating was optimized several times. Different polymers such as PLGA, PLA, and PVA were tested. Moreover, different coating methods were investigated, specifically spray coating vs dip coating. Overall, I found that dip coating PVA cross-linked with sodium trimetaphosphate (STMP) produced the smoothest coating with the least artifacts. PVA also exhibited beneficial properties, including elasticity, mechanical strength, hemocompatibility, and sustained baculovirus delivery. The high elasticity yet mechanical strength enabled stent expansion and deployment without disrupting the smooth stent coating. Moreover, the stent coating sustained baculovirus delivery over ten days enabling gene expression for the desired therapeutic window. The stent was also non-toxic and did not affect cell proliferation or viability. The stent system also inhibited platelet adhesion and whole blood coagulation, which is important to prevent initial thrombosis stages. The stent also did not induce any hemolysis.

The fifth and final thesis paper completes the thesis objectives, developing a gene- and drug-eluting stent for atherosclerotic treatment. I report an optimized stent based off the viral dosage, gene expression, stent coating, and elution timeframe. The sustained drug elution addresses the final stent complication, long term inflammation and restenosis.

CHAPTER 8: A gene- and drug-eluting (GDES) stent coating to
promote re-endothelialization and prevent restenosis due to
atherosclerosis

Sabrina Schaly¹, Paromita Islam¹, Jacqueline L. Boyajian¹, Rahul Thareja¹, Ahmed Abosalha^{1,2}, Karan Arora¹, Dr. Dominique Shum-Tim³, and Dr. Satya Prakash^{1,*}

¹ Biomedical Technology and Cell Therapy Research Laboratory, Department of Biomedical Engineering, Faculty of Medicine and Health Sciences, McGill University, 3775 University Street, Montreal, Quebec, H3A 2B4, Canada

² Pharmaceutical Technology Department, Faculty of Pharmacy, Tanta University, Tanta 31111, Egypt

³ Division of Cardiac Surgery, Royal Victoria Hospital, McGill University Health Centre, McGill University, Faculty of Medicine and Health Sciences, Montreal, Quebec, H3G 2M1, Canada

* Corresponding author satya.prakash@mcgill.ca

Author contributions: I am the first author and contributed to all experiments and manuscript preparation.

Science Advances

(To be submitted)

Abstract

Coronary artery disease (CAD) occurs in one out of every 20 people over 20, creating a significant health and economic burden worldwide. One common cause of CAD is atherosclerosis (plaque build-up) which includes endothelial dysfunction, inflammation, and smooth muscle cell hyperproliferation. Currently, a bare-metal stent (BMS) or drug-eluting stent (DES) is used to force open the artery. However, current stents lead to complications, including blood clotting, inflammation, and arterial re-narrowing leading to reintervention, heart failure, stroke, and death. To mitigate these complications, a novel gene- and drug-eluting stent (GDES) was developed. The stent was synthesized by dip-coating a BMS into a polyvinyl alcohol and Everolimus solution and loaded passively with baculoviruses expressing NOS3. The gene and drug are eluted over 10 and 86 days, respectively. The gene, NOS3, promotes endothelial cell proliferation, prevents smooth muscle cell hyperproliferation, reduces reactive oxygen species production, and induces endothelial cell migration. The two-week gene expression is sufficient to leave behind a fully reformed endothelial lining, preventing downstream complications. Meanwhile, the 86-day Everolimus elution prevents inflammation or neointimal hyperplasia progression. The stent coating and system are non-cytotoxic and hemocompatible. The dissolvable and anti-thrombotic stent coating remains intact during expansion and demonstrates slow, uniform degradation. Overall, the gene and drug elution work together to mitigate current cardiovascular stent complications by promoting endothelial health and preventing downstream inflammation and hyperproliferation.

Keywords: Atherosclerosis, coronary artery disease, drug-eluting stent, gene-eluting stent, thrombosis, restenosis, nitric oxide

Introduction

Coronary artery disease (CAD) is defined as the obstruction of arteries supplying the heart with nutrients and oxygen. CAD is the third leading cause of death yearly, generating a large health and economic burden [16]. Around one out of 20, people have CAD [15]. The obstructed arteries can be attributed to atherosclerosis, including calcification, inflammation, endothelial dysfunction and neointimal hyperplasia [14]. In CAD, low-density lipoprotein accumulates, leading to endothelial dysfunction and immune cell accumulation. The endothelial cells become dysfunctional and begin expressing new receptors, inflammatory cytokines, and reactive oxygen species [144], [196]. This causes the medial layer of smooth muscle cells to hyperproliferate (termed neointimal hyperplasia), leading to arterial narrowing (termed restenosis). Plaque formation and calcification occur over time, further contributing to arterial dysfunction. All of this leads to the proliferation of the medial cell layer (neointimal hyperplasia), inflammation, and more plaque development, all narrowing the blood vessel and creating a positive feedback loop. Eventually, a necrotic core can form within the plaque and occlude off generating thrombi.

One of the main treatments for CAD includes implanting a stent. A stent is used to force open the artery and has successfully saved millions of lives [25]. The bare-metal stents (BMS), typically composed of 316L stainless steel or nitinol, can effectively open the artery and allow blood passage. However, this bare stent design has the highest occurrence of thrombosis and restenosis, 18 % and 2 %, respectively [59]. Further complications arise at the stent site due to incomplete endothelial regrowth and vascular SMC proliferation. This can lead to blood vessel narrowing and blood clot [35]. Blood vessel narrowing (restenosis) is defined as a >50 % narrowing of a blood vessel's diameter and occurs in 5-10 % of cases using current drug-eluting stents [36].

Consequently, drug-eluting stents (DES) have evolved to prevent arterial wall thickening and dampen the immune response to prevent inflammation.

Typically, stent implantation induces a chronic vascular response and inflammation leading to neointimal hyperplasia (SMC proliferation). DES vary in shape, coating, and drug type. Some common drugs eluted from stents include Paclitaxel, Sirolimus, Everolimus, and Tacrolimus [60], [61], [63]. Common polymer coatings include a combination of PBMA, polyvinylidene fluoride (PVDF-HF), poly(hexyl methacrylate) (PHMA), polyvinylpyrrolidone (PVP), and polyvinyl alcohol (PVA) for their strength and drug retention abilities.

A DES can prevent smooth muscle proliferation and blood vessel re-narrowing. However, the drug also prevents endothelial cell proliferation and regrowth. This approach reduced the risk of thrombosis and myocardial infarction, but not in-stent restenosis when compared to the first generation of DES [59]. A study involving 31,379 people showed no difference in mortality between BMS and DES [61], [62]. This indicates that although these DES are superior to BMS at first, they have a comparable efficacy after one-year. Overall, the rate of complications (blood clots and blood vessel re-narrowing) is still relatively high at 5-10 % and needs to be addressed by future generations of stents [36].

Permanent polymers used in the first generation of DES, are associated with delayed healing and triggering inflammation. This increases the risk of late and very late thrombosis [64]. There are currently several biodegradable stent coatings on the market (Osrsiro, Ultimaster, Synergy, BioMatrix Nobori, Combo, and BioMartix Flex®) [26]. These stents have polymer coatings that degrade within three to nine months after deployment. However, recent studies have shown no difference in short-term safety or efficacy compared to DES and had a higher risk of collapse or mechanical failure [65], [67], [68]. An alternative dissolvable option, to prevent

polymer-induced inflammation, includes polyvinyl alcohol (PVA) and gelatin. Both of these polymers are biocompatible and easily modifiable properties to optimize for a stent coating [167], [201].

To improve current DES, a dissolvable PVA stent coating that elutes nitric oxide synthase 3 and Everolimus will be investigated. Nitric oxide synthase 3 (NOS3) is produced by functional endothelial cells and generates nitric oxide using L-arginine [191]. Nitric oxide regulates cell proliferation, promotes blood vessel vasodilation, and inhibits bacterial growth. NOS3 and nitric oxide are known for their role in cardiovascular health. Specifically, nitric oxide (NO) can dose-dependently reduce blood pressure and arterial stiffening [45]. It also prevents endothelial cell dysfunction and reduces platelet activation which would lead to thrombosis. NO has shown promise in some pre-clinical trials however, to further improve the gene delivery, a baculovirus will be used. Baculoviruses are insect cell viruses with an excellent safety and efficiency profile [81], [106], [107]. They provide a high but transient gene delivery, ideal for stent applications to initiate endothelial healing the first two to three weeks.

Results

The coated EucaCCFlex Eucatech stent ® (Weil am Rhein, Germany) was used as a base. The stent was coated in PVA or PVA-gelatin mixtures and imaged under an SEM to observe the coating integrity (Figure 31). The stent struts were entirely encased in the coating with an unobstructed inner diameter for blood flow. Visually and under SEM, the stent coating remained smooth and intact even during a one-minute expansion at 9 atm. Moreover, uniform degradation was observed over two months at normal and accelerated conditions. A smooth surface and uniform degradation are important to prevent thrombosis.

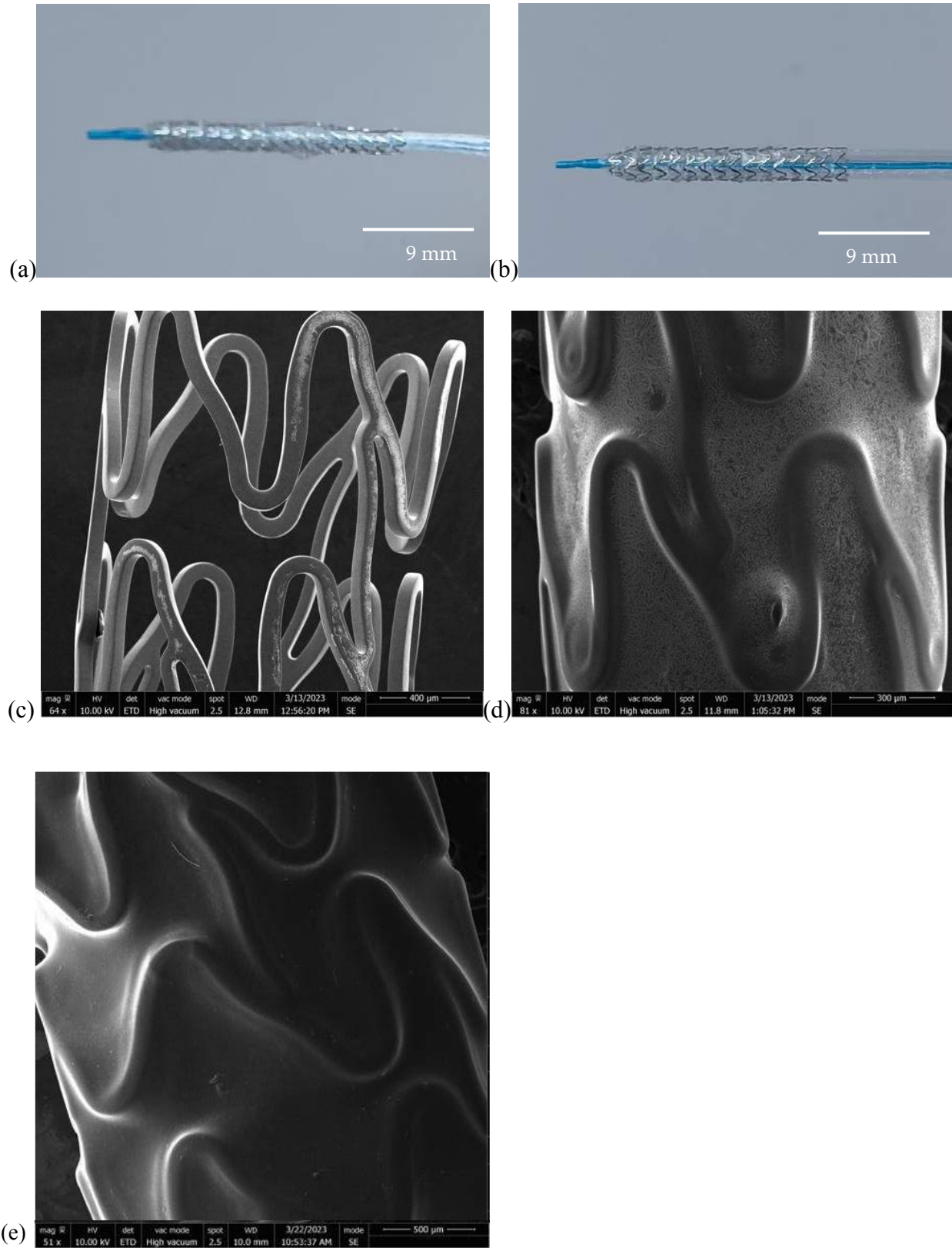
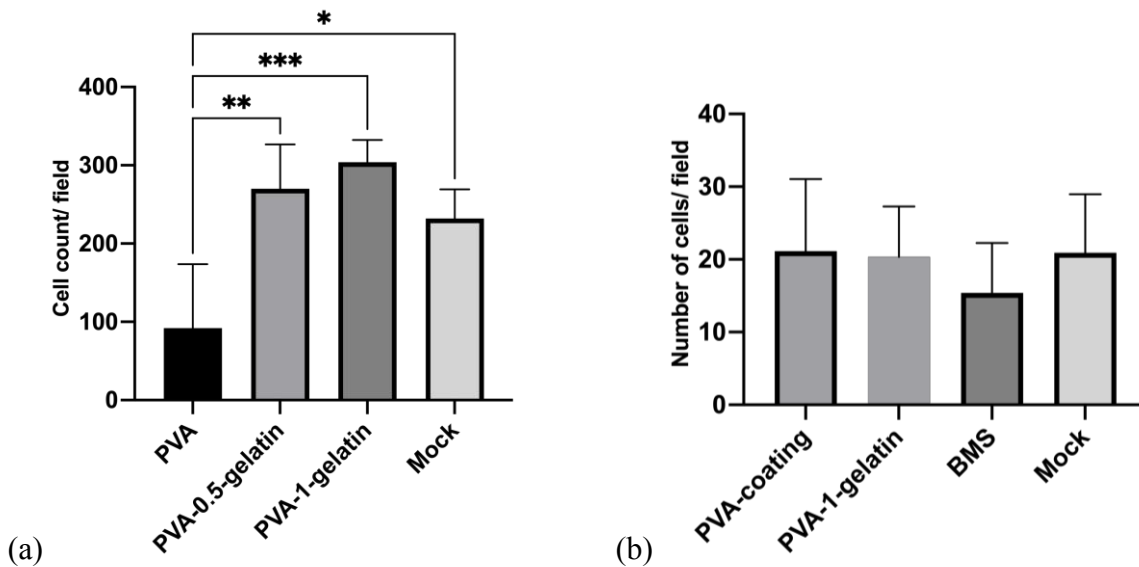


Figure 29. PVA-coated stent morphology under SEM

(a) PVA-coated Eucatech AG stent before expansion. (b) PVA-coated Eucatech AG stent after expansion at 9 atm for one minute. (c) Bare-metal stent under a SEM. (d) Initial PVA-coated Eucatech AG CCFlex stent under a SEM. (e) Expanded PVA-coated Eucatech AG CCFlex stent under SEM

The cytotoxicity and hemocompatibility of the stent were also investigated as part of the medical device fabrication process (Figure 30). HUVEC adhesion was significantly promoted with the addition of gelatin to the PVA. The 1 % (*m/v*) gelatin addition showed the most significant cell adhesion compared to PVA and was used for subsequent studies. There was no significant difference between platelet adherence to the PVA coating, PVA-gelatin coatings, or BMS. The hemolysis percentages were below 2 % after one hour of incubation, indicating they were non-hemolytic. The addition of gelatin supported surface blood coagulation compared to the PVA coating alone. However, significantly less blood coagulated on all the synthesized coatings compared to the BMS ($0.0005 < p\text{-value} < 0.00005$). Moreover, no significant change cell proliferation and viability was observed after stent incubation for two days.



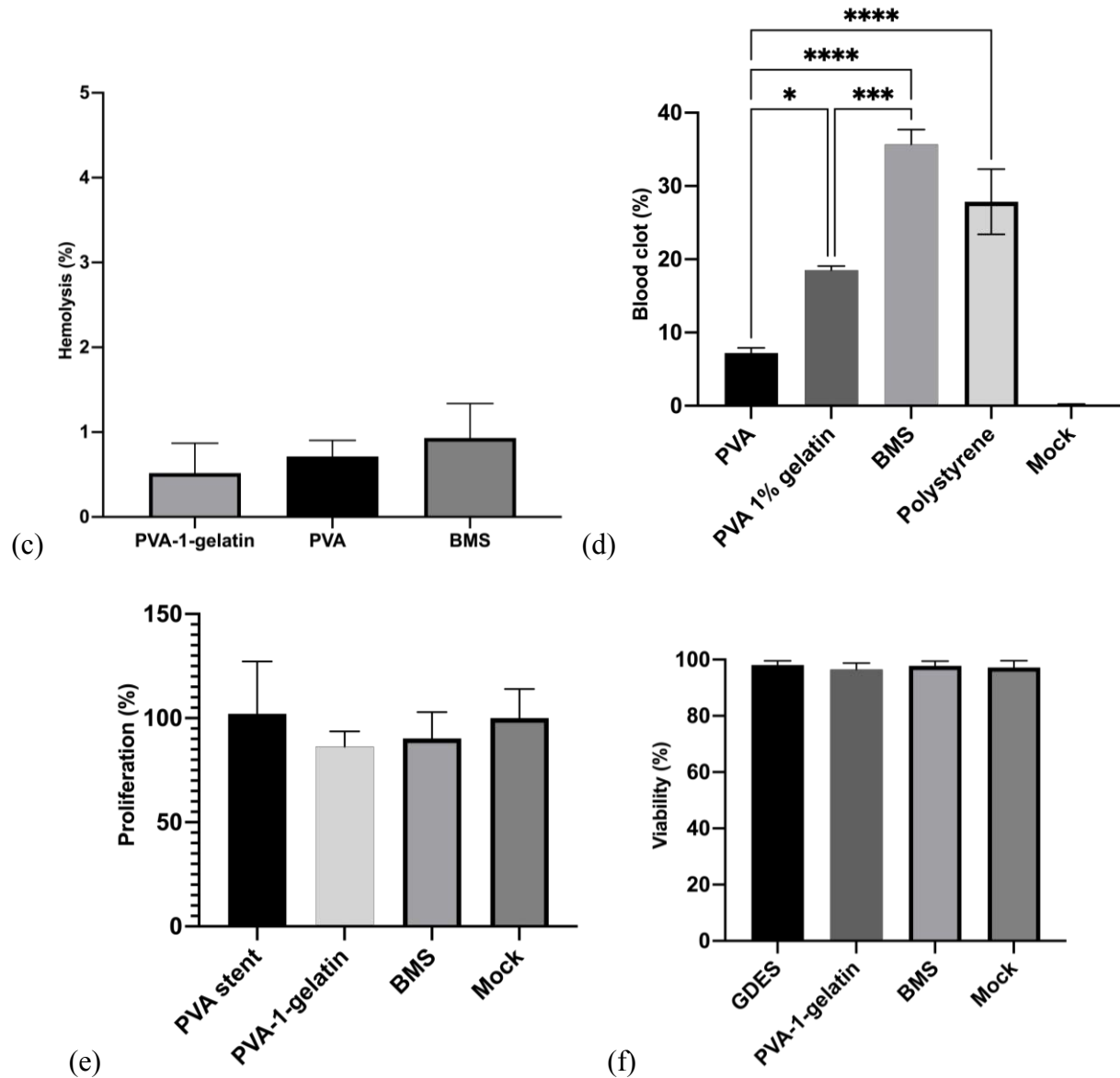
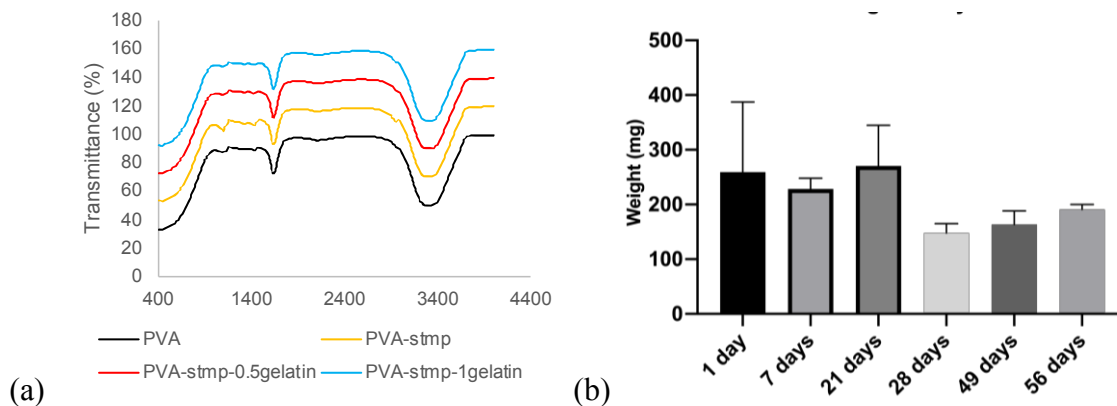


Figure 30. Cell adhesion and blood compatibility for the stent coatings

(a) HUVEC adhesion to the stents. (b) Platelet adhesion to the stents. (c) Hemolysis percent after incubation with the stents for one hour. (d) Blood coagulation on different stents. (e) Cell proliferation after stent incubation for 48 hours. (f) Cell viability after stent incubation for 48 hours.

The chemical and mechanical properties of the stent and coating were also investigated using FTIR, tensile testing, and swelling tests (Figure 31). ATR-FTIR confirmed the conjugation

of STMP and gelatin. The key peaks for PVA were presenting including, 3300 cm^{-1} (OH group), 1100 cm^{-1} (C-O stretching), and 720 cm^{-1} and 1400 cm^{-1} (CH_2 in PVA). FTIR analysis also revealed peaks around 1060 and 1230 cm^{-1} due to the addition of the STMP crosslinker and PO_3^- bond creation. The addition of gelatin also has a characteristic peak due to the N-H stretching ($3200\text{-}3600\text{ cm}^{-1}$). The amide bond within the gelatin also adds a peak at $1540\text{-}1650\text{ cm}^{-1}$. The modulus of elasticity was $1.47 \pm 0.3\text{ MPa}$ and calculated at 60% strain. Two samples slipped before breaking, and the third sample broke at 600% stretch. The Storage and Loss modulus was $1099.2 \pm 282.4\text{ Pa}$ and $93.14 \pm 7.3\text{ Pa}$, respectively. The hydrogel stent coating also remained stable over 56 days at a swelling ratio of approximately 1.5. The swelling ratio and change in weight over time did not differ significantly at typical physiological conditions ($37\text{ }^\circ\text{C}$) compared to accelerated conditions (150 rpm). A gradual degradation of the PVA stent coating was observed over 56 days. Comparatively, the PVA-gelatin coatings degraded almost fully within two weeks.



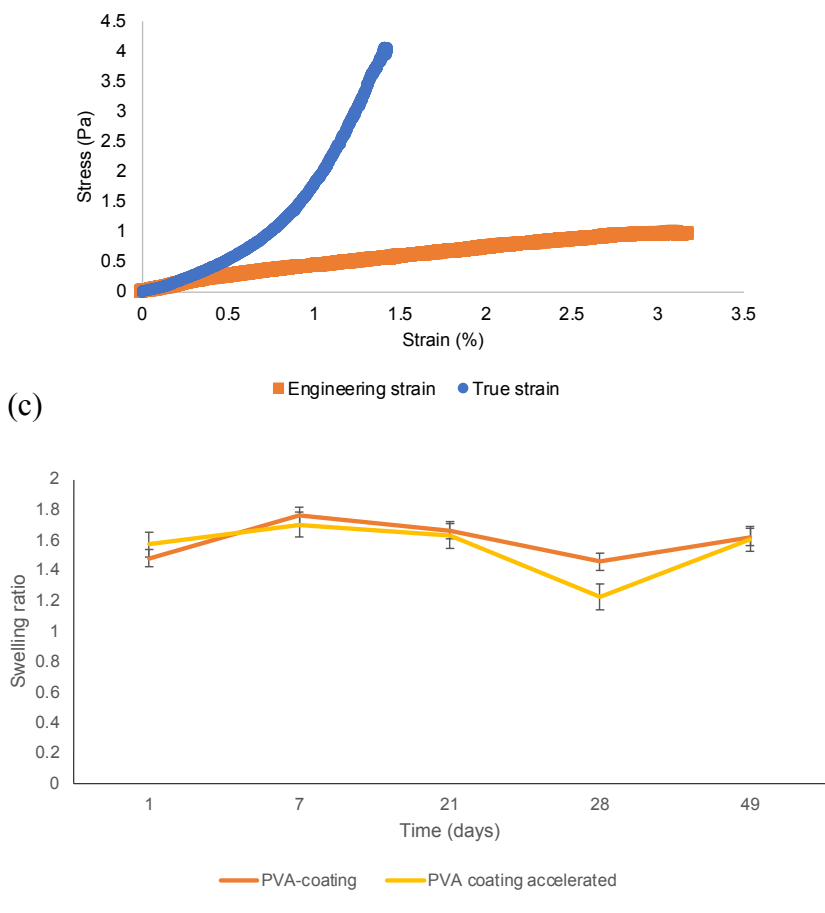
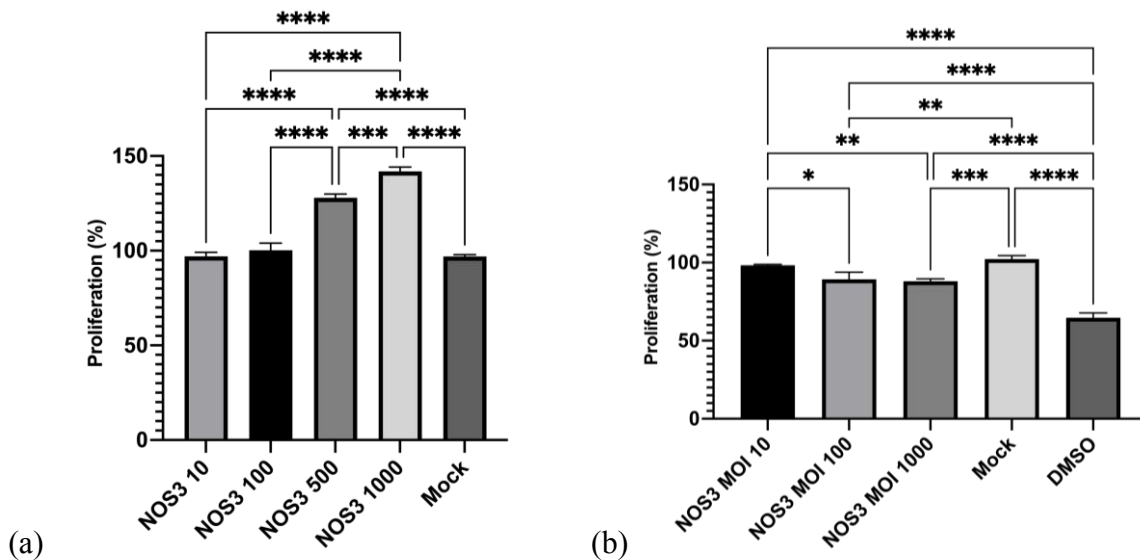


Figure 31. Stent coating characterization and degradation

(a) ATR-FTIR of the PVA-STMP stent coating compared to PVA alone. (b) PVA coating stability (weight loss) over time. (c) Uniaxial tensile testing of the PVA stent coating. (d) The swelling ratio of the stent coating over time at normal and accelerated conditions (150 rpm and 37 °C).

A baculovirus expressing enhanced green fluorescent protein (EGFP) in insect cells and NOS3 in mammalian cells was produced using a polyhedron and cytomegalovirus promoter, respectively. The stock titration of the baculovirus expressing NOS3 was 3.5×10^8 TU/mL. The virus stock was diluted in HBSS to obtain the required concentration for use. The baculovirus was loaded passively onto the stent using the swelling capacity of the coating.

NOS3 expression from the baculovirus also demonstrated favourable characteristics, including improved cell proliferation, cell migration, angiogenesis, and regulate ROS levels (Figure 32). High doses of NOS3 (MOI 500 and 1000) were shown to promote endothelial cell proliferation ($p < 0.00005$) significantly. However, it had the opposite impact on SMCs, significantly reducing their proliferation in a dose-dependent manner. During CAD, the local artery is under an inflammatory response. To mimic this *in vitro*, the cells were pretreated with LPS and $IFN\gamma$. Next, the cells were transduced with the baculovirus to see if NOS3 expression could regulate the reactive oxygen species (ROS) production. Favourably, NOS3 reduced ROS back to base levels with a significant decrease ($p < 0.00005$) in ROS-positive cells compared to the LPS and $IFN\gamma$ groups. NOS3 also generated a significant dose-dependent increase in cell migration following wounding. With an MOI as low as five still produces a significant impact ($p < 0.00005$). When NOS3 and L-NAME were added, a non-selective inhibitor of nitric oxide synthase, cell migration was no longer significantly promoted [214]. NOS3 also created a dose-dependent increase in nodes and branching length in an angiogenesis assay, although not significant.



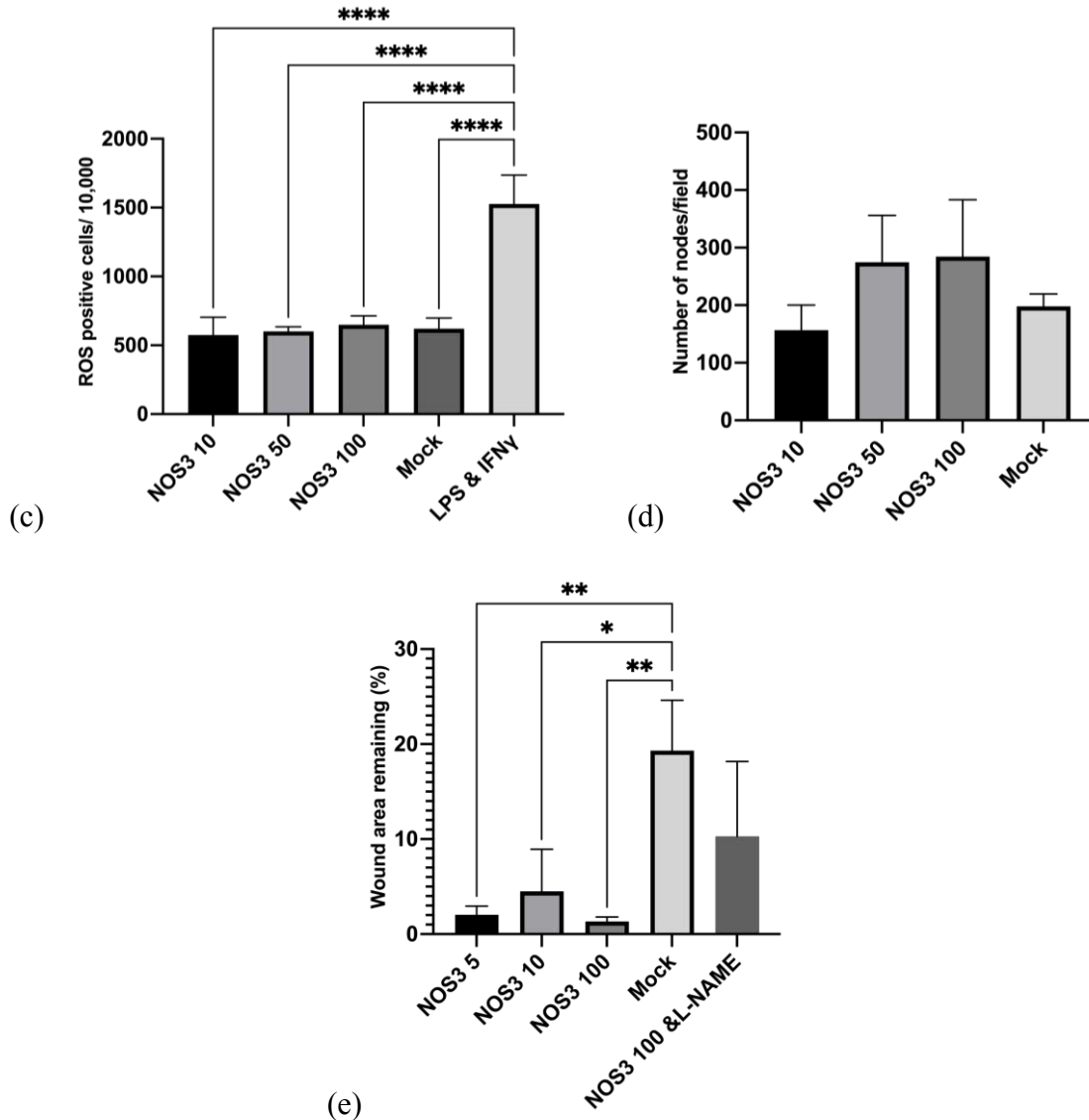
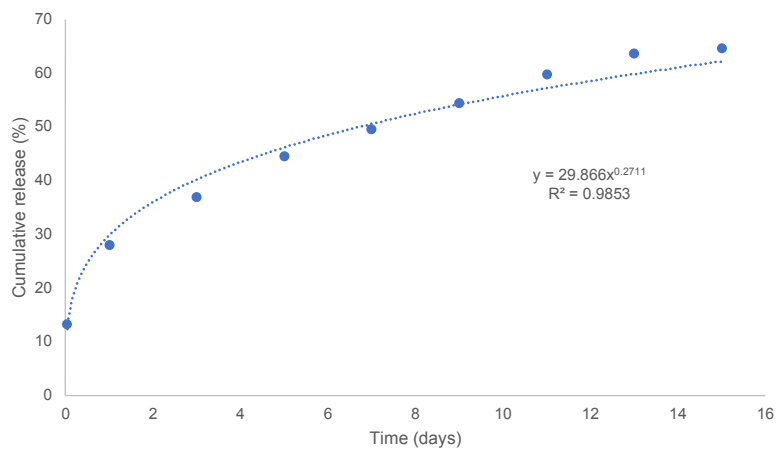


Figure 32. NOS3 gene expression and therapeutic effect

(a) HUVEC proliferation after NOS3 delivery via baculoviruses. (b) SMC proliferation after NOS3 delivery via baculoviruses. (c) Scratch assay after NOS3 delivery (24 hpi) indicating cell migration induction after 12 hours. (d) ROS production after LPS IFN γ treatment followed by BV transduction. (e) Angiogenesis assay using cell media acquired after NOS3-BV transduction. (Please see the Appendix for additional data).

First, Everolimus was loaded via direct incorporation into the PVA stent coating. The baculovirus, expressing NOS3, was loaded onto the stent using passive loading over 12 hours. The

drug was eluted in a sustained manner over the 15 days tested. A curve was fitted to the elution graph ($R^2 = 0.9853$) to predict the elution over an extended time (Figure 33a-b). The solved equation predicted that the drug would be fully eluted in 86 days. Baculovirus elution was also sustained over 8 to 10 days (Figure 33c). The loading efficiency was $18.54 \pm 1.6 \%$ for a 33 mm stent. Gelatin was also incorporated into the PVA hydrogel coating and investigated. Gelatin has been shown to preserve DNA and baculovirus stability [188], [189]. Gelatin is a natural polymer that promotes cell attachment and would be beneficial for promoting re-endothelialization [171]. Gelatin prolonged BV elution by two days and improved baculovirus viability. Adding 0.5 % (*m/v*) and 1 % (*m/v*) gelatin resulted in a loading efficiency of $25.3 \pm 0.5 \%$ and $30.5 \pm 1.0 \%$, respectively. Thus, the PVA coating with 1 % (*m/v*) gelatin was tested further compared to PVA alone. The baculovirus elution was also tested in high serum conditions to confirm that the virus was not inactivated. Similar baculovirus elution and viability were observed from the stent coating in HBSS and 50 % serum (Figure 33d).



(a)

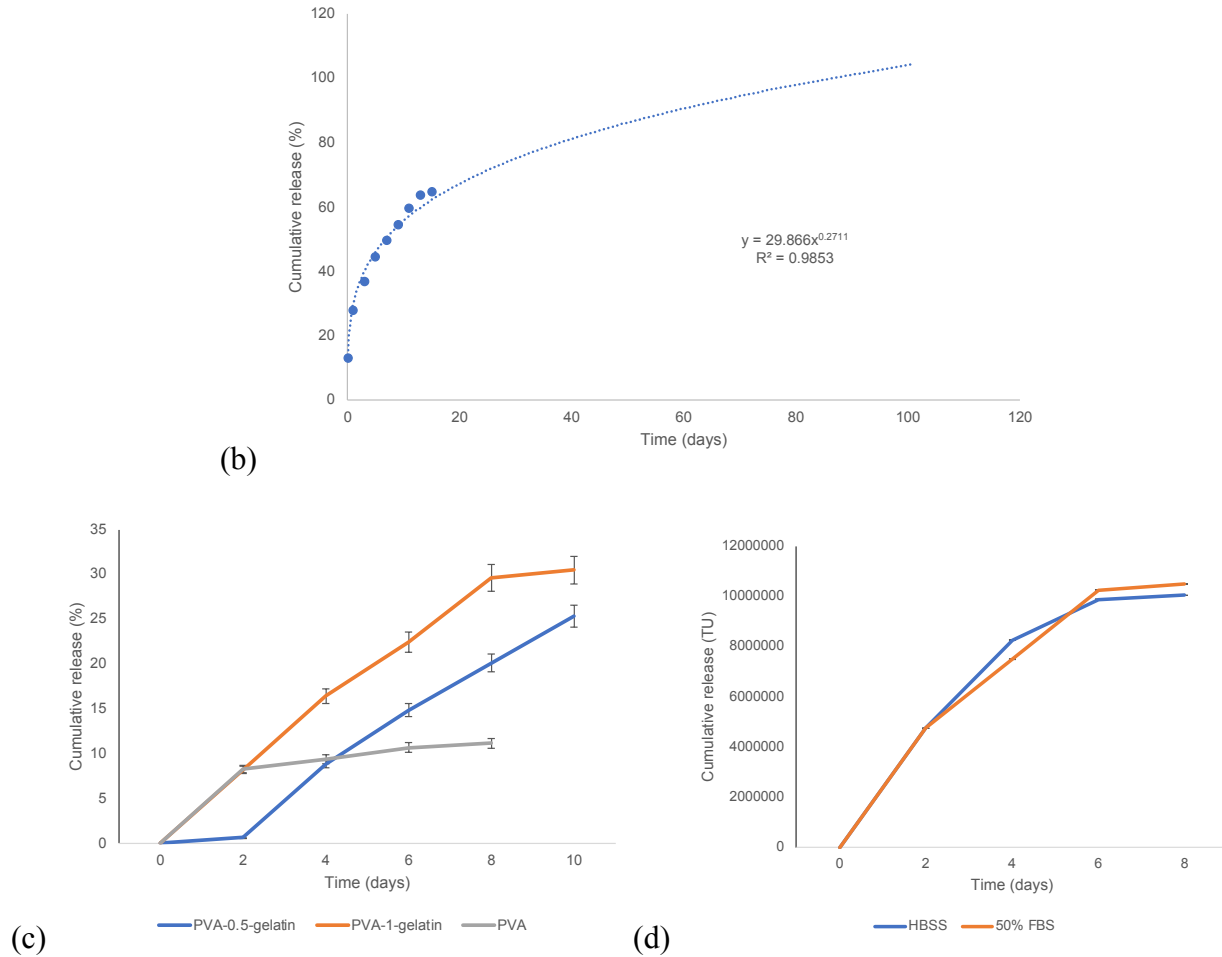
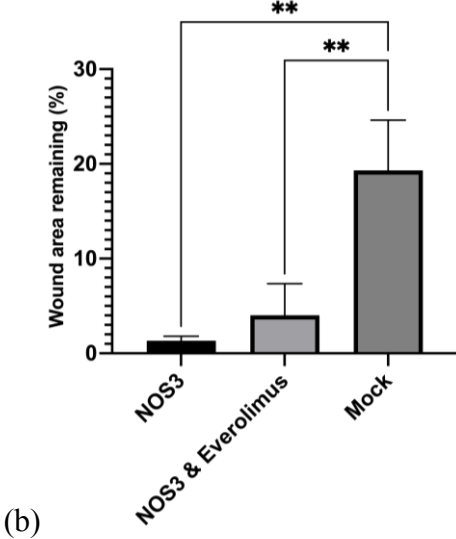
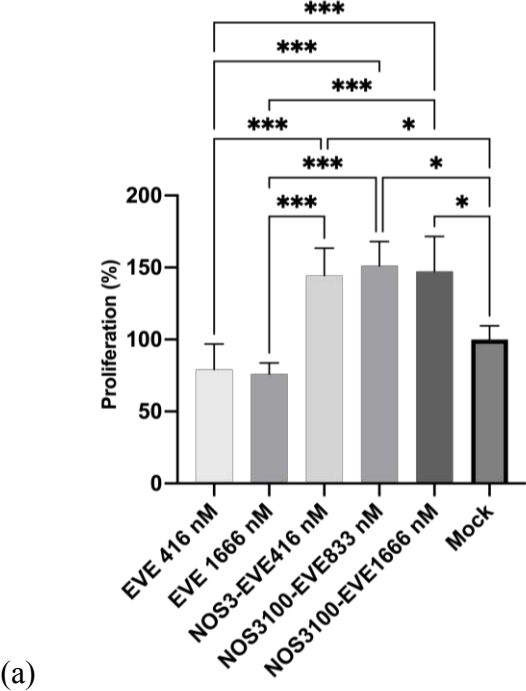


Figure 33. NOS3 and Everolimus (EVE) elution from the stent

(a) EVE elution from the stent over time. (b) EVE elution from the stent over time predictive model. (c) BV elution from different stent hydrogel coatings. (d) BV elution in 50 (v/v) % serum and HBSS. (e) HUVEC proliferation 24 hours after gene or drug addition.

The therapeutic effects of NOS3 were maintained despite the Everolimus elution (Figure 34). NOS3 and Everolimus together still significantly improved endothelial cell proliferation ($p < 0.05$). Comparatively, the drug further reduced SMC proliferation and was selected for its known anti-inflammatory response. The NOS3-induced cell migration in the wound healing assay

remained significant compared to the mock ($p < 0.005$). Adding Everolimus did not impact the wound-healing ability of NOS3.



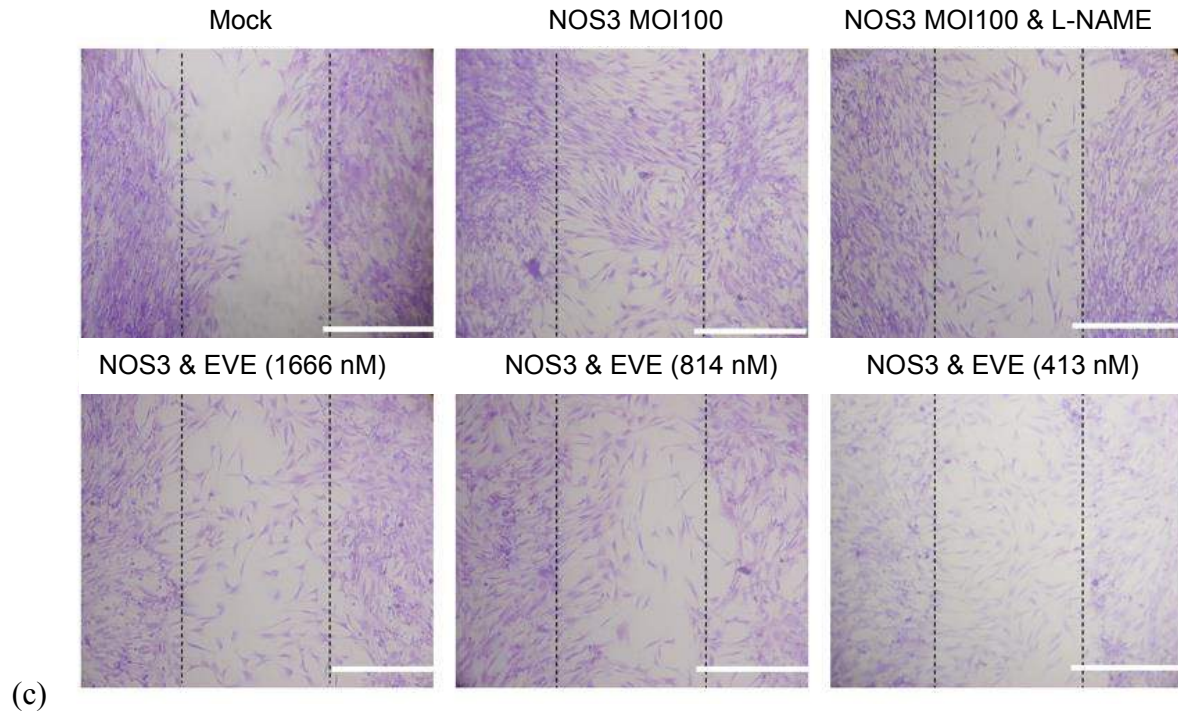


Figure 34. NOS3 and Everolimus (EVE) elution and therapeutic effect together

(a) HUVEC proliferation 48 hours after gene and drug are added. (b) Wound area remaining (%) after gene and drug addition. (c) Brightfield images of the crystal violet stained cells 12 hours after scratching. Scale bar= 0.05 mm.

Discussion

To mitigate current stenting complications, the novel stent should be mechanically stable, promote endothelial health, inhibit restenosis, and be anti-thrombotic. The gene- and drug-eluting stent (GDES) presented here prevented endothelial dysfunction, thrombosis, and smooth muscle cell hyperproliferation, which can contribute to restenosis [36], [65], [67], [68].

Three different stent coatings were investigated, PVA, PVA-0.5%-gelatin, and PVA-1%-gelatin. The composition of the stent coatings was confirmed using FTIR with distinct peaks for STMP and gelatin. Adding 0.5 % or 1 % (*m/v*) gelatin significantly improved cellular adhesion ($p < 0.005$ vs. $p < 0.0005$) compared to the PVA coating. There was no difference in hemolysis,

platelet adhesion, blood coagulation, cell proliferation, or cell viability after stent incubation, indicating all stent systems were non-cytotoxic and hemocompatible. The addition of gelatin also significantly improved the loading efficiency.

The following steps were followed to load the stent with baculovirus and drug. First, the stent was loaded directly with the drug, Everolimus, during fabrication. The drug was estimated to elute over 86 days, comparable to current drug-eluting stents such as Eucalimus® [215]. The baculovirus, expressing NOS3, was loaded next using passive diffusion. The baculovirus was eluted over 10 days with a loading efficiency of $18.54 \pm 1.6 \%$ when 5×10^7 TU were incubated. The loading efficiency increased with the addition of gelatin to the coating. Specifically, 0.5 % (*m/v*) and 1 % (*m/v*) gelatin led to a loading efficiency of $25.3 \pm 0.5 \%$ and $30.5 \pm 1.0 \%$, respectively. Comparatively, the PVA coating alone had a loading efficiency of $15.6 \pm 1.6 \%$. However, gelatin also reduced the mechanical stability and resulted in a coating degradation of under two weeks. Thus, the PVA coating was suggested for future stent coatings.

The stent coatings swelled on average 1.5-fold, which helps it comply with the stent deployment and expansion. The PVA coating on the Eucatech® chromium cobalt stent was highly elastic enabling expansion without deformation or fractures. Degradation was uniform over the 56 days tested at accelerated conditions. These properties are essential for preventing thrombosis. Good tensile strength with a Modulus of Elasticity of 1.47 ± 0.3 MPa. The stent coating has a lower modulus of elasticity (1.47 ± 0.3 MPa) compared to 193 GPa for stainless steel and 45 GPa for magnesium-based stents [211].

Promoting endothelial health and re-endothelialization would prevent several downstream complications, such as restenosis due to SMC hyperproliferation and inflammation. Specifically, NOS3 created a dose-dependent increase in endothelial cell proliferation, with the highest dose

creating a highly significant increase ($p < 0.00005$). This is a favorable characteristic to promote re-endothelialization and prevent downstream restenosis. The wound healing assay revealed significantly promoted cell migration ($p < 0.05$) to assist with re-endothelialization following stent implantation. L-NAME was also added since it is a known inhibitor of nitric oxide synthase [214]. When L-NAME was added, the elevated migratory effect diminished, indicating that NOS3 was responsible for creating the therapeutic effect. NOS3 also promotes angiogenesis (although not significant), which would help transport nutrients and oxygen to the endothelial cells and promote their health.

Restenosis often results from inflammation, vascular smooth muscle cell hyperproliferation, and extracellular matrix formation [216]. Inflammation and reactive oxygen species (ROS) production is common within a diseased coronary artery and contribute to restenosis and disease pathogenesis [217], [218]. Thus, to mitigate ROS production, NOS3 was added after LPS-induction. NOS3 created a dose-dependent decrease in ROS production which may help regulate the inflammatory environment. NOS3 also generated a dose-dependent decrease in SMC proliferation which would help prevent restenosis due to hyperproliferation. Moreover, the PVA coating can be a physical barrier to the SMCs to prevent restenosis development. Everolimus also inhibits mTOR, a major growth regulator, to prevent inflammation [60]. Everolimus-eluting stents have a better bioavailability due to their higher affinity for FKBP12 protein which inhibits smooth muscle division in the G1 and G2 phase. Moreover, the drug also prevents T cell proliferation mitigating a pronounced immune reaction and inflammation [60]. In this study, Everolimus was shown to reduce cell proliferation, preventing SMC hyperproliferation. However, the cell migration stimulated by NOS3 was maintained despite Everolimus delivery. This indicates that the two molecules can be delivered together without counteracting each other.

PVA is common in several different medical device applications due to its inherent safety and anti-thrombotic properties [186]. The PVA stent coating supported this showing no signs of significant platelet adhesion, blood coagulation, or hemolysis. The coating was also smooth with no cracks or breaks, which helps prevent thrombosis. Nitric oxide is also known for its anti-thrombotic and antibacterial properties [177][180]. Specifically, nitric oxide inhibits platelet adhesion preventing the initial blood clotting stage.

Future studies should be conducted *in vivo* to confirm the therapeutic efficacy and safety. The gene- and drug-eluting stent can also be scaled to fit different arteries and geometries. The coating can even be integrated into upcoming fully biodegradable stents to mitigate further complications and improve the quality of life of those impacted by PAD.

Overall, the dual-action stent may effectively mitigate complications seen with current stents. Nitric oxide delivery regulates blood coagulation, prevents platelet adhesion, prevents thrombosis, prevents SMC proliferation, and promotes endothelial health and migration for re-endothelialization [180]. Meanwhile, Everolimus prevents inflammation and SMC hyperproliferation. The stent is also mechanically sound, anti-thrombotic, non-cytotoxic, and contains a dissolvable coating to prevent polymer-induced inflammation.

Conclusion

The novel gene- and drug-eluting (GDES) stent coating shows favourable properties *in vitro*. The dual factor elution assists with re-endothelialization, inhibiting inflammation, and preventing smooth muscle cell proliferation leading to restenosis. The stent coating is also flexible, without cracks or breakage during expansion or degradation, to reduce the risk of thrombosis. The PVA stent coating is hemocompatible and fully dissolvable, reducing the risk of polymer-induced inflammation long-term. Overall, the stent system may improve clinical outcomes by mitigating

complications such as thrombosis, restenosis, polymer-induced inflammation, and endothelial dysfunction.

Materials and Methods

Stent coating process

The PVA-coating technique was adapted from a previous study [201]. Briefly, 20 mL of 10 % (*m/v*) PVA was made in sterile water at 90 °C and 700 rpm. Next, 200 µL of 15 % (*m/v*) STMP was added, stirring the solution for five minutes. Finally, 80 µL of 30 % (*m/v*) NaOH was added to the PVA solution and stirred for one hour. Next, the CCFlex Eucatech® stent was dipped into the PVA solution and dried for 15 minutes. This process was repeated three times. After the third dip, the coated tube was placed in a -20 °C freezer overnight. The next day, the PVA-coated stent was dried fully overnight and sterilized using ethanol and sterile water washes before final drying. After the stent was fully dried, it was stored in the fridge until use. For the PVA-gelatin coatings, the same method was employed except 0.5 % or 1 % (*m/v*) gelatin was added prior to STMP and NaOH.

Stent coating morphology with scanning electron microscopy (SEM)

A high vacuum and a 10 kV voltage were used with the FEI 450 Quanta SEM at the Facility for Electron Microscopy Research (FEMR).

Swelling and degradation studies

The coated stents were immersed into HBSS and incubated at 37 °C. For accelerated testing, the stents were also shaken at 150 rpm. At the designated time points, the stents were blotted dry and weighed to determine their initial swelling ratio and the coating degradation over time. The following equation was used to calculate the swelling ratio:

$$\text{Swelling ratio} = \text{Weight}_{\text{swollen}} / \text{Weight}_{\text{dry}}$$

Tensile testing

To perform the tensile testing, a thin film PVA coating was generated using the same stent synthesis method mentioned above. Once the PVA sheet was fully dried a 3D printed ‘cookie cutter’ was used to cut out a dumbbell shape as described in ISO37:2017. The thickness of the films was measured in triplicate using a Mitutoyo Litematic VL-50A. Next, the thin films were tested on a Shimadzu Uniaxial tensile and compression tester with a strain rate of 1 %. Sandpaper was added to the clamps to help secure the PVA and prevent slipping.

Mammalian cell culture (human smooth muscle and umbilical vein endothelial cells)

Human umbilical vein endothelial cells (HUVECs) and smooth muscle cells (SMCs) were cultured at 37 °C in a 5 % CO₂ incubator. The HUVECs were cultured in complete endothelial growth media (Sigma Aldrich, St. Louis, MI, USA). The SMCs (Coriell Institute for Medical Research, Camden, NJ, USA) were cultured in M199 media supplemented with 10 % (*v/v*) FBS and 0.02 mg/mL endothelial cell growth supplement (Sigma Aldrich, Burlington, Massachusetts, United States). The cell media was changed every second day and the cells were subcultured just prior to confluency. All cells were used before passage five.

Insect cell culture (Sf9 cells)

Sf9 cells (Novagen, Sigma Aldrich, Burlington, Massachusetts, United States) were maintained at 27 °C in T75 flasks or 250 mL shaker flasks with BacVector media. The shaker flasks were rotated at 130 rpm. The cells were subcultured two to three times per week to maintain exponential growth.

Gene cloning and baculovirus (BV) production

The nitric oxide synthase 3 (NOS3) gene was purchased from GenScript (Piscataway, NJ, USA). EcoRI and NotI restriction enzymes (Thermo Fisher, Waltham, Massachusetts, USA) were used to cut out the gene of interest (GOI). The gene fragment was then ligated into a PakBak9 plasmid (GenScript) following the CMV promoter from using Instant Sticky End Ligase (NEB, Ipswich, Massachusetts, USA). The pBakPak9 vector already contained an enhanced green fluorescent protein (EGFP) under polyhedron control. The complete plasmid was then transformed into chemically competent DH5 alpha *E. Coli* (Thermo Fisher). The colonies containing the GOI and ampicillin resistance were selected and amplified. The plasmid was then purified from the *E. coli* using NEB's plasmid purification kit. The final plasmid structures were confirmed using a restriction enzyme gel check and NanoDrop (Thermo Fisher, Waltham, Massachusetts, USA) and used for all future steps.

Baculovirus transfection

One hour before the transfection, 0.5×10^6 Sf9 cells/well were seeded into a 12-well plate. Next, 40 μ L of PBS, 200 ng of the plasmid, 200 ng of the flashBAC, and 0.48 μ L of TransIT reagent were mixed and incubated for 15 minutes at room temperature. Next, 0.5 mL of the insect media was aspirated off, leaving 0.5 mL remaining. The baculovirus transfection mix was then added dropwise to the wells. PBS was used as a mock control. The plate was incubated overnight and the next day, 0.5 mL of BacVector media was added to each well. The plate was then incubated for another four days before the media containing the Po baculovirus stock was harvested.

Baculovirus (BV) amplification

The P₀ baculovirus stock was for amplification and to obtain a high virus titer. First, 100 mL of Sf9 cells were diluted to a concentration of 2×10^6 Sf9 cells/mL in a shake flask. Next, 0.5 mL of the original P₀ baculovirus stock was added to the cells and the flask was incubated for

three-four days. The EGFP expression was checked daily and when all cells expressed EGFP the virus was harvested. Next, the cells were centrifuged at $300 \times g$ for 20 minutes and the viral suspension media (P₁) was collected and stored in the dark at 4 °C.

Baculovirus titration

The baculovirus P₁ stock was titrated using a fluorescent titering assay. First, 5×10^5 Sf9 cells/well were seeded into a 12-well plate and incubated for one hour. The virus was diluted in 10-fold increments during incubation using insect cell medium. The cell media was then aspirated off the Sf9 cells and 100 µL of the virus dilution was added to each well. The plate was incubated for one hour and then an addition 0.5 mL of insect cell media was added to each well and incubated at 27 °C. The next day, the number of fluorescent cells was counted in each well with less than 40 % of fluorescent cells. The following equation was used to calculate the titration:

Transduction Units (TU)/mL = (number of cells transduced x percent of fluorescent cells × dilution factor)/(transduction volume in mL)

Baculovirus transduction

First, 1×10^4 mammalian cells/well were seeded into a 96 black well plate with a clear bottom (Corning 3603, Thermo Fisher, Waltham, MA, USA) and incubated overnight at 37 °C with 5 % CO₂. The next day, the cell media was removed, and the designated amount of baculovirus was added to each well. The baculovirus was incubated with the cells for three hours before being aspirated and replaced with fresh cell media. The plate was then incubated as before for 24 to 48 hours before being used in the experiments described below. The cell media supernatant was aspirated off and used immediately or stored at -80 °C for future experiments.

Reverse transcription-quantitative polymerase chain reaction (RT-qPCR)

For RT-qPCR, cells were transduced with different MOIs of the NOS3-expressing baculovirus. Twenty-four hours after transduction, the cell RNA was extracted using an RNA extraction kit (Bio Basic, Markham, ON, Canada) and used immediately or stored at -80 °C until use. Primers for NOS3 and a reference gene (Beta-actin) were purchased from Bio-Rad (Hercules, CA, USA). The RNA, primers, and polymerase solution were mixed as described by the Luna Universal One-Step RT-qPCR kit (New England Biolabs, Ipswich, MA, USA). The reaction was run on an Illumina Eco Real-Time PCR machine ® (San Diego, CA, USA) for 45 cycles with 35 seconds (denaturation), 55 °C for 35 seconds (annealing), and 72 °C for 25 seconds (extension).

MTT proliferation assay

For the MTT proliferation assay, the baculovirus transduction protocol was followed as described above. The next day (24 hpi), 50 µL of 5 mg/mL MTT was added to each well and incubated for three hours. Next, 35 µL of 37 % (v/v) HCl was added to 10 mL of isopropanol. This solution was mixed and 100 µL was added to each well and mixed via pipetting. The absorbance of the plate was measured at 570 nm using an EnSpire multimode plate reader.

To evaluate the impact of the stent on cell proliferation, the coated stents or BMS were added to a 24-well plate containing mammalian cells. After incubation, the stent was removed and 200 µL of 5 mg/mL MTT was added to each well. The cells were then incubated for three hours and a 0.04 N HCl solution diluted in isopropanol was added and mixed thoroughly. The cell supernatant containing the dissolved MTT was placed into a 96-well plate and read at 570 nm using the same EnSpire plate reader as above.

Live Dead assay

For the live dead assay the mammalian cells were transduced as described above. After 24 or 48 hours, a 2 × live dead stain was diluted in 10 mL of cell media using 50 µL of 1 mM Calcein

AM and 50 μL of 2.5 mg/mL Propidium Iodide. Next, 100 μL of the the live dead stain was added to each well. The plate was incubated for 30 minutes and then imaged using the same Operetta microscope system. The live dead cell count was performed using Columbus. A similar approach was adopted with direct incubation of the coated stent to determine the impact of the stent coatings on cell viability, in a 24-well plate.

Reactive oxygen species (ROS) assay

Cells were pre-treated with lipopolysaccharide (LPS) and interferon-gamma ($\text{IFN}\gamma$) to induce an inflammatory environment. Next, the cells were transduced with different MOIs of the baculovirus to determine if the gene expression reduces ROS production. The transduction protocol was followed as above. Forty-eight hours after LPS treatment a ROS kit (Abcam 186029, Waltham, Boston, USA) was used to measure ROS production as described by the supplier.

Endothelial tube formation assay (angiogenesis assay)

To determine the angiogenic properties of the baculovirus-eluted genes, an endothelial tube formation assay was performed as previously described [163]. Cultrex® reduced growth factor basement membrane (Bio-Techne, Minneapolis, MN, USA) was added to the bottom of each well of a 96-well plate. The plate was then incubated for 30 minutes before 2×10^4 HUVECs/well were seeded on top. Finally, 50 μL of cell media supernatant from previously transduced cells was added. The cells were incubated at 37 °C in a 5 % CO_2 incubator for four hours or until well-defined vasculature could be seen. Cell media containing VEGF or DMSO were used as positive and negative controls, respectively.

***In vitro* scratch assay**

An *in vitro* scratch assay was performed as previously described with slight modifications [212]. Again, HUVECs were seeded into 96-well plates and grown until confluency. Once they

were confluent, the cells were transduced with different MOIs of the baculovirus for three hours. The virus inoculum was aspirated, and fresh media was added. Twenty-four hours after baculovirus transduction, the wells were scraped with a p200 pipette tip. After twelve hours, the wells were imaged when some wounds had healed. The images were analyzed using an ImageJ plugin [162].

Baculovirus release from the stent

The coated stent was dried overnight at 37 °C before incubating the stent in a baculovirus stock solution overnight to allow for passive absorption. Compared to direct incorporation, passive absorption was selected to maintain virus activity. The stent was incubated at 27 °C overnight before removing the stent and placing it into a new well. Next, 1 mL of HBSS or 50 % (*v/v*) fetal bovine serum (FBS) was added to cover the stent. The HBSS or FBS was removed and replaced with fresh solutions at designated times to determine the amount of baculovirus released over time.

Everolimus release

The PVA stent coating was incubated directly with Everolimus dissolved in DMSO at the desired concentration. The stent coating was incubated in HBSS at 37 °C. At the designated time points, the HBSS was removed and read at 280 nm absorbance (NanoDrop, Thermo Fisher) as described elsewhere [219]. Fresh HBSS replaced the old supernatant.

Cell adhesion to stent coatings

To determine if the stent coatings promoted cellular adhesion. Thin films of the hydrogels were created and seeded on the bottom of a 24-well plate. The hydrogels were dried overnight and then swollen in cell media for one hour. After one hour, the cell media was removed and HUVECs were seeded onto the hydrogels. Empty tissue treated wells were used as a control. The seeded hydrogels were incubated at 37 °C for two hours. After the two hours, the hydrogels were washed

with HBSS to remove any unattached cells. The hydrogels were then fixed in 3.7 % (v/v) formaldehyde for 15 minutes and washed with PBS. Finally, the hydrogels were stained with 0.1 % (m/v) crystal violet to visualize the cells under a brightfield microscope. The cells were counted using ImageJ.

Hemolysis

Whole blood samples from two individuals (Male 49, Hispanic and female 29, white; Innovative Research Inc, Novi, Michigan) were used for the hemolysis test. Whole blood was extracted by the company, directly into sodium citrate coated tubes. The stents were immersed into 1 mL of PBS in a 2 mL centrifuge tube. Next, 4 mL of citrated blood was mixed with 5 mL PBS and 0.1 mL of the diluted blood was added to each sample. The stents were incubated at 37 °C for one hour and then centrifuged at 1000 rpm for 10 minutes. The supernatant, containing the lysed hemoglobin, was pipetted into a 96-well plate. The plate was read at 545 nm. A standard curve for the hemolysis was also generated using dilutions of PBS and deionized water to calculate the hemolysis percentage. The negative and positive control was PBS and deionized water, respectively. The following equation was used to determine the percent hemolysis.

$$\text{Hemolysis (\%)} = ((\text{OD}_{\text{sample}} - \text{OD}_{\text{negative control}}) / (\text{OD}_{\text{positive}} - \text{OD}_{\text{negative}})) \times 100\%$$

Platelet adhesion to stent coatings

Platelet adhesion to the stent coatings was performed as previously described [213]. Briefly, platelet-rich plasma (PRP) was obtained by centrifuging whole blood at 1000 × g for 20 minutes. The platelet concentration was calculated using a hemocytometer (952 ± 98 platelets/μL). Meanwhile, the stents were added to a 24-well plate and washed with PBS. The stents were then covered with 200 μL of the PRP and incubated for one hour at 37 °C. After the incubation, the stents were carefully removed and washed with PBS. The stents were then incubated with 100

μL of 2 % (*m/v*) Triton X-100 for 30 minutes at 37 °C to lyse the adherent platelets. The lysed platelet solution was used in an LDH assay (Abcam, Waltham, Boston, USA) following the supplier's instructions. A standard curve for platelet concentration and NADH activity was created to calculate platelet adherence to the stent coatings.

Stent coating-induced whole blood clotting

Whole blood clotting on the stent coatings was evaluated using whole blood samples from two individuals (Male 49, Hispanic and female 29, white; Innovative Research Inc, Novi, Michigan) [160]. The coated stents were placed into a 24-well plate and incubated in PBS for one hour. Next, 7 μL of whole blood was pipetted onto the surface of each stent. After 15, 30 and 45 minutes of incubation, deionized water was added to each sample and incubated for five minutes to induce hemolysis. The resulting supernatant was removed, and the absorbance was read on a 96-well plate at 540 nm. Tissue culture treated wells and blood added directly to deionized water were used as controls.

Statistical analysis

All results are reported as a mean \pm standard deviation (SD) of triplicates, p-values less than 0.05 were considered significant. One-way ANOVAs with post-hoc Tukey's test on GraphPad Prism (version 9.0.0 for Windows, GraphPad Software, San Diego, California USA, www.graphpad.com) were used for data analysis.

Funding: This work was supported by a research grant from the Canadian Institute of Health Research to Dominique Shum-Tim and Satya Prakash (CIHR grant 252743). S.S. is fully funded by the Canadian Graduate Scholarship-Doctoral Award from the Natural Sciences and Engineering Research Council (NSERC, 569661-2022). P.I. is funded by the Islamic Development Bank

Scholarship (2020-245622). R.T. and K.A. is funded by the Canadian Graduate Scholarship-Master's from NSERC. A.A. is fully funded by a scholarship from the Ministry of Higher Education of the Arab Republic of Egypt.

Data Availability Statement: All data is presented in the manuscript.

Acknowledgments: We thank the Facility for Electron Microscopy Research of McGill University (SEM equipment), McGill Chemistry Characterization Facility (ATR-FTIR), Prof. Leask's lab (tensile tester), and the McGill University Imaging and Molecular Biology Platform (Fluorescent Operetta Microscope) for their equipment and services.

Copyright: This is an open-access article under the CC BY-NC-ND license (<http://creativecommons.org/licenses/by-nc-nd/4.0/>).

CHAPTER 9: General discussion

Atherosclerosis is a disease characterized by the buildup of fatty deposits within arteries leading to the obstruction of blood flow and severe complications. In atherosclerosis, low-density lipoprotein (LDL) accumulates, leading to endothelial dysfunction and immune cell accumulation. The high LDL levels and endothelial dysfunction cause the medial cell layer to hyperproliferate (termed neointimal hyperplasia). The LDL continues to accumulate in the artery and commences an inflammatory reaction. The activated immune cells translocate into the subendothelial space. Particularly, monocytes are known to translocate and differentiate into inflammatory macrophages [2]. The macrophages take up the LDL and differentiate into foam cells. The foam cells release more growth factors and cytokines promoting SMC migration and proliferation contributing to neointimal hyperplasia.

During the SMC migration and proliferation, extracellular matrix remodeling can also occur, leading to stiff, stenotic, and calcified blood vessel walls. Several studies have reported that high levels of C-reactive protein (CRP) and reactive-oxygen species (ROS) contribute to the inflammatory response and disease progression [144], [196]. The immune cells and macrophages eventually become overextended and undergo apoptosis, releasing pro-thrombotic factors, damaging microvessels, and contributing to a necrotic core [3]. Plaque erosion and rupture can cause thrombi formation, further obstructing blood flow and leading to clinical complications. These factors create a positive feedback loop contributing further to neointimal hyperplasia, inflammation, and plaque development, all narrowing the blood vessel.

Both coronary artery disease (CAD) and peripheral artery disease (PAD) can be caused by atherosclerosis. CAD is characterized as a disease of the blood vessels and heart. Coronary artery disease, or cardiovascular disease, is the third leading cause of death yearly, generating a large

health and economic burden [16]. Around one out of 20, people have CAD [15]. Comparatively, peripheral artery disease (PAD) affects nearly one in five people over 60, with an estimated 200 million new cases each year worldwide [5], [6]. More recent data suggests that PAD is also infiltrating younger generations, with one to four percent of people aged 25 to 29 diagnosed with PAD [7]. People with PAD report a worse quality of life, higher work impairment, and use more healthcare resources compared to people without PAD [8]. Moreover, complications and disabilities associated with PAD have a larger burden on women and people in developing countries [7], [9]. PAD often comes with significant pain, discomfort, limb ischemia, stroke, and increases the risk of major cardiovascular events such as myocardial infarction, stroke, and coronary artery disease [4]. The obstructed blood flow can also lead to chronic wounds that have difficulty healing.

This thesis presents a novel baculovirus-based delivery system and stent for treating atherosclerosis involved in PAD and CAD. To achieve this, four aims were developed; 1) evaluate baculovirus gene delivery safety, 2) optimize the baculovirus delivery system for sustained elution, 3) investigate the therapeutic effect of three different genes (ADAMTS13, NOS3, and VEGFA) eluted from a fully dissolvable stent, and 4) investigate a gene- and drug-eluting stent to improve clinical outcomes.

1) Baculovirus safety investigation

Research Objective I: To design gene-eluting (ADAMTS13, VEGFA, & NOS3) baculoviruses and evaluate their safety, stability, and efficacy *in vitro* for gene therapy applications.

Challenges for gene therapy include the high cost, gene or protein instability, potential off-target effects, low efficiency, and lack of sustained and stable expression [220]. However,

baculovirus can address these issues making gene therapy feasible and more accessible to all. Baculoviruses can easily be stored at various temperatures, including 4 °C and -80 °C lasting over a year with a high infectivity [190]. However, they must be protected from light to maintain high viability, which is not an issue for the stent implantation [187]. Baculoviruses are safe for the mass production of proteins, antibodies, vaccines, and other components [125], [221]. Moreover, the high efficiency and ease of baculovirus production make them a feasible option for mass production of therapeutics and even personalized medicine.

Baculoviruses are known to be highly efficient gene delivery vehicles to several cell types [222]. However, SMC and HUVEC efficiency have not been reported with this virus type. Moreover, most papers perform the virus transduction at temperatures below typical physiological conditions (37 °C). For efficient baculovirus stent delivery, transduction must be efficient at physiological conditions and in high serum conditions thus these conditions were tested *in vitro*. Here, baculovirus gene delivery was significantly more efficient than typical plasmid delivery. The baculovirus was stable at physiological temperatures and could significantly increase gene levels relative to the initial dosage.

Direct baculovirus administration has not been studied extensively. The baculovirus safety was confirmed in human smooth muscle and endothelial cells *in vitro*. Overall, no evidence of genotoxicity, cytotoxicity, or changes in lysosomal activity was observed. Moreover, early signs of inflammation indicated by C-reactive protein and reactive oxygen species production were not observed. Baculovirus delivery was also hemocompatible, which is essential for all direct human therapy applications. Specifically, no hemolysis or change in blood clotting activity was observed with baculovirus incubation. The thesis paper reports that baculovirus gene delivery is safe even at high doses (MOI 1000). These results support the use of baculoviruses in cancer therapy, vaccine

production, and tissue engineering applications [82]–[84]. Overall, this paper and thesis demonstrates that baculovirus gene therapy is safe, efficient, stable, and feasible.

2) Baculovirus delivery system optimization

Research Objective II: To create a baculovirus delivery platform to optimize the therapeutic timeframe, efficacy, and safety.

Research Objective III: To develop a wound dressing to treat the chronic wounds commonly associated with PAD.

Given that baculovirus gene delivery is safe for direct human applications, controlled and sustained delivery is a crucial step for human therapeutic applications. Hydrogel delivery systems were synthesized for customizable and controlled baculovirus delivery enabling gene delivery over a range of days. The hydrogel properties were optimized to create a flexible yet mechanically sound stent or stent coating.

Natural and biodegradable polymers were investigated to mitigate off-target effects and toxicity. First, an alginate-chitosan hydrogel system was created with sustained baculovirus delivery over ten days. The hydrogel system was antimicrobial, swelled severalfold, hemocompatible, promoted blood coagulation, and was stable over a month. However, the blood coagulation properties and low mechanical strength did not make it suitable for a stent coating. Beneficially, these properties are required for chronic wound treatment. Thus, the hydrogel system developed was investigated for treating the chronic wounds associated with limb ischemia from PAD. Overall, the VEGFA eluted from the baculovirus hydrogel significantly improved angiogenesis, cell migration, wound healing, and cell proliferation. This generates a favourable wound-healing environment.

An ideal wound dressing should be antimicrobial and provide a moist environment [148]. The wound dressing also promoted cell migration, angiogenesis, and epithelialization to help regenerate the damaged tissue [158],[151]. This promising approach for chronic wound treatment meets all these wound dressing requirements. Non-healing wounds and ulcers occur in one-two out of every 100 people [223]. In the US alone, chronic wounds affect 6.5 million people, costing the healthcare system 25 billion dollars [224]. Chronic wounds may be attributed to reactive oxygen species, inflammatory cytokines, senescent cells, low growth factor production, infection, and endothelial cell dysfunction [225]. The gene-eluting wound dressing has the potential to improve clinical outcomes through improved healing, comfort, and reduced risk of infection and amputation.

As for the stent investigation, another natural polymer was investigated, polyvinyl alcohol (PVA). PVA is dissolvable and anti-thrombotic [167], [201]. Different polymers (gelatin, polyethylene glycol, and chitosan) and synthesis methods were investigated to optimize the PVA delivery system. The PVA-based hydrogels investigated here sustained baculovirus elution from five to 25 days, depending on the hydrogel composition. The quantity of viable baculovirus loaded significantly declined with each freeze-thaw from one to four (15.3 ± 2.9 % vs. 0.9 ± 0.5 %, respectively). The addition of gelatin to the hydrogels protected baculovirus viability during the freeze-thaw cycles, resulting in one of the highest loading capacities of 94.6 ± 1.2 % with elution over 23 days. Adding chitosan, PEG-8000, and gelatin to the hydrogels altered the properties of the hydrogel, including swelling, blood coagulation, and antimicrobial effects for different therapeutic applications. Passive absorption of the baculovirus into PVA hydrogels exhibited the highest baculovirus loading (96.4 ± 0.6 %) with elution over 25 days. The PVA-based hydrogels exhibited good blood compatibility and were non-cytotoxic to SMCs and HUVECs. The delivery

system can be further customized by adding other polymers, loading methods, or additional freeze-thaw cycles. These alterations can change the hydrogel's mechanical properties and gene elution, specific to each therapeutic application. This proof of concept has clinical applications as a medical device or stent coating by improving blood compatibility, preventing thrombosis, and preventing infection. Overall, the PVA-based hydrogel delivery of baculoviruses to mammalian cells is efficient, safe, and customizable.

3) Tri-gene eluting dissolvable stent

Research Objective IV: To optimize the baculovirus doses, gene expression, polymer selection, and mechanical properties to fabricate an optimized dissolvable peripheral stent.

Fully biodegradable or dissolvable stents offer several advantages such as eliminating the foreign body (the stent), which could reduce the risk of thrombosis [28]. Complete biodegradation of the stent would also support normal vasomotion and luminal movement. Specifically, polyvinyl alcohol (PVA) has the required mechanical strength and elasticity of a stent [31]–[34]. It also demonstrated uniform degradation, hemocompatibility (no platelet or blood coagulation,) and swelling behaviour to assist with self-expansion. Next, an early-stage intervention to promote endothelial health could prevent current downstream complications including thrombosis, in-stent restenosis, calcification, and low patency. Given the literature, promoting proper endothelial function would appear to prevent LDL accumulation, immune cell infiltration, inflammation, and smooth muscle cell hyperproliferation. To promote endothelial health, baculoviruses' expressing three genes (ADAMTS13, NOS3, and VEGFA) were loaded onto the stent to assist with endothelial cell regulation.

Nitric oxide synthase 3 (NOS3) is produced by functional endothelial cells and generates nitric oxide using L-arginine [191]. Nitric oxide regulates cell proliferation, promotes blood vessel

vasodilation, and inhibits bacterial growth. NOS3 and nitric oxide are known for their role in cardiovascular health. Specifically, nitric oxide (NO) can dose-dependently reduce blood pressure and arterial stiffening [45]. It also prevents endothelial cell dysfunction and reduces platelet activation which would lead to thrombosis. Here, we report that nitric oxide delivery prevents SMC proliferation, promotes endothelial proliferation, reduces ROS production, and promotes cell migration. These properties are beneficial in a stent application for its re-endothelialization, anti-restenotic, and anti-thrombotic properties.

Vascular endothelial cell growth factor A (VEGFA) is known to be one of the most potent pro-angiogenic factors and plays a key role in wound healing [30–32]. Specifically, VEGFA promotes endothelial cell migration, proliferation, and capillary tube formation. Furthermore, intradermal VEGF injections have accelerated diabetic wound-healing [151], [152]. We report that baculovirus VEGFA delivery promoted cell proliferation, migration, and angiogenesis as reported elsewhere [137]. These properties are beneficial for promoting endothelial health and re-endothelialization following stent implantation.

Finally, ADAMTS13 cleaves vWF, which prevents platelet aggregation and blood clotting. High vWF and low ADAMTS13 levels are associated with major cardiovascular events and thrombosis [114], [199]. ADAMTS13 is naturally secreted from healthy endothelial cells and was selected for its potential anti-thrombotic properties [208]. ADAMTS13 is a metalloproteinase that cleaves large multimers called von Willebrand factor (vWF) into smaller pieces and prevents early stages of platelet aggregation [199], [200]. This would have a beneficial antithrombotic property for the stent. ADAMTS13 delivery was functional and cleaved vWF [199]. The anti-thrombotic activity of ADAMTS13 can work additively with the PVA coating. ADAMTS13 and NOS3 were

found to work additively to promote re-endothelialization, prevent inflammation, and prevent thrombosis and thus were used in the stent systems.

Overall, the baculovirus-eluting dissolvable stent fabricated here may mitigate current peripheral stent complications, including in-stent restenosis, endothelial dysfunction, and thrombosis. The genes delivered by the baculovirus promote endothelial recovery, endothelial migration, and prevent inflammation. The gene delivery matches the therapeutic timeline while maintaining a very high safety profile (no signs of cytotoxicity, inflammation, or hemotoxicity). The genes and PVA provide an anti-thrombotic coating by preventing platelet adhesion and blood coagulation. The PVA stent also acts as a physical barrier to prevent SMC hyperproliferation. Meanwhile, the stent itself demonstrated sufficient mechanical strength yet flexibility to improve patency. These improvements may reduce complications and improve clinical outcomes, mitigating PAD's health and economic burden.

The novel stent system can potentially mitigate complications associated with PAD stenting and improve clinical outcomes. Specifically, the stent system can promote endothelial function, stimulate re-endothelialization, inhibit neointimal hyperplasia, and prevent in-stent restenosis while improving patency. The stent was shown to be safe and efficient, providing a superior option for people suffering from PAD or CAD. This can relieve both the health and economic burden of atherosclerosis related complications.

4) A gene- and drug-eluting coronary artery stent

Research Objective V: To optimize the gene and drug concentration and elution from coronary stent coating to mitigate current complications and improve clinical outcomes.

To mitigate current stenting complications (thrombosis and restenosis), a novel gene- and drug-eluting (GDES) stent was also developed. The novel gene- and drug-eluting (GDES) stent coating

shows favourable properties *in vitro*. The smooth stent coating that remains intact during expansion and demonstrates slow, uniform degradation. The stent coating is also flexible, without cracks or breakage during expansion or degradation to reduce the risk of thrombosis. A cross-linker (STMP) improves the tensile strength of the coating which can stretch up to 600 % allowing for stent expansion and arterial movement. The stent system is non-cytotoxic and hemocompatible providing an antithrombotic coating that physically prevents SMC hyperproliferation. The fully dissolvable coating also reduces the risk of long-term polymer-induced inflammation. The gene and drug are eluted over 10 and 86 days, respectively. The gene, NOS3, promotes endothelial cell proliferation, prevents SMC proliferation, reduces ROS production, and induces cell migration. The two-week gene expression enables time for a fully developed endothelial lining to form, preventing downstream complications. The 86-day drug elution prevents any inflammation or neointimal hyperplasia that may occur. The dual factor elution assists with re-endothelialization, inhibiting inflammation, and preventing smooth muscle cell proliferation leading to restenosis. Overall, the stent system may improve clinical outcomes by mitigating current complications such as thrombosis, restenosis, polymer-induced inflammation, and endothelial dysfunction.

CHAPTER 10: Limitations and future recommendations

Although this work is comprehensive and fulfills all research objectives there are limitations and future directions. Future work should focus on the next stage of pre-clinical research for all presented work. All *in vitro* work showed promising results suggesting that *in vivo* studies are warranted.

Chronic and non-healing wounds are common in people with PAD due to inadequate blood flow. Common complications with chronic wound dressings include infection, poor adherence, lack of moisture control, low cell regeneration, inadequate exudate (fluid) management, allergic reaction, pain during removal, and high cost. However, the wound dressing presented here addresses all these complications and thus should be tested further in pre-clinical and eventually clinical studies. The microcapsule hydrogels should be tested in conjugation with classic bandages and dressing to accelerate healing, prevent infection, and provide moisture control.

Both peripheral and cardiac stents are used to treat atherosclerosis. Both stent types have similar complications including restenosis, thrombosis, in-stent fractures, limited flexibility, limited sizes, allergic reactions, calcification, and long lesions. The dissolvable stent and PVA stent coating presented here address these issues. Further stent coating optimization could be investigated. Specifically, a coating that promotes endothelial cell adhesion while preventing platelet, protein, and immune cell adhesion. This would further assist with re-endothelialization and stent patency. The next steps include testing the stent systems *in vivo* to confirm their therapeutic efficacy. Specifically, a swine model, following FDA guidelines, would result in the quickest translation to practice. Finally, different peripheral and cardiac stenting locations should be investigated more thoroughly for changes in fluid dynamics and anatomy that come with it. Computational modeling could also be employed to predict drug elution patterns, fluid dynamics,

and stent efficacy. Given favourable outcomes, the stents should be tested long-term in a pre-clinical setting before moving onto a small clinical trial.

CHAPTER 11: Conclusion

This thesis presents the design, optimization, and engineering of baculovirus gene delivery platforms for treating atherosclerosis present in coronary and peripheral artery disease. The baculovirus delivery system was extensively investigated for its safety and efficacy. The *in vitro* efficacy and safety of baculovirus gene delivery was confirmed using the main cells that populate the artery (SMCs and HUVECs). Given that the baculovirus was safe and effective, a delivery system was needed to extend the gene expression over the therapeutic window. Thus, alginate-chitosan and PVA-based hydrogel systems were investigated and optimized for the baculovirus delivery. The antimicrobial and hemostatic properties of the alginate-chitosan hydrogel were beneficial for treating the chronic wounds often seen in PAD patients. Comparatively, a PVA or PVA-gelatin hydrogel demonstrated the most favourable properties for stent fabrication. A fully dissolvable stent was then made from PVA that eluted three different genes to help prevent atherosclerosis progression. The three genes worked additively to recover a healthy endothelium and leave behind fully reformed vasculature. A bare-metal stent was also coated in PVA and PVA-gelatin. The stent coating eluted a gene and drug to create dual action stent. The novel stent coating significantly reduced inflammation while promote endothelial recovery and growth. Overall, the thesis provides a comprehensive investigation into a gene- and/or drug-eluting stent to treat atherosclerosis present in PAD and CAD.

CHAPTER 12: Summary and claimed original contributions to knowledge

The main goal of this thesis was to design a new stent to treat atherosclerosis. Towards this goal, the following original contributions were reported:

1. Baculovirus transduction and gene delivery is efficient even at physiological temperatures.
2. Baculovirus administration and gene delivery is safe even at high doses (MOI of 1000).
3. Baculovirus administration and gene delivery showed no signs of cytotoxicity, genotoxicity, inflammation, hemolysis, thrombosis, or lysosomal hijacking at therapeutic doses.
4. Baculovirus gene therapy is hemocompatible.
 - a. Baculoviruses do not alter blood clotting time.
 - b. Baculoviruses do not cause hemolysis.
5. Baculoviruses gene delivery can efficiently transduce even in serum (up to 50 % tested).
6. Wound dressings composed of alginate-chitosan hydrogels sustain baculovirus delivery and viability over ten days.
7. Alginate-chitosan hydrogel dressings have a baculovirus encapsulation efficiency of 99.9 %.
8. Baculovirus-eluting alginate-chitosan hydrogels demonstrate antimicrobial properties by preventing bacterial growth, promoted blood coagulation, and swelling to incorporate bacterial and cellular debris.

9. Alginate-chitosan hydrogels eluting baculovirus (that expressed VEGFA) have therapeutic potential in wound dressing for chronic wounds common in people with PAD.
10. Baculovirus gene delivery hydrogels (alginate-chitosan, PVA, PVA-gelatin, PVA-PEG, and PVA-chitosan) are customizable and sustain virus delivery using different polymers incorporated into PVA-based hydrogels.
11. In baculovirus-eluting PVA hydrogels, elution can be customized from five to 23 days using different polymers added to the PVA base.
12. PVA-based hydrogel loading efficiency ranged from 0.4 % to 96.4 %.
13. Passive baculovirus loading onto PVA hydrogels allows sustained baculovirus delivery over 25 days.
14. Adding gelatin to PVA hydrogels significantly improves baculovirus stability over time and even over multiple freeze-thaw cycles.
15. Baculoviruses are stable, safe, and efficient at physiological conditions promoting their use in countless gene therapy applications in human, veterinary, and environmental applications.
16. PVA-based hydrogel elution of NOS3 baculovirus gene delivery shows angiogenic properties by promoting HUVEC proliferation and migration.
17. NOS3 baculovirus gene delivery from PVA hydrogels is also anti-inflammatory by regulating ROS production.
18. NOS3 expression from baculovirus eluted from PVA hydrogels inhibits smooth muscle cell proliferation providing anti-restenotic properties.

19. Stent delivery of baculoviruses expressing ADAMTS13 creates an anti-inflammatory state by reducing ROS production.
20. Stent delivery of baculoviruses expressing ADAMTS13 cleaves vWF, preventing platelet aggregation and providing anti-thrombotic properties.
21. Stent delivery of baculoviruses expressing VEGFA provides angiogenic, proliferative, and wound-healing properties important for endothelial health and re-endothelialization.
22. Stent delivery of ADAMTS13 and NOS3 (via baculovirus vectors) demonstrate superior angiogenic, anti-inflammatory, anti-thrombotic, and anti-restenotic (cell-type dependent proliferation) compared to one gene alone.
23. Dissolvable PVA stent coatings cross-linked with STMP creates a smooth coating that is anti-thrombotic, flexible, and mechanically strong.
24. The engineered PVA stent coating is capable of passive baculovirus loading and sustained elution.
25. PVA stent coatings can elute baculovirus over ten days even in high serum conditions, the main component of blood.
26. Dissolvable PVA stents cross-linked with STMP and then fully dried possess the proper mechanical properties to act as a self-expandable and dissolvable peripheral stent.
27. The PVA stent coating has properties that can combat peripheral and coronary stenting complications (low patency, thrombosis, and in-stent restenosis).
28. Baculovirus gene delivery can work in synergy with Everolimus release. Specifically, neither appear to impact the therapeutic function and both significantly decrease SMC proliferation.

29. The PVA hydrogel stent coating is effective baculovirus and Everolimus delivery systems.
30. The PVA hydrogel stent coating does not stimulate platelet adhesion or blood coagulation making it anti-thrombotic.
31. PVA-gelatin stent coatings improve cellular adhesion without promoting platelet or blood accumulation.

The three medical devices presented address critical limitations of current technology. All three devices had significant therapeutic potential, excellent safety margin, and no cytotoxicity effects and

Chronic wounds are common in PAD whereby the reduced blood flow lead to non-healing ulcers and wounds. The alginate-chitosan wound dressing meets all requirements for a novel wound dressing. The natural polymers mitigate the risk of allergic reaction and cost. The six-fold swelling nature of the hydrogel also provides moisture control and fluid management. Moreover, chitosan is antimicrobial showing a bacterial zone of growth inhibition. The VEGFA expression from baculoviruses promotes endothelial cell migration and angiogenesis to stimulate wound healing. Overall, the wound dressing addresses key issues with current dressings including infection, poor adherence, lack of moisture control, low cell regeneration, inadequate exudate (fluid) management, allergic reaction, pain during removal, and high cost.

The dissolvable peripheral stent elutes three genes to assists with cell regulation and preventing inflammation. The genes initiate endothelial regulation and help prevent consequential issues such as thrombosis, restenosis, and calcification. Moreover, the PVA base degrades over time leaving behind fully formed vasculature and preventing long term polymer induced inflammation. The

dissolvable PVA material is also flexible mitigating the risk of stent fracture and easily customizable for a range of lesion sizes. Overall, the novel stent properties address current stenting complications including restenosis, thrombosis, in-stent fractures, limited flexibility, limited sizes, allergic reactions, calcification, and long lesions.

The cardiac stent uses a dual action mechanism with both drug and gene-eluting. The novel stent coating address current stenting complications including restenosis, thrombosis, limited sizes, allergic reactions, and calcification. The gene and drug work short and long term to prevent restenosis, thrombosis, and downstream calcification. Moreover, the natural components and polymers used mitigate the risk of allergic reaction.

Appendix

Figure 15a-b

03-Aug	Name	Analysed arc	Nb extreme	Nb nodes	Nb junctions	Nb master j	Nb master s	tot. master s	Nb meshes	total meshes	Nb peaces	Nb segment	Nb branches	Nb isol. Seg	total length	total branchi	total seg len	total branchi	total isolatec	branching in	mesh index
V1	V_9859-tr	1166886	82	260	76	27	47	6811	14	209135	154	83	60	11	11580	10791	6449	4342	789	107.483	252.259
V2	IMG_9860-tr	1066716	107	360	97	33	55	6734	13	151092	203	106	87	10	12290	11655	6346	5309	635	72.943	204.061
V		1116801	94.5	310	86.5	30	51	6772.5	13.5	180113.5	178.5	94.5	73.5	10.5	11935	11223	6397.5	4825.5	712	90.213	228.16
M1	IMG_9874-tr	950796	70	200	56	28	45	5556	14	123032	118	67	34	17	9308	7904	5349	2555	1404	157.324	198.429
M3	M_jpocqg cqr	875952	61	182	52	18	31	4303	8	90470	109	58	43	8	8312	7688	3971	3637	704	92.349	239.056
M2	Mock_9875-r	895860	78	227	69	26	42	6008	12	142813	142	75	56	11	10770	10050	5669	4381	720	101.232	231.077
M		907536	69.6666667	203	59	24	39.3333333	5289	11.3333333	118771.667	123	66.6666667	44.3333333	12	9463.33333	8520.66667	4996.33333	3524.33333	942.666667	116.968333	222.854
03-Aug	Name	Analysed arc	Nb extreme	Nb nodes	Nb junctions	Nb master j	Nb master s	tot. master s	Nb meshes	total meshes	Nb peaces	Nb segment	Nb branches	Nb isol. Seg	total length	total branchi	total seg len	total branchi	total isolatec	branching in	mesh index
M1	1637048	26	17	5	8	30	4713	4	6761	36	22	2	12	7941	5294	5221	73	2647	2610.5	589.125	1690.2
M2	1656480	27	25	6	10	26	5035	3	8841	41	23	9	9	10548	9936	5690	4246	612	632.222	503.5	2947
M3	1725680	24	140	38	22	42	17937	18	201710	75	56	14	5	22722	22228	18027	4201	494	1287.643	815.318	11206.1
V1	1732032	43	160	47	45	114	23862	31	374097	129	101	13	15	35438	32049	26526	5523	3389	2040.462	530.267	12067.6
V2	1699944	67	95	28	39	84	18955	18	268530	112	69	19	24	28730	23797	21445	2352	4933	1128.884	486.026	14918.3
V3-tr	1605884	52	156	46	40	91	23910	28	397005	128	94	16	18	38183	34055	26182	7873	4128	1636.375	597.75	14178.8
Angio DMSO	1389680	23	3	1	2	4	371	0	0	17	5	3	9	2134	1826	578	1248	308	192.667	185.5	0
Angio DMSO	1359412	8	0	0	0	4	461	0	0	8	4	0	4	2619	569	569	0	2050	0	0	0
Angio DMSO	1336167	9	19	5	2	9	1452	3	5907	17	12	1	4	2224	1651	1611	40	573	1611	726	1969

Where M is for Mock and V is for VEGF

Figure 15d-h

at 6h and 12h										
	Name	Area mm^2	Area %	Width mm	Std Dev mm	Area mm^2	std dev	Area % avg	Std dev	Label
2 hours	V1 wound 2h	0.569	17.641	0.489	0.12	0.41533333	0.20089881	12.8726667	6.22380465	V
	V2 wound 2h	0.489	15.145	0.51	0.136					
	V3 wound 2h	0.188	5.832	0.045	0.192					
	M1 wound 2h	0.948	29.374	0.707	0.109	0.72833333	0.19104014	22.5653333	5.92188824	Mock
	M2 wound 2h	0.636	19.709	0.47	0.121					
	M3 wound 2h	0.601	18.613	0.499	0.121					
12 hours	V1 wound 12h	0.224	6.954	0.311	0.118	0.172	0.0488774	5.33	1.5274973	V
	V1 wound 12h	0.127	3.922	0.087	0.079					
	V3 wound 12h	0.165	5.114	0.246	0.087					
	M1 wound 12h	0.093	2.897	0.218	0.113	0.12066667	0.02482606	3.74266667	0.7585317	Mock
	M2 wound 12h	0.141	4.363	0.259	0.089					
	M3 wound 12h	0.128	3.968	0.087	0.079					
12h	V1 wound 12h	0.278	8.603	0.31	0.143	0.21466667	0.07557998	6.64866667	2.3397445	
	V1 wound 12h	0.131	4.056	0.089	0.079					V
	V3 wound 12h	0.235	7.287	0.313	0.117					
	M1 wound 12h	0.17	5.258	0.281	0.121	0.249	0.14031037	7.70566667	4.34731231	
	M2 wound 12h	0.411	12.725	0.422	0.137					Mock
	M3 wound 12h	0.166	5.134	0.258	0.252					
15 variance, 1 threshold										

Where M is for Mock and V is for VEGF

Figure 24 & 34: Wound healing assay

		Wound healing assay											
HUVEC June		Area mm^2	Area %	Width mm	Std Dev	Avg area mm	Avg Area %	11		Avg area mm	Avg Area %		
1	A2.JPG	0.02	1.423	0.083	0.044	0.05733333	5.67866667		A	0.05733333	5.67866667		
4	A3.JPG	0.083	8.81	0.199	0.041				Alginate	0.07733333	7.845		
5	A100.JPG	0.069	6.803	0.173	0.048				Chitosan	0.03366667	3.22966667		
6	ALG1.JPG	0.11	11.006	0.168	0.103	0.07733333	7.845		Mock	0.20666667	19.318		
9	ALG2.JPG	0.075	7.034	0.068	0.197				BV-VEGFA	0.032	2.82666667		
10	ALG3.JPG	0.047	5.495	0.052	0.116								
24	Chit mp1.JPG	0.054	5.027	0.141	0.069	0.03366667	3.22966667		bv-v vs mock	P(T<=t) one-	0.02432025		
28	Chit mp2.JPG	0.025	2.456	0.115	0.056				chit vs mock	P(T<=t) one-	0.0108592		
29	Chit mp3.JPG	0.022	2.206	0.08	0.062				alg vs mock	P(T<=t) one-	0.01943851		
19	MOCK2.JPG	0.258	24.453	0.358	0.157	0.20666667	19.318		chit vs alg	P(T<=t) one-	0.01358778		
20	MOCK3.JPG	0.144	13.863	0.222	0.096				alg vs bv	P(T<=t) one-	0.15371269		
39	MOCK1.JPG	0.218	19.638	0.266	0.089				chit vs bv	P(T<=t) one-	0.45181449		
31	v1.JPG	0.005	0.438	0.048	0.019	0.032	2.82666667						
33	v2.JPG	0.006	0.562	0.039	0.019								
34	v3.JPG	0.085	7.48	0.183	0.071								
3	AN1.JPG	0.039	3.526	0.133	0.069	0.03333333	2.91266667						
6	AN2.JPG	0.037	3.027	0.096	0.119								
8	AN3.JPG	0.024	2.185	0.073	0.04								
9	ANV1.JPG	0.075	7.2	0.249	0.109	0.055	5.50166667						
11	ANV2.JPG	0.018	1.521	0.071	0.043								
13	ANV3.JPG	0.072	7.784	0.154	0.112								
17	ANVD1.JPG	0.083	7.827	0.174	0.084	0.04266667	4.002						
21	ANVD2.JPG	0.025	2.221	0.09	0.065								
23	ANVD3.JPG	0.02	1.958	0.1	0.036								
27	ARG1.JPG	0.057	4.999	0.098	0.032	0.05766667	5.096						
30	ARG2.JPG	0.055	4.826	0.146	0.114								
33	ARG3.JPG	0.061	5.463	0.125	0.066								
36	AV1.JPG	0.025	2.043	0.079	0.061	0.108	9.79233333						
37	AV2.JPG	0.285	25.889	0.372	0.162								
42	AV3.JPG	0.014	1.445	0.057	0.062								
46	LNAME.JPG	0.228	19.37	0.327	0.173	0.11533333	10.271						
52	LNAME2.JPG	0.052	5.34	0.176	0.083								
55	LNAME3.JPG	0.066	6.103	0.194	0.072								
58	N1.JPG	0.009	0.825	2.62E-04	0.067	0.01433333	1.32833333						
61	n2.JPG	0.019	1.748	0.055	0.043								
64	N3.JPG	0.015	1.412	0.069	0.052								
66	NV1.JPG	0.023	2.098	0.079	0.043	0.02033333	1.77066667						
70	NV2.JPG	0.014	1.192	0.054	0.063								
72	NV3.JPG	0.024	2.022	0.122	0.062								
76	PAM1.JPG	0.046	3.99	0.09	0.072	0.082	6.79433333						
78	PAM2.JPG	0.031	2.481	0.101	0.067								
87	PAM3.JPG	0.169	13.912	0.236	0.131								

Figure 24 & 34: Angiogenesis assay

02-Aug angiogenesis assay																						
Name	Analysed are	Nb extreme	Nb nodes	Nb junctions	Nb master j.	Nb master s	tot. master s	Nb meshes	total mesh	Nb peaces	Nb segment	Nb branches	Nb isol.	Seg.	total length	total branch	total seg len	total branch total	isolate	branching inf	mesh index	mean mesh
ADAM1	1998700	26	49	16	27	61	14253	10	472610	59	41	10	8	26964	21808	15961	5847	5156	1596.1	527.889	47261	
Screenshot 2	4170628	46	146	41	36	79	36487	20	1342978	101	70	18	13	49441	43810	38303	5507	5631	2127.944	1013.528	67148.9	
Screenshot 2	4099508	56	133	40	34	76	34252	23	1970212	108	70	22	16	51540	48536	35964	12572	3004	1634.727	1007.412	85661.4	
Screenshot 2	3166016	46	116	36	29	78	22388	22	711699	99	66	20	13	39866	33707	23803	9904	6159	1190.15	772	32350	
AN	4034756	78	134	39	52	129	36961	22	900493	140	89	24	27	51459	44663	40853	3810	6796	1702.208	710.788	40931.5	
Screenshot 2	4044740	71	154	45	37	95	35777	26	951004	132	82	31	19	57320	50295	39731	10564	7025	1281.645	966.946	36577.1	
Screenshot 2	3886248	29	894	258	157	280	37551	121	2374534	399	371	27	1	39806	39701	37607	2094	105	1392.852	239.178	19624.2	
Screenshot 2	3041096	55	142	39	31	72	20494	16	435269	110	68	28	14	39533	31373	23273	8100	8160	831.179	661.097	27204.3	
ANV	3934168	67	121	35	31	75	35930	21	1621915	107	62	23	22	51828	42744	38131	4613	9084	1657.87	1159.032	77234	
Screenshot 2	3863356	64	93	30	34	85	33737	17	991204	106	65	18	23	49866	42476	36477	5999	7390	2026.5	992.265	58306.1	
Screenshot 2	3098195	91	158	49	38	107	37328	30	1105917	159	99	29	31	59004	46918	41909	5009	12086	1445.138	982.316	38897.2	
ANV_8308-tr	3498357	45	125	39	28	61	23385	22	1166016	91	59	19	13	40804	34369	23764	10605	6435	1250.737	835.179	59000.7	
AV_8289-tr	3498357	88	1333	382	183	360	39284	175	1802443	615	543	56	16	44791	43722	39982	3740	1069	713.964	214.667	10299.7	
AV_8290-tr	3498357	32	146	46	33	68	27454	21	960771	98	74	16	8	43906	39774	28563	11211	4132	1785.188	831.939	45751	
AV_8291-tr	3498357	36	174	51	47	99	30378	27	624290	120	90	24	6	44221	40091	32911	7180	4130	1371.292	646.34	23121.9	
AV_8292-tr	3498357	62	989	284	130	268	45659	141	1824418	449	408	26	15	50213	48631	46086	2545	1582	1772.538	351.223	12939.1	
Mock_8316-t	3498357	26	119	35	24	56	20425	14	323471	84	63	16	5	30007	28117	21666	6451	1890	1354.125	851.042	23108.1	
Mock_8320-t	3498357	39	86	26	19	39	20373	10	501686	72	45	15	12	27264	26432	20374	5558	832	1391.6	1072.263	50168.6	
Mock_8322-t	3498357	57	143	43	23	55	17088	17	216118	106	67	21	18	23298	21166	17488	3678	2132	832.762	742.957	12718.2	
Mock_8323-t	3498357	41	83	25	16	39	16226	16	198399	67	42	9	16	25341	23621	16798	6823	1720	1866.444	1014.125	12399.9	
NOS3_8272-t	3498357	46	801	237	123	234	41370	107	1896512	378	341	30	7	47855	46962	41566	5396	893	1385.533	336.341	17724.4	
NOS3_8274-t	3498357	36	54	16	26	64	16726	9	628687	60	37	10	13	32719	21921	18378	3543	10798	1837.8	643.308	69854.1	
NOS3_8275-t	3498357	59	1027	298	155	296	45367	140	2008089	477	427	41	9	50949	50108	45886	4522	841	1111.854	292.629	14343.5	
NOS3_8276-t	3498357	37	91	25	24	63	18906	14	630777	77	52	13	12	37415	27885	20166	7719	9530	1551.231	787.75	45055.5	
NV_8295-tr	3498357	39	62	17	18	53	18312	11	822136	66	39	15	12	37485	28959	20367	8592	8526	1357.8	1017.333	74739.6	
NV_8299-tr	3498357	42	109	32	36	87	25427	18	673368	102	71	20	11	40797	36662	28284	8378	4135	1414.2	706.306	37409.3	
NV_8300-tr	3498357	74	540	149	76	146	39596	72	1587748	268	215	32	21	50425	47113	40034	7079	3312	1251.062	521	22052.1	
NV_8301-tr	3498357	116	1013	295	131	261	41448	123	1844514	505	414	68	23	50312	48361	42065	6296	1951	618.603	316.397	14993.1	
VEGF_8278-t	3498357	56	1076	294	136	276	46552	139	2061132	470	424	36	10	52019	51221	47435	3786	798	1317.639	342.294	14828.3	
VEGF_8279-t	3498357	95	1627	464	218	440	53625	216	2195739	748	668	67	13	61109	59604	54747	4857	1505	817.119	245.986	10165.5	
VEGF_8280-t	3498357	66	104	30	46	107	26640	17	713101	125	81	22	22	43992	35533	30241	5292	8459	1374.591	579.13	41947.1	

References

- [1] L. Badimon and G. Vilahur, “Thrombosis formation on atherosclerotic lesions and plaque rupture,” *J. Intern. Med.*, vol. 276, no. 6, pp. 618–632, Dec. 2014, doi: <https://doi.org/10.1111/joim.12296>.
- [2] L. Badimon, R. F. Storey, and G. Vilahur, “Update on lipids, inflammation and atherothrombosis,” *Thromb. Haemost.*, vol. 105, no. S 06, pp. S34–S42, 2011.
- [3] R. Virmani *et al.*, “Atherosclerotic plaque progression and vulnerability to rupture: angiogenesis as a source of intraplaque hemorrhage.,” *Arterioscler. Thromb. Vasc. Biol.*, vol. 25, no. 10, pp. 2054–2061, Oct. 2005, doi: 10.1161/01.ATV.0000178991.71605.18.
- [4] G. Agnelli, J. J. F. Belch, I. Baumgartner, P. Giovvas, and U. Hoffmann, “Morbidity and mortality associated with atherosclerotic peripheral artery disease: A systematic review,” *Atherosclerosis*, vol. 293, pp. 94–100, 2020, doi: <https://doi.org/10.1016/j.atherosclerosis.2019.09.012>.
- [5] American College of Cardiology, “Peripheral artery disease by the numbers.” 2018, [Online]. Available: <https://www.acc.org/latest-in-cardiology/articles/2018/10/25/12/42/number-check-peripheral-artery-disease-by-the-numbers>.
- [6] M. H. Criqui and V. Aboyans, “Epidemiology of Peripheral Artery Disease,” *Circ. Res.*, vol. 116, no. 9, pp. 1509–1526, 2015, doi: 10.1161/CIRCRESAHA.116.303849.
- [7] F. G. R. Fowkes *et al.*, “Comparison of global estimates of prevalence and risk factors for peripheral artery disease in 2000 and 2010: a systematic review and analysis,” *Lancet*, vol. 382, no. 9901, pp. 1329–1340, 2013.
- [8] E. Marrett, M. daCosta DiBonaventura, and Q. Zhang, “Burden of peripheral arterial disease in Europe and the United States: a patient survey,” *Health Qual. Life Outcomes*, vol. 11, no. 1, p. 175, 2013, doi: 10.1186/1477-7525-11-175.
- [9] U. K. A. Sampson *et al.*, “Global and Regional Burden of Death and Disability From Peripheral Artery Disease: 21 World Regions, 1990 to 2010,” *Glob. Heart*, vol. 9, no. 1, pp. 145–158.e21, 2014, doi: <https://doi.org/10.1016/j.gheart.2013.12.008>.
- [10] C. G. Kohn, M. J. Alberts, W. F. Peacock, T. J. Bunz, and C. I. Coleman, “Cost and inpatient burden of peripheral artery disease: Findings from the National Inpatient Sample,” *Atherosclerosis*, vol. 286, pp. 142–146, 2019, doi: <https://doi.org/10.1016/j.atherosclerosis.2019.05.026>.
- [11] A. S. S. *et al.*, “Major Adverse Limb Events and Mortality in Patients With Peripheral Artery Disease,” *J. Am. Coll. Cardiol.*, vol. 71, no. 20, pp. 2306–2315, May 2018, doi: 10.1016/j.jacc.2018.03.008.
- [12] B. Sigvant, F. Lundin, and E. Wahlberg, “The Risk of Disease Progression in Peripheral Arterial Disease is Higher than Expected: A Meta-Analysis of Mortality and Disease Progression in Peripheral Arterial Disease,” *Eur. J. Vasc. Endovasc. Surg.*, vol. 51, no. 3, pp. 395–403, 2016, doi: <https://doi.org/10.1016/j.ejvs.2015.10.022>.
- [13] M. Pabon *et al.*, “Sex Differences in Peripheral Artery Disease,” *Circ. Res.*, vol. 130, no. 4, pp. 496–511, 2022, doi: 10.1161/CIRCRESAHA.121.320702.
- [14] R. D. Shahjehan and B. S. Bhutta, “Coronary artery disease,” in *StatPearls [Internet]*, StatPearls Publishing, 2022.
- [15] Centers for Disease Control and Prevention, “Heart Disease Facts.” 2012, [Online]. Available: <http://www.cdc.gov/heartdisease/facts.htm>.

- [16] “Global, regional, and national age-sex-specific mortality for 282 causes of death in 195 countries and territories, 1980-2017: a systematic analysis for the Global Burden of Disease Study 2017,” *Lancet (London, England)*, vol. 392, no. 10159, pp. 1736–1788, Nov. 2018, doi: 10.1016/S0140-6736(18)32203-7.
- [17] T. A. Gaziano, A. Bitton, S. Anand, S. Abrahams-Gessel, and A. Murphy, “Growing epidemic of coronary heart disease in low-and middle-income countries,” *Curr. Probl. Cardiol.*, vol. 35, no. 2, pp. 72–115, 2010.
- [18] C. Huang, J. Huang, Y. Tian, X. Yang, and D. Gu, “Sugar sweetened beverages consumption and risk of coronary heart disease: a meta-analysis of prospective studies,” *Atherosclerosis*, vol. 234, no. 1, pp. 11–16, 2014.
- [19] W. H. Organization, *A prioritized research agenda for prevention and control of noncommunicable diseases*. World Health Organization, 2011.
- [20] D. Mozaffarian *et al.*, “Heart disease and stroke statistics—2015 update: a report from the American Heart Association,” *Circulation*, vol. 131, no. 4, pp. e29–e322, 2015.
- [21] M. Rayner, S. Allender, P. Scarborough, and B. H. F. H. P. R. Group, “Cardiovascular disease in Europe,” *Eur. J. Cardiovasc. Prev. Rehabil.*, vol. 16, no. 2_suppl, pp. S43–S47, 2009.
- [22] G. Zhang, C. Yu, M. Zhou, L. Wang, Y. Zhang, and L. Luo, “Burden of Ischaemic heart disease and attributable risk factors in China from 1990 to 2015: findings from the global burden of disease 2015 study,” *BMC Cardiovasc. Disord.*, vol. 18, no. 1, p. 18, Feb. 2018, doi: 10.1186/s12872-018-0761-0.
- [23] A. Reda *et al.*, “Gender-related differences in risk factors and treatment strategies in patients with acute coronary syndrome across Egypt: part of the Cardio-Risk Project,” *Atheroscler. Suppl.*, vol. 100, no. 33, p. e2, 2018.
- [24] G. H. Bevan and K. T. White Solaru, “Evidence-Based Medical Management of Peripheral Artery Disease,” *Arterioscler. Thromb. Vasc. Biol.*, vol. 40, no. 3, pp. 541–553, 2020, doi: 10.1161/ATVBAHA.119.312142.
- [25] S. Bangalore *et al.*, “Bare metal stents, durable polymer drug eluting stents, and biodegradable polymer drug eluting stents for coronary artery disease: Mixed treatment comparison meta-analysis,” *BMJ*, vol. 347, no. November, pp. 1–20, 2013, doi: 10.1136/bmj.f6625.
- [26] D. H. Lee and J. M. d. la T. Hernandez, “The newest generation of drug-eluting stents and beyond,” *Eur. Cardiol. Rev.*, vol. 13, no. 1, pp. 54–59, 2018, doi: 10.15420/ecr.2018:8:2.
- [27] S. Venkatraman and F. Boey, “Release profiles in drug-eluting stents: Issues and uncertainties,” *J. Control. Release*, vol. 120, no. 3, pp. 149–160, 2007, doi: 10.1016/j.jconrel.2007.04.022.
- [28] D. Hoare, A. Bussooa, S. Neale, N. Mirzai, and J. Mercer, “The Future of Cardiovascular Stents: Bioresorbable and Integrated Biosensor Technology,” *Adv. Sci.*, vol. 6, no. 20, p. 1900856, Oct. 2019, doi: <https://doi.org/10.1002/advs.201900856>.
- [29] J. Zhu *et al.*, “Biosafety and efficacy evaluation of a biodegradable magnesium-based drug-eluting stent in porcine coronary artery,” *Sci. Rep.*, vol. 11, no. 1, p. 7330, 2021, doi: 10.1038/s41598-021-86803-0.
- [30] H. Hermawan, D. Dubé, and D. Mantovani, “Developments in metallic biodegradable stents,” *Acta Biomater.*, vol. 6, no. 5, pp. 1693–1697, 2010, doi: <https://doi.org/10.1016/j.actbio.2009.10.006>.
- [31] M.-C. Lin, C.-W. Lou, J.-Y. Lin, T. A. Lin, Y.-S. Chen, and J.-H. Lin, “Biodegradable

- Polyvinyl Alcohol Vascular Stents: Structural Model and Mechanical and Biological Property Evaluation.,” *Mater. Sci. Eng. C. Mater. Biol. Appl.*, vol. 91, pp. 404–413, Oct. 2018, doi: 10.1016/j.msec.2018.05.030.
- [32] M.-C. Lin *et al.*, “Using spray-coating method to form PVA coronary artery stents: structure and property evaluations,” *J. Polym. Res.*, vol. 25, no. 4, p. 101, 2018, doi: 10.1007/s10965-018-1497-3.
- [33] C. J. Boyer *et al.*, “3D Printing for Bio-Synthetic Biliary Stents,” *Bioengineering*, vol. 6, no. 1. 2019, doi: 10.3390/bioengineering6010016.
- [34] Y. Nagakawa, S. Fujita, S. Yunoki, T. Tsuchiya, S. Suye, and T. Itoi, “Self-expandable hydrogel biliary stent design utilizing the swelling property of poly(vinyl alcohol) hydrogel,” *J. Appl. Polym. Sci.*, vol. 137, no. 28, p. 48851, Jul. 2020, doi: <https://doi.org/10.1002/app.48851>.
- [35] M. Joner *et al.*, “Pathology of Drug-Eluting Stents in Humans. Delayed Healing and Late Thrombotic Risk,” *J. Am. Coll. Cardiol.*, vol. 48, no. 1, pp. 193–202, 2006, doi: 10.1016/j.jacc.2006.03.042.
- [36] V. Farooq, B. D. Gogas, and P. W. Serruys, “Restenosis: Delineating the numerous causes of drug-eluting stent restenosis,” *Circ. Cardiovasc. Interv.*, vol. 4, no. 2, pp. 195–205, 2011, doi: 10.1161/CIRCINTERVENTIONS.110.959882.
- [37] J. R. Laird, “Limitations of Percutaneous Transluminal Angioplasty and Stenting for the Treatment of Disease of the Superficial Femoral and Popliteal Arteries,” *J. Endovasc. Ther.*, vol. 13, no. 2_suppl, pp. II-30-II-40, Feb. 2006, doi: 10.1177/15266028060130S207.
- [38] J. Almasri *et al.*, “A systematic review and meta-analysis of revascularization outcomes of infrainguinal chronic limb-threatening ischemia,” *J. Vasc. Surg.*, vol. 69, no. 6, pp. 126S-136S, 2019, doi: 10.1016/j.jvs.2018.01.071.
- [39] I. I. Pipinos *et al.*, “The myopathy of peripheral arterial occlusive disease: part 1. Functional and histomorphological changes and evidence for mitochondrial dysfunction,” *Vasc. Endovascular Surg.*, vol. 41, no. 6, pp. 481–489, 2008.
- [40] I. I. Pipinos *et al.*, “Basic Science Review: The Myopathy of Peripheral Arterial Occlusive Disease: Part 2. Oxidative Stress, Neuropathy, and Shift in Muscle Fiber Type,” *Vasc. Endovascular Surg.*, vol. 42, no. 2, pp. 101–112, Apr. 2008, doi: 10.1177/1538574408315995.
- [41] B. D. Klugherz *et al.*, “Gene delivery from a DNA controlled-release stent in porcine coronary arteries,” *Nat. Biotechnol.*, vol. 18, no. 11, pp. 1181–1184, 2000, doi: 10.1038/81176.
- [42] Y. Nakayama, K. Ji-Youn, S. Nishi, H. Ueno, and T. Matsuda, “Development of high-performance stent: Gelatinous photogel-coated stent that permits drug delivery and gene transfer,” *J. Biomed. Mater. Res.*, vol. 57, no. 4, pp. 559–566, Dec. 2001, doi: [https://doi.org/10.1002/1097-4636\(20011215\)57:4<559::AID-JBM1202>3.0.CO;2-H](https://doi.org/10.1002/1097-4636(20011215)57:4<559::AID-JBM1202>3.0.CO;2-H).
- [43] K. Egashira *et al.*, “Local Delivery of Anti-Monocyte Chemoattractant Protein-1 by Gene-Eluting Stents Attenuates In-Stent Stenosis in Rabbits and Monkeys,” *Arterioscler. Thromb. Vasc. Biol.*, vol. 27, no. 12, pp. 2563–2568, Dec. 2007, doi: 10.1161/ATVBAHA.107.154609.
- [44] J. Wang *et al.*, “miR-22 eluting cardiovascular stent based on a self-healable spongy coating inhibits in-stent restenosis,” *Bioact. Mater.*, vol. 6, no. 12, pp. 4686–4696, 2021, doi: <https://doi.org/10.1016/j.bioactmat.2021.04.037>.

- [45] V. Kapil, E. Weitzberg, J. O. Lundberg, and A. Ahluwalia, “Clinical evidence demonstrating the utility of inorganic nitrate in cardiovascular health,” *Nitric Oxide*, vol. 38, pp. 45–57, 2014, doi: <https://doi.org/10.1016/j.niox.2014.03.162>.
- [46] M. H. Kural *et al.*, “Fas ligand and nitric oxide combination to control smooth muscle growth while sparing endothelium,” *Biomaterials*, vol. 212, pp. 28–38, 2019, doi: <https://doi.org/10.1016/j.biomaterials.2019.05.011>.
- [47] J. Rao, H. Pan Bei, Y. Yang, Y. Liu, H. Lin, and X. Zhao, “Nitric Oxide-Producing Cardiovascular Stent Coatings for Prevention of Thrombosis and Restenosis.,” *Front. Bioeng. Biotechnol.*, vol. 8, p. 578, 2020, doi: 10.3389/fbioe.2020.00578.
- [48] D. H. Walter *et al.*, “Local Gene Transfer of phVEGF-2 Plasmid by Gene-Eluting Stents,” *Circulation*, vol. 110, no. 1, pp. 36–45, Jul. 2004, doi: 10.1161/01.CIR.0000133324.38115.0A.
- [49] J. Yang *et al.*, “The prevention of restenosis in vivo with a VEGF gene and paclitaxel co-eluting stent,” *Biomaterials*, vol. 34, no. 6, pp. 1635–1643, 2013, doi: 10.1016/j.biomaterials.2012.11.006.
- [50] T. A. Kost and J. P. Condreay, “Recombinant baculoviruses as mammalian cell gene-delivery vectors,” *Trends Biotechnol.*, vol. 20, no. 4, pp. 173–180, 2002, doi: 10.1016/S0167-7799(01)01911-4.
- [51] N. Cheshenko, N. Krougliak, R. C. Eisensmith, and V. A. Krougliak, “A novel system for the production of fully deleted adenovirus vectors that does not require helper adenovirus,” *Gene Ther.*, vol. 8, no. 11, pp. 846–854, 2001, doi: 10.1038/sj.gt.3301459.
- [52] P. Wang, R. R. Granados, and M. L. Shuler, “Studies on serum-free culture of insect cells for virus propagation and recombinant protein production,” *J. Invertebr. Pathol.*, vol. 59, no. 1, pp. 46–53, 1992, doi: [https://doi.org/10.1016/0022-2011\(92\)90110-P](https://doi.org/10.1016/0022-2011(92)90110-P).
- [53] A. Paul, C. B. Elias, D. Shum-Tim, and S. Prakash, “Bioactive baculovirus nanohybrids for stent based rapid vascular re-endothelialization,” *Sci. Rep.*, vol. 3, no. 1, p. 2366, 2013, doi: 10.1038/srep02366.
- [54] H. Tang, R. R. Vanderpool, J. Wang, and J. X. J. Yuan, “Targeting L-arginine-nitric oxide-cGMP pathway in pulmonary arterial hypertension,” *Pulm. Circ.*, vol. 7, no. 3, pp. 569–571, 2017, doi: 10.1177/2045893217728261.
- [55] J. R. Klinger and P. J. Kadowitz, “The Nitric Oxide Pathway in Pulmonary Vascular Disease,” *Am. J. Cardiol.*, vol. 120, no. 8, Supplement, pp. S71–S79, 2017, doi: <https://doi.org/10.1016/j.amjcard.2017.06.012>.
- [56] A. K. Pandey *et al.*, “Mechanisms of VEGF (Vascular Endothelial Growth Factor) Inhibitor-Associated Hypertension and Vascular Disease,” *Hypertension*, vol. 71, no. 2, pp. e1–e8, Feb. 2018, doi: 10.1161/HYPERTENSIONAHA.117.10271.
- [57] M. Geindreau, F. Ghiringhelli, and M. Bruchard, “Vascular Endothelial Growth Factor, a Key Modulator of the Anti-Tumor Immune Response,” *International Journal of Molecular Sciences*, vol. 22, no. 9. 2021, doi: 10.3390/ijms22094871.
- [58] J. T. B. Crawley, R. De Groot, Y. Xiang, B. M. Luken, and D. A. Lane, “Unraveling the scissile bond: How ADAMTS13 recognizes and cleaves von Willebrand factor,” *Blood*, vol. 118, no. 12, pp. 3212–3221, 2011, doi: 10.1182/blood-2011-02-306597.
- [59] B. Doyle *et al.*, “Outcomes of stent thrombosis and restenosis during extended follow-up of patients treated with bare-metal coronary stents.,” *Circulation*, vol. 116, no. 21, pp. 2391–2398, Nov. 2007, doi: 10.1161/CIRCULATIONAHA.107.707331.
- [60] H. H. van Rossum, F. P. H. T. M. Romijn, N. P. M. Smit, J. W. de Fijter, and J. van Pelt,

- Everolimus and sirolimus antagonize tacrolimus based calcineurin inhibition via competition for FK-binding protein 12*, vol. 77, no. 7. 2009.
- [61] E. P. Navarese *et al.*, “First-generation versus second-generation drug-eluting stents in current clinical practice: Updated evidence from a comprehensive meta-analysis of randomised clinical trials comprising 31 379 patients,” *Open Hear.*, vol. 1, no. 1, 2014, doi: 10.1136/openhrt-2014-000064.
- [62] R. Piccolo *et al.*, “Drug-eluting or bare-metal stents for percutaneous coronary intervention: a systematic review and individual patient data meta-analysis of randomised clinical trials,” *Lancet*, vol. 393, no. 10190, pp. 2503–2510, Jun. 2019, doi: 10.1016/S0140-6736(19)30474-X.
- [63] M.-C. Morice *et al.*, “Direct stenting of de novo coronary stenoses with tacrolimus-eluting versus carbon-coated carbostents. The randomized JUPITER II trial,” *EuroIntervention J. Eur. Collab. with Work. Gr. Interv. Cardiol. Eur. Soc. Cardiol.*, vol. 2, no. 1, pp. 45–52, May 2006.
- [64] T. Palmerini *et al.*, “Stent thrombosis with drug-eluting stents: Is the paradigm shifting?,” *J. Am. Coll. Cardiol.*, vol. 62, no. 21, pp. 1915–1921, 2013, doi: 10.1016/j.jacc.2013.08.725.
- [65] P. K. Bundhun, M. Pursun, and F. Huang, “Biodegradable polymer drug-eluting stents versus first-generation durable polymer drug-eluting stents: A systematic review and meta-analysis of 12 randomized controlled trials,” *Medicine (Baltimore)*, vol. 96, no. 47, pp. e8878–e8878, Nov. 2017, doi: 10.1097/MD.0000000000008878.
- [66] K. Gao *et al.*, “Efficacy and safety of polymer-free stent versus polymer-permanent drug-eluting stent in patients with acute coronary syndrome: a meta-analysis of randomized control trials,” *BMC Cardiovasc. Disord.*, vol. 17, no. 1, p. 194, 2017, doi: 10.1186/s12872-017-0603-5.
- [67] M. J. Lipinski *et al.*, “Scaffold Thrombosis After Percutaneous Coronary Intervention With ABSORB Bioresorbable Vascular Scaffold: A Systematic Review and Meta-Analysis,” *JACC. Cardiovasc. Interv.*, vol. 9, no. 1, pp. 12–24, Jan. 2016, doi: 10.1016/j.jcin.2015.09.024.
- [68] G. El-Hayek *et al.*, “Meta-Analysis of Randomized Clinical Trials Comparing Biodegradable Polymer Drug-Eluting Stent to Second-Generation Durable Polymer Drug-Eluting Stents,” *JACC. Cardiovasc. Interv.*, vol. 10, no. 5, pp. 462–473, Mar. 2017, doi: 10.1016/j.jcin.2016.12.002.
- [69] G. Nakazawa *et al.*, “Anti-CD34 antibodies immobilized on the surface of sirolimus-eluting stents enhance stent endothelialization,” *JACC. Cardiovasc. Interv.*, vol. 3, no. 1, pp. 68–75, Jan. 2010, doi: 10.1016/j.jcin.2009.09.015.
- [70] P. P. Karjalainen and W. Namas, “Titanium-nitride-oxide-coated coronary stents: insights from the available evidence,” *Ann. Med.*, vol. 49, no. 4, pp. 299–309, Jun. 2017, doi: 10.1080/07853890.2016.1244353.
- [71] A. Paul *et al.*, “A nanobiohybrid complex of recombinant baculovirus and Tat/DNA nanoparticles for delivery of Ang-1 transgene in myocardial infarction therapy,” *Biomaterials*, vol. 32, no. 32, pp. 8304–8318, 2011, doi: <https://doi.org/10.1016/j.biomaterials.2011.07.042>.
- [72] J. Yang *et al.*, “The prevention of restenosis in vivo with a VEGF gene and paclitaxel co-eluting stent,” *Biomaterials*, vol. 34, no. 6, pp. 1635–1643, 2013, doi: <https://doi.org/10.1016/j.biomaterials.2012.11.006>.

- [73] A. Paul, W. Shao, D. Shum-Tim, and S. Prakash, "The attenuation of restenosis following arterial gene transfer using carbon nanotube coated stent incorporating TAT/DNAAng1+Vegf nanoparticles," *Biomaterials*, vol. 33, no. 30, pp. 7655–7664, 2012, doi: <https://doi.org/10.1016/j.biomaterials.2012.06.096>.
- [74] F. Sharif *et al.*, "Gene-eluting stents: Adenovirus-mediated delivery of eNOS to the blood vessel wall accelerates re-endothelialization and inhibits restenosis," *Mol. Ther.*, vol. 16, no. 10, pp. 1674–1680, 2008, doi: 10.1038/mt.2008.165.
- [75] L. E. Volkman and P. A. Goldsmith, "In Vitro Survey of Autographa californica Nuclear Polyhedrosis Virus Interaction with Nontarget Vertebrate Host Cells," *Appl. Environ. Microbiol.*, vol. 45, no. 3, pp. 1085–1093, 1983, [Online]. Available: <https://pubmed.ncbi.nlm.nih.gov/16346229>.
- [76] L. K. Miller, A. J. Lingg, and L. A. Bulla, "Bacterial, viral, and fungal insecticides," *Science (80-.)*, vol. 219, no. 4585, pp. 715–721, 1983.
- [77] M. J. Adang and L. K. Miller, "Molecular cloning of DNA complementary to mRNA of the baculovirus Autographa californica nuclear polyhedrosis virus: location and gene products of RNA transcripts found late in infection," *J. Virol.*, vol. 44, no. 3, pp. 782–793, 1982.
- [78] Y. C. Hu, C. T. Tsai, Y. J. Chang, and J. H. Huang, "Enhancement and prolongation of baculovirus-mediated expression in mammalian cells: focuses on strategic infection and feeding," *Biotechnol Prog*, vol. 19, no. 2, pp. 373–379, 2003, doi: 10.1021/bp025609d.
- [79] D. Palmberger, I. B. H. Wilson, I. Berger, R. Grabherr, and D. Rendic, "Sweetbac: A new approach for the production of mammalianised glycoproteins in insect cells," *PLoS One*, vol. 7, no. 4, pp. 1–8, 2012, doi: 10.1371/journal.pone.0034226.
- [80] J. J. Aumiller, H. Mabashi-Asazuma, A. Hillar, X. Shi, and D. L. Jarvis, "A new glycoengineered insect cell line with an inducibly mammalianized protein N-glycosylation pathway," *Glycobiology*, vol. 22, no. 3, pp. 417–428, Mar. 2012, doi: 10.1093/glycob/cwr160.
- [81] T. A. Kost and J. P. Condreay, "Recombinant baculoviruses as mammalian cell gene-delivery vectors," *Trends Biotechnol.*, vol. 20, no. 4, pp. 173–180, 2002, doi: [https://doi.org/10.1016/S0167-7799\(01\)01911-4](https://doi.org/10.1016/S0167-7799(01)01911-4).
- [82] M. A. Cheever and C. S. Higano, "PROVENGE (Sipuleucel-T) in Prostate Cancer: The First FDA-Approved Therapeutic Cancer Vaccine," *Clin. Cancer Res.*, vol. 17, no. 11, pp. 3520–3526, 2011, doi: 10.1158/1078-0432.Ccr-10-3126.
- [83] A. Monie, C.-F. Hung, R. Roden, and T. C. Wu, "Cervarix: a vaccine for the prevention of HPV 16, 18-associated cervical cancer," *Biologics*, vol. 2, no. 1, pp. 97–105, 2008, [Online]. Available: <https://pubmed.ncbi.nlm.nih.gov/19707432>.
- [84] R. A. A. Muzzarelli, M. El Mehtedi, C. Bottegoni, A. Aquili, and A. Gigante, "Genipin-Crosslinked Chitosan Gels and Scaffolds for Tissue Engineering and Regeneration of Cartilage and Bone," *Mar. Drugs*, vol. 13, no. 12, pp. 7314–7338, 2015, doi: 10.3390/md13127068.
- [85] C. Y. Wang, F. Li, Y. Yang, H. Y. Guo, C. X. Wu, and S. Wang, "Recombinant baculovirus containing the diphtheria toxin A gene for malignant glioma therapy," *Cancer Res*, vol. 66, no. 11, pp. 5798–5806, 2006, doi: 10.1158/0008-5472.Can-05-4514.
- [86] P. Balani, J. Boulaire, Y. Zhao, J. Zeng, J. Lin, and S. Wang, "High mobility group box2 promoter-controlled suicide gene expression enables targeted glioblastoma treatment," *Mol Ther*, vol. 17, no. 6, pp. 1003–1011, 2009, doi: 10.1038/mt.2009.22.

- [87] W. Huang *et al.*, “Suppression of gastric cancer growth by baculovirus vector-mediated transfer of normal epithelial cell specific-1 gene,” *World J Gastroenterol*, vol. 14, no. 38, pp. 5810–5815, 2008, doi: 10.3748/wjg.14.5810.
- [88] W. Y. Luo *et al.*, “Development of the hybrid Sleeping Beauty-baculovirus vector for sustained gene expression and cancer therapy,” *Gene Ther.*, vol. 19, no. 8, pp. 844–851, 2012, doi: 10.1038/gt.2011.129.
- [89] C.-Y. Lin *et al.*, “The healing of critical-sized femoral segmental bone defects in rabbits using baculovirus-engineered mesenchymal stem cells,” *Biomaterials*, vol. 31, no. 12, pp. 3222–3230, 2010.
- [90] J. J. Treanor *et al.*, “Protective efficacy of a trivalent recombinant hemagglutinin protein vaccine (FluBlok®) against influenza in healthy adults: A randomized, placebo-controlled trial,” *Vaccine*, vol. 29, no. 44, pp. 7733–7739, 2011, doi: <https://doi.org/10.1016/j.vaccine.2011.07.128>.
- [91] N. Muñoz *et al.*, “Epidemiologic classification of human papillomavirus types associated with cervical cancer,” *N Engl J Med*, vol. 348, no. 6, pp. 518–527, 2003, doi: 10.1056/NEJMoa021641.
- [92] V. Ferreira, H. Petry, and F. Salmon, “Immune Responses to AAV-Vectors, the Glybera Example from Bench to Bedside,” *Front Immunol*, vol. 5, p. 82, 2014, doi: 10.3389/fimmu.2014.00082.
- [93] T. Bin Emran *et al.*, “Baculovirus-Induced Fast-Acting Innate Immunity Kills Liver-Stage Plasmodium,” *J. Immunol.*, vol. 201, no. 8, p. 2441, 2018, doi: 10.4049/jimmunol.1800908.
- [94] D. S. Fedson and P. Dunnill, “New approaches to confronting an imminent influenza pandemic,” *Perm. J.*, vol. 11, no. 3, p. 63, 2007.
- [95] “Draft landscape of covid-19 candidate vaccines.” WHO, [Online]. Available: <https://www.who.int/publications/m/item/draft-landscape-of-covid-19-candidate-vaccines>.
- [96] L. Lu, Y. Ho, and J. Kwang, “Suppression of porcine arterivirus replication by baculovirus-delivered shRNA targeting nucleoprotein,” *Biochem. Biophys. Res. Commun.*, vol. 340, no. 4, pp. 1178–1183, 2006.
- [97] J. K. Rätty *et al.*, “Enhanced Gene Delivery by Avidin-Displaying Baculovirus,” *Mol. Ther.*, vol. 9, no. 2, pp. 282–291, 2004, doi: <https://doi.org/10.1016/j.yymthe.2003.11.004>.
- [98] Y.-K. Kim *et al.*, “Receptor-mediated gene delivery by folate-PEG-baculovirus in vitro,” *J. Biotechnol.*, vol. 131, no. 3, pp. 353–361, 2007, doi: <https://doi.org/10.1016/j.jbiotec.2007.07.938>.
- [99] P. Meysami, F. Rezaei, S. M. Marashi, M. M. Amiri, E. Bakker, and T. Mokhtari-Azad, “Antitumor effects of a recombinant baculovirus displaying anti-HER2 scFv expressing Apoptin in HER2 positive SK-BR-3 breast cancer cells,” *Future Virol.*, vol. 14, no. 3, pp. 139–152, 2019.
- [100] C. Ono *et al.*, “Innate immune response induced by baculovirus attenuates transgene expression in mammalian cells,” *J Virol*, vol. 88, no. 4, pp. 2157–2167, 2014, doi: 10.1128/jvi.03055-13.
- [101] M. Takahama *et al.*, “The RAB2B-GARIL5 Complex Promotes Cytosolic DNA-Induced Innate Immune Responses,” *Cell Rep*, vol. 20, no. 12, pp. 2944–2954, 2017, doi: 10.1016/j.celrep.2017.08.085.
- [102] W.-H. Lo, S.-M. Hwang, C.-K. Chuang, C.-Y. Chen, and Y.-C. Hu, “Development of a hybrid baculoviral vector for sustained transgene expression,” *Mol. Ther.*, vol. 17, no. 4,

- pp. 658–666, 2009.
- [103] X. Wang, Z. Ao, L. Chen, G. Kobinger, J. Peng, and X. Yao, “The Cellular Antiviral Protein APOBEC3G Interacts with HIV-1 Reverse Transcriptase and Inhibits Its Function during Viral Replication,” *J. Virol.*, vol. 86, no. 7, pp. 3777 LP – 3786, Apr. 2012, doi: 10.1128/JVI.06594-11.
- [104] T.-A. Hsu, J. J. Eiden, P. Bourgarel, T. Meo, and M. J. Betenbaugh, “Effects of co-expressing chaperone BiP on functional antibody production in the baculovirus system,” *Protein Expr. Purif.*, vol. 5, no. 6, pp. 595–603, 1994.
- [105] M. Kool, J. W. Voncken, F. L. J. Van Lier, J. Tramper, and J. M. Vlak, “Detection and analysis of *Autographa californica* nuclear polyhedrosis virus mutants with defective interfering properties,” *Virology*, vol. 183, no. 2, pp. 739–746, 1991.
- [106] C. Hofmann, V. Sandig, G. Jennings, M. Rudolph, P. Schlag, and M. Strauss, “Efficient gene transfer into human hepatocytes by baculovirus vectors,” *Proc. Natl. Acad. Sci.*, vol. 92, no. 22, pp. 10099–10103, 1995, doi: 10.1073/pnas.92.22.10099.
- [107] V. Sandig, C. Hofmann, S. Steinert, G. Jennings, P. Schlag, and M. Strauss, “Gene transfer into hepatocytes and human liver tissue by baculovirus vectors,” *Hum Gene Ther*, vol. 7, no. 16, pp. 1937–1945, 1996, doi: 10.1089/hum.1996.7.16-1937.
- [108] K. Lundstrom, “Latest development in viral vectors for gene therapy,” *Trends Biotechnol.*, vol. 21, no. 3, pp. 117–122, 2003, doi: [https://doi.org/10.1016/S0167-7799\(02\)00042-2](https://doi.org/10.1016/S0167-7799(02)00042-2).
- [109] E. Marshall, “Gene Therapy Death Prompts Review of Adenovirus Vector,” *Science (80-.)*, vol. 286, no. 5448, pp. 2244–2245, 1999, doi: 10.1126/science.286.5448.2244.
- [110] N.-D. van Loo, E. Fortunati, E. Ehlert, M. Rabelink, F. Grosveld, and B. J. Scholte, “Baculovirus Infection of Nondividing Mammalian Cells: Mechanisms of Entry and Nuclear Transport of Capsids,” *J. Virol.*, vol. 75, no. 2, pp. 961–970, 2001, doi: 10.1128/jvi.75.2.961-970.2001.
- [111] M. Lohela, M. Bry, T. Tammela, and K. Alitalo, “VEGFs and receptors involved in angiogenesis versus lymphangiogenesis,” *Curr. Opin. Cell Biol.*, vol. 21, no. 2, pp. 154–165, 2009, doi: <https://doi.org/10.1016/j.ceb.2008.12.012>.
- [112] L. Loffredo *et al.*, “Imbalance between nitric oxide generation and oxidative stress in patients with peripheral arterial disease: Effect of an antioxidant treatment,” *J. Vasc. Surg.*, vol. 44, no. 3, pp. 525–530, 2006, doi: <https://doi.org/10.1016/j.jvs.2006.05.023>.
- [113] A. Paul, C. B. Elias, D. Shum-Tim, and S. Prakash, “Bioactive baculovirus nanohybrids for stent based rapid vascular re-endothelialization,” *Sci. Rep.*, vol. 3, pp. 1–9, 2013, doi: 10.1038/srep02366.
- [114] M. Tscharre *et al.*, “Von Willebrand Factor and ADAMTS13 and long-term outcomes in patients undergoing percutaneous coronary intervention,” *Thromb. Res.*, vol. 196, pp. 31–37, 2020, doi: <https://doi.org/10.1016/j.thromres.2020.08.018>.
- [115] J. de Haro Miralles, E. Martínez-Aguilar, A. Florez, C. Varela, S. Bleda, and F. Acin, “Nitric oxide: link between endothelial dysfunction and inflammation in patients with peripheral arterial disease of the lower limbs☆,” *Interact. Cardiovasc. Thorac. Surg.*, vol. 9, no. 1, pp. 107–112, Jul. 2009, doi: 10.1510/icvts.2008.196428.
- [116] H. Li and U. Förstermann, “Nitric oxide in the pathogenesis of vascular disease,” *J. Pathol.*, vol. 190, no. 3, pp. 244–254, Feb. 2000, doi: [https://doi.org/10.1002/\(SICI\)1096-9896\(200002\)190:3<244::AID-PATH575>3.0.CO;2-8](https://doi.org/10.1002/(SICI)1096-9896(200002)190:3<244::AID-PATH575>3.0.CO;2-8).
- [117] L. S. Ulanova *et al.*, “Development of methods for encapsulation of viruses into polymeric nano- and microparticles for aquaculture vaccines,” *J. Appl. Polym. Sci.*, vol. 131, no. 17,

- pp. 8785–8796, 2014, doi: 10.1002/app.40714.
- [118] C. E. Mora-Huertas, H. Fessi, and A. Elaissari, “Polymer-based nanocapsules for drug delivery,” *Int. J. Pharm.*, vol. 385, no. 1–2, pp. 113–142, 2010, doi: 10.1016/j.ijpharm.2009.10.018.
- [119] T. M. S. Chang, “ARTIFICIAL CELL evolves into nanomedicine, biotherapeutics, blood substitutes, drug delivery, enzyme/gene therapy, cancer therapy, cell/stem cell therapy, nanoparticles, liposomes, bioencapsulation, replicating synthetic cells, cell encapsulation/scaffold, biosorbent/immunosorbent haemoperfusion/plasmapheresis, regenerative medicine, encapsulated microbe, nanobiotechnology, nanotechnology,” *Artif. Cells, Nanomedicine Biotechnol.*, vol. 47, no. 1, pp. 997–1013, 2019, doi: 10.1080/21691401.2019.1577885.
- [120] K. Y. Lee and D. J. Mooney, “Alginate: properties and biomedical applications,” *Prog. Polym. Sci.*, vol. 37, no. 1, pp. 106–126, Jan. 2012, doi: 10.1016/j.progpolymsci.2011.06.003.
- [121] S. G. Mohyuddin *et al.*, “Effect of chitosan on blood profile, inflammatory cytokines by activating TLR4/NF- κ B signaling pathway in intestine of heat stressed mice,” *Sci. Rep.*, vol. 11, no. 1, p. 20608, 2021, doi: 10.1038/s41598-021-98931-8.
- [122] S.-H. Min, K. C. Park, and Y. Il Yeom, “Chitosan-mediated non-viral gene delivery with improved serum stability and reduced cytotoxicity,” *Biotechnol. Bioprocess Eng.*, vol. 19, no. 6, pp. 1077–1082, 2014, doi: 10.1007/s12257-014-0450-5.
- [123] M. N. Singh, K. S. Y. Hemant, M. Ram, and H. G. Shivakumar, “Microencapsulation: A promising technique for controlled drug delivery,” *Res. Pharm. Sci.*, vol. 5, no. 2, pp. 65–77, Jul. 2010, [Online]. Available: <https://pubmed.ncbi.nlm.nih.gov/21589795>.
- [124] H. Chen *et al.*, “Preparation and characterization of novel polymeric microcapsules for live cell encapsulation and therapy,” *Cell Biochem. Biophys.*, vol. 47, no. 1, pp. 159–167, 2007, doi: 10.1385/CBB:47:1:159.
- [125] S. Schaly, M. Ghebretatios, and S. Prakash, “Baculoviruses in Gene Therapy and Personalized Medicine,” *Biologics*, vol. 15, pp. 115–132, 2021, doi: 10.2147/BTT.S292692.
- [126] M. L. Fabre, P. N. Arrías, T. Masson, M. L. Pidre, and V. Romanowski, “Chapter 11 - Baculovirus-Derived Vectors for Immunization and Therapeutic Applications,” M. M. B. T.-E. and R. V. P. Ennaji, Ed. Academic Press, 2020, pp. 197–224.
- [127] A. Paul, W. Shao, S. Abbasi, D. Shum-Tim, and S. Prakash, “PAMAM dendrimer-baculovirus nanocomplex for microencapsulated adipose stem cell-gene therapy: In vitro and in vivo functional assessment,” *Mol. Pharm.*, vol. 9, no. 9, pp. 2479–2488, 2012, doi: 10.1021/mp3000502.
- [128] M. Mansouri *et al.*, “Highly efficient baculovirus-mediated multigene delivery in primary cells,” *Nat. Commun.*, vol. 7, no. 1, p. 11529, 2016, doi: 10.1038/ncomms11529.
- [129] S. Rousseau, F. Houle, and J. Huot, “Integrating the VEGF signals leading to actin-based motility in vascular endothelial cells,” *Trends Cardiovasc. Med.*, vol. 10, no. 8, pp. 321–327, 2000.
- [130] L. Lamalice, F. Houle, and J. Huot, “Phosphorylation of Tyr1214 within VEGFR-2 triggers the recruitment of Nck and activation of Fyn leading to SAPK2/p38 activation and endothelial cell migration in response to VEGF,” *J. Biol. Chem.*, vol. 281, no. 45, pp. 34009–34020, 2006.
- [131] S. Prakash, A. Paul, A. A. Khan, and D. Shum-Tim, “BacMam virus transduced

- cardiomyoblasts can be used for myocardial transplantation using AP-PEG-A microcapsules: Molecular cloning, preparation, and in vitro analysis,” *J. Biomed. Biotechnol.*, vol. 2010, 2010, doi: 10.1155/2010/858094.
- [132] L.-Y. Sung *et al.*, “Efficient gene delivery into cell lines and stem cells using baculovirus,” *Nat. Protoc.*, vol. 9, no. 8, pp. 1882–1899, 2014, doi: 10.1038/nprot.2014.130.
- [133] M. Heli, R. Johanna, G. Leona, M. Varpu, R. Hilkkka, and O.-B. Christian, “Baculovirus Entry into Human Hepatoma Cells,” *J. Virol.*, vol. 79, no. 24, pp. 15452–15459, Dec. 2005, doi: 10.1128/JVI.79.24.15452-15459.2005.
- [134] M. Scarcella *et al.*, “The Key Role of Lysosomal Protease Cathepsins in Viral Infections.,” *Int. J. Mol. Sci.*, vol. 23, no. 16, Aug. 2022, doi: 10.3390/ijms23169089.
- [135] S. E. McNeil, *Challenges for Nanoparticle Characterization*, vol. 697. 2011.
- [136] S. Schaly, P. Islam, A. Abosalha, J. L. Boyajian, D. Shum-Tim, and S. Prakash, “Alginate-Chitosan Hydrogel Formulations Sustain Baculovirus Delivery and VEGFA Expression Which Promotes Angiogenesis for Wound Dressing Applications.,” *Pharmaceuticals (Basel)*, vol. 15, no. 11, Nov. 2022, doi: 10.3390/ph15111382.
- [137] A. S. R. Maharaj and P. A. D’Amore, “Roles for VEGF in the adult,” *Microvasc. Res.*, vol. 74, no. 2, pp. 100–113, 2007, doi: <https://doi.org/10.1016/j.mvr.2007.03.004>.
- [138] R. Valencia-Quintana *et al.*, “Evaluation of the genotoxic potential of dimethyl sulfoxide (DMSO) in meristematic cells of the root of *Vicia faba*,” *Toxicol. Environ. Health Sci.*, vol. 4, no. 3, pp. 154–160, 2012, doi: 10.1007/s13530-012-0130-9.
- [139] M. Mittal, M. R. Siddiqui, K. Tran, S. P. Reddy, and A. B. Malik, “Reactive oxygen species in inflammation and tissue injury.,” *Antioxid. Redox Signal.*, vol. 20, no. 7, pp. 1126–1167, Mar. 2014, doi: 10.1089/ars.2012.5149.
- [140] T. Gotoh, N. Ando, and K. I. Kikuchi, “Analysis of inactivation of AcMNPV under various conditions by the ELVA method,” *Biosci. Biotechnol. Biochem.*, vol. 72, no. 7, pp. 1973–1976, 2008, doi: 10.1271/bbb.80105.
- [141] R. B. Hitchman, R. D. Possee, and L. A. King, “High-throughput baculovirus expression in insect cells,” in *Recombinant Gene Expression*, Springer, 2012, pp. 609–627.
- [142] O. de coopération et de développement économiques, *Test No. 487: In vitro mammalian cell micronucleus test*. OECD Publishing, 2016.
- [143] A. R. T. Machado *et al.*, “Cytotoxic, genotoxic, and oxidative stress-inducing effect of an l-amino acid oxidase isolated from *Bothrops jararacussu* venom in a co-culture model of HepG2 and HUVEC cells,” *Int. J. Biol. Macromol.*, vol. 127, pp. 425–432, 2019, doi: <https://doi.org/10.1016/j.ijbiomac.2019.01.059>.
- [144] N. R. Sproston and J. J. Ashworth, “Role of C-Reactive Protein at Sites of Inflammation and Infection.,” *Front. Immunol.*, vol. 9, p. 754, 2018, doi: 10.3389/fimmu.2018.00754.
- [145] N. Alexandre *et al.*, “In vitro and in vivo evaluation of blood coagulation activation of polyvinyl alcohol hydrogel plus dextran-based vascular grafts,” *J. Biomed. Mater. Res. - Part A*, vol. 103, no. 4, pp. 1366–1379, 2015, doi: 10.1002/jbm.a.35275.
- [146] M. Jerebtsova, M. L. Batshaw, and X. Ye, “Humoral Immune Response to Recombinant Adenovirus and Adeno-Associated Virus after In Utero Administration of Viral Vectors in Mice,” *Pediatr. Res.*, vol. 52, no. 1, pp. 95–104, 2002, doi: 10.1203/00006450-200207000-00018.
- [147] T. Velnar, T. Bailey, and V. Smrkolj, “The Wound Healing Process: An Overview of the Cellular and Molecular Mechanisms,” *J. Int. Med. Res.*, vol. 37, no. 5, pp. 1528–1542,

- Oct. 2009, doi: 10.1177/147323000903700531.
- [148] A. Singh *et al.*, “Meta-analysis of Randomized Controlled Trials on Hydrocolloid Occlusive Dressing Versus Conventional Gauze Dressing in the Healing of Chronic Wounds,” *Asian J. Surg.*, vol. 27, no. 4, pp. 326–332, 2004, doi: [https://doi.org/10.1016/S1015-9584\(09\)60061-0](https://doi.org/10.1016/S1015-9584(09)60061-0).
- [149] Z. Değim, “Use of microparticulate systems to accelerate skin wound healing,” *J. Drug Target.*, vol. 16, no. 6, pp. 437–448, Jan. 2008, doi: 10.1080/10611860802088572.
- [150] S. Liu *et al.*, “Injectable hydrogels based on silk fibroin peptide grafted hydroxypropyl chitosan and oxidized microcrystalline cellulose for scarless wound healing,” *Colloids Surfaces A Physicochem. Eng. Asp.*, vol. 647, p. 129062, 2022, doi: <https://doi.org/10.1016/j.colsurfa.2022.129062>.
- [151] H. Brem *et al.*, “Mechanism of Sustained Release of Vascular Endothelial Growth Factor in Accelerating Experimental Diabetic Healing,” *J. Invest. Dermatol.*, vol. 129, no. 9, pp. 2275–2287, 2009, doi: <https://doi.org/10.1038/jid.2009.26>.
- [152] N. Ferrara, H.-P. Gerber, and J. LeCouter, “The biology of VEGF and its receptors,” *Nat. Med.*, vol. 9, no. 6, pp. 669–676, 2003, doi: 10.1038/nm0603-669.
- [153] G. A. A. U.-M. Martău MihaelaAU - Vodnar, Dan C.TI - The Use of Chitosan, Alginate, and Pectin in the Biomedical and Food Sector—Biocompatibility, Bioadhesiveness, and Biodegradability, “No Title,” *Polymers*, vol. 11, no. 11. 2019, doi: 10.3390/polym11111837.
- [154] S. Tandon, B. Singh, S. Kapoor, and S. Mangal, “Comparison of Effect of pH Modulation on Wound Healing with Topical Application of Citric Acid Versus Superoxide Ions.,” *Niger. J. Surg. Off. Publ. Niger. Surg. Res. Soc.*, vol. 26, no. 2, pp. 122–126, 2020, doi: 10.4103/njs.NJS_14_19.
- [155] K. S. Agrawal, A. V. Sarda, R. Shrotriya, M. Bachhav, V. Puri, and G. Nataraj, “Acetic acid dressings: Finding the Holy Grail for infected wound management.,” *Indian J. Plast. Surg. Off. Publ. Assoc. Plast. Surg. India*, vol. 50, no. 3, pp. 273–280, 2017, doi: 10.4103/ijps.IJPS_245_16.
- [156] S. Li *et al.*, “Antibacterial Hydrogels.,” *Adv. Sci. (Weinheim, Baden-Wurtemberg, Ger.)*, vol. 5, no. 5, p. 1700527, May 2018, doi: 10.1002/advs.201700527.
- [157] Y. K. Kim *et al.*, “Hybrid of baculovirus and galactosylated PEI for efficient gene carrier,” *Virology*, vol. 387, no. 1, pp. 89–97, 2009, doi: 10.1016/j.virol.2009.02.001.
- [158] L. Yang *et al.*, “Vascular endothelial growth factor promotes fibrosis resolution and repair in mice.,” *Gastroenterology*, vol. 146, no. 5, pp. 1339–50.e1, May 2014, doi: 10.1053/j.gastro.2014.01.061.
- [159] N. G. Heatley, “A method for the assay of penicillin,” *Biochem. J.*, vol. 38, no. 1, p. 61, 1944.
- [160] R. M. Sabino and K. C. Popat, “Evaluating Whole Blood Clotting in vitro on Biomaterial Surfaces.,” *Bio-protocol*, vol. 10, no. 3, p. e3505, Feb. 2020, doi: 10.21769/BioProtoc.3505.
- [161] D. W. Leung, G. Cachianes, W. J. Kuang, D. V Goeddel, and N. Ferrara, “Vascular endothelial growth factor is a secreted angiogenic mitogen.,” *Science*, vol. 246, no. 4935, pp. 1306–1309, Dec. 1989, doi: 10.1126/science.2479986.
- [162] A. Suarez-Arnedo, F. Torres Figueroa, C. Clavijo, P. Arbeláez, J. C. Cruz, and C. Muñoz-Camargo, “An image J plugin for the high throughput image analysis of in vitro scratch wound healing assays,” *PLoS One*, vol. 15, no. 7, p. e0232565, Jul. 2020, [Online].

Available: <https://doi.org/10.1371/journal.pone.0232565>.

- [163] I. Arnaoutova and H. K. Kleinman, “In vitro angiogenesis: endothelial cell tube formation on gelled basement membrane extract,” *Nat. Protoc.*, vol. 5, no. 4, pp. 628–635, 2010, doi: 10.1038/nprot.2010.6.
- [164] K. Koizumi *et al.*, “Anti-angiogenic effects of dimethyl sulfoxide on endothelial cells.,” *Biol. Pharm. Bull.*, vol. 26, no. 9, pp. 1295–1298, Sep. 2003, doi: 10.1248/bpb.26.1295.
- [165] G. Carpentier *et al.*, “Angiogenesis Analyzer for ImageJ — A comparative morphometric analysis of ‘Endothelial Tube Formation Assay’ and ‘Fibrin Bead Assay,’” *Sci. Rep.*, vol. 10, no. 1, p. 11568, 2020, doi: 10.1038/s41598-020-67289-8.
- [166] M. Teodorescu, M. Bercea, and S. Morariu, “Biomaterials of PVA and PVP in medical and pharmaceutical applications: Perspectives and challenges,” *Biotechnol. Adv.*, vol. 37, no. 1, pp. 109–131, 2019, doi: <https://doi.org/10.1016/j.biotechadv.2018.11.008>.
- [167] N. Alexandre *et al.*, “Biocompatibility and hemocompatibility of polyvinyl alcohol hydrogel used for vascular grafting--In vitro and in vivo studies.,” *J. Biomed. Mater. Res. A*, vol. 102, no. 12, pp. 4262–4275, Dec. 2014, doi: 10.1002/jbm.a.35098.
- [168] C. C. DeMerlis and D. R. Schoneker, “Review of the oral toxicity of polyvinyl alcohol (PVA).,” *Food Chem. Toxicol. an Int. J. Publ. Br. Ind. Biol. Res. Assoc.*, vol. 41, no. 3, pp. 319–326, Mar. 2003, doi: 10.1016/s0278-6915(02)00258-2.
- [169] S. Wu *et al.*, “Poly(vinyl alcohol) Hydrogels with Broad-Range Tunable Mechanical Properties via the Hofmeister Effect,” *Adv. Mater.*, vol. 33, no. 11, p. 2007829, Mar. 2021, doi: <https://doi.org/10.1002/adma.202007829>.
- [170] N. Jain, V. K. Singh, and S. Chauhan, “A review on mechanical and water absorption properties of polyvinyl alcohol based composites/films,” vol. 26, no. 5–6, pp. 213–222, 2017, doi: 10.1515/jmbm-2017-0027.
- [171] K. Da Silva, P. Kumar, S. F. van Vuuren, V. Pillay, and Y. E. Choonara, “Three-Dimensional Printability of an ECM-Based Gelatin Methacryloyl (GelMA) Biomaterial for Potential Neuroregeneration,” *ACS Omega*, vol. 6, no. 33, pp. 21368–21383, Aug. 2021, doi: 10.1021/acsomega.1c01903.
- [172] S. Petros, T. Tesfaye, and M. Ayele, “A Review on Gelatin Based Hydrogels for Medical Textile Applications,” *J. Eng.*, vol. 2020, p. 8866582, 2020, doi: 10.1155/2020/8866582.
- [173] M. G. Chuc-Gamboa *et al.*, “The Effect of PEGDE Concentration and Temperature on Physicochemical and Biological Properties of Chitosan,” *Polymers (Basel)*, vol. 11, no. 11, p. 1830, Nov. 2019, doi: 10.3390/polym11111830.
- [174] M. B. Mellott, K. Searcy, and M. V Pishko, “Release of protein from highly cross-linked hydrogels of poly(ethylene glycol) diacrylate fabricated by UV polymerization,” *Biomaterials*, vol. 22, no. 9, pp. 929–941, 2001, doi: [https://doi.org/10.1016/S0142-9612\(00\)00258-1](https://doi.org/10.1016/S0142-9612(00)00258-1).
- [175] M. Akhlaq *et al.*, “Methotrexate-Loaded Gelatin and Polyvinyl Alcohol (Gel/PVA) Hydrogel as a pH-Sensitive Matrix,” *Polymers*, vol. 13, no. 14, 2021, doi: 10.3390/polym13142300.
- [176] S. Das and U. Subuddhi, “Controlled delivery of ibuprofen from poly(vinyl alcohol)-poly(ethylene glycol) interpenetrating polymeric network hydrogels.,” *J. Pharm. Anal.*, vol. 9, no. 2, pp. 108–116, Apr. 2019, doi: 10.1016/j.jpha.2018.11.007.
- [177] M. C. Frost, M. M. Reynolds, and M. E. Meyerhoff, “Polymers incorporating nitric oxide releasing/generating substances for improved biocompatibility of blood-contacting medical devices.,” *Biomaterials*, vol. 26, no. 14, pp. 1685–1693, May 2005, doi:

- 10.1016/j.biomaterials.2004.06.006.
- [178] Y. Yuan, Y. Shang, Y. Zhou, J. Guo, and F. Yan, “Enabling Antibacterial and Antifouling Coating via Grafting of a Nitric Oxide-Releasing Ionic Liquid on Silicone Rubber,” *Biomacromolecules*, vol. 23, no. 6, pp. 2329–2341, Jun. 2022, doi: 10.1021/acs.biomac.2c00077.
- [179] G. Fleming, J. Aveyard, J. L. Fothergill, F. McBride, R. Raval, and R. A. D’Sa, “Nitric Oxide Releasing Polymeric Coatings for the Prevention of Biofilm Formation.,” *Polymers (Basel)*, vol. 9, no. 11, Nov. 2017, doi: 10.3390/polym9110601.
- [180] Y. Chen *et al.*, “A tough nitric oxide-eluting hydrogel coating suppresses neointimal hyperplasia on vascular stent,” *Nat. Commun.*, vol. 12, no. 1, p. 7079, 2021, doi: 10.1038/s41467-021-27368-4.
- [181] X. Zhou, C. Hou, T.-L. Chang, Q. Zhang, and J. F. Liang, “Controlled released of drug from doubled-walled PVA hydrogel/PCL microspheres prepared by single needle electrospraying method,” *Colloids Surfaces B Biointerfaces*, vol. 187, p. 110645, 2020, doi: <https://doi.org/10.1016/j.colsurfb.2019.110645>.
- [182] T. Kimura *et al.*, “Preparation of poly(vinyl alcohol)/DNA hydrogels via hydrogen bonds formed on ultra-high pressurization and controlled release of DNA from the hydrogels for gene delivery.,” *J. Artif. organs Off. J. Japanese Soc. Artif. Organs*, vol. 10, no. 2, pp. 104–108, 2007, doi: 10.1007/s10047-006-0367-7.
- [183] F. M. Boyce and N. L. Bucher, “Baculovirus-mediated gene transfer into mammalian cells,” *Proc. Natl. Acad. Sci.*, vol. 93, no. 6, pp. 2348–2352, 1996, doi: 10.1073/pnas.93.6.2348.
- [184] V. Jones, J. E. Grey, and K. G. Harding, “Wound dressings.,” *BMJ*, vol. 332, no. 7544, pp. 777–780, Apr. 2006, doi: 10.1136/bmj.332.7544.777.
- [185] L. Fan, H. Yang, J. Yang, M. Peng, and J. Hu, “Preparation and characterization of chitosan/gelatin/PVA hydrogel for wound dressings.,” *Carbohydr. Polym.*, vol. 146, pp. 427–434, Aug. 2016, doi: 10.1016/j.carbpol.2016.03.002.
- [186] M. F. A. Cutiongco *et al.*, “Submillimeter Diameter Poly(Vinyl Alcohol) Vascular Graft Patency in Rabbit Model.,” *Front. Bioeng. Biotechnol.*, vol. 4, p. 44, 2016, doi: 10.3389/fbioe.2016.00044.
- [187] D. L. Jarvis and A. J. Garcia, “Long-term stability of baculoviruses stored under various conditions.,” *Biotechniques*, vol. 16, no. 3, pp. 508–513, Mar. 1994.
- [188] V. L. Truong-Le, J. T. August, and K. W. Leong, “Controlled Gene Delivery by DNA–Gelatin Nanospheres,” *Hum. Gene Ther.*, vol. 9, no. 12, pp. 1709–1717, Aug. 1998, doi: 10.1089/hum.1998.9.12-1709.
- [189] L. Rose, H. M. Aliabadi, and H. Uludağ, “Gelatin coating to stabilize the transfection ability of nucleic acid polyplexes.,” *Acta Biomater.*, vol. 9, no. 7, pp. 7429–7438, Jul. 2013, doi: 10.1016/j.actbio.2013.03.029.
- [190] H. Jorio, R. Tran, and A. Kamen, “Stability of serum-free and purified baculovirus stocks under various storage conditions.,” *Biotechnol. Prog.*, vol. 22, no. 1, pp. 319–325, 2006, doi: 10.1021/bp050218v.
- [191] G. H. Oliveira-Paula, R. Lacchini, and J. E. Tanus-Santos, “Endothelial nitric oxide synthase: From biochemistry and gene structure to clinical implications of NOS3 polymorphisms.,” *Gene*, vol. 575, no. 2 Pt 3, pp. 584–599, Jan. 2016, doi: 10.1016/j.gene.2015.09.061.
- [192] J. R. Hall, K. R. Rouillard, D. J. Suchyta, M. D. Brown, M. J. R. Ahonen, and M. H.

- Schoenfisch, “Mode of Nitric Oxide Delivery Affects Antibacterial Action,” *ACS Biomater. Sci. Eng.*, vol. 6, no. 1, pp. 433–441, Jan. 2020, doi: 10.1021/acsbio.2c01384.
- [193] R. Namivandi-Zangeneh *et al.*, “Nitric Oxide-Loaded Antimicrobial Polymer for the Synergistic Eradication of Bacterial Biofilm,” *ACS Macro Lett.*, vol. 7, no. 5, pp. 592–597, May 2018, doi: 10.1021/acsmacrolett.8b00190.
- [194] C. Kenoutis *et al.*, “Baculovirus-mediated gene delivery into Mammalian cells does not alter their transcriptional and differentiating potential but is accompanied by early viral gene expression.” *J. Virol.*, vol. 80, no. 8, pp. 4135–4146, Apr. 2006, doi: 10.1128/JVI.80.8.4135-4146.2006.
- [195] N. Navneet *et al.*, “Pathology of Peripheral Artery Disease in Patients With Critical Limb Ischemia,” *J. Am. Coll. Cardiol.*, vol. 72, no. 18, pp. 2152–2163, Oct. 2018, doi: 10.1016/j.jacc.2018.08.002.
- [196] S. Steven, A. Daiber, J. F. Doppeide, T. Münzel, and C. Espinola-Klein, “Peripheral artery disease, redox signaling, oxidative stress – Basic and clinical aspects,” *Redox Biol.*, vol. 12, pp. 787–797, 2017, doi: <https://doi.org/10.1016/j.redox.2017.04.017>.
- [197] F. T. Silveira *et al.*, “Stent fractures in the superficial femoral artery: predisposing factors and their implications.” *J. Vasc. Bras.*, vol. 21, p. e20200014, 2022, doi: 10.1590/1677-5449.202000142.
- [198] S. Dierk *et al.*, “Prevalence and clinical impact of stent fractures after femoropopliteal stenting,” *J. Am. Coll. Cardiol.*, vol. 45, no. 2, pp. 312–315, Jan. 2005, doi: 10.1016/j.jacc.2004.11.026.
- [199] M. A. H. Sonneveld, M. P. M. de Maat, and F. W. G. Leebeek, “Von Willebrand factor and ADAMTS13 in arterial thrombosis: a systematic review and meta-analysis,” *Blood Rev.*, vol. 28, no. 4, pp. 167–178, 2014, doi: <https://doi.org/10.1016/j.blre.2014.04.003>.
- [200] P. M. Mannucci, C. Capoferri, and M. T. Canciani, “Plasma levels of von Willebrand factor regulate ADAMTS-13, its major cleaving protease,” *Br. J. Haematol.*, vol. 126, no. 2, pp. 213–218, 2004.
- [201] Y. J. Jeong, Y. Yao, T. H. Mekonnen, and E. K. F. Yim, “Changing Compliance of Poly(Vinyl Alcohol) Tubular Scaffold for Vascular Graft Applications Through Modifying Interlayer Adhesion and Crosslinking Density,” *Front. Mater.*, vol. 7, no. January, pp. 1–16, 2021, doi: 10.3389/fmats.2020.595295.
- [202] T. Cheng *et al.*, “A rapid and efficient method to express target genes in mammalian cells by baculovirus.” *World J. Gastroenterol.*, vol. 10, no. 11, pp. 1612–1618, Jun. 2004, doi: 10.3748/wjg.v10.i11.1612.
- [203] A. Abdellaoui and H. Al-Khaffaf, “C-Reactive Protein (CRP) as a Marker in Peripheral Vascular Disease,” *Eur. J. Vasc. Endovasc. Surg.*, vol. 34, no. 1, pp. 18–22, 2007, doi: <https://doi.org/10.1016/j.ejvs.2006.10.040>.
- [204] T. P. Singh, D. R. Morris, S. Smith, J. V Moxon, and J. Golledge, “Systematic Review and Meta-Analysis of the Association Between C-Reactive Protein and Major Cardiovascular Events in Patients with Peripheral Artery Disease,” *Eur. J. Vasc. Endovasc. Surg.*, vol. 54, no. 2, pp. 220–233, 2017, doi: <https://doi.org/10.1016/j.ejvs.2017.05.009>.
- [205] P. Libby and P. M. Ridker, “Inflammation and atherosclerosis: role of C-reactive protein in risk assessment,” *Am. J. Med.*, vol. 116, no. 6, pp. 9–16, 2004.
- [206] L. A. Brito, S. Chandrasekhar, S. R. Little, and M. M. Amiji, “Non-viral eNOS gene

- delivery and transfection with stents for the treatment of restenosis,” *Biomed. Eng. Online*, vol. 9, pp. 1–14, 2010, doi: 10.1186/1475-925X-9-56.
- [207] S. É. Michaud, S. Dussault, J. Groleau, P. Haddad, and A. Rivard, “Cigarette smoke exposure impairs VEGF-induced endothelial cell migration: Role of NO and reactive oxygen species,” *J. Mol. Cell. Cardiol.*, vol. 41, no. 2, pp. 275–284, 2006, doi: <https://doi.org/10.1016/j.yjmcc.2006.05.004>.
- [208] R. Tati *et al.*, “Phenotypic Expression of ADAMTS13 in Glomerular Endothelial Cells,” *PLoS One*, vol. 6, no. 6, p. e21587, Jun. 2011, [Online]. Available: <https://doi.org/10.1371/journal.pone.0021587>.
- [209] H. E. Von Der Leyen *et al.*, “Gene therapy inhibiting neointimal vascular lesion: in vivo transfer of endothelial cell nitric oxide synthase gene.,” *Proc. Natl. Acad. Sci.*, vol. 92, no. 4, pp. 1137–1141, 1995.
- [210] Y. Nagakawa, S. Fujita, S. Yunoki, T. Tsuchiya, S. ichiro Suye, and T. Itoi, “Self-expandable hydrogel biliary stent design utilizing the swelling property of poly(vinyl alcohol) hydrogel,” *J. Appl. Polym. Sci.*, vol. 137, no. 28, pp. 1–9, 2020, doi: 10.1002/app.48851.
- [211] P. Poncin and J. Proft, “Stent tubing: Understanding the desired attributes,” *Med. Device Mater. - Proc. Mater. Process. Med. Devices Conf. 2003*, no. September, pp. 253–259, 2003.
- [212] C.-C. Liang, A. Y. Park, and J.-L. Guan, “In vitro scratch assay: a convenient and inexpensive method for analysis of cell migration in vitro,” *Nat. Protoc.*, vol. 2, no. 2, pp. 329–333, 2007, doi: 10.1038/nprot.2007.30.
- [213] S. Braune, S. Zhou, H. Hereon, and F. Jung, “Quantification of adherent platelets on polymer-based biomaterials . Comparison of colorimetric and microscopic assessment,” no. September, 2015, doi: 10.3233/CH-151995.
- [214] Z. Wu *et al.*, “Inhibition of eNOS by L-NAME resulting in rat hind limb developmental defects through PFKFB3 mediated angiogenetic pathway,” *Sci. Rep.*, vol. 10, no. 1, p. 16754, 2020, doi: 10.1038/s41598-020-74011-1.
- [215] M. Viecca, V. Vizzi, G. Alessandrino, G. Scarpini, A. Colombo, and M. Di Biasi, “TWO YEARS CLINICAL OUTCOMES OF PATIENTS TREATED WITH EUCALIMUS SIROLIMUS-ELUTING STENTS A REAL WORLD EXPERIENCE,” *Studies*, vol. 14, p. 15, 2022.
- [216] D. J. Omeh and E. Shlofmitz, “Restenosis,” 2019.
- [217] V. Lubrano and S. Balzan, “Enzymatic antioxidant system in vascular inflammation and coronary artery disease.,” *World J. Exp. Med.*, vol. 5, no. 4, pp. 218–224, Nov. 2015, doi: 10.5493/wjem.v5.i4.218.
- [218] H. Sellak, E. Franzini, J. Hakim, and C. Pasquier, “Reactive oxygen species rapidly increase endothelial ICAM-1 ability to bind neutrophils without detectable upregulation,” 1994.
- [219] D. Sharmila, A. L. Rao, and L. Kalyani, “Development and Validation of Stability-indicating High Performance Liquid Chromatographic Method for the Estimation of Everolimus in Tablets.,” *Indian J. Pharm. Sci.*, vol. 77, no. 5, pp. 599–604, 2015, doi: 10.4103/0250-474x.169044.
- [220] X. Pan *et al.*, “Applications and developments of gene therapy drug delivery systems for genetic diseases,” *Asian J. Pharm. Sci.*, vol. 16, no. 6, pp. 687–703, 2021, doi: <https://doi.org/10.1016/j.ajps.2021.05.003>.

- [221] J. J. Treanor *et al.*, “Dose-Related Safety and Immunogenicity of a Trivalent Baculovirus-Expressed Influenza-Virus Hemagglutinin Vaccine in Elderly Adults,” *J. Infect. Dis.*, vol. 193, no. 9, pp. 1223–1228, Apr. 2006, [Online]. Available: <http://www.jstor.org/stable/30086531>.
- [222] Y. C. Hu, “Baculovirus as a highly efficient expression vector in insect and mammalian cells,” *Acta Pharmacol. Sin.*, vol. 26, no. 4, pp. 405–416, 2005, doi: 10.1111/j.1745-7254.2005.00078.x.
- [223] F. Gottrup, “A specialized wound-healing center concept: importance of a multidisciplinary department structure and surgical treatment facilities in the treatment of chronic wounds,” *Am. J. Surg.*, vol. 187, no. 5, Supplement 1, pp. S38–S43, 2004, doi: [https://doi.org/10.1016/S0002-9610\(03\)00303-9](https://doi.org/10.1016/S0002-9610(03)00303-9).
- [224] C. K. Sen *et al.*, “Human skin wounds: a major and snowballing threat to public health and the economy.,” *Wound repair and regeneration : official publication of the Wound Healing Society [and] the European Tissue Repair Society*, vol. 17, no. 6. United States, pp. 763–771, 2009, doi: 10.1111/j.1524-475X.2009.00543.x.
- [225] R. G. Frykberg and J. Banks, “Challenges in the Treatment of Chronic Wounds.,” *Adv. wound care*, vol. 4, no. 9, pp. 560–582, Sep. 2015, doi: 10.1089/wound.2015.0635.